CROSS TALK BETWEEN THE IMMUNE SYSTEM AND METABOLISM

EDITED BY: Jixin Zhong, Wen Kong and Jie Chen
PUBLISHED IN: Frontiers in Endocrinology

frontiers Research Topics

frontiers

ISSN 1664-8714
ISBN 978-2-88966-170-1
DOI 10.3389/978-2-88966-170-1

About Frontiers

Frontiers is more than just an open-access publisher of scholarly articles: it is a pioneering approach to the world of academia, radically improving the way scholarly research is managed. The grand vision of Frontiers is a world where all people have an equal opportunity to seek, share and generate knowledge. Frontiers provides immediate and permanent online open access to all its publications, but this alone is not enough to realize our grand goals.

Frontiers Journal Series

The Frontiers Journal Series is a multi-tier and interdisciplinary set of open-access, online journals, promising a paradigm shift from the current review, selection and dissemination processes in academic publishing. All Frontiers journals are driven by researchers for researchers; therefore, they constitute a service to the scholarly community. At the same time, the Frontiers Journal Series operates on a revolutionary invention, the tiered publishing system, initially addressing specific communities of scholars, and gradually climbing up to broader public understanding, thus serving the interests of the lay society, too.

Dedication to Quality

Each Frontiers article is a landmark of the highest quality, thanks to genuinely collaborative interactions between authors and review editors, who include some of the world's best academicians. Research must be certified by peers before entering a stream of knowledge that may eventually reach the public - and shape society; therefore, Frontiers only applies the most rigorous and unbiased reviews.
Frontiers revolutionizes research publishing by freely delivering the most outstanding research, evaluated with no bias from both the academic and social point of view. By applying the most advanced information technologies, Frontiers is catapulting scholarly publishing into a new generation.

What are Frontiers Research Topics?

Frontiers Research Topics are very popular trademarks of the Frontiers Journals Series: they are collections of at least ten articles, all centered on a particular subject. With their unique mix of varied contributions from Original Research to Review Articles, Frontiers Research Topics unify the most influential researchers, the latest key findings and historical advances in a hot research area! Find out more on how to host your own Frontiers Research Topic or contribute to one as an author by contacting the Frontiers Editorial Office: researchtopics@frontiersin.org

CROSS TALK BETWEEN THE IMMUNE SYSTEM AND METABOLISM

Topic Editors:
Jixin Zhong, Case Western Reserve University, United States
Wen Kong, Huazhong University of Science and Technology, China
Jie Chen, Xiamen University, China

Citation: Zhong, J., Kong, W., Chen, J., eds. (2020). Cross Talk Between the Immune System and Metabolism. Lausanne: Frontiers Media SA.
doi: 10.3389/978-2-88966-170-1

Table of Contents

frontiers in Endocrinology

EDITORIAL
published: 24 September 2020
doi: 10.3389/fendo.2020.00588

Editorial: Cross Talk Between the Immune System and Metabolism

Jie Chen[1], *Wen Kong*[2] *and Jixin Zhong*[3,4]*

[1] Jiangxi Provincial People's Hospital Affiliated to Nanchang University, Nanchang, China, [2] Department of Endocrinology, Wuhan Union Hospital, Tongji Medical College, Huazhong University of Science and Technology, Wuhan, China, [3] Department of Rheumatology and Immunology, Tongji Hospital, Tongji Medical College, Huazhong University of Science and Technology, Wuhan, China, [4] Department of Medicine, Case Western Reserve University, Cleveland, OH, United States

Keywords: immune system, metabolism, metabolic disease, chronic inflammation, metabolic dysregulation

Editorial on the Research Topic

Cross Talk Between the Immune System and Metabolism

Metabolic dysregulation leads to a number of diseases including diabetes, obesity, hypertension, gout and rheumatoid arthritis (RA). These diseases have been associated with chronic inflammatory processes. To date, increasing evidence indicates that immune system plays an important role in the process of metabolic diseases. For example, the activation of type 1 immunity was identified in obesity-associated metabolic dysfunction (1). Metabolism has been shown to play a critical role in RA, a chronic autoimmune disease with involvement of a series of pro-inflammatory and immune-regulatory cytokines and mediators (2, 3). Innate immunity is also of key importance in the pathogenesis of gout (4). Although the association between the immune system and metabolic diseases have been well-recognized, the understanding of immune-related mechanisms of these diseases are not fully understood. This special issue exhibits a number of original research articles and review papers on the topic of cross talk between the immune system and metabolism.

As a central immune organ, the thymus provides a place for naive T cell differentiation, development and maturation. With thymic senescence, the epithelial network shrinks and is replaced by adipose tissue, leading to a decline of its immune function (5). Meanwhile, beige adipose tissue plays a key role in metabolism. By investigating the beige-specific and beige-indicative markers and metabolic profile (OCR/ECAR ratio), Banfai et al. reported in this issue that thymic adipose tissue emerging with senescence was actually beige adipose tissue, which builds a bridge between immune organ and metabolic tissue. T cells develop within the thymus and play a central role in adaptive immunity. Sirtuins are nicotine adenine dinucleotide (NAD+)-dependent enzymes involved in the cell metabolism (6). A review by Jonathan L et al. summarized some recent progresses in the role of sirtuins in regulating adaptive immunity (Warren and MacIver).

Alarmins play vital roles in innate and adaptive immune responses and participate in a wide range of pathophysiological processes such as inflammation and oncogenesis (7). Guo et al. investigated how sodium butyrate exerts its anti-inflammatory activity by inhibiting an "alarmin," HMGB1, and thus exhibits an anti-diabetic effect in type 1 diabetes. Shang et al. examined the role of another alarmin, IL-33, in an animal model of human gout, MSU-induced inflammation. A review by Tu and Yang summarizes the potential mechanisms of IL-33/ST2 axis in the metabolic disorders.

Hormones have regulatory effects on immunologic processes. In this special issue, a research by Porchas-Quijada et al. evaluated the relationship of anti-ghrelin autoantibodies with clinical, body-composition, and metabolic parameters in RA patients. Their findings support the previously reported functions of these natural autoantibodies as carriers and modulators of the stability and physiological function of natural hormones Porchas-Quijada et al.. In addition, a mini review by

Edited and reviewed by:
Cunming Duan,
University of Michigan, United States

***Correspondence:**
Jixin Zhong
zhongjixin620@163.com

Specialty section:
This article was submitted to Experimental Endocrinology, a section of the journal Frontiers in Endocrinology

Received: *03 July 2020*
Accepted: *20 July 2020*
Published: *24 September 2020*

Citation:
Chen J, Kong W and Zhong J (2020) Editorial: Cross Talk Between the Immune System and Metabolism. Front. Endocrinol. 11:588. doi: 10.3389/fendo.2020.00588

Montesinos and Pellizas summarized the cellular and molecular mechanisms involved in thyroid hormones effects on innate immunity. In recent years, studies into the microbiomes have revealed their close relationship with human diseases (8). A study by Ning et al. investigated the alterations of urinary microbiome in gout patients, indicating the new prospects for microbiome in the diagnosis and treatment of gout.

Metabolic disorder can lead to serious complications. For instance, diabetic cardiomyopathy and encephalopathy are common severe complications of diabetes that cause mortality and morbidity in diabetic patients. Using mouse models of diabetes, Bhusal et al. investigated the role of LCN2 in the pathogenesis of diabetic encephalopathy, which help explain the pathogenic mechanisms that cause this complication. Ying et al. found that Phloretin prevented diabetic cardiomyopathy, possibly by suppressing the interaction between Nrf2 and Keap 1. Their work indicates a suppressive effect of Phloretin in high glucose-induced injury of cardiomyocytes. Intensive anti-diabetic therapy in diabetic patients may cause hypoglycemia, which has been found to be associated with an increased risk for adverse cardiovascular outcomes and all-cause mortality (9). In this special issue, Wei et al. investigated the association between hypoglycemia as assessed by continuous glucose monitoring and the major adverse cardiovascular events or all-cause mortality.

Collectively, the original research and review articles in this special issue cover a series of important aspects in the field of interaction between the immune system and metabolism, which may provide new insights into the diagnosis and treatment of metabolic diseases and their complications.

AUTHOR CONTRIBUTIONS

All authors listed have made a substantial, direct and intellectual contribution to the work, and approved it for publication.

FUNDING

This work was supported by grants from National Natural Science Foundation of China (81974254 and 81670431), Jiangxi Provincial Natural Science Foundation (20202ACBL206011), and Outstanding Innovation Team of Jiangxi Provincial People's Hospital (no. 19-008).

REFERENCES

1. Donath MY, Dalmas E, Sauter NS, Boni-Schnetzler M. Inflammation in obesity and diabetes: islet dysfunction and therapeutic opportunity. *Cell Metab.* (2013) 17:860–72. doi: 10.1016/j.cmet.2013.05.001
2. Chen Z, Bozec A, Ramming A, Schett G. Anti-inflammatory and immune-regulatory cytokines in rheumatoid arthritis. *Nat Rev Rheumatol.* (2019) 15:9–17. doi: 10.1038/s41584-018-0109-2
3. Pucino V, Certo M, Varricchi G, Marone G, Ursini F, Rossi FW, et al. Metabolic checkpoints in rheumatoid arthritis. *Front Physiol.* (2020) 11: 347. doi: 10.3389/fphys.2020.00347
4. So AK, Martinon F. Inflammation in gout: mechanisms and therapeutic targets. *Nat Rev Rheumatol.* (2017) 13 639–47. doi: 10.1038/nrrheum.2017.155
5. Palmer DB, The effect of age on thymic function. *Front Immunol.* (2013) 4:316. doi: 10.3389/fimmu.2013.00316
6. Watroba M, Dudek I, Skoda M, Stangret A, Rzodkiewicz P, Szukiewicz D. Sirtuins, epigenetics and longevity. *Ageing Res Rev.* (2017) 40:11–9. doi: 10.1016/j.arr.2017.08.001
7. Yang Han Z, Oppenheim JJ. Alarmins and immunity. *Immunol Rev.* (2017) 280:41–56. doi: 10.1111/imr.12577
8. Young VB, The role of the microbiome in human health and disease: an introduction for clinicians. *BMJ.* (2017) 356:j831. doi: 10.1136/bmj.j831
9. Group AS, Gerstein HC, Miller ME, Genuth S, Ismail-Beigi F, Buse JB, et al. Long-term effects of intensive glucose lowering on cardiovascular outcomes. *N Engl J Med.* (2011) 364:818–28. doi: 10.1056/NEJMoa1006524

Conflict of Interest: The authors declare that the research was conducted in the absence of any commercial or financial relationships that could be construed as a potential conflict of interest.

frontiers in Endocrinology

ORIGINAL RESEARCH
published: 25 October 2018
doi: 10.3389/fendo.2018.00630

Sodium Butyrate Ameliorates Streptozotocin-Induced Type 1 Diabetes in Mice by Inhibiting the HMGB1 Expression

Yu Guo[1†], Zheng Xiao[1†], Yanan Wang[1], Weihua Yao[1], Shun Liao[1], Bo Yu[1], Jianqiang Zhang[1], Yanxiang Zhang[1,2], Bing Zheng[1,2], Boxu Ren[1,2*] and Quan Gong[1,2*]*

[1] Department of Immunology, School of Medicine, Yangtze University, Jingzhou, China, [2] Clinical Molecular Immunology Center, School of Medicine, Yangtze University, Jingzhou, China

OPEN ACCESS

Edited by:
Jie Chen,
Xiamen University, China

Reviewed by:
Hsien-Hui Chung,
National Cheng Kung University, Taiwan
Sonia Liao,
University of Electronic Science and Technology of China, China

***Correspondence:**
Bing Zheng
hxzheng@yangtzeu.edu.cn
Boxu Ren
boxuren188@163.com
Quan Gong
gongquan1998@163.com

[†]These authors have contributed equally to this work

Specialty section:
This article was submitted to Experimental Endocrinology, a section of the journal Frontiers in Endocrinology

Received: 04 August 2018
Accepted: 04 October 2018
Published: 25 October 2018

Citation:
Guo Y, Xiao Z, Wang Y, Yao W, Liao S, Yu B, Zhang J, Zhang Y, Zheng B, Ren B and Gong Q (2018) Sodium Butyrate Ameliorates Streptozotocin-Induced Type 1 Diabetes in Mice by Inhibiting the HMGB1 Expression. Front. Endocrinol. 9:630. doi: 10.3389/fendo.2018.00630

Type 1 diabetes (T1D) is an autoimmune disease characterized by the immune cell-mediated progressive destruction of pancreatic β-cells. High-mobility group box 1 protein (HMGB1) has been recognized as a potential immune mediator to enhance the development of T1D. So we speculated that HMGB1 inhibitors could have anti-diabetic effect. Sodium butyrate is a short fatty acid derivative possessing anti-inflammatory activity by inhibiting HMGB1. In the current study, we evaluated the effects of sodium butyrate in streptozotocin (STZ)-induced T1D mice model. Diabetes was induced by multiple low-dose injections of STZ (40 mg/kg/day for 5 consecutive days), and then sodium butyrate (500 mg/kg/day) was administered by intraperitoneal injection for 7 consecutive days after STZ treatment. Blood glucose, incidence of diabetes, body weight, pancreatic histopathology, the amounts of $CD4^+$T cell subsets, IL-1β level in serum and pancreatic expressions levels of HMGB1, and NF-κB p65 protein were analyzed. The results showed that sodium butyrate treatment decreased blood glucose and serum IL-1β, improved the islet morphology and decreased inflammatory cell infiltration, restored the unbalanced Th1/Th2 ratio, and down-regulated Th17 to normal level. In addition, sodium butyrate treatment can inhibit the pancreatic HMGB1 and NF-κB p65 protein expression. Therefore, we proposed that sodium butyrate should ameliorate STZ-induced T1D by down-regulating NF-κB mediated inflammatory signal pathway through inhibiting HMGB1.

Keywords: sodium butyrate, HMGB1, Th1/Th2, type 1 diabetes, streptozotocin

INTRODUCTION

Diabetes, as a non-communicable disease, has become the major cause of mortality and disease burden in the world. In recent decades, the incidence of diabetes has increased continuously that the estimated morbidity of diabetes in China was 10.9% in 2013 according to the latest published national survey (1). Type 1 diabetes (T1D) is characterized by the chronic hyperglycemia resulting from an immunologic disorder in which the autoreactive immune cells attack insulin-producing pancreatic β-cells (2). T1D is also known as juvenile-onset diabetes because it usually occurs in children and young adults (3). So far, the most suitable treatment for T1D is still insulin.

However, the usage of insulin is restricted because of the inevitable chronical cardiovascular complications caused by unmanageable blood glucose and destruction of β-cells (4). Recently, alloislet transplantation has been becoming an appealing method for T1D treatment is, but therapeutic approaches are limited due to deficiency of donor (5). In recent onset of T1D, the insulitis is usually present that is characterized by immune cell inflammatory infiltration within pancreatic islets (6, 7), the process is thought to be important for autoimmune diabetes progression (8). Consequently, it is reasonable to prevent or treat T1D with some anti-inflammatory agents.

High-mobility group box 1 protein (HMGB1), a highly conserved chromosomal protein, can be passively released from damaged cells or secreted from immune cells. It was recognized as an innate signal to mediate the autoimmune initiation and progression of the systemic lupus erythematosus and rheumatoid arthritis (9, 10). HMGB1 was also recognized to be involved in the development of both type 1 and 2 diabetes (11–13). In the type 1 diabetes model, streptozotocin (STZ) is a widely used diabetogenic agent (14), Previous studies have shown that HMGB1 is activated and the expression is increased in STZ-induced diabetic mice (15, 16). In addition, Extracellular HMGB1 was also discovered as proinflammatory cytokine (17, 18). Comparing with early-acting role of TNF-α and IL-1, HMGB1 was identified as a late-acting cytokine to influence the progression of sepsis (19), so we speculated that anti-HMGB1 therapeutics would become an effective approach to treat inflammation-related autoimmune disease. For example, administration of anti-HMGB1 antibody reduced the diabetes incidence and delayed the onset of diabetes in NOD mice (11). Sodium butyrate, a short fatty acid derivative, is present in human diet such as butter and cheese and it is also notably produced in the large intestine through fermentation of dietary fiber (20). It can act as a direct HMGB1 antagonist, and showed the effects to attenuate myocardial ischemia/reperfusion injury (21), to protect against acute lung injury (ALI) induced by severe burn (22), and to reduce pancreas injury in severe acute pancreatitis (23), through modulating the expression of HMGB1.

Given the role of HMGB1 in T1D initiation and progression (11, 15, 16). And sodium butyrate, as a specific HMGB1 antagonist, has shown anti-inflammatory effect in various animal models, so whether sodium butyrate have some protective effect on the T1D development through inhibiting the HMGB1? In current study, we reported the potential beneficial effects of sodium butyrate in STZ-induced type 1 diabetes mouse model and its underlying molecular mechanisms.

MATERIALS AND METHODS

Animals

Male BALB/c mice (6–8 weeks, 25 ± 2 g) were purchased from Wuhan Centers for Disease Prevention & Control and the mice were bred and maintained in a pathogen-free facility, where kept the room temperature about 25°C, humidity about 50%, a standard 12 h dark/light cycles. The studies were in accordance with protocols approved by the Institutional Animal Care and Use Committee (IACUC) at the Yangtze University. The diabetes was induced by treating the male BALB/c mice multiple low doses of STZ (Sigma-Aldrich, Shanghai, China). Namely, the mice were received intraperitoneal injection of STZ at a dose of 40 mg/kg/day (dissolved in 0.1 mol/L citrate buffer, pH 4.5) for 5 consecutive days. Non-diabetic mice were received with an equal volume of vehicle. To observe the diabetic status of the mice, the non-fasting glucose from tail blood sampling were monitored by a glucose meter (OneTouch, LifeScan). Diabetes onset were diagnosed when blood glucose level >16.7 mmol (300 mg/dl) on 2 consecutive tests (24).

Drug Treatment

Sodium butyrate (Sigma-Aldrich, Shanghai, China) were dissolved in 0.9% sodium chloride solution and administered by intraperitoneal injection of 500 mg/kg/day at day 6 after STZ injection, the treatment were followed for 7 consecutive days.

Serum Collection

The mice were sacrificed at the end of experiment, after anesthetized with diethyl ether, the blood were collected using retro-orbital venous plexus puncture and then stayed at room temperature for 30 min, separated the serum through centrifugation at 12,000× g for 15 min at 4°C. The sera were kept at −70°C for ELISA.

ELISA for Cytokine Assay

The amount of IL-1β in serum was determined using a commercial kit (MultiSciences, Hangzhou, China) according to the manufacturers' instructions.

Histological and Morphological Analyses

The mice pancreases were removed and fixed in 4% formaldehyde at room temperature for 24 h, then the fixed tissues were infiltrated with paraffin, three series of 4 μm thick sections were prepared and subsequently subjected to standard hematoxylin and eosin staining to assess the pancreatic histopathologic changes.

Flow Cytometry Analysis of $CD4^+$T Cell Subsets

$CD4^+$T cell subsets from the spleen and pancreatic lymph nodes (PLNs) were determined by flow cytometry. Briefly, the lymphocyte were isolated from fresh spleen and PLNs by mechanical dissociation, then centrifuged and adjusted the supernatant cell number to 2×10^6, erythrocytes were lysed using red cell lysis buffer (Tiangen, Beijing, China), washed twice with RPMI-1640 (containing 10% FBS), added 0.5 μl PMA and BFA (MultiSciences, Hangzhou, China) and incubated for 5 h, followed by incubation with PE-labeled IL-4, PE-labeled IL-17A, FITC-labeled CD4, and APC-labeled IFN-γ (BD Pharmingen, Shanghai, China) at 4°C for 30 min. The cells were then subjected to flow cytometry analysis.

Western Blot Analysis

Pancreas tissues were homogenized in the RIPA lysis buffer (MultiSciences, Hangzhou, China) containing various inhibitors. The lysates were separated by 10% SDS-PAGE and then electrotransferred onto polyvinylidene difluoride (PVDF)

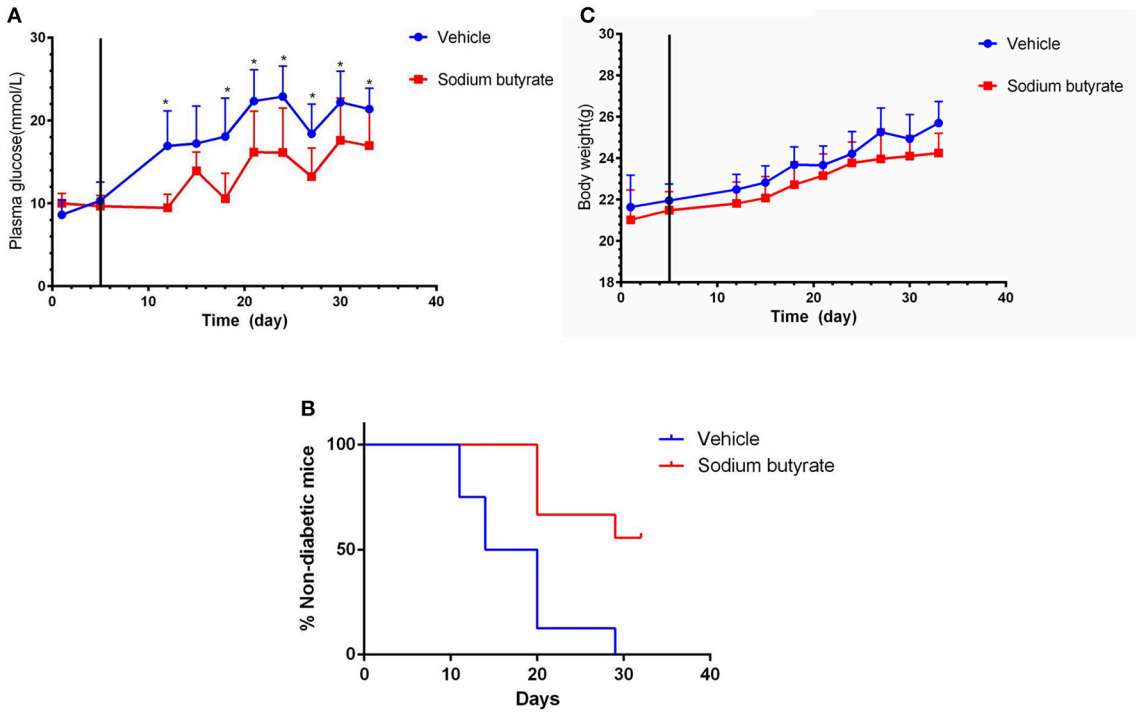

FIGURE 1 | Sodium butyrate treatment decreases blood glucose level and delays the onset of diabetes. Male BALB/c mice received STZ treatment by i.p. route at a dose of 40 mg/kg/day for 5 consecutive days. Sodium butyrate (dose of 500 mg/kg/day, $n = 9$) or vehicle treatment ($n = 8$) from day 6 (solid line labeled) for 7 consecutive days after the last STZ injection. **(A)** STZ induced diabetic mice exhibited lower blood glucose when receiving sodium butyrate treatment compared with vehicle from day 11 (*$p < 0.05$). **(B)** Treatment with sodium butyrate decreased diabetes incidence and delayed the onset of diabetes (*$p < 0.01$). **(C)** Sodium butyrate treatment had no effect on the body weight of the diabetic mice.

membranes. The membranes were incubated with primary antibody for the protein of interest or anti-β-Actin, the membranes were washed with Tris-buffered saline with Tween and incubated with HRP-conjugated secondary antibody. Immunoreactivity was detected using an enhanced chemiluminescence reagent (MultiSciences, Hangzhou, China).

Statistical Analysis

Results are shown as mean ± standard deviation (SD). Graphical presentation and statistical analyses were carried out with GraphPad Prism software. The Student's *t*-test were used for comparison of the mean for two groups (plasma glucose and body weight).The difference of diabetes onset between groups were determined using the log-rank (Mantel–Cox) test. Comparisons between groups for cytokine secretion, the amount of $CD4^+$T cell subsets and western blot were performed by one-way ANOVA. $P < 0.05$ was considered statistically significant.

RESULTS

Administration of Sodium Butyrate Decreases Plasma Glucose and Delays the Onset of Diabetes

To determine the effect of sodium butyrate on diabetes, the mice were intraperitoneal injected with 500 mg/kg sodium butyrate after the STZ injection. Vehicle-treated mice developed hyperglycaemia within 7 day after the last STZ injection, whereas the mice administrated with sodium butyrate exhibited lower non-fasting serum glucose levels compared with vehicle group (**Figure 1A**). Although sodium butyrate can't block the progression of diabetes, sodium butyrate treatment significantly postponed the development of diabetes (**Figure 1B**). The incidence of diabetes (non-fasting blood glucose level > 16.7 mmol) was first observed in vehicle group at day 12 compared with sodium butyrate group at day 21. In addition, we have also monitored the effect of sodium butyrate on the body weight and food intake of diabetic mice, but there was no significant difference between vehicle and sodium butyrate group (**Figure 1C** and **Supplementary Figure 1**).

Pancreatic Histopathologic Changes Are Improved by Sodium Butyrate

Histological examination of mice pancreases were performed to evaluate the effect of sodium butyrate on STZ-induced mice. As shown in **Figure 2**, the healthy mice had intact islet morphology. However, islet boundary became a little vague and cell number inside islet decreased in diabetic mice. Moreover, heavy inflammatory cell infiltration at one side was evident. Here, although sodium butyrate treatment could not prevent the inflammatory cells infiltration, morphology of islet was improved when compared with vehicle group.

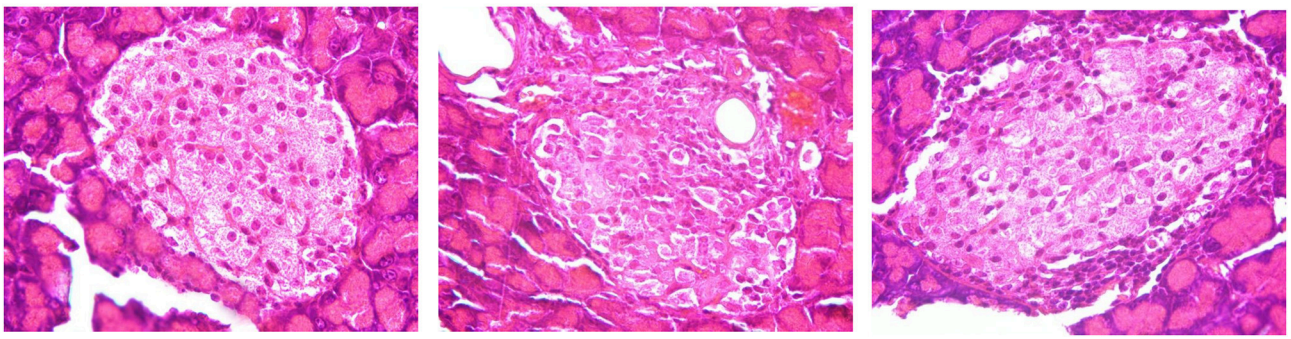

FIGURE 2 | Sodium butyrate treatment ameliorates the pancreatic histopathologic changes. Hematoxylin and eosin staining of pancreases from healthy mice, vehicle group, and sodium butyrate treated mice (H&E staining, magnification 1000×).

The Ratio of Th1/Th2 and Th17 Cells Are Regulated by Sodium Butyrate

It has been reported that the pathogenesis of some inflammatory diseases are associated with the imbalance of Th1/Th2 and Th17 cells (25–27). We determined whether the anti-diabetic effect of sodium butyrate are related with the changes of Th1/Th2 in the spleen and Th17 cells in PLNs. As shown in **Figure 3**, vehicle treated diabetic mice showed a higher percentage of Th1 and lower percentage of Th2 compared with non-diabetic mice. More importantly, the ratio of Th1/Th2 and Th17 cells in diabetic mice are higher than non-diabetic mice. Whereas, sodium butyrate regulated the increased ratio to a relative low level that was closed to health non-diabetic mice. These results demonstrated that sodium butyrate should exhibit the anti-diabetic effect through modulating the unbalanced Th1/Th2 and decreased Th17 cells to the normal level.

Proinflammatory Cytokine IL-1β Are Down-Regulated in Sodium Butyrate Treated Diabetic Mice

Considering the role of proinflammatory cytokines on the pathogenesis of diabetes, population with detectable levels of circulating IL-1β cytokines have increased risk to develop diabetes (28–30). We speculate that sodium butyrate could relieve diabetes reflected by decreased level of IL-1β. As expected, diabetic mice showed increased levels of IL-1β, but sodium butyrate treatment significant decreased the level (**Figure 4**). The data suggested that sodium butyrate could inhibit proinflammatory response of diabetes.

Sodium Butyrate Inhibits the Pancreatic HMGB1 and NF-κB p65 Protein Expression

Pancreatic HMGB1 and NF-κB p65 protein expression were analyzed by western blot. Results showed that both HMGB1 and NF-κB p65 protein expression were up-regulated in diabetic mice compared with healthy non-diabetic mice, in contrast, the protein expression was markedly down-regulated in the mice treated with sodium butyrate compared with diabetic mice (**Figure 5**).

DISCUSSION

Current strategies for T1D treatment include lifelong insulin delivery, maintaining normal glycemic level, eating healthy foods, and keeping to a healthy weight. As is known to us, people with diabetes have a higher risk to develop one or more complications, so it is important to control and maintain the blood glucose within the normal level.

HMGB1, a highly conserved non-histone nuclear protein, was proven to be involved in the pathogenesis of inflammatory and autoimmune disease (31), and it can serve as endogenous alarmin to alert the innate immune system to promote host defense or tissue repair. The role of HMGB1 in autoimmune disease was first confirmed in rheumatoid arthritis (RA) (32). Extranuclear HMGB1expression was increased in the synovia of patients and animal models with rheumatoid arthritis (RA), and blockade of HMGB1 expression in experimental animal models can attenuate the RA (32, 33). In addition, HMGB1 was also involved in pathogenesis of systemic lupus erythematosus (SLE), the patients with SLE show increased level of HMGB1 in the epidermis, and the increased plasma levels of HMGB1 correlated closely with disease activity (34). T1D is also an autoimmune disease characterized by destruction of the insulin secreting β-cells, previous study has shown that HMGB1 seems to be involved in T1D pathogenesis and it can act as a potent innate alarmin to mediate the initiation and progression during T1D development in NOD mice, a model of spontaneous T1D (11). When NOD mice were treated with HMGB1 neutralizing antibody, the insulitis progression was significantly inhibited and the diabetes incidence was also decreased (11). HMGB1 was also thought to be involved in the pathogenesis of type 2 diabetes (T2D) (35). It has been reported that serum HMGB1 level was increased in patients with T2D, and *in vitro* study showed that high glucose can activate HMGB1 expression in mesangial cells (35). A recent investigation about the effect of

A

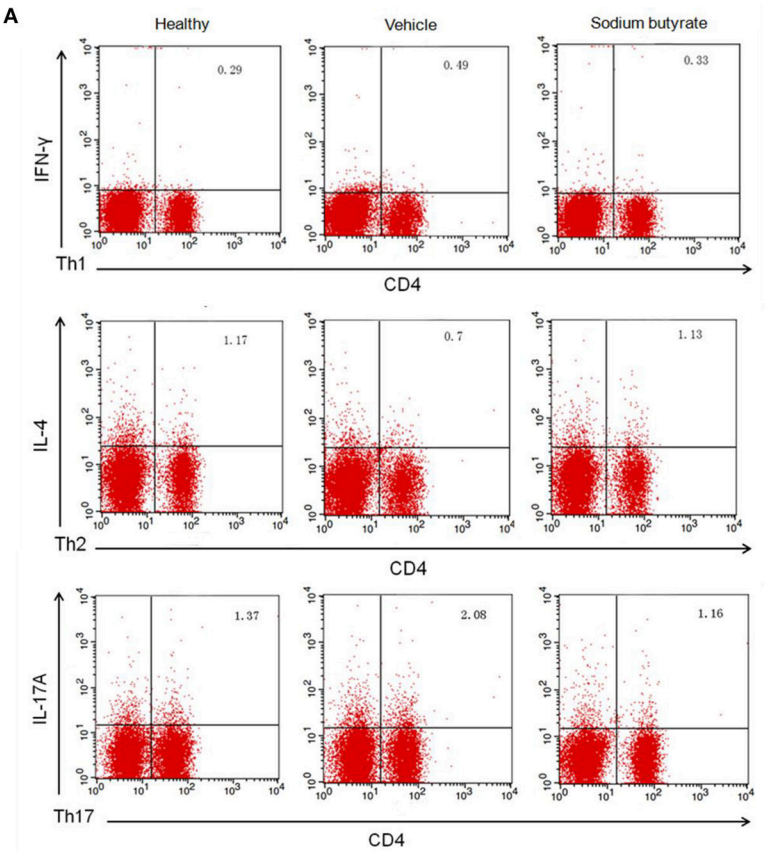

B

Group	Splenic Th1	Splenic Th2	Splenic Th1/ Th2	PLNs' Th17
Healthy	0.26±0.04	1.12±0.07	0.23±0.08	1.45±0.03
Vehicle	0.51±0.02*	0.74±0.07*	0.72±0.07**	1.88±0.10**
Sodium butyrate	0.30±0.08$^{\#}$	1.01±0.11	0.30±0.06$^{\#\#}$	1.12±0.05$^{\#\#}$

FIGURE 3 | Sodium butyrate treatment regulates $CD4^+$ T cell subsets **(A)**. Splenic and PLNs' lymphocyte originated from sodium butyrate treated mice ($n = 5$), vehicle group ($n = 5$) and healthy mice ($n = 3$) were harvested for CD4, IL-4, IFN-γ, and IL-17A staining. The percentages of Th1, Th2, and Th17 cells were determined by flow cytometric analysis **(B)**. The data are listed in the table as means ± SD of three independent experiment. The ratio of splenic Th1/Th2 and Th17 cell in PLNs was significantly higher than healthy mice, whereas sodium butyrate treatment restored unbalanced Th1/Th2 and regulated Th17 cells to normal level. $^*p < 0.05$, $^{**}p < 0.01$ vs. healthy group, $^{\#}p<0.05$, $^{\#\#}p<0.01$ vs. vehicle group.

HMGB1 on high concentration glucose induced mesothelial cells (MCs) injury also demonstrated that high glucose promoted HMGB1 translocation and secretion from the nucleus of MCs (36). Moreover, it has also been reported that high glucose can induce retinal pericytes, vascular smooth muscle cells and human aortic endothelial cells to secret HMGB1 (37–39). So it is undoubted that HMGB1 expression could be activated under high glucose induction.

Based on the potential role of HMGB1 in the pathogenesis of diabetes, It was presumed that HMGB1 inhibitors would probably affect the diabetes onset. Sodium butyrate is a well-known short fatty acid derivative and exhibits good anti-inflammatory property through inhibiting HMGB1 expression. It has been proven that sodium butyrate showed protective effect in myocardial ischemia/reperfusion, severe sepsis and ALI by inhibiting HMGB1 (21, 22, 40, 41). Sodium butyrate can also improve the performance of diabetic complications (42, 43). For example, sodium butyrate showed protective effect against diabetic nephropathy (DN) (42). In a high fat diet (HFD)-induced type II diabetic model, cardiac function and metabolic dysfunction were improved by sodium butyrate (43). In addition, sodium butyrate can prevent the insulin resistance in HFD-induced obese mice (44).

$CD4^+$ T helper (Th) cells are major T cell subsets that play a vital role in mediating immune responses. According to cytokine production and specialized functions, the Th cells

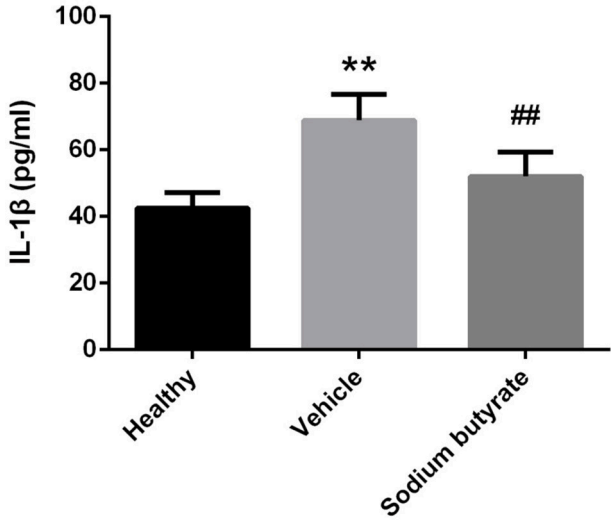

FIGURE 4 | Sodium butyrate down-regulates proinflammatory cytokine IL-1β expression in diabetic mice. Levels of serum cytokine IL-1β in sodium butyrate treatment ($n = 9$), vehicle group ($n = 8$) and healthy group ($n = 5$) mice were assessed by ELISA. The IL-1β level is increased in diabetic mice compared with normal, whereas sodium butyrate inhibit its expression. $^{**}p < 0.01$ vs. healthy group, $^{\#\#}p < 0.01$ vs. vehicle group.

can be classified into at least four distinct Th phenotypes (Th1, Th2, Th17, and T-regulatory cells). Th1 cells were responded for cellular immunity through secreting interferon (IFN)-γ (45), Th1 cells were thought to be involved in the insulin-producing β-cell destruction in the pancreatic islets (46). Whereas, Th2 cells were mainly involved in mediating humoral immunity and would actually protect against autoimmune disease (47). Induction of Th2 cells could lead to dominant protective effect against T1D development (48). Previous study had shown that Th1/Th2 imbalance could contribute to pathogenesis of some autoimmune diseases (26). Th17 cells, another subset of $CD4^+$T cells, can produce proinflammatory cytokine IL-17 and induce inflammation to mediate autoimmune pathology. Some evidence indicated that Th17 cell and its related cytokines had significant effects on the onset and progression of T1D in both human and animals (25, 27).

In this study, we evaluated the potential anti-diabetic effect of sodium butyrate in a STZ-induced T1D mice model. Multiple low dose injection of STZ led to pronounced pancreatic insulititis, followed by β-cell destruction and plasma glucose elevation (14), then the HMGB1 was passively released from damaged β-cell (11), and it acted as proinflammatory cytokine to enhance the inflammatory response. We found that sodium butyrate exhibited the protective effect on streptozotocin-induced type 1 diabetes in mice. Sodium butyrate treatment decreased the

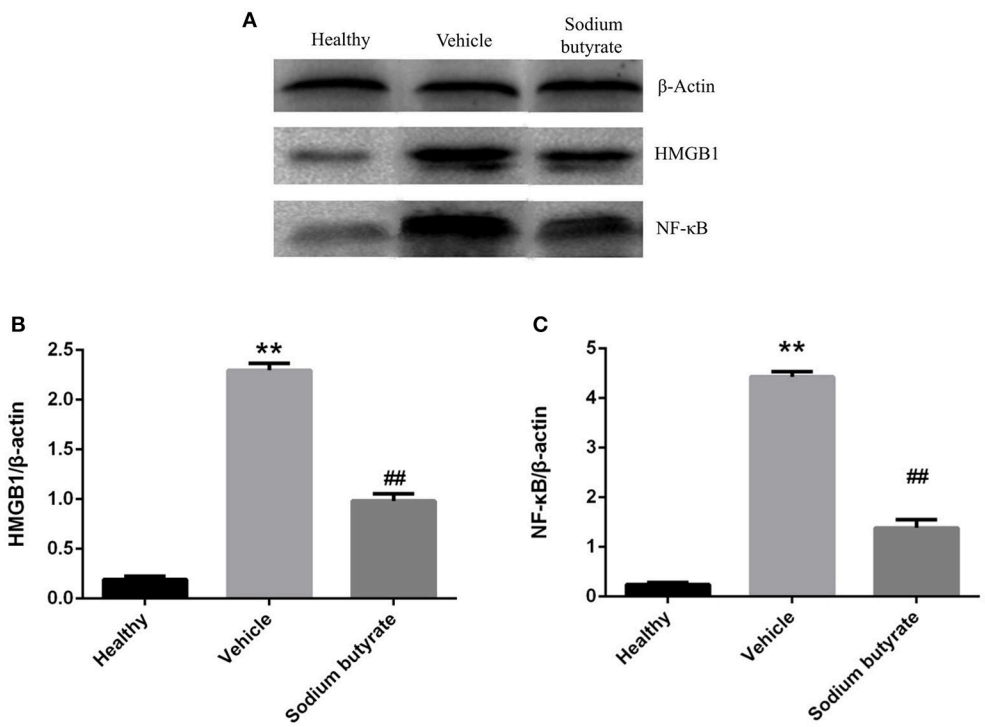

FIGURE 5 | Sodium butyrate inhibits the pancreatic HMGB1 and NF-κB p65 protein expression **(A)**. Western blot analysis of pancreatic HMGB1 and NF-κB p65 protein expression from sodium butyrate group ($n = 5$), vehicle group ($n = 5$), and healthy group mice ($n = 3$). Both HMGB1 and NF-κB p65 expression were increased in diabetic mice compared with healthy group, however, sodium butyrate down-regulated their expression **(B,C)**. Quantitative analysis of A results are representative of three independent experiments and data represent the mean ± SD. $^{**}p < 0.01$ vs. healthy group, $^{\#\#}p < 0.01$ vs. vehicle group.

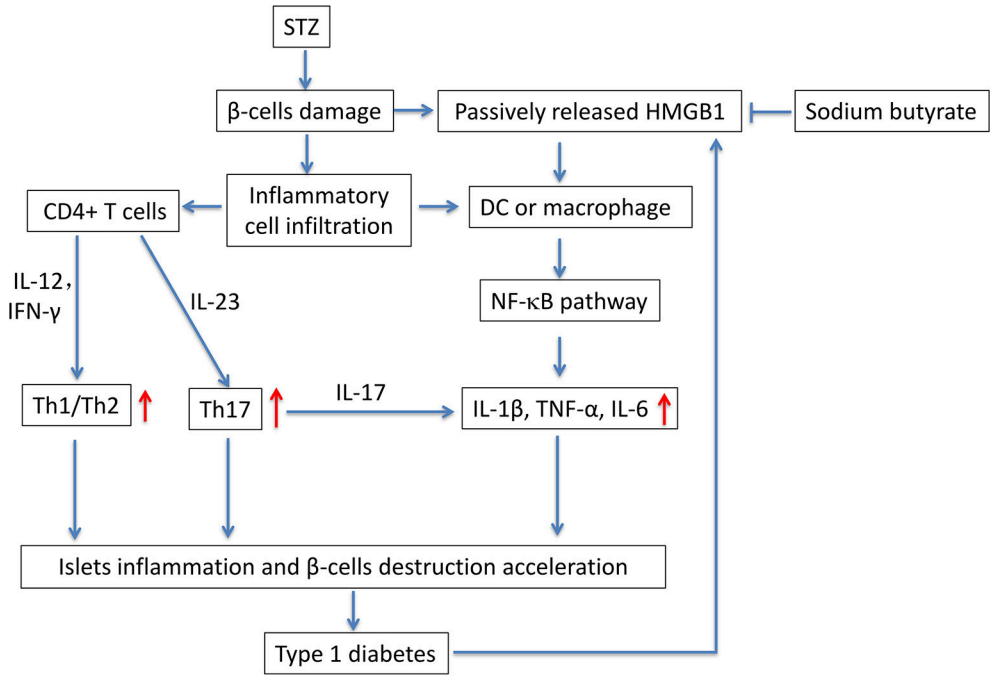

FIGURE 6 | The potential mechanism of sodium butyrate on STZ-induced type 1 diabetes. STZ, specifically destroys pancreatic β-cells. The damaged β-cells passively release HMGB1 (11). At the same time, the islets are infiltrated by inflammatory cells such as DCs, macrophages and T cells. Naïve $CD4^+$ T cells are differentiated into effector Th1 and/or Th17 cells based on their cytokine microenvironment. In addition, the released extracellular HMGB1 targets DCs or macrophage via the corresponding surface receptor(s), induces a signaling cascade and activates NF-κB pathway (12), therefore leading to the production of proinflammatory cytokines IL-1β, TNF-α, and IL-6 (49). the unbalanced Th1/Th2/Th17 and proinflammatory cytokines further accelerate the islets inflammation and β-cells destruction and lead to the onset of type 1 diabetes. Sodium butyrate, as a direct HMGB1 antagonist, could down-regulate the expression of HMGB1 and mediate the balance of Th1/Th2/Th17 paradigm, thus attenuating type 1 diabetes.

level of plasma glucose and delayed the onset of diabetes. In order to investigate the mechanism of beneficial effects of sodium butyrate for T1D, we first analyzed the phenotypes of $CD4^+$ T cells. The results showed that ratio of Th1/Th2 and Th17 were increased in diabetic mice, and sodium butyrate treatment significantly decreased the proportion of Th1/Th2 in spleen and Th17 from PLNs. As aforementioned, Th1 and Th17 cell are closely associated with onset and development of T1D. So it is not difficult to speculate that sodium butyrate could recover the balance of Th1/Th2 and inhibit theTh17 cell to the normal level. Th17 initiated the inflammation through stimulating the production of proinflammatory cytokines, IL-1β, IL-6, and TNF-α and in turn accelerated β-cell destruction (49). And our results demonstrated that sodium butyrate treatment did decrease the level of IL-1β in serum. To further address the underlying mechanism of sodium butyrate, we determined the NF-κB p65 expression. Because NF-κB is an important transcription factor that regulates the inflammatory gene expression. An *in vitro* study showed high glucose mimicking diabetes can lead to the activation of NF-κB and subsequent increased expression of inflammatory chemokines and cytokines (35, 50). In our study, NF-κB p65 expression was increased in diabetic mice, indicating NF-κB signaling pathway is involved in pathogenesis of the streptozotocin-induced type 1 diabetes model. Whereas treatment with sodium butyrate can inhibit the NF-κB p65 levels. Therefore, the main results can be summarized in **Figure 6**. Briefly, STZ directly targets and destroys pancreatic β-cells, then HMGB1 was passively released from damaged β-cells (11), and interacts with DCs or macrophage via the corresponding surface receptor(s), induces a signaling cascade and activates NF-κB pathway (12), therefore leading to the production of proinflammatory cytokines (such as IL-1β), the cytokines together with unbalanced Th1/Th2/Th17 accelerate the islets inflammation and β-cells destruction and finally develop into diabetes, high glucose would promote HMGB1 expression and further aggravate the diabetic condition through positive feedback effect of HMGB1 and high glucose. Whereas, sodium butyrate, as a direct HMGB1 antagonist, could down-regulate the expression of HMGB1 and mediate the balance of Th1/Th2/Th17 paradigm, thus attenuating type 1 diabetes.

Additionally, emerging evidences have implicated that gut bacterial composition may be associated with disease development and progression of T1D in both animal and human (51, 52). And a recently study has also suggested that short chain fatty acids (including sodium butyrate) treatment to rat breeders can ameliorates T1D in the offspring through reshaping the intestinal microbiota (53). So we speculate that sodium butyrate, to some extent, could restore the balance of intestinal flora to maintain metabolic homeostasis in the STZ-induced T1D mice. And we would perform experiments to observe the

effect of sodium butyrate on intestinal microbiota composition in the future, such as *Lactobacillus* and *Bifidobacterium* that are associated with the progression of T1D (54).

Altogether, our data suggest that sodium butyrate ameliorates STZ-induced type 1 diabetes. The beneficial effects could be attributed to the effects of sodium butyrate on restoring the unbalanced Th1/Th2/Th17 paradigm and inhibiting NF-κB-mediated inflammatory pathway. Therefore, sodium butyrate would become a beneficial dietary supplementation for T1D patients.

AUTHOR CONTRIBUTIONS

YG and ZX searched related literatures and made the mice model of STZ-induced T1D. WY was responsible for blood glucose monitoring. SL and BY performed the ELISA and western blot. YW and JZ performed the flow cytometry analysis and statistical analysis. YZ was responsible for histological and morphological analysis. QG and BR designed the experiment and supervised the project. BZ wrote the manuscript with contribution from all authors.

FUNDING

This work was supported by Natural Science Foundation of Hubei Province (2015CFA080).

ACKNOWLEDGMENTS

We gratefully thank Dr. Feng Qian for the critical reading of the manuscript.

SUPPLEMENTARY MATERIAL

The Supplementary Material for this article can be found online at: https://www.frontiersin.org/articles/10.3389/fendo.2018.00630/full#supplementary-material

REFERENCES

1. Wang L, Gao M, Zhang M, Huang Z, Zhang D, Deng Q, et al. Prevalence and ethnic pattern of diabetes and prediabetes in China in 2013. *JAMA* (2017) 317:2515–23. doi: 10.1001/jama.2017.7596
2. von Herrath M, Peakman M, Roep B. Progress in immune-based therapies for type 1 diabetes. *Clin Exp Immunol.* (2013) 172:186–202. doi: 10.1111/cei.12085
3. Patterson CC, Dahlquist GG, Gyurus E, Green A, Soltesz G. Incidence trends for childhood type 1 diabetes in Europe during 1989-2003 and predicted new cases 2005-20: a multicentre prospective registration study. *Lancet* (2009) 373:2027–33. doi: 10.1016/S0140-6736(09)60568-7
4. Davidson MH. Cardiovascular risk factors in a patient with diabetes mellitus and coronary artery disease: therapeutic approaches to improve outcomes: perspectives of a preventive cardiologist. *Am J Cardiol.* (2012) 110(Suppl. 9):43b—9b. doi: 10.1016/j.amjcard.2012.08.033
5. Robertson RP Islet transplantation a decade later and strategies for filling a half-full glass. *Diabetes* (2010) 59:1285–91. doi: 10.2337/db09-1846
6. Campbell-Thompson ML, Atkinson MA, Butler AE, Chapman NM, Frisk G, Gianani R, et al. The diagnosis of insulitis in human type 1 diabetes. *Diabetologia* (2013) 56:2541–3. doi: 10.1007/s00125-013-3043-5
7. Willcox A, Richardson SJ, Bone AJ, Foulis AK, Morgan NG. Analysis of islet inflammation in human type 1 diabetes. *Clin Exp Immunol.* (2009) 155:173–81. doi: 10.1111/j.1365-2249.2008.03860.x
8. Coppieters KT, Dotta F, Amirian N, Campbell PD, Kay TW, Atkinson MA, et al. Demonstration of islet-autoreactive CD8 T cells in insulitic lesions from recent onset and long-term type 1 diabetes patients. *J Exp Med.* (2012) 209:51–60. doi: 10.1084/jem.20111187
9. Pisetsky DS. The complex role of DNA, histones and HMGB1 in the pathogenesis of SLE. *Autoimmunity* (2014) 47:487–93. doi: 10.3109/08916934.2014.921811
10. Andersson U. Erlandsson-Harris H. HMGB1 is a potent trigger of arthritis. *J Internal Med.* (2004) 255:344–50. doi: 10.1111/j.1365-2796.2003.01303.x
11. Han J, Zhong J, Wei W, Wang Y, Huang Y, Yang P, et al. Extracellular high-mobility group box 1 acts as an innate immune mediator to enhance autoimmune progression and diabetes onset in NOD mice. *Diabetes* (2008) 57:2118–27. doi: 10.2337/db07-1499
12. Zhang S, Zhong J, Yang P, Gong F, Wang CY. HMGB1, an innate alarmin, in the pathogenesis of type 1 diabetes. *Int J Clin Exp Pathol.* (2009) 3:24–38.
13. Zhao D, Wang Y, Tang K, Xu Y. Increased serum HMGB1 related with HbA1c in coronary artery disease with type 2 diabetes mellitus. *Int J Cardiol.* (2013) 168:1559–60. doi: 10.1016/j.ijcard.2012.12.073
14. Like AA, Rossini AA. Streptozotocin-induced pancreatic insulitis: new model of diabetes mellitus. *Science* (1976) 193:415–7. doi: 10.1126/science.180605
15. Szasz T, Wenceslau CF, Burgess B, Nunes KP, Webb RC. Toll-Like receptor 4 activation contributes to diabetic bladder dysfunction in a murine model of type 1 diabetes. *Diabetes* (2016) 65:3754–64. doi: 10.2337/db16-0480
16. Zhang H, Zhang R, Chen J, Shi M, Li W, Zhang XC. High mobility group box1 inhibitor glycyrrhizic acid attenuates kidney injury in streptozotocin-induced diabetic rats. *Kidney Blood Pressure Res.* (2017) 42:894–904. doi: 10.1159/000485045
17. Chen G, Ward MF, Sama AE. Wang H. Extracellular HMGB1 as a proinflammatory cytokine. *J Interferon Cytokine Res.* (2004) 24:329–33. doi: 10.1089/107999004323142187
18. Erlandsson Harris H, Andersson U. Mini-review: the nuclear protein HMGB1 as a proinflammatory mediator. *Eur J Immunol.* (2004) 34:1503–12. doi: 10.1002/eji.200424916
19. Czura CJ, Tracey KJ. Targeting high mobility group box 1 as a late-acting mediator of inflammation. *Crit Care Med.* (2003) 31(Suppl. 1):S46–50. doi: 10.1097/00003246-200301001-00007
20. Li H, Gao Z, Zhang J, Ye X, Xu A, Ye J, et al. Sodium butyrate stimulates expression of fibroblast growth factor 21 in liver by inhibition of histone deacetylase 3. *Diabetes* (2012) 61:797–806. doi: 10.2337/db11-0846
21. Hu X, Zhang K, Xu C, Chen Z, Jiang H. Anti-inflammatory effect of sodium butyrate preconditioning during myocardial ischemia/reperfusion. *Exp Therapeut. Med.* (2014) 8:229–32. doi: 10.3892/etm.2014.1726
22. Liang X, Wang RS, Wang F, Liu S, Guo F, Sun L, et al. Sodium butyrate protects against severe burn-induced remote acute lung injury in rats. *PLoS ONE* (2013) 8:e68786. doi: 10.1371/journal.pone.0068786
23. Zhang T, Xia M, Zhan Q, Zhou Q, Lu G, An F. Sodium butyrate reduces organ injuries in mice with severe acute pancreatitis through inhibiting HMGB1 expression. *Digestive Dis Sci.* (2015) 60:1991–9. doi: 10.1007/s10620-015-3586-z
24. Castro CN, Barcala Tabarrozzi AE, Winnewisser J, Gimeno ML, Antunica Noguerol M, Liberman AC, et al. Curcumin ameliorates autoimmune diabetes. evidence in accelerated murine models of type 1 diabetes. *Clin Exp Immunol.* (2014) 177:149–60. doi: 10.1111/cei.12322
25. Martin-Orozco N, Chung Y, Chang SH, Wang YH, Dong C. Th17 cells promote pancreatic inflammation but only induce diabetes efficiently in lymphopenic hosts after conversion into Th1 cells. *Eur J Immunol.* (2009) 39:216–24. doi: 10.1002/eji.200838475

26. Lenschow DJ, Herold KC, Rhee L, Patel B, Koons A, Qin HY, et al. CD28/B7 regulation of Th1 and Th2 subsets in the development of autoimmune diabetes. *Immunity* (1996) 5:285–93. doi: 10.1016/S1074-7613(00)80323-4
27. Annunziato F, Cosmi L, Santarlasci V, Maggi L, Liotta F, Mazzinghi B, et al. Phenotypic and functional features of human Th17 cells. *J Exp Med.* (2007) 204:1849–61. doi: 10.1084/jem.20070663
28. Huang J, Yang Y, Hu R, Chen L. Anti-interleukin-1 therapy has mild hypoglycemic effect in type 2 diabetes. *Diab obes Metab.* (2017) 20:1024–8. doi: 10.1111/dom.13140
29. Spranger J, Kroke A, Mohlig M, Hoffmann K, Bergmann MM, Ristow M, et al. Inflammatory cytokines and the risk to develop type 2 diabetes: results of the prospective population-based European prospective investigation into cancer and nutrition (EPIC)-Potsdam Study. *Diabetes* (2003) 52:812–7. doi: 10.2337/diabetes.52.3.812
30. Cucak H, Hansen G, Vrang N, Skarsfeldt T, Steiness E, Jelsing J. The IL-1beta receptor antagonist SER140 postpones the onset of diabetes in female nonobese diabetic mice. *J Diab Res.* (2016) 2016:7484601. doi: 10.1155/2016/7484601
31. Harris HE, Andersson U, Pisetsky DS. HMGB1: A multifunctional alarmin driving autoimmune and inflammatory disease. *Nat Rev Rheumatol.* (2012) 8:195–202. doi: 10.1038/nrrheum.2011.222
32. Taniguchi N, Kawahara KI, Yone K, Hashiguchi T, Yamakuchi M, Goto M, et al. High mobility group box chromosomal protein 1 plays a role in the pathogenesis of rheumatoid arthritis as a novel cytokine. *Arthritis Rheumat.* (2003) 48:971–81. doi: 10.1002/art.10859
33. Kokkola R, Li J, Sundberg E, Aveberger AC, Palmblad K, Yang H, et al. Successful treatment of collagen-induced arthritis in mice and rats by targeting extracellular high mobility group box chromosomal protein 1 activity. *Arthrit Rheumat.* (2003) 48:2052–8. doi: 10.1002/art.11161
34. Jiang W, Pisetsky DS. Expression of high mobility group protein 1 in the sera of patients and mice with systemic lupus erythematosus. *Ann Rheumatic Dis.* (2008) 67:727–8. doi: 10.1136/ard.2007.074484
35. Chen Y, Qiao F, Zhao Y, Wang Y, Liu G. HMGB1 is activated in type 2 diabetes mellitus patients and in mesangial cells in response to high glucose. *Int J Clin Exp Pathol* (2015) 8:6683–91.
36. Chu YN, Wang Y, Zheng ZH, Lin YL, He R, Liu J, et al. Proinflammatory effect of high glucose concentrations on HMrSV5 cells via the autocrine effect of HMGB1. *Front Physiol.* (2017) 8:762. doi: 10.3389/fphys.2017.00762
37. Wang Y, Shan J, Yang W, Zheng H, Xue S. High Mobility Group Box 1 (HMGB1) mediates high-glucose-induced calcification in vascular smooth muscle cells of saphenous veins. *Inflammation* (2013) 36:1592–604. doi: 10.1007/s10753-013-9704-1
38. Kim JC, Kim S, Sohn E, Kim JS. Cytoplasmic translocation of high-mobility group box-1 protein is induced by diabetes and high glucose in retinal pericytes. *Mol Med Rep.* (2016) 14:3655–61. doi: 10.3892/mmr.2016.5702
39. Yao DC, Brownlee M. Hyperglycemia-induced reactive oxygen species increase expression of the receptor for advanced glycation end products (RAGE) and RAGE ligands. *Diabetes* (2010) 59:249–55. doi: 10.2337/db09-0801
40. Zhang LT, Yao MY, Lu QJ, Yan JX, Yu Y, Sheng YZ. Sodium butyrate prevents lethality of severe sepsis in rats. *Shock* (2007) 27:672–7. doi: 10.1097/SHK.0b013e31802e3f4c
41. Li N, Liu XX, Hong M, Huang XZ, Chen H, Xu JH, et al. Sodium butyrate alleviates LPS-induced acute lung injury in mice via inhibiting HMGB1 release. *Int Immunopharmacol.* (2018) 56:242–8. doi: 10.1016/j.intimp.2018.01.017
42. Dong WP, Jia Y, Liu XX, Zhang H, Li T, Huang WL, et al. Sodium butyrate activates NRF2 to ameliorate diabetic nephropathy possibly via inhibition of HDAC. *J Endocrinol.* (2017) 232:71–83. doi: 10.1530/JOE-16-0322
43. Zhang L, Du J, Yano N, Wang H, Zhao YT, Dubielecka PM, et al. Sodium butyrate protects -against high fat diet-induced cardiac dysfunction and metabolic disorders in type II diabetic mice. *J Cell Biochem.* (2017) 118:2395–408. doi: 10.1002/jcb.25902
44. Gao ZG, Yin J, Zhang J, Ward RE, Martin RJ, Lefevre M, et al. Butyrate improves insulin sensitivity and increases energy expenditure in mice. *Diabetes* (2009) 58:1509–17. doi: 10.2337/db08-1637
45. Mosmann TR, Cherwinski H, Bond MW, Giedlin MA, Coffman RL. Two types of murine helper T cell clone. I. definition according to profiles of lymphokine activities and secreted proteins. *J Immunol.* (1986) 136:2348–57.
46. Katz JD, Benoist C, Mathis D. T helper cell subsets in insulin-dependent diabetes. *Science* (1995) 268:1185–8. doi: 10.1126/science.7761837
47. Hedegaard CJ, Krakauer M, Bendtzen K, Lund H, Sellebjerg F, Nielsen CH. T helper cell type 1 (Th1), Th2 and Th17 responses to myelin basic protein and disease activity in multiple sclerosis. *Immunology* (2008) 125:161–9. doi: 10.1111/j.1365-2567.2008.02837.x
48. Suarez-Pinzon WL, Rabinovitch A. Approaches to type 1 diabetes prevention by intervention in cytokine immunoregulatory circuits. *Int J Exp Diab Res.* (2001) 2:3–17. doi: 10.1155/EDR.2001.3
49. Abdel-Moneim A, Bakery HH, Allam G. The potential pathogenic role of IL-17/Th17 cells in both type 1 and type 2 diabetes mellitus. *Biomed Pharmacother.* (2018) 101:287–92. doi: 10.1016/j.biopha.2018.02.103
50. Miao F, Gonzalo IG, Lanting L, Natarajan R. *In vivo* chromatin remodeling events leading to inflammatory gene transcription under diabetic conditions. *J Biol Chem.* (2004) 279:18091–7. doi: 10.1074/jbc.M311786200
51. Markle JGM, Frank DN, Mortin-Toth S, Robertson CE, Feazel LM, Rolle-Kampczyk U, et al. Sex differences in the gut microbiome drive hormone-dependent regulation of autoimmunity. *Science* (2013) 339:1084–8. doi: 10.1126/science.1233521
52. Alkanani AK, Hara N, Gottlieb PA, Ir D, Robertson CE, Wagner BD, et al. Alterations in intestinal microbiota correlate with susceptibility to type 1 diabetes. *Diabetes* (2015) 64:3510–20. doi: 10.2337/db14-1847
53. Needell JC, Ir D, Robertson CE, Kroehl ME, Frank DN, Zipris D. Maternal treatment with short-chain fatty acids modulates the intestinal microbiota and immunity and ameliorates type 1 diabetes in the offspring. *PLoS ONE* (2017) 12:e0183786. doi: 10.1371/journal.pone.0183786
54. Patterson E, Marques TM, O'Sullivan O, Fitzgerald P, Fitzgerald GF, Cotter PD, et al. Streptozotocin-induced type-1-diabetes disease onset in Sprague-Dawley rats is associated with an altered intestinal microbiota composition and decreased diversity. *Microbiology-Sgm* (2015) 161:182–93. doi: 10.1099/mic.0.082610-0

Conflict of Interest Statement: The authors declare that the research was conducted in the absence of any commercial or financial relationships that could be construed as a potential conflict of interest.

frontiers in Endocrinology

ORIGINAL RESEARCH
published: 20 December 2018
doi: 10.3389/fendo.2018.00774

Phloretin Prevents Diabetic Cardiomyopathy by Dissociating Keap1/Nrf2 Complex and Inhibiting Oxidative Stress

Yin Ying[1†], *Jiye Jin*[2†], *Li Ye*[3], *Pingping Sun*[1], *Hui Wang*[1] *and Xiaodong Wang*[4*]

[1] Department of Pharmacy, Tongde Hospital of Zhejiang Province, Hangzhou, China, [2] Department of Rehabilitation, Tongde Hospital of Zhejiang Province, Hangzhou, China, [3] Department of Nursing, Tongde Hospital of Zhejiang Province, Hangzhou, China, [4] Department of Vascular Surgery, Tongde Hospital of Zhejiang Province, Hangzhou, China

Hyperglycemia induces chronic inflammation and oxidative stress in cardiomyocyte, which are the main pathological changes of diabetic cardiomyopathy (DCM). Treatment aimed at these processes may be beneficial in DCM. Phloretin (PHL), a promising natural product, has many pharmacological activities, such as anti-inflammatory, anticancer, and anti-oxidative function. The aim of this study was to investigate whether PHL could ameliorate the high glucose-mediated oxidation, hypertrophy, and fibrosis in H9c2 cells and attenuate the inflammation- and oxidation-mediated cardiac injury. In this study, PHL induced significantly inhibitory effect on the expression of pro-inflammatory, hypertrophy, pro-oxidant, and fibrosis cytokines in high glucose-stimulated cardiac H9c2 cells. Furthermore, PHL decreased the levels of serum lactate dehydrogenase, aspartate aminotransferase, and creatine kinase-MB, and attenuated the progress in the fibrosis, oxidative stress, and pathological parameters via Kelch-like ECH-associated protein 1 (Keap1)/nuclear factor E2-related factor 2 (Nrf2) pathway in diabetic mice. In additional, molecular modeling and immunoblotting results confirmed that PHL might obstruct the interaction between Nrf2 and Keap1 through direct binding Keap1, and promoting Nrf2 expression. These results provided evidence that PHL could suppress high glucose-induced cardiomyocyte oxidation and fibrosis injury, and that targeting Keap1/Nrf2 may provide a novel therapeutic strategy for human DCM in the future.

Keywords: phloretin, Nrf2, Keap1, diabetic cardiomyopathy, oxidative stress

OPEN ACCESS

Edited by:
Jie Chen,
Xiamen University, China

Reviewed by:
Xiaoqiang Tang,
Sichuan University, China
Hsien-Hui Chung,
National Cheng Kung University, Taiwan

***Correspondence:**
Xiaodong Wang
wangxiaodong155@gmail.com

[†]These authors have contributed equally to this work

Specialty section:
This article was submitted to Experimental Endocrinology, a section of the journal Frontiers in Endocrinology

Received: *04 October 2018*
Accepted: *10 December 2018*
Published: *20 December 2018*

Citation:
Ying Y, Jin J, Ye L, Sun P, Wang H and Wang X (2018) Phloretin Prevents Diabetic Cardiomyopathy by Dissociating Keap1/Nrf2 Complex and Inhibiting Oxidative Stress. Front. Endocrinol. 9:774. doi: 10.3389/fendo.2018.00774

INTRODUCTION

Diabetes mellitus (DM) is an emerging global health problem. Diabetic cardiomyopathy (DCM) is the one of the major complications of diabetes that causes mortality and morbidity in diabetic patients (1). DCM starts with diastolic dysfunction in patients with type-1 (T1DM) or type-2 (T2DM). Previous studies showed that DCM presented with structural and functional abnormalities of the myocardium, leading to increased risks for myocardial fibrosis, ventricular hypertrophy, and heart failure (2, 3). There are several physiological mechanisms related to the pathogenesis for DCM, including insulin resistance signaling, cardiac inflammation, oxidative stress, endoplasmic reticulum stress, etc. (4). Increasingly, evidence demonstrated that oxidative stress may be the most common feature linking diabetes-induced alterations to the development of cardiac dysfunction.

The Keap1/Nrf2 pathway is the most crucial anti-oxidative mechanism that protects cells from oxidative stress (5). Nrf2 is a master regulator of redox status and cellular detoxification responses by inducing the expression of multiple downstream anti-oxidant genes, including heme oxygenase (HO-1), nicotinamide adenine dinucleotide phosphate-H (NADPH), quininoxidoreductase-1 (NQO-1), and glutamate-cysteine ligase catalytic (GCLC) (6). Recently, it was reported that Nrf2 prevented T2DM-induced cardiac injury (7). Furthermore, another study indicated that fibroblast growth factor-21 (FGF21) prevented diabetic cardiomyopathy via AMPK-AKT2-Nrf2 mediated anti-oxidation and lipid-lowering effects in the heart (8). Therefore, controlling cytoprotective oxidative stress response enzymes in DCM via Keap1/Nrf2 pathway targeting is a potential important strategy.

Phloretin (PHL, **Figure 1A**) is a dihydrochalcone flavonoid found in peel and root skin of frequently consumed vegetables and fruits. PHL showed numerous biological and pharmacological activities, such as anti-inflammatory, antioxidant, and anti-cancer in various disease models (9–12). Previously, our group found that PHL significantly inhibited tert-Butyl hydroperoxide (TBHP) induced oxidation. However, the potential of PHL for the treatment of DCM and the molecular mechanisms underlying the actions of PHL remain unclear. In this study, we evaluated the protective effect of PHL in hyperglycemia-induced oxidative stress and cardiac injury *in vitro* and *in vivo*. Subsequently, molecular modeling and immunoblotting were used to explore the underlying mechanisms and possible targets of PHL. Our results revealed that PHL could prevent cardiac injury in T1DM by attenuating hyperglycemia-induced oxidative stress and hypertrophy. We identified Keap1, a negative regulator of Nrf2, as the possible target for PHL. Overall, our study provided crucial evidence that PHL may be a novel therapeutic agent for the treatment of DCM.

MATERIALS AND METHODS

Reagents, Cell Culture and Treatment

Phloretin (purity 98%, verified by high-performance liquid chromatography; molecular weight = 274.27) was purchased from Aladdin (Shanghai, China). Phloretin was dissolved in DMSO for *in vitro* experiments and in CMC-Na (0.5%) for *in vivo* experiments, both stored at 4°C for further use. H9c2 embryonic rat heart-derived cell line was purchased from the Shanghai Institute of Biochemistry and Cell Biology (Shanghai, China) and cultured in DMEM medium (Gibco, Eggenstein, Germany) including 5.5 mmol/l of D-glucose supplemented with 10% FBS, 100 U/ml of penicillin, and 100 mg/ml of streptomycin. For the high glucose-treated group (HG), cells were incubated with a DMEM medium, which was contained 33 mmol/L of glucose. Glucose and streptozotocin (STZ) were obtained from Sigma-Aldrich (St. Louis, MO). Haematoxylin-eosin (H&E) was purchased from Beyotime (Nantong, China). Masson's trichrome kits was obtained in Solarbio (Beijing, China).

Antibodies for Nrf2 (#12721), TGF-β (#3711), Keap1 (#8047), GAPDH (#5174), and secondary antibodies (mouse #7076, rat #7077) were obtained from Cell Signaling Technology (Danvers, USA). RIPA lysis buffer was purchased from Boster Biological technology (Wuhan, China).

Animals and Treatment

Male C57BL/6 mice weighing 20–22 g were obtained from Zhejiang Animal Center (Hangzhou, China). The mice were housed at a constant room temperature with a 12:12 h light-dark cycle and fed with a standard rodent diet and water. All animal experimental procedures complied with the "The Detailed Rules and Regulations of Medical Animal Experiments Administration and Implementation" (Document No. 1998–55, Ministry of Public Health, PR China), and were approved by the Tongde Hospital of Zhejiang Province Animal Policy and Welfare Committee (Approval Document No. SCXK2014-0001).

Eighteen mice were randomly divided into three groups. Twelve mice were received intraperitoneal (i.p.) injection of STZ at the dose of 100 mg/kg formulated in 100 mM citrate buffer (pH 4.5) for 1 time, blood glucose levels were detected using a glucometer, control animals received buffered saline only. Six mice treated with phloretin at 10 mg/kg through i.g. after injection STZ 8 days. At Day 56 after STZ induction, the mice were killed under anesthesia, and then blood samples were collected. At the time of death, the heart tissues were removed.

Determination of Serum Aspartate Aminotransferase (AST), Lactate Dehydrogenase (LDH) and Creatine Kinase (CK-MB), Malondialdehyde (MDA), and Superoxide Dismutase (SOD)

Serum levels of AST, LDH, and CK-MB and supernatant levels of MDA and SOD were analyzed by commercial ELISA kits refer to the manufacturers' instruction (Nanjing Jiancheng Bioengineering Institute, Nanjing, China).

Heart Histopathology

Heart tissue was fixed in 10% formalin for 24 h, embedded in paraffin, and sectioned at 5 μm. Then, the heart sections were deparaffinized, rehydrated, and stained with hematoxylin and eosin (H&E). Cardiac fibrosis was tested by Masson's trichrome staining for collagen deposition as described previously. To estimate the extent of damage, the specimen was observed under a light microscope (Nikon, Japan).

Cell Cytotoxicity

Before PHL treatment, seeding cells into 96-well plates with 5,000 cells/well. Adding PHL into wells with various doses and incubated for 24 h. After treatment, MTT was added to each well (1 mg/ml), incubated at 37°C for 4 h. The formazan crystal was dissolved with DMSO, 150 μL/well. The absorbance was detected at 490 nm on a microplate reader. Cell cytotoxicity was expressed as the percentage of MTT reduction compared to control.

Rhodamine Phalloidine Staining

For hypertrophy, cells were fixed with 4% paraformaldehyde, permeabilized with 0.1% Triton X-100, and stained with rhodamine phalloidin at a concentration of 50 μg/mL for 30 min. Nuclei were stained with the DAPI at room temperature for

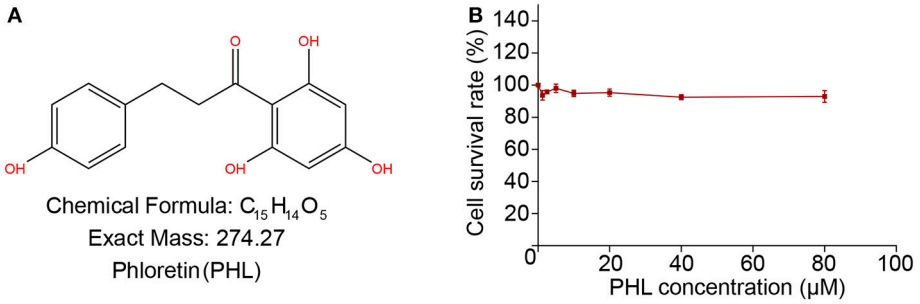

FIGURE 1 | The chemical structure of Phloretin **(A)**. MTT assay tests the effect of PHL on H9c2 survival rate after 24 h treatment **(B)**.

5 min. Immunofluorescence was viewed and captured using Nikon fluorescence microscope (Nikon, Japan).

RNA Isolation and Real-Time PCR (q-PCR)

Total RNA was extracted from the heart tissues and cells by using Trizol reagent (Invitrogen, Carlsbad, CA) according to each manufacturer's protocol. Both reverse transcription and quantitative PCR were carried out using a two-step M-MLV Platinum SYBR Green qPCR SuperMix-UDG kit (Invitrogen, Carlsbad, CA). Eppendorf Mastercycler ep realplex detection system (Eppendorf, Hamburg, Germany) was applied to q-PCR analysis. The primers of genes including NQO-1, HO-1, Nrf2, GCLC, CTGF, collagen-1, TGF-β, ANP, BNP, β-MyHC, and β-actin were obtained from Invitrogen (Shanghai, China). The primer sequences were listed in **Table S1**. Comparative cycle time (Ct) was used to determine fold differences between samples and normalized to β-actin.

Western Blot Analysis

Heart tissues and harvested cell pellets were homogenized in RIPA lysis buffer (Santa Cruz Biotechnology, Santa Cruz, CA) to obtain total protein or nuclear protein extracted using a nuclei isolation kit (NUC201, Sigma-Aldrich). Western blot assay was performed for target protein quantification, as described previously. The proteins were separated by 10% sodium dodecyl sulfate (SDS)-polyacrylamide gel electrophoresis (PAGE) and transferred to a nitrocellulose membrane. Membranes were blocked with 5% non-fat milk for 1 h and incubated overnight at 4°C with the specific antibodies over-night in 4°C. Immunoreactive bands were detected by incubating with secondary antibody conjugated with horseradish peroxidase and visualizing using enhanced chemiluminescence reagents (Bio-Rad, Hercules, CA). The amounts of the proteins were analyzed using Image J analysis software and normalized to GAPDH.

Co-immunoprecipitation (Co-IP) Analysis

Nrf2 was co-precipitated with Keap1 from cardiac tissues to detect the association of Nrf2 with Keap1. Cardiac tissue extracts (500 μg) were incubated with anti-Nrf2 antibody (0.5 μg) at 4°C overnight and then precipitated with protein A agarose (Beyotime, Shanghai, China) for 3 h. The Keap1/Nrf2 complex level in the beads was further detected by western blot.

Intracellular ROS Measurement

The ROS production was measured by using the ROS-sensitive dye, 2,7-dichlorodihydrofluorescein diacetate (DCFH-DA, Beyotime Biotechnology, China) as an indicator, as described previously. To measure ROS production in tissues and cell, dihydroethidium (DHE) staining was performed as described previously (13).

Construction of the Initial Structure of the Keap1/PHL Complex

The atomic co-ordinates of mouse Keap1 was download from the Protein Data Bank (PDB code: 5CGJ) (14). Next, the structure of Keap1 was preprocessed by VMD software (15). The AutoDock 4.2.6 package were used to predict the possible binding pose between Keap1 and PHL (16). Before molecular docking, the Keap1 and PHL were prepared by AutoDockTools 1.5.6 package, including adding missing hydrogen atoms and Gasteiger partial charges. After that, a grid box size of 22.5 Å × 22.5 Å × 22.5 Å was assigned, which covered almost the entire binding site of Keap1. During molecular docking, trials of 100 dockings, Lamarckian Genetic Algorithm (LGA) was used to globe conformational sampling, and other parameters were set as default. The lowest predicted binding energy conformation was used to further molecular dynamics (MD) simulation analysis.

Conventional Molecular Dynamics (MD) Simulation and Gaussian Accelerated Molecular Dynamics (GaMD) Simulation

The structural optimization of PHL was conducted using B3LYP combined with 6 – 31+G* basis set and RESP fitting method was applied for charge derivation based on the optimal conformation. The ff14SB force field was employed for the Keap1 protein and the general amber force field (gaff2) for the PHL (17, 18). The Keap1/PHL complex was solvated into TIP3P water box with boundary extended 12 Å away from any solute atom. The counter ions of Na^+ were added to maintain the electroneutrality.

Before productive simulation, three consecutive minimization stages were applied to relax the system, including 5,000 steps of steepest descent and 5,000 steps of conjugate gradient steps. Firstly, energy minimization of only hydrogen atoms, followed by water molecules and counter ions, were performed

with harmonic constraint potential of a 5.0 kcal mol^{-1} $Å^{-2}$. Thereafter, the whole system was minimized without any constraint. The systems were gradually heated to 310 K in 100 ps, followed by 600 ps density equilibration. Finally, 200 ns conventional MD simulations and 400 ns GaMD simulation were performed in the NPT ensemble and NVT ensemble, respectively. In particular, the dual potential boost method was employed in the GaMD simulation (19, 20). The boost parameters were calculated from an initial ∼4 ns NVT conventional MD simulation. During these simulations, the temperature were maintained by the Langevin temperature equilibration scheme (21). The long-range electrostatic interaction (cutoff = 10.0 Å) was used to evaluate direct space interaction with the particle-mesh Ewald (PME) method (22). All bonds involving hydrogen atoms were constrained by using the SHAKE algorithm (23). The simulation trajectories were processed by CPPTRAJ module in Amber 16 package (24). The Binding free energy decomposition was calculated by molecular mechanics/generalized Born surface area (MM/GBSA) method based on 200 snapshots extracted from the last 40 ns conventional MD simulation trajectory.

Statistical Analysis

Statistical analysis was performed using Student's *t*-test, and ANOVA as appropriate, with Tukey or Bonferroni *post hoc*-tests. All data were analyzed with GraphPad Prism 5.0 (Graphpad Software, Inc.); $p < 0.05$ were considered significant.

RESULTS

The Cytotoxicity of PHL

We investigated the cytotoxicity of PHL on H9c2 cells by MTT assay. As shown in **Figure 1B**, treatment of H9c2 cells with increasing concentrations of PHL (2.5, 5, 10, 20, 40, and 80 μM) for 24 h showed that even at 80 μM, PHL was relatively non-toxic to H9c2 cells. These results indicated that PHL had no obvious toxic effect on H9c2 cells. Finally, 10 μM PHL was selected for subsequent *in vitro* experiments.

PHL Reduced Hyperglycemia-Induced ROS Levels Through Regulation of Nrf2 Antioxidant Responses in H9c2 Cells

A large amount of evidence have shown that reactive oxygen species (ROS) play an important role in the pathogenesis of DCM (25). Therefore, we investigated the effect of PHL on hyperglycemia-induced oxidative stress. Firstly, we measured the effects of PHL on hyperglycemia-induced ROS generation and redox status markers. The hyperglycemia-induced group demonstrated markedly increased ROS generation, which significantly reduced by pre-treatment with PHL in hyperglycemia-induced H9c2 cells (**Figure 2A**). PHL also decreased the levels of MDA, a natural byproduct of lipid peroxidation (**Figure 2B**) and enhanced the enzyme SOD activity (**Figure 2C**). Dihydroethidium (DHE) reacts with superoxide anions to form a red fluorescent product, allowing signal visualization, and measurement of intracellular ROS in H9c2 cells. As shown in **Figure 2H**, PHL attenuated hyperglycemia-induced ROS production. These findings indicated that PHL is a potential inhibitor for hyperglycemia-induced ROS production.

As reported as Foresti et al. (26), hyperglycemia downregulated Nrf2 *in vitro* and *in vivo*. Nrf2 regulates the transcription of genes coding for anti-oxidant and detoxifying proteins, such as HO-1, NADPH, NQO-1, glutathione peroxidase-2, GCLC, and glutathione S-transferase. As shown in **Figure 2D**, the hyperglycemia-mediated downregulation of Nrf2 was prevented by the pre-treatment with PHL. Subsequently, we evaluated the expression levels of Nrf2, NQO-1, and HO-1 by pre-treating H9c2 cells with PHL for 30 min, followed by stimulation with high glucose (33 mM) for 24 h. The gene expression showed that Nrf2 (**Figure 2E**), NQO-1 (**Figure 2F**), and HO-1 (**Figure 2G**) were significantly increased in the PHL pre-treated group despite hyperglycemia induction. These results indicated that PHL inhibited the hyperglycemia-induced oxidation through Nrf2 gene in H9c2 cells.

PHL Attenuated Hyperglycemia-Induced Cell Fibrosis and Hypertrophy in H9c2 Cells

Myocardial fibrosis and hypertrophy are the major mechanisms contributing to cardiomyocyte remodeling in DCM (2, 27), so we assessed the effect of PHL on hyperglycemia-induced cardiac fibrosis and hypertrophy in H9c2 cells. As shown in **Figure 3A**, increased protein levels of hypertrophy marker atrial natriuretic peptide (ANP) and fibrosis marker TGF-β were observed in hyperglycemia-induced cells. These increases were significantly ablated by PHL pre-treatment. Meanwhile, RT-qPCR analysis revealed that PHL inhibited hyperglycemia-induced increases in hypertrophy factors, including ANP (**Figure 3C**), brain natriuretic peptide (BNP, **Figure 3D**) and β-myosin heavy chain (β-MyHC, **Figure 3E**) as well as fibrosis factors, such as transforming growth factor-β (TGF-β, **Figure 3F**), collagen-1 (**Figure 3G**), and connective tissue growth factor (CTGF, **Figure 3H**) gene expression. Rhodamine phalloidin staining also demonstrated an ablated hyperglycemia-induced cell size increase by PHL pre-treatment (**Figure 3B**).

PHL Prevented Cardiomyocyte Injury in Diabetic Mice

The *in vitro* experiments clearly showed that PHL could reduce oxidative stress, hypertrophy and fibrosis in H9c2 cells. Next, we evaluated the protected effects of PHL on heart *in vivo*. As shown in **Figures 4A–C**, PHL significantly inhibited the hyperglycemia-induced upregulation of biochemical markers LDH (**Figure 4A**), CK-MB (**Figure 4B**) and AST (**Figure 4C**) of myocardial injury. The H&E stain revealed that the hyperglycemia-stimulated hearts had structural abnormalities, namely disorganized myofibers. Heart tissues from PHL treatment group showed no significant structural changes compared to the control (CON) group (**Figure 4D**). Investigation of hypertrophy related genes in heart tissues revealed that PHL significantly attenuated the high expression levels of ANP (**Figure 4E**), BNP (**Figure 4F**), and β-MyHC (**Figure 4G**) found in diabetic mice. However, PHL treatment did not significantly affect fasting weight and blood

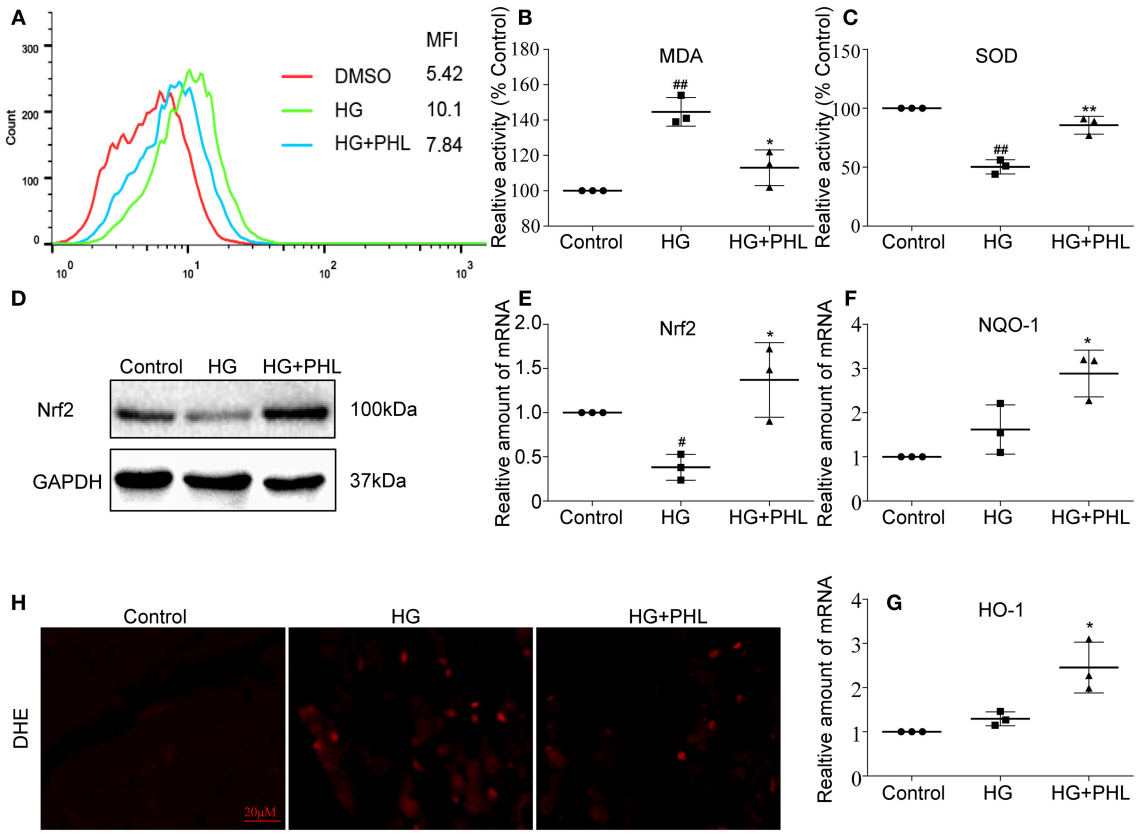

FIGURE 2 | PHL reduced hyperglycemia-induced ROS levels through induction of Nrf2 anti-oxidant responses in H9c2 cells. **(A)** PHL inhibited high glucose-induced ROS generation. H9c2 (1 * 10^6) cells pretreated with PHL (10 μM) for 1 h were incubated with HG (33 mM) for 3 h. DCFH-DA probes loaded and cells were processed by flow cytometry analysis for O_2 level, and mean fluorescence intensity (MFI) value was determined. **(B,C)** H9c2 (5 * 10^5) cells pretreated with PHL (10 μM) for 1 h and incubated with HG (33 mM) for 6 h. Levels of malondialdehyde (MDA) **(B)** in lysates prepared from H9c2 cells and enzymatic activity of superoxide dismutase (SOD) **(C)** as measured using colorimetric assays. **(D)** H9c2 (1 * 10^6) cells were pre-treated with PHL (10 μM) for 1 h and then incubated with HG (33 mM) for 12 h. The cell lysates were immunoblotted for Nrf2, with GAPDH as a loading control. **(E–G)** Total RNAs were extracted and the mRNA levels of Nrf2, HO-1, and NQO-1 were detected by RT-qPCR. Cells were treated as in **(B)**. **(H)** Staining of cultured H9c2 cells with DHE. DHE generates red fluorescence product (ethidium) in the presence of ROS. Cells were treated as in **(A)**. Data are presented as mean ± SEM. $^*P < 0.05$, $^{**}P < 0.01$ vs. HG group; $^{\#}P < 0.05$, $^{\#\#}P < 0.01$ vs. Control group.

sugar (**Figures S1A,B**), suggesting that the cardiac protective effects of PHL were not related to metabolic changes.

PHL Inhibited Cardiac Oxidative Stress and Fibrosis in the Diabetic Myocardium

To identify potential pharmacological activity for PHL protection *in vivo*, a series of biomarkers related to oxidation and fibrosis were investigated. Firstly, DHE staining showed that PHL attenuated the increase in ROS level in DCM (**Figure 5A**). Next, connective tissue collagen and histopathology of the hearts from PHL treated and untreated diabetic mice were assessed using Masson's trichrome stain. PHL effectively inhibited the fibrotic process of DCM (**Figure 5B**). As shown in **Figures 5C–E**, the expression levels of HO-1, NQO-1, GCLC in DCM tissues were upregulated by PHL. Additionally, in agreement with the histopathology, the high TGF-β (**Figure 5F**), collagen-1 (**Figure 5G**), and CTGF (**Figure 5H**) were significantly downregulated in DCM. These results suggested that the protective effect of PHL on cardiomyocyte in hyperglycemia-induced DCM might be related to its anti-oxidant and anti-fibrotic function.

PHL Targeted Keap1 Leading to Dissociation of the Keap1/Nrf2 Complex

Keap1/Nrf2 signaling pathway play a major role in regulating oxidative stress (28). Increasing evidence showed that Keap1/Nrf2 signaling pathway regulates inflammation, fibrosis and endoplasmic reticulum stress (ER stress) in DCM (29, 30). The *in vitro* study revealed that PHL promoted Nrf2 expression in hyperglycemia stimulation but the target and mechanism remained unclear. Previous studies indicated that Nrf2 maintains an inactive state in the cytoplasm under unstressed conditions bound to its inhibitor Keap1 (29), a vital regulator of the anti-oxidant response. Dissociation of the protein-protein interaction between Nrf2 and Keap1 leads to expression of detoxifying anti-oxidant enzymes. Thus, molecular modeling

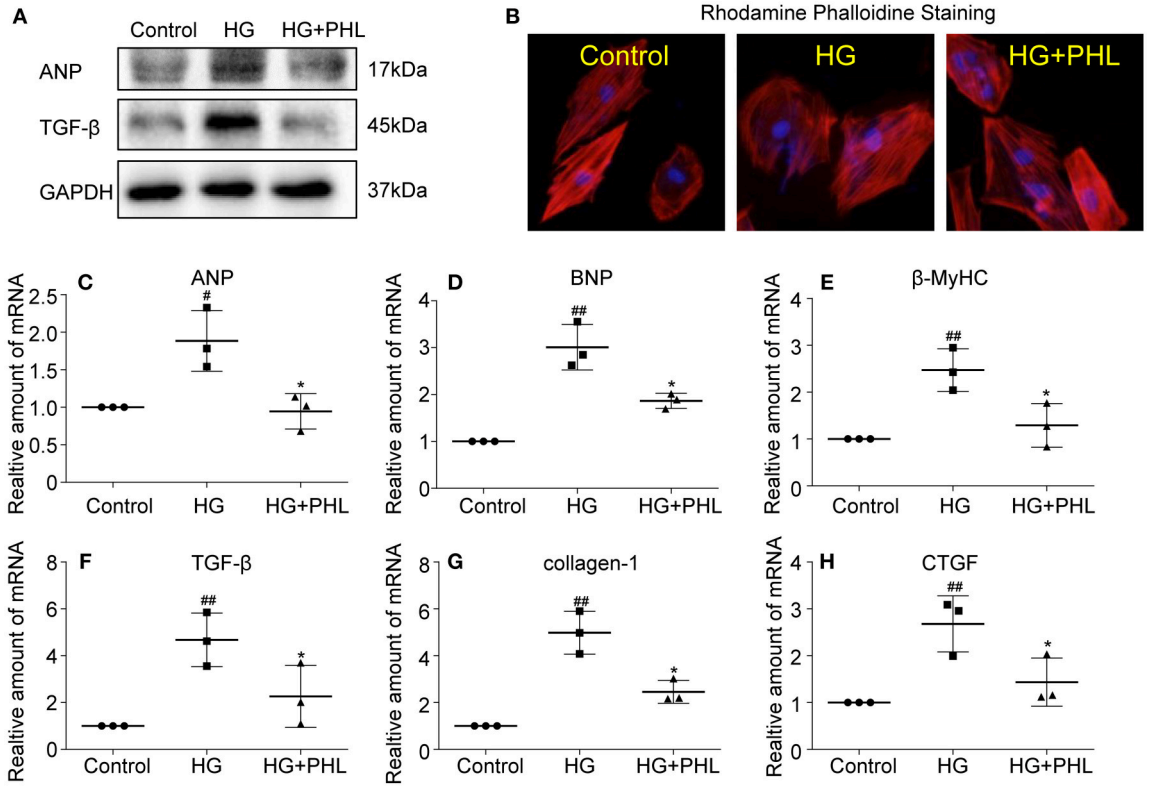

FIGURE 3 | PHL reduced hyperglycemia-induced hypertrophy and fibrosis in H9c2 cells. H9c2 ($1 * 10^6$) cells were pre-treated with PHL (10 μM) for 1 h and then incubated with HG (33 mM) for 24 h. **(A)** The cell lysates were immunoblotted for ANP, TGF-β, with GAPDH as a loading control. **(B)** The cell sizes were detected by Rhodamine Phalloidin/DAPI immunofluorescence staining. Total RNAs were extracted and the mRNA levels of ANP **(C)**, BNP **(D)**, β-MyHC **(E)**, TGF-β **(F)**, collagen-1 **(G),** and CTGF **(H)** were detected by RT-qPCR. Data are presented as mean ± SEM. $^*P < 0.05 < 0.01$ vs. HG group; $^{\#}P < 0.05$, $^{\#\#}P < 0.01$ vs. Control group.

and immunoblotting analysis were applied, focusing particularly on the hydrophobic binding site of Keap1.

Molecular docking was used to generate the initial structure and molecular dynamics (MD) simulations were applied to investigate the dynamic behavior. In order to monitor the stability of Keap1/phloretin complex during MD simulation, the root-mean-square deviations (RMSDs) of the backbone atoms (C_α) of Keap1 and the heavy atoms of PHL were analyzed (**Figure S2**). As shown in **Figures S2A,B**, the RMSD values of the backbone atoms of Keap1 and the heavy atoms of phloretin have a small fluctuation during the whole conventional MD simulation. GaMD simulation indicated that the Keap1/PHL complex was relatively stable. To gain an insight into the roles of individual residues in determining the interaction between Keap1 and PHL, the binding free energy decomposition was carried out. As shown in **Figure 6A**, the 10 most contributed residues were Gly-511, Ile-559, Gly-558, Ala-366, Val-512, Val-465, Val-606, Gly-464, Gly-605, and Gly-417. The predominant interactions were hydrogen bonds (residues of Ile-559, Gly-511, and Val-512) and hydrophobic interactions (**Figures 6A,B**).

Due to possible energy barriers between various intermediate states, conventional MD simulations cannot sample the conformational ensembles. Hence, an enhanced sampling technique to speed up the conformational sampling and take conformational samples at various intermediate states is needed. The traditional enhanced sampling methods often require predefined reaction coordinates (RCs), such as RMSD, atom distances, eigenvectors generated from the principal component analysis, which usually requires rich experience of the simulated systems. Nevertheless, the enhanced sampling method of GaMD simulation avoids such a requirement. Compared with conventional MD simulation, GaMD simulation can take samples at various intermediate states by adding a harmonic boost potential to smoothen the system potential energy surface, which are not accessible to conventional MD simulations. Therefore, the enhanced sampling method, GaMD simulation, was carried out to enhance conformational sampling (19, 20). Alignment of the representative structures from conventional MD and GaMD simulations exhibited high similarity with minor adjustments, indicating that PHL in the binding site of Keap1 was sufficiently stable (**Figure 6C**). The principal component analysis (PCA) further supported this observation (**Figure 6D**). Theoretically, when principal components are plotted against each other, similar structures are clustered and each cluster shows a different protein conformational state. As shown in **Figure 6D**, only one cluster was observed, the target for PHL

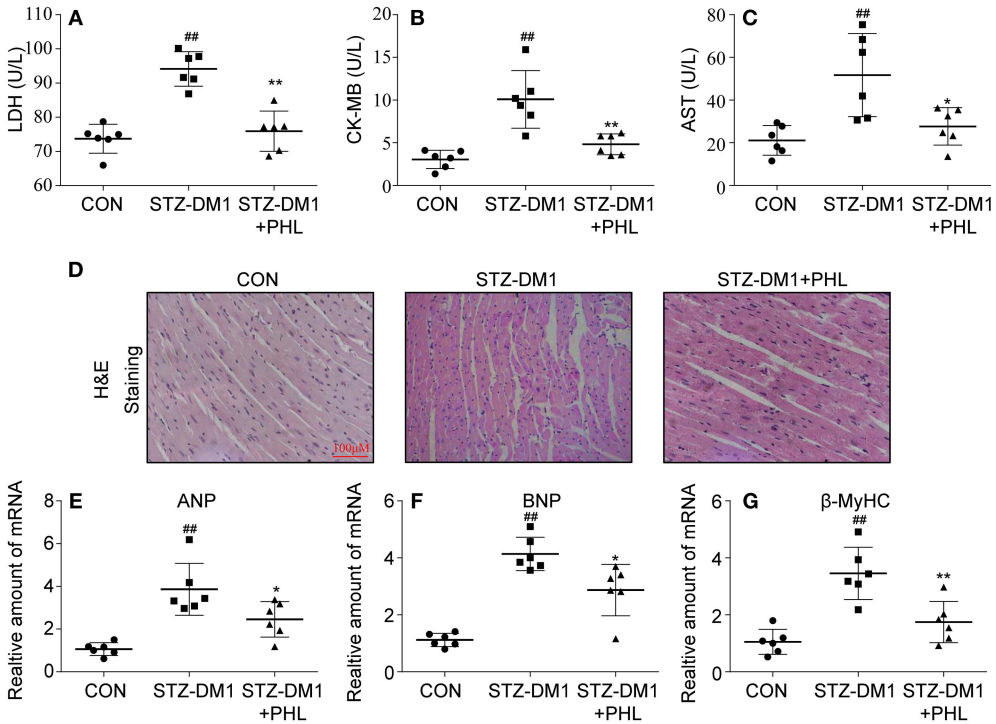

FIGURE 4 | PHL attenuated diabetes-induced cardiac injury. Diabetes mellitus was induced in male C57BL/6 mice by a single intraperitoneal (i.p.) injection of 100 mg/kg STZ and mice with fasting-blood glucose >12 mM were considered diabetes and then diabetic mice were orally treated with phloretin (PHL, 10 mg/kg), or vehicle by gavage once every 2 days for 8 weeks, which was administrated in diabetic mice. Serum levels of LDH **(A)**, CK-MB **(B),** and AST **(C)** were determined using indicated kits (Six mice in each group were used for above analysis). **(D)** Representative images from H&E sections of heart tissues are shown, ×400 amplification. **(E–G)** The mRNA expression levels of ANP **(E)**, BNP **(F),** and β-MyHC **(G)** in myocardial tissues of each group were determined by real-time qPCR. Six mice in each group were used for above analysis. $^{*}P < 0.05$, $^{**}P < 0.01$ vs. STZ-DM1 group; $^{\#\#}P < 0.01$ vs. CON group.

is likely to be Keap1. To verify this theory, the expressions of Keap1/Nrf2 complex in the heart tissues were assessed that the expressions level of Nrf2 in diabetic heart tissues. The results showed that the expression of Nrf2 was significantly lower and the levels of Keap1/Nrf2 complex was a little higher in diabetic heart tissues, while PHL inhibited this process (**Figure 6E** and **Figure S4**). In summary, the computational and experiment results demonstrated that Keap1 may be the direct target for PHL to exert anti-oxidative effects and promoted Nrf2 expression for the protective effects in DCM.

DISCUSSION

It has been well-established that persistent hyperglycemia in diabetic patients induce cardiomyocyte hypertrophy, myocardial inflammation, fibrosis, and apoptosis (1, 2, 5, 8). As observed in our study, high glucose induced oxidative stress, hypertrophy, and fibrosis in myocardial cells and diabetic mice (**Figures 2–5**). Current therapies for DCM focus on intensive blood glucose control (31). However, this strategy does not prevent the development of cardiac complications associated with hyperglycemia. Treatment with anti-diabetics, such as miglitol, significantly reduced the blood glucose via different mechanisms *in vivo*, while the diabetic complications remained (32). Moreover, a few studies showed that anti-inflammatory agents prevented the development of cardiac and renal injury in streptozotocin (STZ)-induced diabetic mice (2). Meanwhile, a large number of targets, such as TLR4 and FGFR as well as fatty acid-induced cardiac remodeling have been investigated (33, 34). Therefore, we speculate that there are unknown mechanisms contributing to cardiac fibrosis, cardiac remodeling, and cell death.

Recently, natural products have been increasingly evaluated for their effects on cardiovascular diseases. Most notably, flavonoids exhibited properties of inflammation, oxidant stress, cell death, and fibrosis by direct or indirect mechanisms (35, 36). It was recently been reported that several flavonoids, such as quercetin, kaempferol, liquiritin, and baicalein exhibited multiple effects in diabetic complications by inhibiting inflammation, oxidation and fibrosis (37–40). PHL, a natural flavonoid compound derived from apples and pears, was shown to reduce myocardial hypertrophy in acute models of heart disease (41). In addition, PHL prevents high-fat diet-induced obesity and improves metabolic homeostasis through anti-oxidative effect (42). However, to-date, no data is available regarding the effects of PHL on DCM. In this study, we investigated the activities and mechanisms of PHL in an *in vivo* model for DCM. Following STZ injection for 10 weeks, cardiac remodeling including hypertrophy, cardiomyocyte disorganization, and fibrosis were observed in the hearts of diabetic mice. Interestingly, oral PHL

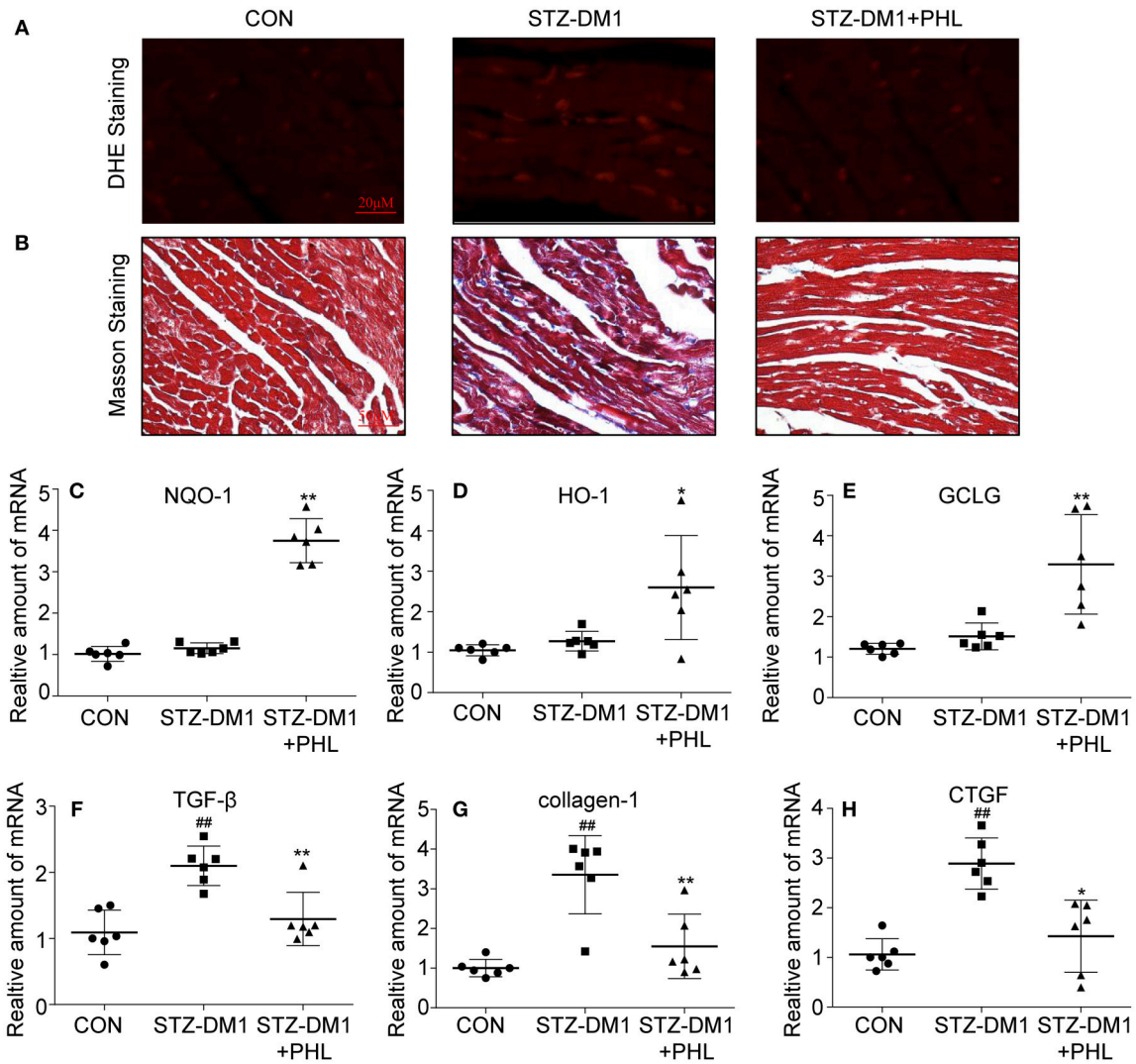

FIGURE 5 | PHL inhibited cardiac oxidative stress and fibrosis in the diabetic myocardium. **(A)** Representative images for DHE staining using the frozen section of heart tissues as described in Materials and Methods (1000× magnification). **(B)** Assessment of cardiac fibrosis by Masson's Trichrome staining (400× magnification). **(C–H)** The mRNA expression levels of HO-1 **(C)**, NQO-1 **(D)**, GCLC **(E)**, TGF-β **(F)**, collagen-1 **(G),** and CTGF **(H)** in myocardial tissues of each group were determined by real-time qPCR. Six mice in each group were used for above analysis. $^{*}P < 0.05$, $^{**}P < 0.01$ vs. STZ-DM1 group; $^{\#\#}P < 0.01$ vs. CON group.

(10 mg/kg) attenuated cardiac remodeling without any effects on the glucose level or body weight of diabetic mice (**Figure S1**, **Figures 2**–**5**). Similar biochemical results were reflected in hyperglycemia-treated H9c2 cells (**Figures 2**, **3**). It is interesting that PHL attenuated MDA level and upregulated Nrf2, HO-1, and NQO-1 expressions *in vitro* (**Figure 2**). These findings suggested that PHL has a potential therapeutic effect in DCM, likely through decreased cardiac oxidative stress.

Increasing evidence has shown that oxidative stress plays an important role in the pathophysiology of hyperglycemic induction of cardiovascular disease (43, 44). Cardiac oxidative stress is associated with increased cardiac fibrosis and cell death, leading to the development of severe heart failure (43, 44). Excess oxidation results in ROS aggregation in tissues. In metabolic disease, sustained production of ROS is critical to the development of cardiac injuries. ROS induced mitochondrial DNA has been proposed to be particularly susceptible to oxidative damage. In this study, PHL significantly reduced hyperglycemia-induced ROS accumulation in H9c2 cells and heart tissues from diabetic mice (**Figure 2A** and **Figure 5A**). There is an increasing recognition that Keap1/Nrf2 pathway activation can be beneficial for DCM, as it has been recognized as a key regulator of anti-oxidant defense system by mediating the expression of anti-oxidant genes, such as HO-1, GCLC, NAPD-H, and NQO-1. While hyperglycemia reduced the expression of Nrf2, HO-1, and NQO-1, PHL markedly upregulated these genes *in vitro* and *in vivo* (**Figure 2**, **Figure 5**). Interestingly, Keap1 was increased by hyperglycemia, but PHL downregulated Keap1

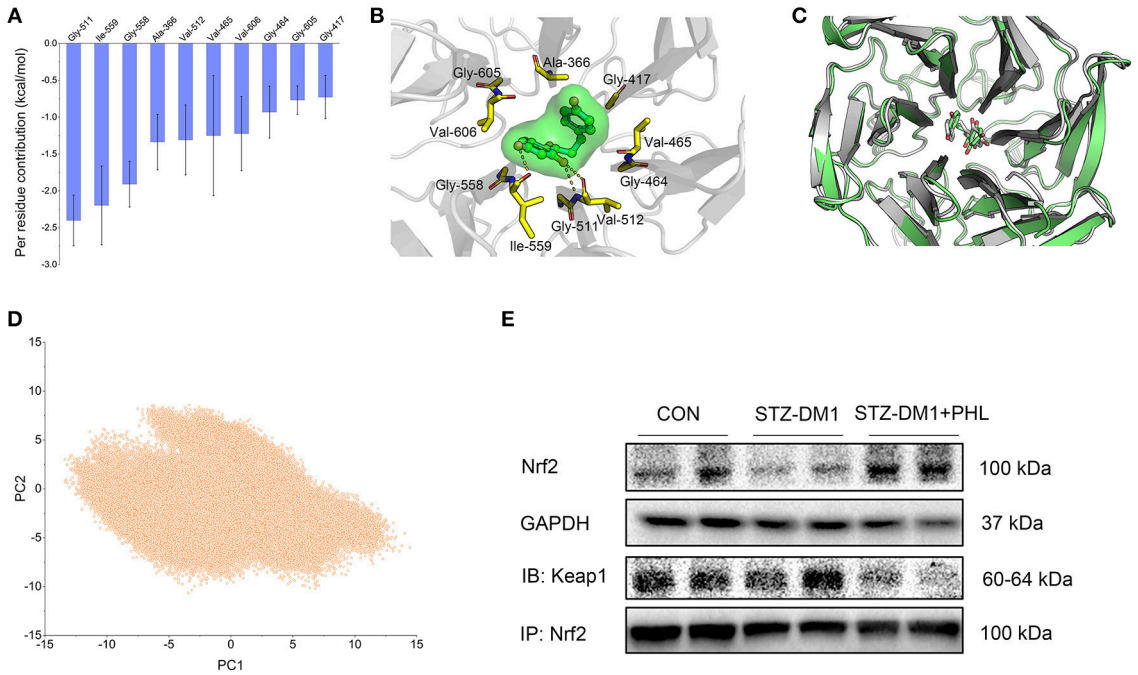

FIGURE 6 | PHL targeted Keap1 to disassemble the Keap1/Nrf2 complex. **(A)** Per-residue of top 10 contribution to the binding free energy; **(B)** Structural analysis of the most 10 contributors of Keap1 to PHL, hydrogen bonds are colored yellow; **(C)** Alignment of the representative structures between from conventional MD simulation and from GaMD simulation; **(D)** PCA scatter plot of 200,000 snapshots from GaMD simulation along the first two principal components. **(E)** Immunoblotting analysis of Nrf2 expression and Co-Immunoprecipitation analysis of Nrf2 and Keap1 complex in lysates prepared from heart tissues. GAPDH was used as a loading control.

protein levels. Using molecular modeling and immunoblotting, PHL was determined to bind to Keap1 via hydrogen bonds and hydrophobic interactions (**Figures 6A–D**), which subsequently resulted in increased available Nrf2.

In conclusion, this study demonstrated that PHL could prevent the hyperglycemia-induced cardiac injury. The possible mechanism involved, in prevention of oxidative stress and related cytoprotective effect, could be through degradation of Keap1 and upregulation of Nrf2 expressions, leading to downstream regulation of key detoxifying enzymes (**Figures 2–6** and **Figure S3**). Thus, PHL could be a candidate for treating diabetic complications, especially for DCM. In addition, conventional MD and GaMD simulations (**Figures 6A–D**) supported the hypothesized mechanism whereby PHL protected cardiomyocyte from hyperglycemia through disruption of the interaction between Keap1 and Nrf2. Co-IP and western blot analyses also supported this hypothesis (**Figure 6E** and **Figure S4**). However, it is still not clear whether PHL induced Nrf2 transcription and led to elimination of ROS or whether PHL inhibited Keap1/Nrf2 complex first and the subsequent antioxidant response. And the mechanism of PHL how to induced Nrf2 transcription is unknown. The approach using shRNA knockdown *in vitro* with hyperglycemia would be more robust to solve these shortages. This is a limitation of this study.

Overall, this study strongly supports PHL as a promising natural agent via increased Nrf2 expression dissociation of Keap1/Nrf2 complex, leading to decreased cardiac oxidative stress in DCM. At the same time, this study also highlighted Keap1/Nrf2 pathway as a potential therapeutic target for DCM management.

AUTHOR CONTRIBUTIONS

YY and JJ who originally designed the project, performed the research, analyzed data, and wrote the manuscript draft. PS, HW, and LY performed partial experiments and data collection. XW were responsible for revising the manuscript. All authors approved the final version of the manuscript.

FUNDING

Financial support was provided by Natural Science Foundation of Zhejiang Province of China (LQ14H280003) and Zhejiang Medical and Health Science Technology Project (2013KYB062), and Zhejiang Chinese Medical and Health Technology Project (2019ZA030).

SUPPLEMENTARY MATERIAL

The Supplementary Material for this article can be found online at: https://www.frontiersin.org/articles/10.3389/fendo.2018.00774/full#supplementary-material

REFERENCES

1. Jia G, Hill MA, Sowers JR. Diabetic cardiomyopathy: an update of mechanisms contributing to this clinical entity. *Circ Res.* (2018) 122:624–38. doi: 10.1161/CIRCRESAHA.117.311586
2. Chen H, Yang X, Lu K, Lu C, Zhao Y, Zheng S, et al. Inhibition of high glucose-induced inflammation and fibrosis by a novel curcumin derivative prevents renal and heart injury in diabetic mice. *Toxicol Lett.* (2017) 278:48–58. doi: 10.1016/j.toxlet.2017.07.212
3. Hu X, Rajesh M, Zhang J, Zhou S, Wang S, Sun J, et al. Protection by dimethyl fumarate against diabetic cardiomyopathy in type 1 diabetic mice likely via activation of nuclear factor erythroid-2 related factor 2. *Toxicol Lett.* (2018) 287:131–41. doi: 10.1016/j.toxlet.2018.01.020
4. Pan J, Guleria RS, Zhu S, Baker KM. Molecular mechanisms of retinoid receptors in diabetes-induced cardiac remodeling. *J Clin Med.* (2014) 3:566–94. doi: 10.3390/jcm3020566
5. Miyata T, Suzuki N, van Ypersele de Strihou C. Diabetic nephropathy: are there new and potentially promising therapies targeting oxygen biology? *Kidney Int.* (2013) 84:693–702. doi: 10.1038/ki.2013.74
6. Lu M, Ji J, Jiang Z, You Q. The keap1-Nrf2-ARE pathway as a potential preventive and therapeutic target: an update. *Med Res Rev.* (2016) 36:924–63. doi: 10.1002/med.21396
7. Vaamonde-Garcia C, Courties A, Pigenet A, Laiguillon M, Sautet A, Houard X, et al. The nuclear factor-erythroid 2-related factor/heme oxygenase-1 axis is critical for the inflammatory features of type 2 diabetes-associated osteoarthritis. *J Biol Chem.* (2017) 292:14505–15. doi: 10.1074/jbc.M117.802157
8. Yang H, Feng A, Lin S, Yu L, Lin X, Yan X, et al. Fibroblast growth factor-21 prevents diabetic cardiomyopathy via AMPK-mediated antioxidation and lipid-lowering effects in the heart. *Cell Death Dis.* (2018) 9:227. doi: 10.1038/s41419-018-0307-5
9. Huang W, Fang L, Liou C. Phloretin attenuates allergic airway inflammation and oxidative stress in asthmatic mice. *Front Immunol.* (2017) 8:134. doi: 10.3389/fimmu.2017.00134
10. Fenton R, Chou C, Stewart G, Smith C, Knepper M. Urinary concentrating defect in mice with selective deletion of phloretin-sensitive urea transporters in the renal collecting duct. *Proc Natl Acad Sci USA.* (2004) 101:7469–74. doi: 10.1073/pnas.0401704101
11. Zhang S, Qin C, Safe S. Flavonoids as aryl hydrocarbon receptor agonists/antagonists: effects of structure and cell context. *Environ Health Perspect.* (2003) 111:1877–82. doi: 10.1289/ehp.6322
12. Jones R, Parker M, Morris M. Quercetin, morin, luteolin, and phloretin are dietary flavonoid inhibitors of monocarboxylate transporter 6. *Mol Pharm.* (2017) 14:2930–6. doi: 10.1021/acs.molpharmaceut.7b00264
13. Gao J, Liu R, Wu J, Liu Z, Li J, Zhou J, et al. The use of chitosan based hydrogel for enhancing the therapeutic benefits of adipose-derived MSCs for acute kidney injury. *Biomaterials* (2012) 33:3673–81. doi: 10.1016/j.biomaterials.2012.01.061
14. Winkel AF, Engel CK, Margerie D, Kannt A, Szillat H, Glombik H, et al. Characterization of RA839, a noncovalent small molecule binder to keap1 and selective activator of Nrf2 signaling. *J Biol Chem.* (2015) 290:28446–55. doi: 10.1074/jbc.M115.678136
15. Humphrey W, Dalke A, Schulten K. VMD: visual molecular dynamics. *J Mol Graph.* (1996) 14:33–8, 27–8. doi: 10.1016/0263-7855(96)00018-5
16. Morris GM, Huey R, Lindstrom W, Sanner MF, Belew RK, Goodsell DS, et al. AutoDock4 and autodocktools4: automated docking with selective receptor flexibility. *J Comput Chem.* (2009) 30:2785–91. doi: 10.1002/jcc.21256
17. Maier JA, Martinez C, Kasavajhala K, Wickstrom L, Hauser KE, Simmerling C. ff14sb: improving the accuracy of protein side chain and backbone parameters from ff99SB. *J Chem Theory Comput.* (2015) 11:3696–713. doi: 10.1021/acs.jctc.5b00255
18. Wang J, Wolf RM, Caldwell JW, Kollman PA, Case DA. Development and testing of a general amber force field. *J Comput Chem.* (2004) 25:1157–74. doi: 10.1002/jcc.20035
19. Miao Y, McCammon JA. Unconstrained enhanced sampling for free energy calculations of biomolecules: a review. *Mol Simul.* (2016) 42:1046–55. doi: 10.1080/08927022.2015.1121541
20. Miao Y, McCammon JA. Graded activation and free energy landscapes of a muscarinic G-protein-coupled receptor. *Proc Natl Acad Sci USA.* (2016) 113:12162–7. doi: 10.1073/pnas.1614538113
21. Loncharich RJ, Brooks BR, Pastor RW. Langevin dynamics of peptides: the frictional dependence of isomerization rates of N-acetylalanyl-N'-methylamide. *Biopolymers* (1992) 32:523–35. doi: 10.1002/bip.360320508
22. Essmann U, Perera L, Berkowitz ML, Darden T, Lee H, Pedersen LG. A smooth particle mesh Ewald method. *J Chem Phys.* (1995) 103:8577–93. doi: 10.1063/1.470117
23. Kräutler V, Van Gunsteren WF, Hünenberger PH. A fast SHAKE algorithm to solve distance constraint equations for small molecules in molecular dynamics simulations. *J Comput Chem.* (2001) 22:501–8. doi: 10.1002/1096-987X(20010415)22:5<501::AID-JCC1021>3.0.CO;2-V
24. Roe DR, Cheatham TE III. PTRAJ and CPPTRAJ: software for processing and analysis of molecular dynamics trajectory data. *J Chem Theory Comput.* (2013) 9:3084–95. doi: 10.1021/ct400341p
25. Ganugula R, Arora M, Jaisamut P, Wiwattanapatapee R, Jørgensen H, Venkatpurwar V, et al. Nano-curcumin safely prevents streptozotocin-induced inflammation and apoptosis in pancreatic beta cells for effective management of Type 1 diabetes mellitus. *Br J Pharmacol.* (2017) 174:2074–84. doi: 10.1111/bph.13816
26. Foresti R, Bucolo C, Platania C, Drago F, Dubois-Randé J, Motterlini R. Nrf2 activators modulate oxidative stress responses and bioenergetic profiles of human retinal epithelial cells cultured in normal or high glucose conditions. *Pharmacol Res.* (2015) 99:296–307. doi: 10.1016/j.phrs.2015.07.006
27. Guo Y, Zhuang X, Huang Z, Zou J, Yang D, Hu X, et al. Klotho protects the heart from hyperglycemia-induced injury by inactivating ROS and NF-κB-mediated inflammation both *in vitro* and *in vivo*. *Biochim Biophys Acta Mol Basis Dis.* (2018) 1864:238–51. doi: 10.1016/j.bbadis.2017.09.029
28. Filomeni G, De Zio D, Cecconi F. Oxidative stress and autophagy: the clash between damage and metabolic needs. *Cell Death Differ.* (2015) 22:377–88. doi: 10.1038/cdd.2014.150
29. Sykiotis G, Bohmann D. Keap1/Nrf2 signaling regulates oxidative stress tolerance and lifespan in Drosophila. *Dev Cell* (2008) 14:76–85. doi: 10.1016/j.devcel.2007.12.002
30. Periyasamy P, Shinohara T. Age-related cataracts: Role of unfolded protein response, Ca mobilization, epigenetic DNA modifications, and loss of Nrf2/Keap1 dependent cytoprotection. *Prog Retin Eye Res.* (2017) 60:1–19. doi: 10.1016/j.preteyeres.2017.08.003
31. Finan B, Yang B, Ottaway N, Smiley D, Ma T, Clemmensen C, et al. A rationally designed monomeric peptide triagonist corrects obesity and diabetes in rodents. *Nat Med.* (2015) 21:27–36. doi: 10.1038/nm.3761
32. Shimabukuro M, Tanaka A, Sata M, Dai K, Shibata Y, Inoue Y, et al. α-Glucosidase inhibitor miglitol attenuates glucose fluctuation, heart rate variability and sympathetic activity in patients with type 2 diabetes and acute coronary syndrome: a multicenter randomized controlled (MACS) study. *Cardiovasc Diabetol.* (2017) 16:86. doi: 10.1186/s12933-017-0571-1
33. Detillieux K, Sheikh F, Kardami E, Cattini P. Biological activities of fibroblast growth factor-2 in the adult myocardium. *Cardiovasc Res.* (2003) 57:8–19. doi: 10.1016/S0008-6363(02)00708-3
34. Hu N, Zhang Y. TLR4 knockout attenuated high fat diet-induced cardiac dysfunction via NF-κB/JNK-dependent activation of autophagy. *Biochim Biophys Acta Mol Basis Dis.* (2017) 1863:2001–11. doi: 10.1016/j.bbadis.2017.01.010
35. Ribeiro D, Freitas M, Lima J, Fernandes E. Proinflammatory pathways: the modulation by flavonoids. *Med Res Rev.* (2015) 35:877–936. doi: 10.1002/med.21347
36. Selvaraj S, Krishnaswamy S, Devashya V, Sethuraman S, Krishnan U. Influence of membrane lipid composition on flavonoid-membrane interactions: implications on their biological activity. *Prog Lipid Res.* (2015) 58:1–13. doi: 10.1016/j.plipres.2014.11.002
37. Pathak S, Regmi S, Nguyen T, Gupta B, Gautam M, Yong C, et al. Polymeric microsphere-facilitated site-specific delivery of quercetin prevents senescence of pancreatic islets *in vivo* and improves transplantation outcomes in mouse model of diabetes. *Acta Biomater* (2018) 75:287–99. doi: 10.1016/j.actbio.2018.06.006
38. Alkhalidy H, Moore W, Wang Y, Luo J, McMillan R, Zhen W, et al. The flavonoid kaempferol ameliorates streptozotocin-induced diabetes

by suppressing hepatic glucose production. *Molecules* (2018) 23. doi: 10.3390/molecules23092338
39. Zhang Y, Zhang L, Zhang Y, Xu J, Sun L, Li S. The protective role of liquiritin in high fructose-induced myocardial fibrosis via inhibiting NF-κB and MAPK signaling pathway. *Biomed Pharmacother.* (2016) 84:1337–49. doi: 10.1016/j.biopha.2016.10.036
40. Ku S, Bae J. Baicalin, baicalein and wogonin inhibits high glucose-induced vascular inflammation *in vitro* and *in vivo*. *BMB Rep.* (2015) 48:519–24. doi: 10.5483/BMBRep.2015.48.9.017
41. Vineetha V, Soumya R, Raghu K. Phloretin ameliorates arsenic trioxide induced mitochondrial dysfunction in H9c2 cardiomyoblasts mediated via alterations in membrane permeability and ETC complexes. *Eur J Pharmacol.* (2015) 754:162–72. doi: 10.1016/j.ejphar.2015.02.036
42. Alsanea S, Gao M, Liu D. Phloretin prevents high-fat diet-induced obesity and improves metabolic homeostasis. *AAPS J.* (2017) 19:797–805. doi: 10.1208/s12248-017-0053-0
43. Jha J, Ho F, Dan C, Jandeleit-Dahm K. A causal link between oxidative stress and inflammation in cardiovascular and renal complications of diabetes. *Clin Sci.* (2018) 132:1811–36. doi: 10.1042/CS20171459
44. Kiyuna L, Albuquerque R, Chen C, Mochly-Rosen D, Ferreira J. Targeting mitochondrial dysfunction and oxidative stress in heart failure: challenges and opportunities. *Free Radic Biol Med.* (2018) 129:155–68. doi: 10.1016/j.freeradbiomed.2018.09.019

Conflict of Interest Statement: The authors declare that the research was conducted in the absence of any commercial or financial relationships that could be construed as a potential conflict of interest.

frontiers in Endocrinology

REVIEW
published: 30 January 2019
doi: 10.3389/fendo.2019.00026

IL-33 at the Crossroads of Metabolic Disorders and Immunity

Lei Tu[1] *and Lijing Yang*[2]*

[1] Division of Gastroenterology, Union Hospital, Tongji Medical College, Huazhong University of Science and Technology, Wuhan, China, [2] Department of Radiation and Medical Oncology, Zhongnan Hospital, Wuhan University, Wuhan, China

As a cytokine in interleukin-1(IL-1) family, interleukin-33(IL-33) usually exists in the cytoplasm and cell nucleus. When the cells are activated or damaged, IL-33 can be secreted into extracellular and regulate the functions of various immune cells through binding to its specific receptor suppression of tumorigenicity 2 (ST2). Except regulating the function of immune cells including T cells, B cells, dendritic cells (DCs), macrophages, mast cells, and innate lymphoid cells, IL-33 also plays an important role in metabolic diseases and has received an increasing attention. This review summarizes the regulation of IL-33 on different immune cells in lipid metabolism, which will help to understand the pathology of abnormal lipid metabolic diseases, such as atherosclerosis and type 2 diabetes.

Keywords: IL-33, metabolism, diabetes, innate & adaptive immune response, ST2

OPEN ACCESS

Edited by:
Jixin Zhong,
Case Western Reserve University,
United States

Reviewed by:
Yanbo Yu,
Qilu Hospital of Shandong University,
China
Takashi Yazawa,
Asahikawa Medical University, Japan
Fenna Sille,
Johns Hopkins University,
United States

***Correspondence:**
Lijing Yang
yanglijing23@126.com

Specialty section:
This article was submitted to Experimental Endocrinology, a section of the journal Frontiers in Endocrinology

Received: *23 October 2018*
Accepted: *15 January 2019*
Published: *30 January 2019*

Citation:
Tu L and Yang L (2019) IL-33 at the Crossroads of Metabolic Disorders and Immunity. Front. Endocrinol. 10:26. doi: 10.3389/fendo.2019.00026

INTRODUCTION

IL-33, a new member of the IL-1 family, was discovered in 2005 (1) while its receptor ST2 containing intracellular domain Toll/IL-1R (TIR) was found in BALB/c-3t3 mouse fibroblasts in 1989 (1, 2). The receptor complex of IL-33 is composed of ST2 and interleukin-1 receptor accessory protein (IL-1RAcP). IL-33 mediates its biological effect through binding to its specific receptor ST2 (2, 3), whereas the expression of ST2 is restricted and determines the cellular responsiveness to IL-33 treatment (3).Two forms of ST2 have been demonstrated, a membrane-bound form (ST2L) and a soluble form (sST2), the latter which prevents its signaling as the decoy receptor for IL-33. IL-33 is mainly expressed in fibroblasts, epithelial cells and endothelial cells, and especially in high endothelial venules (HEV) (4). Indeed, as designated as an "alarmin," IL-33 is usually released after cell injury to alert the immune system and initiate repair processes. In a recent study, islet mesenchymal-cell-derived IL-33 has been identified as an islet immunoregulatory feature (5). As the receptor of IL-33, ST2 is expressed in many immune cells. IL-33 is a dual-function cytokine. In the absence of inflammatory stimulation, IL-33 is located in the nucleus as a nuclear factor. Once the cell is damaged and/or necrotic, IL-33 can be released from the nucleus and then act as an endogenous "alarmin" (4). The activation signal produced by IL-33/ST2 pathway is transmitted to the cell and a series of signal transmissions activate nuclear factor kappa-light-chain-enhancer of activated B cells (NF-κB) and mitogen-activated protein kinase (MAPK) pathway to regulate immune response (1, 6). Under normal physiological condition, inflammation induced by a dysregulated lipid metabolism is benefit for the maintenance of homeostasis and is controlled to avoid excessive damage to the host. However, if not properly controlled, the inflammatory response will promote the excessive production of lipid metabolites, inflammatory cytokines and adhesion molecules, which lead to acute or chronic diseases (7), such as obesity, non-alcoholic steatohepatitis (NASH), atherosclerosis, and acute cardiovascular events. To date, an increasing body of evidence has demonstrated that IL-33 plays a critical role in the lipid metabolism. This review highlights

the function of IL-33/ST2 axis on different immune cells in the metabolic disorders.

IL-33/ST2L SIGNALING IN INNATE IMMUNE RESPONSES

IL-33 and ST2 have been shown to be expressed in human and murine adipose tissue, and IL-33 expression is strongly correlated with leptin expression in human adipose tissue (8). In addition, administration of IL-33 increases browning of white adipose tissue and energy expenditure in mice (9). These observations show that a critical role of IL-33 played in the adipose tissues homeostasis.

Macrophages have functional plasticity in adipose tissue inflammation, which can exhibit pro-inflammatory or anti-inflammatory function. According to the phenotypes and secreted cytokines, macrophages can be divided into two categories named as classical activated macrophages (CAM, M1 type) and alternatively activated macrophages (AAM, M2 type), respectively. CAM are generated in response to helper T1 cells (Th1 cells)-related cytokines, such as interferon-γ (IFN-γ) and tumor necrosis factor-α (TNF-α), while AAM polarization is linked to the helper T2 cells (Th2 cells)-related cytokines (IL-4 and IL-13) (10). Previous studies showed that AAM could attenuate adipose tissue inflammation and obesity-induced insulin resistance (11–14). It has been showed that ST2 can be detected on the cell surface of macrophages. IL-33 can promote the expression of lipopolysaccharide (LPS) receptor components such as myeloid differentiation factor 2 (MD2), toll-like receptor (TLR) 4, soluble cluster of differentiation 14 (CD14) and myeloid differentiation primary response gene 88 (Myd88), which result in an enhanced inflammatory cytokine production (15). However, IL-33 administration improves glucose tolerance, which is associated with the accumulation of M2 macrophages in adipose tissue of ob/ob mice that are the mutant mice to construct the model of Type II diabetes (16). As the result of purine metabolism disorder, gout is a very common metabolic disease in human (17, 18). Hyperlipidaemia is common in gout patients including increased low-density lipoprotein (LDL) cholesterol and decreased high-density lipoprotein (HDL) cholesterol (19). The serum IL-33 expression is predominantly increased in gout patients compared to healthy controls and positively correlated with the expression of HDL, while negatively correlated with LDL expression (20). It has been reported that the elevated IL-33 level is considerably reduced in renal impairment when compared with normal renal function in gout patients (20–22). These data suggest that IL-33 may prevent the kidney injury through regulating the lipid metabolism, which may be resulted from the AAM polarization.

Although ST2 can be detected on the cell surface of macrophages, IL-33/ST2 signaling cannot directly promote AAM polarization. The involvement of IL-33/ST2 signaling in the differentiation and activation of AAM is associated with type II cytokines induction (23–25). A previous finding showed that a population of cells expressing ST2 in adipose was potential to produce large amounts of Th2 cytokines in response to IL-33 (26). Recent studies have named this population as group 2 innate lymphoid cells (ILC2s), characterized by expressing ST2 receptor, and secreting type 2 cytokines such as IL-5 and IL-13 in response to IL-33 (27–30). In addition, soluble ST2 can prevent ILC2s from IL-33 stimulation (31). Recent observation has shown that ILC2s activation favors macrophages toward a protective AAM, which lead to a reduced lipid storage and decrease gene expression of lipid metabolism and adiposeness (32). Furthermore, it has showed that IL-13Rα2 may act as a critical checkpoint in the protective effect of the IL-33/IL-13 axis in obesity (33). In addition, IL-33 promotes β cell function through islet-resident ILC2s that elicite retinoic acid (RA)-producing capacities in macrophages and dendritic cells via the secretion of IL-13 and colony-stimulating factor 2 (5). These data suggest that IL-33 plays a protective role in the adipose tissue inflammation through regulating macrophage function, which is closely associated with the activation of ILC2 to produce type 2 cytokine and IL-4Rα signaling.

IL-33/ST2L SIGNALING ON T CELL IMMUNE RESPONSES

As a subset of T cells, the regulatory T cells (Tregs) play a critical role in suppressing autoimmune reactivity and have gained an increasing attention in the autoimmune diseases (34). It is shown that an impaired Tregs function is investigated in ST2 gene knockout mice with streptozotocin-induced diabetes, where the glycaemia and β cell loss are severe (35). Indeed, the exogenous IL-33 treatment propagates Tregs expressing the ST2 on the cellular surface, which suggests that the Tregs expansion induced by IL-33 administration is likely to be the result of a direct effect of IL-33 on $ST2L^+$ Tregs (36, 37). Besides, $ST2^+$ DCs stimulated by IL-33 to secrete IL-2, which promotes the selective expansion of $ST2^+$ Tregs vs. non-Tregs, are required for *in vitro* and *in vivo* Tregs expansion (37, 38). In the Th1/Th17-mediated allograft rejection, IL-33 treatment can prevent allograft rejection through increasing ST2 positive Tregs in mice (39). In the mouse model of trinitrobenzene sulfonic acid (TNBS)-induced colitis, dextran sulfate sodium (DSS)-induced colitis or T cell adoptive transfer induced colitis, IL-33 can increase the number of $Foxp3^+$ Tregs (40–42).

The Tregs also play a immunosuppressive function in obesity-associated inflammation (43). Interestingly, studies have also demonstrated that IL-33 maintain homeostasis in adipose tissue. A high level of ST2 expression is observed on human adipose tissue Tregs. Furthermore, IL-33 treatment can induce vigorous population expansion of Tregs in obese mice, and the changes of metabolic parameters are significantly correlated with the increased Tregs (44, 45). IL-33 signaling through the IL-33 receptor ST2 and the myeloid differentiation factor MyD88 pathway is essential for the development and maintenance of Tregs in visceral adipose tissue (44). However, ILC2-intrinsic IL-33 activation is required for Tregs accumulation *in vivo* and is independent of ILC2 type 2 cytokines but partially dependent on direct co-stimulatory interactions via the inducible costimulator ligand (ICOSL)/ICOS pathway

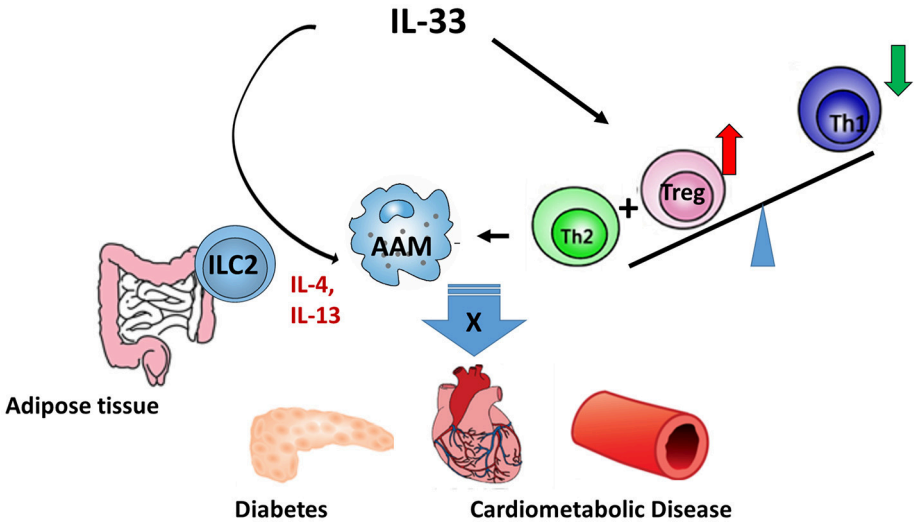

FIGURE 1 | The regulatory role of IL-33 in metabolic diseases. IL-33/ST2 axis regulates metabolic diseases through: (1) promoting AAM polarization; (2) regulating the differentiation and functions of Treg and Th2; and (3) regulating the function of ILC2.

(46). Concordantly, the ST2$^+$ Tregs population is with a higher expression of activated marker ICOS and CD44 (38). Thus, IL-33 plays a protective role in adipose tissue inflammation through directly and indirectly regulating Tregs function.

It has also been reported that increasing severity of insulin resistance and microalbuminuria is strongly correlated with the decreased level of IL-33 in patients with diabetic nephropathy, where an enhanced Th1 and suppressed Th2 response is observed (47). ST2 is selectively and stably expressed on the surface of Th2 cells, and IL-33 can effectively induce the immune response of Th2 cells and the expression of Th2 related cytokines IL-5 and IL-13 without increasing IFN-γ expression (48, 49). These studies suggest that the ST2/IL-33 axis is closely associated with the Th1/Th2 response imbalance in the development of diabetes. Atherosclerosis is characterized by the formation of fibrotic plaques in the major arteries and increased Th1 immune response, which leads to myocardinfal iarction and stroke (50, 51). It has been shown that Th1-to-Th2 shift can reduce the development of atherosclerosis (52, 53). Due to the effect of IL-33 on Th2-type immune response, IL-33 exhibits a protective role in the pathogenesis of atherosclerosis (54). Previous findings also showed that the reduced level of IL-33 might increase the risk of atherosclerosis development for certain individuals (55). These data suggest a crucial role of IL-33 in the lipid metabolism through regulating T cells differentiation.

CONCLUSION

Due to the vital role of IL-33 in the metabolic homeostasis, a sound understanding of the production, regulation, and function of IL-33 will facilitate the treatment of metabolic disorders. The potential mechanisms (**Figure 1**) of IL-33/ST2 axis in the metabolic disorders may include: (1) IL-33 promotes the AAM polarization; (2) IL-33 regulates Tregs and Th2 differentiation and function; and (3) IL-33 regulates the function of ILC2. Notably, the AAM polarization induced by IL-33 depends on Type 2 cytokines, which may be released from ILC2. However, most studies in this area were mainly carried out on animal models and there were limited clinical trials. To what extent IL-33 contributes to metabolic disorders in humans still requires further investigation.

AUTHOR CONTRIBUTIONS

LT and LY reviewed the literature and wrote the first draft. LY finalized the manuscript. LT and LY have read and approved the final manuscript.

FUNDING

This work was supported by the National Natural Science Foundation of China 81700490 to LT.

REFERENCES

1. Schmitz J, Owyang A, Oldham E, Song Y, Murphy E, McClanahan TK, et al. IL-33, an interleukin-1-like cytokine that signals via the IL-1 receptor-related protein ST2 and induces T helper type 2-associated cytokines. *Immunity* (2005) 23:479–90. doi: 10.1016/j.immuni.2005.09.015
2. Baekkevold ES, Roussigne M, Yamanaka T, Johansen FE, Jahnsen FL, Amalric F, et al. Molecular characterization of NF-HEV, a nuclear factor preferentially expressed in human high endothelial venules. *Am J Pathol.* (2003) 163:69–79. doi: 10.1016/S0002-9440(10)63631-0
3. Louten J, Rankin AL, Li Y, Murphy EE, Beaumont M, Moon C, et al. Endogenous IL-33 enhances Th2 cytokine production and T-cell responses

during allergic airway inflammation. *Int Immunol.* (2011) 23:307–15. doi: 10.1093/intimm/dxr006
4. Moussion C, Ortega N, Girard JP. The IL-1-like cytokine IL-33 is constitutively expressed in the nucleus of endothelial cells and epithelial cells *in vivo*: a novel 'alarmin'? *PLoS ONE* (2008) 3:e3331. doi: 10.1371/journal.pone.0003331
5. Dalmas E, Lehmann FM, Dror E, Wueest S, Thienel C, Borsigova M, et al. Interleukin-33-activated islet-resident innate lymphoid cells promote insulin secretion through myeloid cell retinoic acid production. *Immunity* (2017) 47:928–42.e7. doi: 10.1016/j.immuni.2017.10.015
6. Luthi AU, Cullen SP, McNeela EA, Duriez PJ, Afonina IS, Sheridan C, et al. Suppression of interleukin-33 bioactivity through proteolysis by apoptotic caspases. *Immunity* (2009) 31:84–98. doi: 10.1016/j.immuni.2009.05.007
7. Calder PC. n-3 polyunsaturated fatty acids, inflammation, and inflammatory diseases. *Am J Clin Nutr.* (2006) 83 (Suppl. 6):1505S−19S. doi: 10.1093/ajcn/83.6.1505S
8. Zeyda M, Wernly B, Demyanets S, Kaun C, Hammerle M, Hantusch B, et al. Severe obesity increases adipose tissue expression of interleukin-33 and its receptor ST2, both predominantly detectable in endothelial cells of human adipose tissue. *Int J Obes.* (2013) 37:658–65. doi: 10.1038/ijo.2012.118
9. Lee MW, Odegaard JI, Mukundan L, Qiu Y, Molofsky AB, Nussbaum JC, et al. Activated type 2 innate lymphoid cells regulate beige fat biogenesis. *Cell* (2015) 160:74–87. doi: 10.1016/j.cell.2014.12.011
10. Mills CD. Anatomy of a discovery: m1 and m2 macrophages. *Front Immunol.* (2015) 6:212. doi: 10.3389/fimmu.2015.00212
11. Weisberg SP, McCann D, Desai M, Rosenbaum M, Leibel RL, Ferrante AW Jr. Obesity is associated with macrophage accumulation in adipose tissue. *J Clin Investig.* (2003) 112:1796–808. doi: 10.1172/JCI19246
12. Xu H, Barnes GT, Yang Q, Tan G, Yang D, Chou CJ, et al. Chronic inflammation in fat plays a crucial role in the development of obesity-related insulin resistance. *J Clin Investig.* (2003) 112:1821–30. doi: 10.1172/JCI19451
13. Wynn TA, Chawla A, Pollard JW. Macrophage biology in development, homeostasis and disease. *Nature* (2013) 496:445–55. doi: 10.1038/nature12034
14. Chawla A, Nguyen KD, Goh YP. Macrophage-mediated inflammation in metabolic disease. *Nat Rev Immunol.* (2011) 11:738–49. doi: 10.1038/nri3071
15. Espinassous Q, Garcia-de-Paco E, Garcia-Verdugo I, Synguelakis M, von Aulock S, Sallenave JM, et al. IL-33 enhances lipopolysaccharide-induced inflammatory cytokine production from mouse macrophages by regulating lipopolysaccharide receptor complex. *J Immunol.* (2009) 183:1446–55. doi: 10.4049/jimmunol.0803067
16. Miller AM, Asquith DL, Hueber AJ, Anderson LA, Holmes WM, McKenzie AN, et al. Interleukin-33 induces protective effects in adipose tissue inflammation during obesity in mice. *Circ Res.* (2010) 107:650–8. doi: 10.1161/CIRCRESAHA.110.218867
17. Cayley WE Jr. Gout. *BMJ* (2010) 341:c6155. doi: 10.1136/bmj.c6155
18. McCarty DJ, Hollander JL. Identification of urate crystals in gouty synovial fluid. *Ann Intern Med.* (1961) 54:452–60.
19. Takahashi S, Yamamoto T, Moriwaki Y, Tsutsumi Z, Higashino K. Impaired lipoprotein metabolism in patients with primary gout–influence of alcohol intake and body weight. *Br J Rheumatol.* (1994) 33:731–4.
20. Duan L, Huang Y, Su Q, Lin Q, Liu W, Luo J, et al. Potential of IL-33 for preventing the kidney injury via regulating the lipid metabolism in gout patients. *J Diabetes Res.* (2016) 2016:1028401. doi: 10.1155/2016/1028401
21. Chen J, Muntner P, Hamm LL, Jones DW, Batuman V, Fonseca V, et al. The metabolic syndrome and chronic kidney disease in U.S. adults. *Ann Intern Med.* (2004) 140:167–74. doi: 10.7326/0003-4819-140-3-200402030-00007
22. Kurella M, Lo JC, Chertow GM. Metabolic syndrome and the risk for chronic kidney disease among nondiabetic adults. *J Am Soc Nephrol.* (2005) 16:2134–40. doi: 10.1681/ASN.2005010106
23. Li D, Guabiraba R, Besnard AG, Komai-Koma M, Jabir MS, Zhang L, et al. IL-33 promotes ST2-dependent lung fibrosis by the induction of alternatively activated macrophages and innate lymphoid cells in mice. *J Allergy Clin Immunol.* (2014) 134:1422–32.e11. doi: 10.1016/j.jaci.2014.05.011
24. Kurowska-Stolarska M, Stolarski B, Kewin P, Murphy G, Corrigan CJ, Ying S, et al. IL-33 amplifies the polarization of alternatively activated macrophages that contribute to airway inflammation. *J Immunol.* (2009) 183:6469–77. doi: 10.4049/jimmunol.0901575
25. Kurowska-Stolarska M, Kewin P, Murphy G, Russo RC, Stolarski B, Garcia CC, et al. IL-33 induces antigen-specific IL-5$^+$ T cells and promotes allergic-induced airway inflammation independent of IL-4. *J Immunol.* (2008) 181:4780–90. doi: 10.4049/jimmunol.181.7.4780
26. Moro K, Yamada T, Tanabe M, Takeuchi T, Ikawa T, Kawamoto H, et al. Innate production of T(H)2 cytokines by adipose tissue-associated c-Kit$^+$Sca-1$^+$ lymphoid cells. *Nature* (2010) 463:540–4. doi: 10.1038/nature08636
27. Mjosberg JM, Trifari S, Crellin NK, Peters CP, van Drunen CM, Piet B, et al. Human IL-25- and IL-33-responsive type 2 innate lymphoid cells are defined by expression of CRTH2 and CD161. *Nat Immunol.* (2011) 12:1055–62. doi: 10.1038/ni.2104
28. Lefrancais E, Duval A, Mirey E, Roga S, Espinosa E, Cayrol C, et al. Central domain of IL-33 is cleaved by mast cell proteases for potent activation of group-2 innate lymphoid cells. *Proc Nat Acad Sci USA.* (2014) 111:15502–7. doi: 10.1073/pnas.1410700111
29. Johansson K, Malmhall C, Ramos-Ramirez P, Radinger M. Bone marrow type 2 innate lymphoid cells: a local source of interleukin-5 in interleukin-33-driven eosinophilia. *Immunology* (2018) 153:268–78. doi: 10.1111/imm.12842
30. Camelo A, Rosignoli G, Ohne Y, Stewart RA, Overed-Sayer C, Sleeman MA, et al. IL-33, IL-25, and TSLP induce a distinct phenotypic and activation profile in human type 2 innate lymphoid cells. *Blood Adv.* (2017) 1:577–89. doi: 10.1182/bloodadvances.2016002352
31. Hayakawa H, Hayakawa M, Tominaga SI. Soluble ST2 suppresses the effect of interleukin-33 on lung type 2 innate lymphoid cells. *Biochem Biophys Rep.* (2016) 5:401–7. doi: 10.1016/j.bbrep.2016.02.002
32. Molofsky AB, Nussbaum JC, Liang HE, Van Dyken SJ, Cheng LE, Mohapatra A, et al. Innate lymphoid type 2 cells sustain visceral adipose tissue eosinophils and alternatively activated macrophages. *J Exp Med.* (2013) 210:535–49. doi: 10.1084/jem.20121964
33. Duffen J, Zhang M, Masek-Hammerman K, Nunez A, Brennan A, Jones JEC, et al. Modulation of the IL-33/IL-13 axis in obesity by IL-13Ralpha2. *J Immunol.* (2018) 200:1347–59. doi: 10.4049/jimmunol.1701256
34. Miyara M, Ito Y, Sakaguchi S. TREG-cell therapies for autoimmune rheumatic diseases. *Nat Rev Rheumatol.* (2014) 10:543–51. doi: 10.1038/nrrheum.2014.105
35. Zdravkovic N, Shahin A, Arsenijevic N, Lukic ML, Mensah-Brown EP. Regulatory T cells and ST2 signaling control diabetes induction with multiple low doses of streptozotocin. *Mol Immunol.* (2009) 47:28–36. doi: 10.1016/j.molimm.2008.12.023
36. Biton J, Khaleghparast Athari S, Thiolat A, Santinon F, Lemeiter D, Herve R, et al. *In vivo* expansion of activated Foxp3$^+$ regulatory T cells and establishment of a type 2 immune response upon IL-33 treatment protect against experimental arthritis. *J Immunol.* (2016) 197:1708–19. doi: 10.4049/jimmunol.1502124
37. Matta BM, Turnquist HR. Expansion of regulatory T cells *in vitro* and *in vivo* by IL-33. *Methods Mol Biol.* (2016) 1371:29–41. doi: 10.1007/978-1-4939-3139-2_3
38. Matta BM, Lott JM, Mathews LR, Liu Q, Rosborough BR, Blazar BR, et al. IL-33 is an unconventional Alarmin that stimulates IL-2 secretion by dendritic cells to selectively expand IL-33R/ST2$^+$ regulatory T cells. *J Immunol.* (2014) 193:4010–20. doi: 10.4049/jimmunol.1400481
39. Turnquist HR, Zhao Z, Rosborough BR, Liu Q, Castellaneta A, Isse K, et al. IL-33 expands suppressive CD11b$^+$ Gr-1(int) and regulatory T cells, including ST2L$^+$ Foxp3$^+$ cells, and mediates regulatory T cell-dependent promotion of cardiac allograft survival. *J Immunol.* (2011) 187:4598–610. doi: 10.4049/jimmunol.1100519
40. Duan L, Chen J, Zhang H, Yang H, Zhu P, Xiong A, et al. Interleukin-33 ameliorates experimental colitis through promoting Th2/Foxp3$^+$ regulatory T-cell responses in mice. *Mol Med.* (2012) 18:753–61. doi: 10.2119/molmed.2011.00428
41. Schiering C, Krausgruber T, Chomka A, Frohlich A, Adelmann K, Wohlfert EA, et al. The alarmin IL-33 promotes regulatory T-cell function in the intestine. *Nature* (2014) 513:564–8. doi: 10.1038/nature13577
42. Zhu J, Xu Y, Zhu C, Zhao J, Meng X, Chen S, et al. IL-33 induces both regulatory B cells and regulatory T cells in dextran sulfate sodium-induced colitis. *Int Immunopharmacol.* (2017) 46:38–47. doi: 10.1016/j.intimp.2017.02.006

43. Feuerer M, Herrero L, Cipolletta D, Naaz A, Wong J, Nayer A, et al. Lean, but not obese, fat is enriched for a unique population of regulatory T cells that affect metabolic parameters. *Nat Med.* (2009) 15:930–9. doi: 10.1038/nm.2002
44. Vasanthakumar A, Moro K, Xin A, Liao Y, Gloury R, Kawamoto S, et al. The transcriptional regulators IRF4, BATF and IL-33 orchestrate development and maintenance of adipose tissue-resident regulatory T cells. *Nat Immunol.* (2015) 16:276–85. doi: 10.1038/ni.3085
45. Kolodin D, van Panhuys N, Li C, Magnuson AM, Cipolletta D, Miller CM, et al. Antigen- and cytokine-driven accumulation of regulatory T cells in visceral adipose tissue of lean mice. *Cell Metab.* (2015) 21:543–57. doi: 10.1016/j.cmet.2015.03.005
46. Molofsky AB, Van Gool F, Liang HE, Van Dyken SJ, Nussbaum JC, Lee J, et al. Interleukin-33 and interferon-gamma counter-regulate group 2 innate lymphoid cell activation during immune perturbation. *Immunity* (2015) 43:161–74. doi: 10.1016/j.immuni.2015.05.019
47. Anand G, Vasanthakumar R, Mohan V, Babu S, Aravindhan V. Increased IL-12 and decreased IL-33 serum levels are associated with increased Th1 and suppressed Th2 cytokine profile in patients with diabetic nephropathy (CURES-134). *Int J Clin Exp Pathol.* (2014) 7:8008–15.
48. Xu D, Chan WL, Leung BP, Huang F, Wheeler R, Piedrafita D, et al. Selective expression of a stable cell surface molecule on type 2 but not type 1 helper T cells. *J Exp Med.* (1998) 187:787–94.
49. Yin H, Li XY, Jin XB, Zhang BB, Gong Q, Yang H, et al. IL-33 prolongs murine cardiac allograft survival through induction of TH2-type immune deviation. *Transplantation* (2010) 89:1189–97. doi: 10.1097/TP.0b013e3181d720af
50. Hansson GK, Libby P. The immune response in atherosclerosis: a double-edged sword. *Nat Rev Immunol.* (2006) 6:508–19. doi: 10.1038/nri1882
51. Lusis AJ, Mar R, Pajukanta P. Genetics of atherosclerosis. *Ann Rev Genomics Hum Genet.* (2004) 5:189–218. doi: 10.1146/annurev.genom.5.061903.175930
52. Lusis AJ. Atherosclerosis. *Nature* (2000) 407:233–41. doi: 10.1038/35025203
53. de Boer OJ, van der Wal AC, Verhagen CE, Becker AE. Cytokine secretion profiles of cloned T cells from human aortic atherosclerotic plaques. *J Pathol.* (1999) 188:174–9. doi: 10.1002/(SICI)1096-9896(199906)188:2<174::AID-PATH333>3.0.CO;2-3
54. Miller AM, Xu D, Asquith DL, Denby L, Li Y, Sattar N, et al. IL-33 reduces the development of atherosclerosis. *J Exp Med.* (2008) 205:339–46. doi: 10.1084/jem.20071868
55. Hasan A, Al-Ghimlas F, Warsame S, Al-Hubail A, Ahmad R, Bennakhi A, et al. IL-33 is negatively associated with the BMI and confers a protective lipid/metabolic profile in non-diabetic but not diabetic subjects. *BMC Immunol.* (2014) 15:19. doi: 10.1186/1471-2172-15-19

Conflict of Interest Statement: The authors declare that the research was conducted in the absence of any commercial or financial relationships that could be construed as a potential conflict of interest.

frontiers in Endocrinology

ORIGINAL RESEARCH
published: 30 January 2019
doi: 10.3389/fendo.2019.00025

Role of Hippocampal Lipocalin-2 in Experimental Diabetic Encephalopathy

Anup Bhusal[1†], *Md Habibur Rahman*[1†], *In-Kyu Lee*[2] *and Kyoungho Suk*[1,3*]

[1] BK21 Plus KNU Biomedical Convergence Program, Departments of Biomedical Science and Pharmacology, School of Medicine, Kyungpook National University, Daegu, South Korea, [2] Division of Endocrinology and Metabolism, Department of Internal Medicine, School of Medicine, Kyungpook National University, Daegu, South Korea, [3] Brain Science and Engineering Institute, Kyungpook National University, Daegu, South Korea

Diabetic encephalopathy is a severe diabetes-related complication in the central nervous system (CNS) that is characterized by degenerative neurochemical and structural changes leading to impaired cognitive function. While the exact pathophysiology of diabetic encephalopathy is not well-understood, it is likely that neuroinflammation is one of the key pathogenic mechanisms that cause this complication. Lipocalin-2 (LCN2) is an acute phase protein known to promote neuroinflammation via the recruitment and activation of immune cells and glia, particularly microglia and astrocytes, thereby inducing proinflammatory mediators in a range of neurological disorders. In this study, we investigated the role of LCN2 in multiple aspects of diabetic encephalopathy in mouse models of diabetes. Here, we show that induction of diabetes increased the expression of both *Lcn2* mRNA and protein in the hippocampus. Genetic deficiency of *Lcn2* significantly reduced gliosis, recruitment of macrophages, and production of inflammatory cytokines in the diabetic mice. Further, diabetes-induced hippocampal toxicity and cognitive decline were both lower in *Lcn2* knockout mice than in the wild-type animals. Taken together, our findings highlight the critical role of LCN2 in the pathogenesis of diabetic encephalopathy.

Keywords: Lipocalin-2, diabetic encephalopathy, hippocampus, glia, neuroinflammation, cognitive dysfunction

OPEN ACCESS

Edited by:
Jixin Zhong,
Case Western Reserve University, United States

Reviewed by:
Hsien-Hui Chung,
National Cheng Kung University, Taiwan
Xiaoqiang Tang,
Sichuan University, China

***Correspondence:**
Kyoungho Suk
ksuk@knu.ac.kr

[†]*These authors have contributed equally to this work*

Specialty section:
This article was submitted to Experimental Endocrinology, a section of the journal Frontiers in Endocrinology

Received: *25 November 2018*
Accepted: *15 January 2019*
Published: *30 January 2019*

Citation:
Bhusal A, Rahman MH, Lee I-K and Suk K (2019) Role of Hippocampal Lipocalin-2 in Experimental Diabetic Encephalopathy. Front. Endocrinol. 10:25. doi: 10.3389/fendo.2019.00025

INTRODUCTION

Diabetic encephalopathy is one of the most severe microvascular complications of diabetes in the central nervous system (CNS). The measurable manifestations of diabetic encephalopathy include electrophysiological and structural changes, as well as cognitive decline (1, 2). Diabetic encephalopathy involves direct neuronal damage caused by persistent hyperglycemia, a phenomenon referred to as glucose neurotoxicity (1, 3). However, the pathogenesis of this disease is poorly understood and its diagnosis is complicated due to multiple pathogenic pathways involved (4, 5). Cognitive impairment is one of the many consequences of such toxicity that reduces the quality of life of patients (6–9). Studies on both humans and rodents have revealed a close association among hyperglycemia, oxidative stress (10–12), mitochondrial dysfunction (13, 14), and activation of inflammatory pathways (11, 15). These phenomena seem to play a crucial role in the structural and functional damage of neurons in the brain, particularly in the hippocampus, thereby leading to diabetic encephalopathy.

Increasing evidence indicates that inflammation plays an important role in the pathogenesis of diabetic encephalopathy (11, 15). Chronic diabetes initiates an inflammatory response through the

activation of glial cells and the upregulation of pro-inflammatory cytokines in the hippocampus in rodent models of diabetes (16, 17). This inflammatory reaction has been suggested to lead to hippocampal neuronal loss (18, 19) and cognitive decline in diabetic mice (17). Therefore, neuroinflammation and its associated endogenous factors in the brain, particularly in the hippocampus, might be useful targets for the prevention and treatment of diabetic encephalopathy. However, molecular targets that can be used for clinical purposes have not been well-explored.

Lipocalin-2 (LCN2), also called neutrophil gelatinase-associated lipocalin (NGAL), is an acute-phase protein that has been reported to be selectively induced in a variety of tissues in diabetic mice (20, 21). LCN2 is a regulator of immune and inflammatory responses in a range of neurological diseases (22–24). Our previous studies have shown that LCN2 causes gliosis, glial activation, and increased expression of inflammatory cytokines (25–27). This inflammatory microenvironment has been correlated with neurodegenerative phenotypes in several disease models. Further, the circulating levels of LCN2 have been reported to be increased in both rodents (28) and patients with diabetes (29, 30). Based on these observations, we hypothesized that LCN2 might play an important role in the development of diabetic encephalopathy. In this study, we used mouse models of diabetes to examine the pathological role of LCN2 in the progression of diabetic encephalopathy. Our results suggest that LCN2 may contribute to the augmentation of hippocampal inflammation and subsequent pathologies associated with diabetic encephalopathy.

MATERIALS AND METHODS

Mouse Breeding and Maintenance

Male C57BL/6 mice (Samtako, Osan, South Korea) and *Lcn2*-/- mice on pure C57BL/6 background were housed under a 12-h light/dark cycle (lights on from 07:00 to 19:00 h) at a constant ambient temperature of 23 ± 2°C with food and water provided *ad libitum*. *Lcn2*-/- mice were kindly provided by Dr. Shizuo Akira (Osaka University, Japan). *Lcn2*+/+ and *Lcn2*-/- mice were back-crossed for eight to ten generations onto the C57BL/6 background to generate homozygous animals free of background effects on the phenotypes, as previously described (31, 32). All experiments were conducted in accordance with the animal care guidelines of the National Institute of Health and efforts were made to minimize the number of animals used as well as animal suffering. Male *Lcn2* wild-type (WT, *Lcn2*+/+) and *Lcn2*-knockout (KO, *Lcn2*-/-) mice aged 8–10 weeks were used in further experiments.

Diabetes Induction

Age-matched *Lcn2* knockout (KO, *Lcn2*-/-) and *Lcn2* wild-type (WT, *Lcn2*+/+) mice of the same background strain (C57BL/6) were used to study diabetic encephalopathy. Diabetes was induced using two experimental protocols described previously (33, 34) with slight modifications. First, multiple low-dose intraperitoneal injections of streptozotocin (STZ) dissolved in citrate buffer at pH 4.5 (MLDS; 40 mg STZ/kg body weight on 5 consecutive days) were administered to induce both pancreatic β-cytotoxic effects and STZ-specific T-cell-dependent immune reactions. Second, a single high-dose intraperitoneal injection of STZ (HDS; 150 mg/kg body weight) was administered to effect direct toxicity in pancreatic β-cells, which results in necrosis within 48–72 h and causes permanent hyperglycemia. Control mice were injected with the same volume of the citrate buffer. The day of the first STZ injection was termed day 0. Blood samples were collected from the tail vein 1 week after the injection, and glycaemia was determined using an SD CodeFreeTM glucometer (SD Biosensor Inc., Suwon, Korea). Animals with fasting blood glucose values >260 mg/dl were considered diabetic.

High-Fat Diet Model

High-fat diet (HFD) fed mice are a robust and efficient model for type 2 diabetes and are commonly used for both mechanistic studies and as a tool for developing novel therapeutic interventions (35–37). Six-week-old male WT (C57BL/6) mice were fed a HFD in which 20% of the calories were derived from carbohydrates and 60% were derived from fat (D12492 pellets; Research Diets, Inc.). Control animals were fed an isocaloric low-fat diet/control diet (CD) in which 70% of the calories were derived from carbohydrates and 10% were derived from fat (D12450B pellets; Research Diets, Inc.). The mice were housed and maintained on a 12-hr light/dark cycle at 22 ± 2°C. Tissues were rapidly collected by sacrificing the mice according to the experimental time-points, and the samples were immediately stored at −80°C.

Enzyme-Linked Immunosorbent Assay (ELISA)

The levels of LCN2 protein in the hippocampus, CSF, and plasma were assessed using the mouse LCN2 ELISA kit (R&D systems). The assays were performed in 96-well plates using the hippocampal tissue, CSF, or plasma (1:10 or 1:100 dilution) as per the manufacturer's protocol. Mouse recombinant LCN2 was used as a standard at concentrations ranging from 75 to 2,500 pg/ml, and the absorbance was measured at 450 and 540 nm using a microplate reader (Molecular Devices). All measurements were obtained from duplicated assays.

Immunofluorescence Staining

Deeply anesthetized mice were sacrificed and subjected to intracardiac perfusion-fixation using a solution of 0.9% sodium chloride (VWR International, LLC) and 4% paraformaldehyde (Sigma-Aldrich) in 0.1 M phosphate-buffered saline (PBS, pH 7.4). Isolated brains were immersion-fixed in 4% paraformaldehyde for 24 h, and then incubated in 30% sucrose and embedded in optimal cutting temperature (OCT) compound for cryoprotection (Tissue-Tek; Sakura Finetek USA, Torrance, CA). Staining was carried out as described previously (27) with some modifications. Coronal brain sections (20-μm thick) were rinsed in PBS and incubated overnight with the following primary antibodies: rabbit anti-ionized calcium-binding adapter molecule 1 (Iba-1, 1:200; Wako, Osaka, Japan), rabbit anti-glial fibrillary acidic protein (GFAP, 1:1,000; Dako, Carpinteria, CA), and mouse anti-cluster of

differentiation 68 (CD68, 1:200; BMA Biomedicals, Switzerland). Following incubation with primary antibodies, the sections were rinsed and incubated with fluorescein isothiocyanate (FITC)-conjugated and Cy3-conjugated secondary antibodies (1:200; Jackson ImmunoResearch, West Grove, PA). Slides were washed and then coverslipped with VECTASHIELD mounting medium (Vector Laboratories, Burlingame, CA). Images of the immunostained tissues were captured using a fluorescence microscope (Leica Microsystems, DM2500, Wetzlar, Germany).

Cresyl Violet, 4′, 6-Diamidino-2-Phenylindole (DAPI), and Hematoxylin and Eosin (H & E) Staining

Neuronal damage was visualized using DAPI (a fluorescent chromophore that binds to double-stranded DNA in the nuclei of all cells), Cresyl violet (a Nissl stain for evaluating neuronal cell body numbers and features) (Sigma-Aldrich) (38, 39), and H & E staining. Following Cresyl violet staining, the number of pyramidal cells showing a distinct nucleus and nucleolus in each CA1 subfield of the hippocampus were counted (27, 40). For DAPI staining, sections were washed in PBS followed by mounting with VECTASHIELD mounting medium (Vector Laboratories, Burlingame, and CA) (41). Similarly, the tissues were stained with Harris' H & E solution, as described previously (42). Further, the Cresyl violet-, H & E-, and DAPI-stained tissues were visualized using bright field microscopy and fluorescent microscopy, respectively.

Quantitative Real-Time and Traditional Reverse Transcription-Polymerase Chain Reaction (PCR)

Mice were deeply anesthetized and then perfused with normal saline through the aorta to remove the blood. Hippocampal tissues were rapidly dissected, frozen in liquid nitrogen, and homogenized in Trizol reagent (Life Technologies, Carlsbad, CA) for total RNA isolation. Total RNA (2 μg) from each sample was reverse-transcribed into cDNA using a first strand cDNA synthesis kit (MBI Fermentas, Hanover, Germany). Real-time PCR was performed using the one-step SYBR® PrimeScript TM RT-PCR kit (Perfect Real-Time; Takara Bio Inc., Tokyo) and the ABI Prism® 7000 sequence detection system (Applied Biosystems, Foster City, CA), according to the manufacturer's instructions. The 2−ΔΔCT method was used to calculate relative changes in gene expression (43), with glyceraldehyde 3-phosphate dehydrogenase (GAPDH) used as an internal control. The nucleotide sequences of the primers used in the real-time-PCR were as follows: *Lcn2*: forward, 5′-CCC CAT CTC TGC TCA CTG TC-3′; reverse, 5′-TTT TTC TGG ACC GCA TTG-3′; *Tnf-α*: forward, 5′-ATG GCC TCC TCA TCA GTT C-3′; reverse, 5′-TTG GTT TGC TAC GAC GTG-3′; *Il-6*, 5′-AGT TGC CTT CTT GGG ACT GA-3′ (forward) and 5′-TCC ACG ATT TCC CAG AGA AC-3′ (reverse) *Gapdh*: forward, 5′-TGG GCT ACA CTG AGC ACC AG-3′; reverse, 5′-GGG TGT CGC TGT TGA AGT CA-3′. Likewise, the traditional reverse transcription-PCR was performed using a DNA Engine Tetrad Peltier Thermal Cycler (MJ Research, Waltham, MA). To analyze the PCR products, 10 μl of each PCR reaction was electrophoresed on a 1% agarose gel and detected under ultraviolet (UV) light. The nucleotide sequences of the primers used in the traditional reverse transcription-PCR were as follows: *Lcn2*: forward, 5′-ATG TCA ACC TCC ACC TGG TC-3′; reverse, 5′-CAC ACT CAC CCA TTC AG-3′; *Gapdh*: forward, 5′-ACC ACA GTC CAT GCC ATC AC-3′; reverse, 5′-TCC ACC ACC CTG TTG CTG TA-3′.

Novel Object Recognition Test

The novel object recognition (NOR) test was performed as described previously (27, 44, 45). The NOR test was performed over 3 days that included a habituation phase (5 min for 1 day), a training phase (10 min for 1 day), and a test phase (10 min for 1 day) for each mouse. The test was conducted using a metal cylinder (diameter, 7 cm; height, 10 cm) and a rectangular plastic cuboid filled with sand (5 × 5 × 10 cm). During the habituation phase, mice were allowed to acclimatize to the testing arena for 5 min in the absence of objects. During the training session, mice were exposed to two identical objects placed in opposite corners of the arena 3 cm away from the walls, and the mice were allowed to explore the objects for 10 min. During the test session, mice were placed in the arena with the familiar object in its previous location and a novel object in the place of the removed object. The total time spent exploring each object was recorded for 10 min. Exploration was defined as being within 3 cm of an object or touching it with the nose. Objects were thoroughly cleaned between trials to eliminate residual odors. The relative exploration time was measured using a discrimination index [(DI) = (time spent at the novel object—time spent at the familiar object)/(time spent at the novel object + time spent at the familiar object)]. N indicated the time spent near the novel object, while F indicated the time spent near the familiar object. Thus, a positive DI value indicates that the mice spent more time exploring the novel object than the familiar object, whereas a DI of 0 indicates that the mice spent equal amounts of time exploring the two objects.

Y-Maze Test

The Y-maze test was performed as described previously (46) with slight modifications. Spatial cognition was examined using the spontaneous alternation task in the Y-maze apparatus. The Y-maze is a three-arm horizontal maze (length, 40 cm; width, 3 cm; wall height, 12 cm) in which the three arms are at equal angles from one another. The animals were initially placed at the center of the maze and allowed to move freely through it during a 7-min session. The series of arm entries were recorded visually; an arm entry was considered to be completed when the hind paws of the mouse were completely placed within the arm. A spontaneous alternation was defined as an entry into a different arm on each consecutive choice (i.e., ABC, CAB, or BCA, but not BAB). The arms of the maze were cleaned thoroughly with water before each trial in order to remove any residual odors. The percentage of alternations was defined as [(number of alternations)/(total arm entries)] × 100.

Passive Avoidance Test

The step-through passive avoidance test was performed as previously described with minor modifications (47, 48). The test was performed over 3 days, including a habituation phase (day 1), a training phase (day 2), and a test phase (day 3) for each mouse. Briefly, the animals were placed in the light compartment of a two-compartment box (one light, one dark; San Diego Instruments, San Diego, CA) with the door to the dark compartment closed. Following 30 s of exploration, the door was opened. When the mouse entered the dark compartment, the door was closed and the mouse received a single electric shock (0.5 mA, 3 s) on the 2nd day. A retention test was conducted after 24 h, and the step-through latency for the animal to enter the dark compartment was recorded without the use of an electric shock. A maximum latency of 300 s was scored if the animal did not enter the dark compartment at all.

Quantification and Statistical Analysis

For the immunohistochemical analysis, 3–4 tissue sections/animal were used to analyze microscopic images of the hippocampus. For the determination of immunofluorescence intensity, the whole image was selected, and the average intensity was measured using the ImageJ software (National Institutes of Health, Bethesda, MD). The graphs represent an average of all the images. Statistical analyses were performed with GraphPad Software (GraphPad Software, La Jolla, CA, USA). All the results have been presented as the means ± standard errors (SE). Statistical comparisons were performed using the Student's *t*-test. Differences with $p < 0.05$ ($p < 0.05$) were considered statistically significant.

RESULTS

LCN2 Expression Is Increased in the Hippocampus of Diabetic Mice

To study the role of LCN2 in the pathogenesis of diabetic encephalopathy, we used multiple animal models of diabetes in this study, including the multiple low dose STZ injection (MLDS), high dose STZ injection (HDS), and high fat diet (HFD) feeding models. First, intraperitoneal administration of STZ induced diabetes with elevated blood glucose levels in the first week post-injection; the increased blood glucose levels were maintained throughout the study (**Supplementary Figure 1**). Next, we examined the expression of *Lcn2* mRNA and protein following STZ injection using conventional RT-PCR and ELISA, respectively. We found a substantial increase in the expression of *Lcn2* mRNA in hippocampal tissues at 8 weeks post MLDS and 4 weeks post HDS administration (**Figures 1A,C**). Similarly, LCN2 protein level in the hippocampus was significantly increased at 8 and 4 weeks post STZ injection in both models compared to the vehicle-injected control groups (**Figures 1B,D**). HFD-fed mice showed a similar upregulation of *Lcn2* mRNA and increased expression of LCN2 protein in the hippocampus (**Figures 1E,F**). The *Lcn2* mRNA expression data was further confirmed by real time-PCR; our results were consistent with the conventional RT-PCR data (**Supplementary Figures 2A–C**).

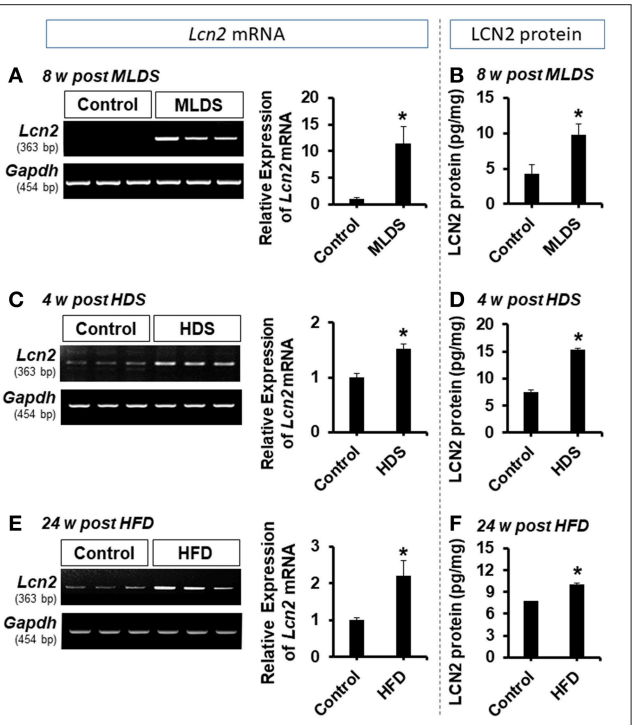

FIGURE 1 | Expression of LCN2 in the hippocampus of diabetic mice. The expression of *Lcn2* mRNA in the hippocampus at 8 w post MLDS and 4 w post HDS injection was assessed by conventional PCR **(A,C)**. Further, the expression level of LCN2 protein in the hippocampus of STZ-induced diabetic mice was estimated by ELISA assay **(B,D)**. Similar upregulation of *Lcn2* mRNA and LCN2 protein was detected in the hippocampus at 24 w post HFD feeding **(E,F)**. *$p < 0.05$ vs. the vehicle-treated control animals; Student's *t*-test; $n = 3$ for each group; data are represented as mean ± SEM. STZ, streptozotocin; MLDS, multiple low dose of STZ; HDS, high dose of STZ; HFD, high fat diet; LCN2, Lipocalin-2; w, weeks; SEM, standard error of the mean.

We predominantly used the MLDS model to investigate the role of LCN2 in the pathogenesis of diabetic encephalopathy because it represents a model of mild type 1 diabetes and closely resembles the pathophysiology observed in human patients (34, 49). The MLDS model is less toxic with a slowly progressive pancreatic β-cell death, and causes gradual elevation of blood glucose levels, minimal muscle weakness and movement abnormalities in mice, thereby providing us with an opportunity to accurately measure animal behavior. We used the HDS model to explore molecular changes and to identify the role of LCN2 in the pathogenesis of diabetic encephalopathy. Further, we also measured the LCN2 level in cerebrospinal fluid (CSF) and blood plasma of the MLDS model mice. The enzyme-linked immunosorbent assay (ELISA) revealed an increased level of LCN2 protein in the CSF and blood plasma of diabetic mice at 8 weeks post MLDS injection, when compared with the vehicle-injected control animals (**Supplementary Figures 2D,E**). These data suggest that induction of diabetes enhances the expression of LCN2 in the hippocampus, CSF, and blood plasma of mice.

Lcn2 Deficiency Reduces Diabetes-Induced Glial Activation, Proliferation, Macrophage Infiltration, and Proinflammatory Cytokine Expression in the Hippocampus

Glial activation and proliferation are well-known pathological features in the CNS across a range of neurological disorders (17, 50). To investigate the role of LCN2 in diabetes-induced changes in glial characteristics, brain sections were immunostained with anti-Iba-1 and anti-GFAP antibodies to label the microglia and astrocytes, respectively (51, 52). Immunofluorescence analysis showed increased immunoreactivity of Iba-1 in the hippocampus of the diabetic mice at 8 weeks (**Figures 2A,B**) and 4 weeks (**Supplementary Figures 3A,B**) post MLDS and HDS injections, respectively. We observed a significant increase in the number of Iba-1-positive microglial cells in the hippocampus of diabetic mice, where microglia exhibited enhanced Iba-1 immunoreactivity with short and thick processes when compared to control mice. These morphological features of the microglia and the increased Iba-1 immunoreactivity in the hippocampus were attenuated in the *Lcn2* KO mice. Similarly, the GFAP-positive astrocytes exhibited increased immunoreactivity and hypertrophic morphology with thick processes in the hippocampus of diabetic mice in comparison with the vehicle-injected control animals; the immunoreactivity and hypertrophic morphology were both significantly reduced in *Lcn2* KO mice. Further, the immunofluorescence-based analyses of CD68 (a macrophage marker in the brain) (53, 54) and Iba-1(a marker for both microglia and macrophages) (55, 56) in the brain tissues from diabetic mice showed a marked increase in the number of infiltrated macrophages in the hippocampus at 8 weeks post-MLDS injection compared with vehicle-injected control animals. Mice with *Lcn2*-deficiency showed a significant decrease in the number of infiltrated macrophages in the hippocampus compared with WT-diabetic animals (**Supplementary Figure 4**).

Furthermore, STZ-induced hyperglycemia increased the expression of *Tnf-α* and *Il-6* mRNA in the hippocampus of diabetic mice, whereas the expression levels of these cytokines were significantly attenuated in the *Lcn2*-deficient mice (**Figure 2C**). These findings indicate that diabetes-induced activation of glial cells and enhanced expression of proinflammatory cytokines in the hippocampus might be direct consequences of pathological inflammation, which is itself modulated by LCN2 activity (52).

Lcn2 Deficiency Attenuates Diabetes-Induced Loss of Hippocampal Neurons

The increased expression of pro-inflammatory cytokines in the brain under diabetic conditions plays an important role in neuronal damage (2, 57). LCN2-mediated glial activation and subsequent inflammatory responses in the diabetic hippocampus led us to investigate the histological changes in the CA1 neurons of the hippocampus. Histological analysis using Cresyl violet and DAPI staining revealed fewer number of neurons in the CA1 of the hippocampus of diabetic mice than in that of vehicle-injected control animals. Moreover, such changes in the diabetic hippocampus were ameliorated by *Lcn2* deficiency (**Figures 3A,B**). Further, the H & E staining data revealed that many of the granular neurons in area CA1 of the hippocampus of WT-diabetic mice were densely stained and showed shrunken appearance with minimal or no cytoplasm compared with control animals. Fewer such degenerative features were found in the granular neurons of *Lcn2* KO mice (**Supplementary Figure 5**). These results indicate that the neurotoxicity in the CA1 region of the hippocampus might be related to the diabetes-induced elevation of LCN2 levels and its contribution to augmented inflammatory processes.

Attenuation of Diabetes-Induced Cognitive Impairment in *Lcn2* KO Mice

To investigate whether the cognitive function of the diabetic mice is impaired and if *Lcn2* deficiency can ameliorate this impairment, we examined the cognitive function of mice using the NOR test, which is based on differential exploration behavior with respect to familiar and new objects, and used to study short-term declarative memory and attention (58). As shown in **Figure 4A**, the discrimination index of the WT-diabetic mice was significantly lower than that of the vehicle-injected control animals. However, *Lcn2*-deficient diabetic mice showed an improved discrimination index compared to the WT-diabetic animals. As an alternative method to confirm whether *Lcn2* deficiency ameliorates diabetes-induced memory dysfunction, we used the Y-maze test, which measures the natural behavioral tendency of mice to explore new environments. Mice typically prefer to investigate a new arm of the maze rather than returning to one that has already been visited. Many parts of the brain, including the hippocampus, are involved in this task (46). Diabetic mice showed a decline in the percentage of spontaneous alteration compared to control animals, indicating an impairment in spatial memory function. However, *Lcn2* deficiency ameliorated this diabetes-induced memory dysfunction (**Figure 4B**). Further, diabetic mice of both genotypes (WT and KO) showed decrease in movement velocity and the number of arm entries at 8 weeks post-MLDS injection, which might be associated with diabetes-induced motor impairments. In line with our findings, several studies have shown a reduction in the number of total arm entries of diabetic mice compared with non-diabetic controls (59–61). Likewise, another study has found a marked reduction in speed and traveling distance of diabetic mice, indicating impairment of exploratory behavior and motor activity (62). In order to address these limitations and to confirm the changes observed in NOR and Y-maze test performances following diabetes, we performed the passive avoidance test, which is fear-aggravated, and requires lesser movement to evaluate learning and memory in rodent models of CNS disorders (48, 63). This behavior requires the association between a normally neutral environment and an aversive stimulus, which is dependent on hippocampal function. In passive avoidance test, we found that the latency during the learning trial did not differ among the experimental and control

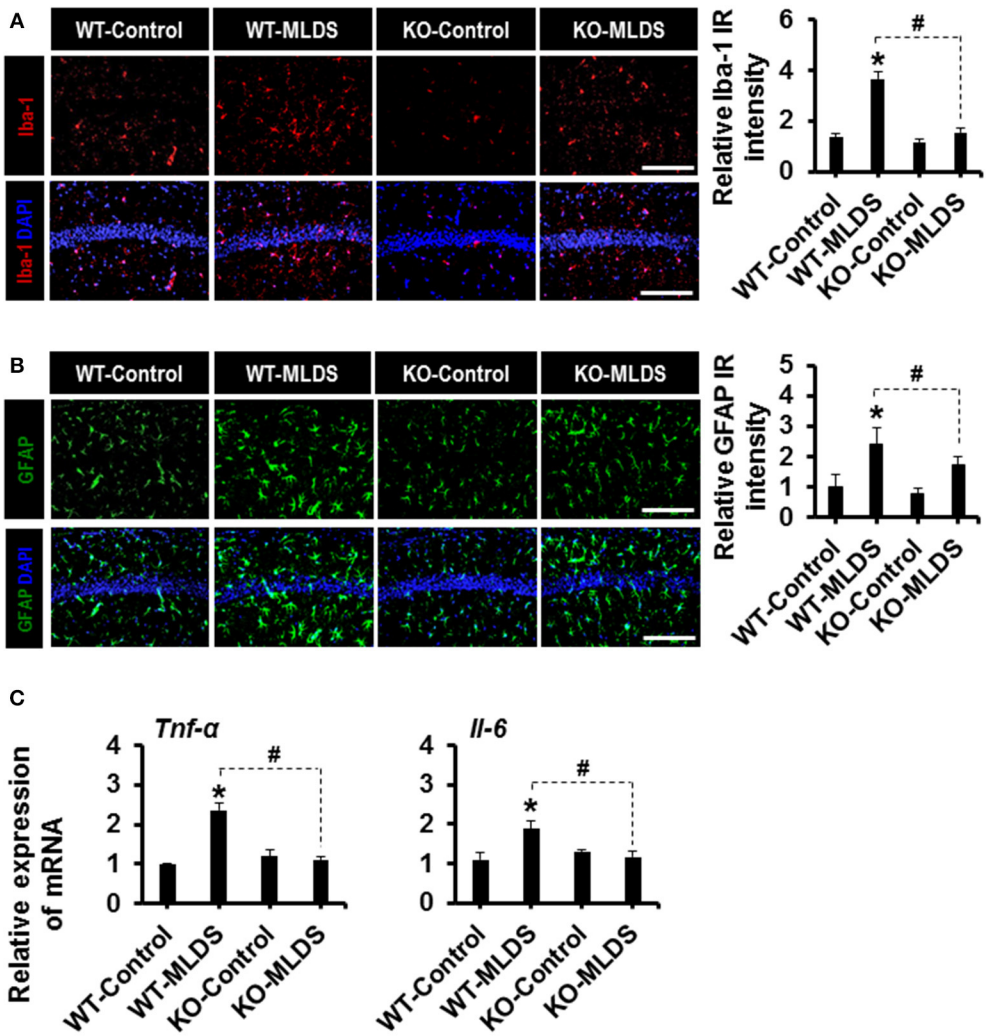

FIGURE 2 | Effect of *Lcn2*-deficiency on diabetes-induced gliosis and proinflammatory cytokines in the hippocampus. Immunoreactivity (IR) of Iba-1 and GFAP was increased in the hippocampus of WT mice at 8 w post MLDS injection, whereas mice with *Lcn-2* deficiency attenuated this increase in IR **(A,B)**. The quantification of relative intensity of IR is presented adjacent to the microscopic images. The expression levels of *Tnf-α* and *Il-6* mRNAs in the hippocampus after 8 weeks of MLDS injection were evaluated by real time PCR **(C)**. *$p < 0.05$ vs. the vehicle-treated control animals; #p<0.05 between the indicated groups; Student's *t*-test; $n = 3$ for each group; data are represented as mean ± SEM. Scale bar, 200 μm. WT, wild type; KO, knockout; MLDS, multiple low dose of STZ; w, weeks; SEM, standard error of the mean.

groups, indicating that all the mice had similar responses to the testing environment and the electric shock. However, as shown in **Figure 4C**, *Lcn2*-deficient mice showed longer latency than the WT-diabetic animals 24 h after the training process. However, we found no significant difference between the vehicle-injected control mice groups. These findings suggest that LCN2 plays a crucial role in the development of cognitive impairment associated with diabetic encephalopathy.

DISCUSSION

Diabetic encephalopathy is one of the most severe complications of diabetes mellitus that involves cognitive dysfunction and an increased incidence of dementia (64–69). Growing evidence points to the role of neuroinflammation in the progression of clinically well-recognized complications of diabetes like encephalopathy (70, 71). Several epidemiological studies have shown a strong link between poor cognitive ability and elevated inflammatory markers in patients with diabetes (72–74). Thus, targeting inflammation might be an important therapeutic strategy for the treatment of diabetic encephalopathy. Inflammation, especially in the hippocampus may lead to impairments in a variety of cognitive domains as it is the center for learning and memory processing in the brain (75, 76). The role of LCN2 in neuroinflammation and cognitive function has already been established. In the current study, we used STZ-induced diabetes and HFD mice models to evaluate the expression level of LCN2 in the

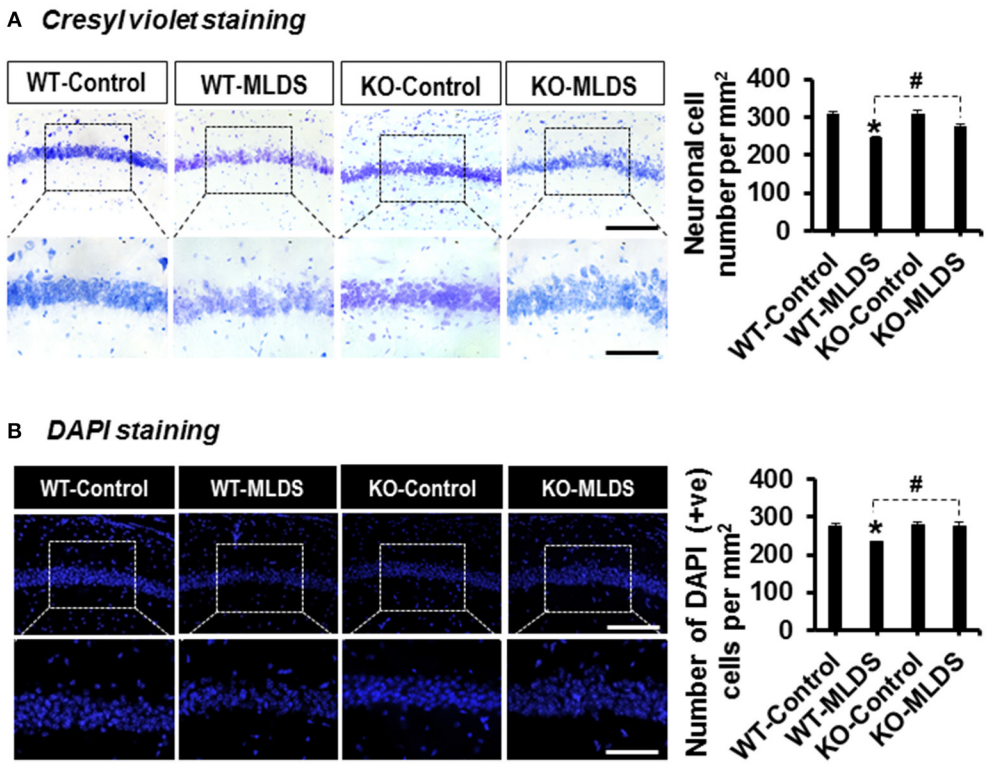

FIGURE 3 | *Lcn2*-deficiency protects hippocampal neurons following diabetes induction. The number of viable neurons in the hippocampal CA1 area was determined using Cresyl violet and DAPI staining at 8 w post MLDS injection. The quantification of hippocampal neuronal number is presented adjacent to the microscopic images **(A,B)**. $^{*}p < 0.05$ vs. the vehicle-treated control animals; $^{\#}p < 0.05$ between the indicated groups; Student's *t*-test; $n = 3$ for each group; data are represented as mean ± SEM. Scale bar, 200 and 100 μm in the original and magnified images, respectively. DAPI, 4′, 6-diamidino-2-phenylindole; WT, wild type; KO, knockout; MLDS, multiple low dose of STZ; w, weeks; +ve, positive; SEM, standard error of mean.

hippocampus. We further employed the MLDS model to study the encephalopathy and associated cognitive impairment in diabetic mice in greater detail. We found that the induction of diabetes through STZ administration and HFD feeding significantly increased the expression of LCN2 in the hippocampus at the level of mRNA and protein. Further, deletion of the *Lcn2* gene ameliorated the diabetes-induced reactive gliosis in the hippocampus seen in the WT-diabetic mice. In addition, the hyperglycemia-induced increase in expression of pro-inflammatory cytokines was significantly attenuated in *Lcn2* KO mice. Moreover, *Lcn2*-deficient mice showed decreased neuronal loss in the CA1 region of the hippocampus following diabetes, an effect that was correlated with improved cognitive behavior in these animals. These results suggest that the diabetes-induced increase in the hippocampal LCN2 level causes neuroinflammation, which may play an important role in the development of diabetic encephalopathy and associated impairments in cognitive function (**Figure 5**).

Several *in vivo* studies have revealed the effect of STZ-induced diabetes on LCN2 expression in the peripheral tissues of rodents (77, 78). In these studies, STZ-induced diabetic rodents showed enhanced expression of LCN2 in the kidney and adipose tissues, respectively. However, the expression of LCN2 in the brain has not yet been studied using a mouse model of STZ-induced diabetes. To our knowledge, this is the first study to report the upregulation of LCN2 and its pathological role in the mouse hippocampus following STZ injection, which is an insulin-deficient diabetes model. As HFD-fed and STZ-injected mice are characterized by hyperinsulinemia and insulinopenic state, respectively, it is important to understand whether the presence or absence of insulin affects the expression of LCN2.

It has been reported that insulin treatment of STZ-induced diabetic mice leads to decreased LCN2 expression in skin excisional wound tissues, which has been proposed as a potential therapeutic target for improving diabetic wound healing (79). Further, HFD-fed mice show insulin resistance and hyperinsulinemia (80). In this condition, insulin cannot be used to correct the diabetic state. It has been reported that proliferator-activated receptor-γ agonist rosiglitazone, an insulin sensitizer, markedly decreases LCN2 expression in both obese mice and humans, which is correlated with a decrease in inflammation and improved insulin sensitivity (20, 28). However, upregulation of LCN2 in 3T3-L1 adipocytes by insulin treatment under hyperglycemic condition has also been reported, suggesting that glucose metabolism is required for the effect of insulin on LCN2 expression (81). In line with this, a human study revealed that circulating LCN2 level is increased after insulin intake, and also

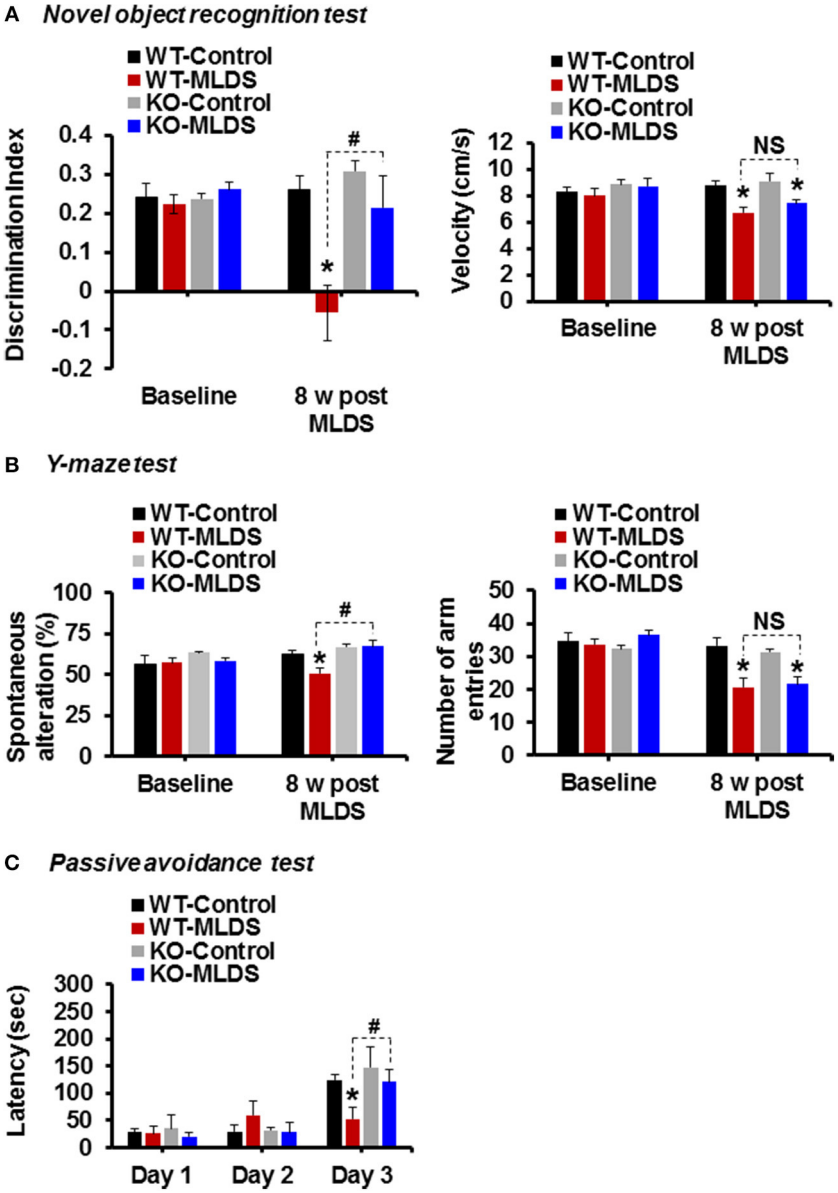

FIGURE 4 | Genetic ablation of the *Lcn2* gene alleviates diabetes-induced cognitive deficits. Memory impairment in diabetic mice was measured using the novel-object recognition, Y-maze, and passive avoidance tests at 8 w post MLDS injection. The discrimination index and velocity are shown **(A)**. Spatial cognition deficit was assessed using the Y-maze test. The number of alternations and total arm entries **(B)** were compared. Cognitive impairment was further evaluated using the passive avoidance test **(C)**. $^{*}p < 0.05$ vs. the vehicle-treated control animals; $^{\#}p < 0.05$ between the indicated groups; Student's *t*-test; $n = 8$–10 for each group; data are represented as mean ± SEM. WT, wild type; KO; knockout; MLDS, multiple low dose of STZ; w, weeks; NS, not significant; SEM, standard error of mean.

highlighted the involvement of both phosphoinositide 3-kinase and mitogen-activated protein kinase signaling pathways in insulin-induced LCN2 upregulation (82). These findings suggest a regulatory role of insulin in mediating the effects of LCN2 in metabolic diseases. Future studies may explain the mechanistic correlation between metabolic hormones and LCN2 induction with respect to neuroinflammation.

Several epidemiological studies have found increased levels of markers and mediators of inflammation in diabetic condition (83, 84). In the brain, microglia and astrocytes are the immune cells, and play a nuanced role in neuroprotection and maintenance of homeostasis (85, 86). However, under pathological conditions, such as diabetes, reactive gliosis is a well-known phenomenon (16, 87, 88). Consistently, in the present study, STZ-induced diabetes caused significant microglial and astrocytic activation 8 weeks after the injection. However, glial activation was attenuated in the *Lcn2* KO diabetic mice compared with WT mice. This result can be compared to our previous

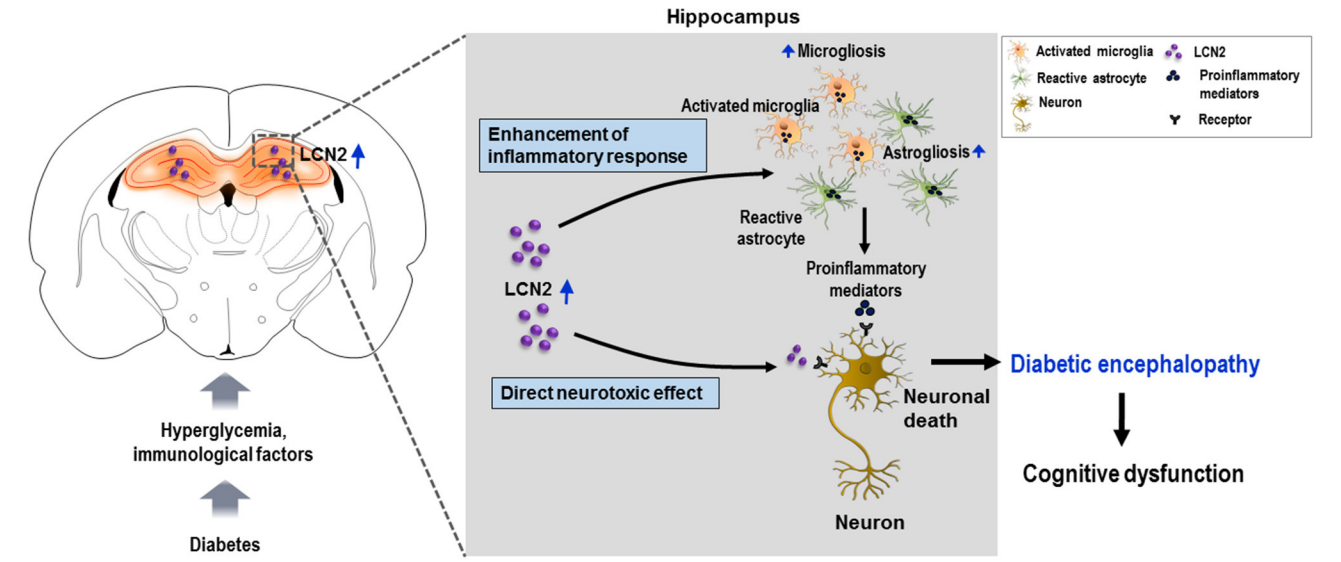

FIGURE 5 | Schematic representation of the role of LCN2 in diabetic encephalopathy. Diabetes leads to the upregulation of LCN2 in the hippocampus. Induction of LCN2 enhances inflammatory activation of microglia and astrocytes, and macrophage infiltration, which causes increased expression and release of proinflammatory mediators such as *Tnf-α* and *Il-6* in the diabetic hippocampus. It is suggested that increased levels of LCN2 and proinflammatory mediators produced as a result may cause hippocampal neurotoxicity and cognitive deficits observed in diabetic mice. LCN2 may also directly induce neuronal damage by interacting with the LCN2 receptor on the surface of neurons, ultimately leading to encephalopathy in the diabetic condition. LCN2, lipocalin-2.

finding, in which LCN2 produced phenotypic changes in glia via Rho-associated protein kinase, and affected their migration by secreting chemokines (52). Further, LCN2 is known to act via autocrine and paracrine mechanisms to activate and recruit macrophages at the site of inflammation (89). These macrophages may further induce inflammatory mediators and exacerbate the immune response. In our study, we observed increased number of macrophages in the hippocampus of diabetic mice. A previous study using fluorescence-activated cell sorting revealed an increase in blood-brain barrier permeability, leading to macrophage infiltration in the brain of db/db mice (90). These findings suggest that the gliosis and macrophage infiltration that occur in the hippocampus of diabetic mice is likely mediated by LCN2, and that deletion of *Lcn2* prevents the inflammatory reactive gliosis and macrophage infiltration associated with encephalopathy.

Activation of immune cells in the brain of diabetic subject has been associated with several manifestations of diabetic encephalopathy (84, 91). This has been attributed to the effects of poorly controlled hyperglycemia that triggers activation of inflammatory transcription factors, such as nuclear factor kappa B, and the release of proinflammatory cytokines (91–93). LCN2 is known to stimulate various immune cells like neutrophils (94), microglia, and astrocytes (27, 95) to produce vital proinflammatory mediators, such as IL-6, IL-8, and TNF-α. In addition, the inflammatory factors released by microglia can activate astrocytes, and factors released from astrocytes may, in turn, activate microglia, further aggravating the situation (96, 97). These neurotoxic inflammatory cytokines, once released under diabetic conditions, might act directly on neurons to induce apoptosis and cell death (98, 99). In our study, WT-diabetic mice showed elevated inflammatory cytokines such as *Tnf-α* and *Il-6* in the hippocampus, which may be due to LCN2-mediated activation of glial cells and recruitment of immune cells therein. Cognitive impairment following HFD consumption is associated with neuroinflammation impairing insulin signaling in the hippocampus of experimental animals (100). Similarly, in STZ-induced diabetic mice, hyperglycemic stress and inflammation progressively worsen the condition in the hippocampus, leading to neurodegeneration and, ultimately, diabetic encephalopathy (4). Based on these findings, it is suggested that LCN2-mediated neuroinflammation may be a potential mechanism underlying diabetic encephalopathy and cognitive deficit in both type 1 and type 2 diabetes mellitus.

Chronic neuroinflammation plays an important role in the onset and progression of various neurodegenerative diseases (101). Neurodegeneration is a condition in which neuronal structure and function are altered, leading to reduced neuronal survival and increased neuronal death in the CNS (102). Recent evidence points to an important role of LCN2 in the pathophysiology of sterile inflammatory conditions like obesity and diabetes (28, 30, 103, 104). However, LCN2 has been shown to have contradictory roles in the development of obesity or diabetes in rodents. An *in vitro* study by Zhang et al. recently demonstrated that exposure of primary adipocytes to recombinant LCN2 protein inhibits the expression of *Tnf-α* mRNA, which is suggested to be mediated by the induction of peroxisome proliferator-activated receptor gamma, a key anti-inflammatory transcription factor (105). On the contrary, Law et al. have shown that LCN2 deficiency attenuates

obesity-induced expression and activity of 12-lipoxygenase and production of TNF-α in the mouse fat tissue (103). However, several studies have reported that LCN2 contributes to immune and inflammatory responses in the brain, eventually leading to the development of neurodegenerative diseases (22, 23, 106, 107). Once released, LCN2 binds to its cell-surface receptor LCN2R to regulate neuroinflammation and cell death (31, 108). In our study, Cresyl violet and DAPI staining revealed significant neuronal loss in the CA1 region of the hippocampus of diabetic WT mice compared to *Lcn2* KO mice, which is consistent with other studies (27, 41). Further, this result was supported by H & E staining. These results suggest that elevated levels of LCN2 in the hippocampus may potentiate neuroinflammation and cause neuronal loss following diabetes.

Various studies indicate that neuroinflammation and neuronal cell death are implicated in diabetes-associated learning and memory deficits (57, 62). Previously, our research group has reported increased LCN2 levels in patients with cognitive impairment (109); these findings are consistent with the study by Dekens et al. (110). In this study, WT-diabetic mice showed poor cognitive function when compared with *Lcn2* KO mice as measured by the NOR, Y-maze, and passive avoidance tests. In chronic conditions such as diabetes, over-secretion of LCN2 in the hippocampus may subsequently aggravate the neural imbalance in the hippocampus, and lead to impaired cognitive function. Our previous findings of LCN2 treatment inducing inflammatory activation of glial cells and having a toxic effect on co-cultured hippocampal neurons supports this notion (27). Other groups have reported a specific role of LCN2 in the decline of cognitive function (111) and suggested that its upregulation following stress reduces dendritic spine density in hippocampal neurons (112). Taken together, these findings suggest that LCN2 can mediate neuroinflammation via activation of glial cells and increased expression of inflammatory cytokines which leads to hippocampal neuronal death and impairs cognitive function across domains in patients with diabetes (**Figure 5**). Thus, LCN2 upregulation in the hippocampus might be a potential pathogenic mechanism leading to further disruption of the hippocampus through neuroinflammation in the diabetic state. Increased level of circulating LCN2 has been considered an inflammatory marker closely associated with insulin resistance and hyperglycemia in patients with diabetes (20). Therefore, the control of hyperglycemia-induced expression of LCN2 or its activity in the hippocampus may be important for neuroprotection in these patients.

In summary, our findings suggest that increased LCN2 expression due to diabetes is critical for the development of several manifestations of diabetic encephalopathy, in which LCN2-mediated inflammatory reaction as well as direct toxicity by interacting with its receptors in the hippocampal neurons of diabetic animals has been proposed as a potential mechanism. The extent to which it can worsen cognitive ability in diabetic mice makes LCN2 a promising target for therapeutic interventions against diabetic encephalopathy.

ETHICS STATEMENT

This study was carried out in accordance with the recommendations of Kyungpook National University Animal Care Committee. The protocol was approved by Kyungpook National University Animal Care Committee.

AUTHOR CONTRIBUTIONS

All authors have made a substantial intellectual contribution to this work, and approved submission of the manuscript. AB and MR designed and performed the research, analyzed the data, and prepared the manuscript. I-KL provided essential reagents. KS directed the study and was involved in all aspects of the experimental design, data analysis, and manuscript preparation.

ACKNOWLEDGMENTS

This work was supported by a grant from the Korea Healthcare Technology R&D Project, Ministry of Health & Welfare, Republic of Korea (HI16C1501) and the Basic Science Research Program through the National Research Foundation (NRF), which is funded by the Korean government (MSIP) (2018R1A2A1A05077118, 2016M3C7A1904148, NRF-2017R1A5A2015391).

SUPPLEMENTARY MATERIAL

The Supplementary Material for this article can be found online at: https://www.frontiersin.org/articles/10.3389/fendo.2019.00025/full#supplementary-material

Supplementary Figure 1 | Blood glucose levels in STZ-induced diabetic mice. After intraperitoneal injection of low dose of STZ (MLDS), blood glucose levels significantly increased within the first week and remained significantly high throughout the course of the study as compared to control non-diabetic animals. $^*p < 0.05$ vs. the vehicle-treated control animals; Student's *t*-test; $n = 4$–6 for each group; data are represented as mean ± SEM. WT, wild type; KO; knockout; MLDS, multiple low dose of STZ; w, weeks; SEM, standard error of mean.

Supplementary Figure 2 | LCN2 expression following diabetes induction. The expression of *Lcn2* mRNA in the hippocampus at 8 w of MLDS **(A)** and 4 w of HDS **(B)** injection, and 24 w post HFD feeding **(C)** was assessed using real-time PCR. Further, the expression levels of LCN2 protein in the CSF **(D)** and blood plasma **(E)** from diabetic mice were estimated using ELISA. $^*p < 0.05$ vs. the vehicle-treated control animals; Student's *t*-test; $n = 3$ for each group; data are represented as mean ± SEM. MLDS, multiple low dose of STZ; HDS, high dose of STZ, HFD, high fat diet; LCN2, Lipocalin-2; PCR, polymerase chain reaction; CSF, cerebrospinal fluid; ELISA, enzyme-linked immunosorbent assay; w, weeks; SEM, standard error of mean.

Supplementary Figure 3 | Effect of *Lcn2*-deficiency on diabetes (HDS)-induced gliosis in the hippocampus. Immunoreactivity (IR) of Iba-1 and GFAP was increased in the hippocampus of WT mice after 4 w of HDS injection, whereas *Lcn-2* deficiency attenuated such an increase in IR **(A,B)**. The quantification of relative intensity of IR is presented adjacent to the microscopic images. $^*p < 0.05$ vs. the vehicle-treated control animals; $\#p < 0.05$ between the indicated groups; Student's *t*-test; $n = 3$ for each group; data are represented as mean ± SEM. Scale bar, 200 μm (Iba-1 stained images) and 100 μm (GFAP-stained images). WT, wild-type; KO, knockout; NS, not significant; HDS, high dose of STZ; w, weeks; SEM, standard error of mean; Iba-1, ionized calcium-binding adapter molecule 1; GFAP, glial fibrillary acidic protein.

Supplementary Figure 4 | Macrophage infiltration in the hippocampus of diabetic mice. To determine the role of *Lcn2*-deficiency in diabetes-induced infiltration of macrophages in the hippocampus, co-immunostaining of CD68 (red) and Iba-1 (green) was performed using brain tissue sections collected from WT and *Lcn2* KO mice at 8 w post-MLDS/vehicle injection. Quantification of $CD68^{+}$/Iba-1^{-} cells (macrophages) is presented adjacent to the representative images. Arrows indicate the $CD68^{+}$ macrophages. $^{*}p < 0.05$ vs. vehicle-treated control animals, $\#p < 0.05$ between the indicated groups, Student's *t*-test; $n = 3$ for each group; data are presented as mean ± SEM. Scale bar, 200 μm. CD68, cluster of differentiation 68; Iba-1, ionized calcium-binding adapter molecule 1; WT, wild type; KO, knockout; MLDS, multiple low doses of streptozotocin; w, weeks; SEM, standard error of the mean.

Supplementary Figure 5 | *Lcn2*-deficiency confers protection against diabetes-induced degeneration of hippocampal granular neurons. To determine the role of LCN2 in diabetes-induced loss of hippocampal tissue integrity and neuronal degeneration, H and E staining was performed using brain tissue sections collected from WT and *Lcn2* KO mice at 8 w post-MLDS/vehicle injection. Quantification of percentage of degenerated neurons in the hippocampus is presented adjacent to the representative images. $^{*}p < 0.05$ vs. vehicle-treated control animals, $\#p < 0.05$ between the indicated groups, Student's *t*-test; $n = 3$ for each group; data are presented as mean ± SEM. Scale bar, 200 and 100 μm in the original and magnified images, respectively. LCN2, lipocalin-2; H and E, hematoxylin and eosin; WT, wild type; KO, knockout; MLDS, multiple low doses of streptozotocin; w, weeks; SEM, standard error of mean.

REFERENCES

1. Cai XJ, Xu HQ, Lu Y. C-peptide and diabetic encephalopathy. *Chin Med Sci J.* (2011) 26:119–25. doi: 10.1016/S1001-9294(11)60031-X
2. Gaspar JM, Baptista FI, Macedo MP, Ambrosio AF. Inside the diabetic brain: role of different players involved in cognitive decline. *ACS Chem Neurosci.* (2016) 7:131–42. doi: 10.1021/acschemneuro.5b00240
3. Tomlinson DR, Gardiner NJ. Glucose neurotoxicity. *Nat Rev Neurosci.* (2008) 9:36–45. doi: 10.1038/nrn2294
4. Sima AA. Encephalopathies: the emerging diabetic complications. *Acta Diabetol.* (2010) 47:279–93. doi: 10.1007/s00592-010-0218-0
5. Vieira LL, de Lima Soares RG, da Silva Felipe SM, de Moura FC, de Castro Brito GA, Pacheco C, et al. Physiological targets for the treatment of diabetic encephalopathy. *Cent Nerv Syst Agents Med Chem.* (2017) 17:78–86. doi: 10.2174/1871524916666160428111015
6. Manschot SM, Brands AM, van der Grond J, Kessels RP, Algra A, Kappelle LJ, et al. Brain magnetic resonance imaging correlates of impaired cognition in patients with type 2 diabetes. *Diabetes* (2006) 55:1106–13. doi: 10.2337/diabetes.55.04.06.db05-1323
7. Kodl CT, Seaquist ER. Cognitive dysfunction and diabetes mellitus. *Endocr Rev.* (2008) 29:494–511. doi: 10.1210/er.2007-0034
8. Moore EM, Mander AG, Ames D, Kotowicz MA, Carne RP, Brodaty H, et al. Increased risk of cognitive impairment in patients with diabetes is associated with metformin. *Diabetes Care* (2013) 36:2981–7. doi: 10.2337/dc13-0229
9. Saedi E, Gheini MR, Faiz F, Arami MA. Diabetes mellitus and cognitive impairments. *World J Diabetes* (2016) 7:412–22. doi: 10.4239/wjd.v7.i17.412
10. Giacco F, Brownlee M. Oxidative stress and diabetic complications. *Circ Res.* (2010) 107:1058–70. doi: 10.1161/CIRCRESAHA.110.223545
11. Muriach M, Flores-Bellver M, Romero FJ, Barcia JM. Diabetes and the brain: oxidative stress, inflammation, and autophagy. *Oxid Med Cell Longev.* (2014) 2014:102158. doi: 10.1155/2014/102158
12. Asmat U, Abad K, Ismail K. Diabetes mellitus and oxidative stress-A concise review. *Saudi Pharm J.* (2016) 24:547–53. doi: 10.1016/j.jsps.2015.03.013
13. Sivitz WI, Yorek MA. Mitochondrial dysfunction in diabetes: from molecular mechanisms to functional significance and therapeutic opportunities. *Antioxid Redox Signal.* (2010) 12:537–77. doi: 10.1089/ars.2009.2531
14. Wang Z, Huang Y, Cheng Y, Tan Y, Wu F, Wu J, et al. Endoplasmic reticulum stress-induced neuronal inflammatory response and apoptosis likely plays a key role in the development of diabetic encephalopathy. *Oncotarget* (2016) 7:78455–72. doi: 10.18632/oncotarget.12925
15. Esposito K, Nappo F, Marfella R, Giugliano G, Giugliano F, Ciotola M, et al. Inflammatory cytokine concentrations are acutely increased by hyperglycemia in humans: role of oxidative stress. *Circulation* (2002) 106:2067–72. doi: 10.1161/01.CIR.0000034509.14906.AE
16. Hwang IK, Choi JH, Nam SM, Park OK, Yoo DY, Kim W, et al. Activation of microglia and induction of pro-inflammatory cytokines in the hippocampus of type 2 diabetic rats. *Neurol Res.* (2014) 36:824–32. doi: 10.1179/1743132814Y.0000000330
17. Oliveira WH, Nunes AK, Franca ME, Santos LA, Los DB, Rocha SW, et al. Effects of metformin on inflammation and short-term memory in streptozotocin-induced diabetic mice. *Brain Res.* (2016) 1644:149–60. doi: 10.1016/j.brainres.2016.05.013
18. Aktas O, Ullrich O, Infante-Duarte C, Nitsch R, Zipp F. Neuronal damage in brain inflammation. *Arch Neurol.* (2007) 64:185–9. doi: 10.1001/archneur.64.2.185
19. Kadlubowska J, Malaguarnera L, Waz P, Zorena K. Neurodegeneration and neuroinflammation in diabetic retinopathy: potential approaches to delay neuronal loss. *Curr Neuropharmacol.* (2016) 14:831–9. doi: 10.2174/1570159X14666160614095559
20. Wang Y, Lam KS, Kraegen EW, Sweeney G, Zhang J, Tso AW, et al. Lipocalin-2 is an inflammatory marker closely associated with obesity, insulin resistance, and hyperglycemia in humans. *Clin Chem.* (2007) 53:34–41. doi: 10.1373/clinchem.2006.075614
21. Kim KE, Jung Y, Min S, Nam M, Heo RW, Jeon BT, et al. Caloric restriction of db/db mice reverts hepatic steatosis and body weight with divergent hepatic metabolism. *Sci Rep.* (2016) 6:30111. doi: 10.1038/srep30111
22. Berard JL, Zarruk JG, Arbour N, Prat A, Yong VW, Jacques FH, et al. Lipocalin 2 is a novel immune mediator of experimental autoimmune encephalomyelitis pathogenesis and is modulated in multiple sclerosis. *Glia* (2012) 60:1145–59. doi: 10.1002/glia.22342
23. Naude PJ, Nyakas C, Eiden LE, Ait-Ali D, van der Heide R, Engelborghs S, et al. Lipocalin 2: novel component of proinflammatory signaling in Alzheimer's disease. *FASEB J.* (2012) 26:2811–23. doi: 10.1096/fj.11-202457
24. Shashidharamurthy R, Machiah D, Aitken JD, Putty K, Srinivasan G, Chassaing B, et al. Differential role of lipocalin 2 during immune complex-mediated acute and chronic inflammation in mice. *Arthritis Rheum.* (2013) 65:1064–73. doi: 10.1002/art.37840
25. Jin M, Kim JH, Jang E, Lee YM, Soo Han H, Woo DK, et al. Lipocalin-2 deficiency attenuates neuroinflammation and brain injury after transient middle cerebral artery occlusion in mice. *J Cereb Blood Flow Metab.* (2014) 34:1306–14. doi: 10.1038/jcbfm.2014.83
26. Kim BW, Jeong KH, Kim JH, Jin M, Kim JH, Lee MG, et al. Pathogenic upregulation of glial Lipocalin-2 in the parkinsonian dopaminergic system. *J Neurosci.* (2016) 36:5608–22. doi: 10.1523/JNEUROSCI.4261-15.2016
27. Kim JH, Ko PW, Lee HW, Jeong JY, Lee MG, Kim JH, et al. Astrocyte-derived lipocalin-2 mediates hippocampal damage and cognitive deficits in experimental models of vascular dementia. *Glia* (2017) 65:1471–90. doi: 10.1002/glia.23174
28. Yan QW, Yang Q, Mody N, Graham TE, Hsu CH, Xu Z, et al. The adipokine lipocalin 2 is regulated by obesity and promotes insulin resistance. *Diabetes* (2007) 56:2533–40. doi: 10.2337/db07-0007
29. Huang Y, Yang Z, Ye Z, Li Q, Wen J, Tao X, et al. Lipocalin-2, glucose metabolism and chronic low-grade systemic inflammation in Chinese people. *Cardiovasc Diabetol.* (2012) 11:11. doi: 10.1186/1475-2840-11-11
30. Elkhidir AE, Eltaher HB, Mohamed AO. Association of lipocalin-2 level, glycemic status and obesity in type 2 diabetes mellitus. *BMC Res Notes* (2017) 10:285. doi: 10.1186/s13104-017-2604-y

31. Flo TH, Smith KD, Sato S, Rodriguez DJ, Holmes MA, Strong RK, et al. Lipocalin 2 mediates an innate immune response to bacterial infection by sequestrating iron. *Nature* (2004) 432:917–21. doi: 10.1038/nature03104
32. Lee S, Kim JH, Kim JH, Seo JW, Han HS, Lee WH, et al. Lipocalin-2 Is a chemokine inducer in the central nervous system: role of chemokine ligand 10 (CXCL10) in lipocalin-2-induced cell migration. *J Biol Chem.* (2011) 286:43855–70. doi: 10.1074/jbc.M111.299248
33. Wang Z, Dohle C, Friemann J, Green BS, Gleichmann H. Prevention of high- and low-dose STZ-induced diabetes with D-glucose and 5-thio-D-glucose. *Diabetes* (1993) 42:420–8. doi: 10.2337/diab.42.3.420
34. O'Brien PD, Sakowski SA, Feldman EL. Mouse models of diabetic neuropathy. *ILAR J.* (2014) 54:259–72. doi: 10.1093/ilar/ilt052
35. Winzell MS, Ahren B. The high-fat diet-fed mouse: a model for studying mechanisms and treatment of impaired glucose tolerance and type 2 diabetes. *Diabetes* (2004) 53 (Suppl. 3):S215–9. doi: 10.2337/diabetes.53.suppl_3.S215
36. Wang CY, Liao JK. A mouse model of diet-induced obesity and insulin resistance. *Methods Mol Biol.* (2012) 821:421–33. doi: 10.1007/978-1-61779-430-8_27
37. Heydemann A. An overview of murine high fat diet as a model for type 2 diabetes mellitus. *J Diabetes Res.* (2016) 2016:2902351. doi: 10.1155/2016/2902351
38. Loesel R, Weigel S, Braunig P. A simple fluorescent double staining method for distinguishing neuronal from non-neuronal cells in the insect central nervous system. *J Neurosci Methods* (2006) 155:202–6. doi: 10.1016/j.jneumeth.2006.01.006
39. Darsalia V, Mansouri S, Ortsater H, Olverling A, Nozadze N, Kappe C, et al. Glucagon-like peptide-1 receptor activation reduces ischaemic brain damage following stroke in Type 2 diabetic rats. *Clin Sci.* (2012) 122:473–83. doi: 10.1042/CS20110374
40. Kuang X, Du JR, Liu YX, Zhang GY, Peng HY. Postischemic administration of Z-Ligustilide ameliorates cognitive dysfunction and brain damage induced by permanent forebrain ischemia in rats. *Pharmacol Biochem Behav.* (2008) 88:213–21. doi: 10.1016/j.pbb.2007.08.006
41. Bouter Y, Dietrich K, Wittnam JL, Rezaei-Ghaleh N, Pillot T, Papot-Couturier S, et al. N-truncated amyloid beta (Abeta) 4-42 forms stable aggregates and induces acute and long-lasting behavioral deficits. *Acta Neuropathol.* (2013) 126:189–205. doi: 10.1007/s00401-013-1129-2
42. Rahman MH, Jha MK, Kim JH, Nam Y, Lee MG, Go Y, et al. Pyruvate dehydrogenase kinase-mediated glycolytic metabolic shift in the dorsal root ganglion drives painful diabetic neuropathy. *J Biol Chem.* (2016) 291:6011–25. doi: 10.1074/jbc.M115.699215
43. Livak KJ, Schmittgen TD. Analysis of relative gene expression data using real-time quantitative PCR and the 2(-Delta Delta CT) Method. *Methods* (2001) 25:402–8. doi: 10.1006/meth.2001.1262
44. Jang E, Kim JH, Lee S, Kim JH, Seo JW, Jin M, et al. Phenotypic polarization of activated astrocytes: the critical role of lipocalin-2 in the classical inflammatory activation of astrocytes. *J Immunol.* (2013) 191:5204–19. doi: 10.4049/jimmunol.1301637
45. Leger M, Quiedeville A, Bouet V, Haelewyn B, Boulouard M, Schumann-Bard P, et al. Object recognition test in mice. *Nat Protoc.* (2013) 8:2531–7. doi: 10.1038/nprot.2013.155
46. Sarnyai Z, Sibille EL, Pavlides C, Fenster RJ, McEwen BS, Toth M. Impaired hippocampal-dependent learning and functional abnormalities in the hippocampus in mice lacking serotonin(1A) receptors. *Proc Natl Acad Sci USA*. (2000) 97:14731–6. doi: 10.1073/pnas.97.26.14731
47. Flood JF, Mooradian AD, Morley JE. Characteristics of learning and memory in streptozocin-induced diabetic mice. *Diabetes* (1990) 39:1391–8. doi: 10.2337/diab.39.11.1391
48. Liu LP, Yan TH, Jiang LY, Hu W, Hu M, Wang C, et al. Pioglitazone ameliorates memory deficits in streptozotocin-induced diabetic mice by reducing brain beta-amyloid through PPARgamma activation. *Acta Pharmacol Sin.* (2013) 34:455–63. doi: 10.1038/aps.2013.11
49. McKillop AM, Moran BM, Abdel-Wahab YH, Gormley NM, Flatt PR. Metabolic effects of orally administered small-molecule agonists of GPR55 and GPR119 in multiple low-dose streptozotocin-induced diabetic and incretin-receptor-knockout mice. *Diabetologia* (2016) 59:2674–85. doi: 10.1007/s00125-016-4108-z
50. Pekny M, Pekna M. Reactive gliosis in the pathogenesis of CNS diseases. *Biochim Biophys Acta* (2016) 1862:483–91. doi: 10.1016/j.bbadis.2015.11.014
51. Lee S, Lee J, Kim S, Park JY, Lee WH, Mori K, et al. A dual role of lipocalin 2 in the apoptosis and deramification of activated microglia. *J Immunol.* (2007) 179:3231–41. doi: 10.4049/jimmunol.179.5.3231
52. Lee S, Park JY, Lee WH, Kim H, Park HC, Mori K, et al. Lipocalin-2 is an autocrine mediator of reactive astrocytosis. *J Neurosci.* (2009) 29:234–49. doi: 10.1523/JNEUROSCI.5273-08.2009
53. Ma Y, Li Y, Jiang L, Wang L, Jiang Z, Wang Y, et al. Macrophage depletion reduced brain injury following middle cerebral artery occlusion in mice. *J Neuroinflammation* (2016) 13:38. doi: 10.1186/s12974-016-0504-z
54. Boddaert J, Bielen KS, Jongers B, Manocha E, Yperzeele L, Cras P, et al. CD8 signaling in microglia/macrophage M1 polarization in a rat model of cerebral ischemia. *PLoS ONE* (2018) 13:e0186937. doi: 10.1371/journal.pone.0186937
55. Greter M, Lelios I, Croxford AL. Microglia versus myeloid cell nomenclature during brain inflammation. *Front Immunol.* (2015) 6:249. doi: 10.3389/fimmu.2015.00249
56. Valdearcos M, Douglass JD, Robblee MM, Dorfman MD, Stifler DR, Bennett ML, et al. Microglial inflammatory signaling orchestrates the hypothalamic immune response to dietary excess and mediates obesity susceptibility. *Cell Metab.* (2017) 26:185–197 e183. doi: 10.1016/j.cmet.2017.05.015
57. Zilliox LA, Chadrasekaran K, Kwan JY, Russell JW. Diabetes and cognitive impairment. *Curr Diab Rep.* (2016) 16:87. doi: 10.1007/s11892-016-0775-x
58. Zou W, Yuan J, Tang ZJ, Wei HJ, Zhu WW, Zhang P, et al. Hydrogen sulfide ameliorates cognitive dysfunction in streptozotocin-induced diabetic rats: involving suppression in hippocampal endoplasmic reticulum stress. *Oncotarget* (2017) 8:64203–16. doi: 10.18632/oncotarget.19448
59. Toyama K, Koibuchi N, Hasegawa Y, Uekawa K, Yasuda O, Sueta D, et al. ASK1 is involved in cognitive impairment caused by long-term high-fat diet feeding in mice. *Sci Rep.* (2015) 5:10844. doi: 10.1038/srep10844
60. Hardigan T, Hernandez C, Ward R, Hoda MN, Ergul A. TLR2 knockout protects against diabetes-mediated changes in cerebral perfusion and cognitive deficits. *Am J Physiol Regul Integr Comp Physiol.* (2017) 312:R927–37. doi: 10.1152/ajpregu.00482.2016
61. Hemmati AA, Alboghobeish S, Ahangarpour A. Effects of cinnamic acid on memory deficits and brain oxidative stress in streptozotocin-induced diabetic mice. *Korean J Physiol Pharmacol.* (2018) 22:257–67. doi: 10.4196/kjpp.2018.22.3.257
62. Pei B, Sun J. Pinocembrin alleviates cognition deficits by inhibiting inflammation in diabetic mice. *J Neuroimmunol.* (2018) 314:42–9. doi: 10.1016/j.jneuroim.2017.11.006
63. Eagle AL, Wang H, Robison AJ. Sensitive assessment of hippocampal learning using temporally dissociated passive avoidance task. *Bio Protoc* (2016) 6:e1821.doi: 10.21769/BioProtoc.1821
64. Biessels GJ, Staekenborg S, Brunner E, Brayne C, Scheltens P. Risk of dementia in diabetes mellitus: a systematic review. *Lancet Neurol.* (2006) 5:64–74. doi: 10.1016/S1474-4422(05)70284-2
65. Cheng G, Huang C, Deng H, Wang H. Diabetes as a risk factor for dementia and mild cognitive impairment: a meta-analysis of longitudinal studies. *Intern Med J.* (2012) 42:484–91. doi: 10.1111/j.1445-5994.2012.02758.x
66. Geijselaers SLC, Sep SJS, Stehouwer CDA, Biessels GJ. Glucose regulation, cognition, and brain MRI in type 2 diabetes: a systematic review. *Lancet Diabetes Endocrinol.* (2015) 3:75–89. doi: 10.1016/S2213-8587(14)70148-2
67. Moheet A, Mangia S, Seaquist ER. Impact of diabetes on cognitive function and brain structure. *Ann N Y Acad Sci.* (2015) 1353:60–71. doi: 10.1111/nyas.12807
68. Mehta BK, Singh KK, Banerjee S. Effect of exercise on type 2 diabetes-associated cognitive impairment in rats. *Int J Neurosci.* (2018). doi: 10.1080/00207454.2018.1526795. [Epub ahead of print].
69. van Gemert T, Wolwer W, Weber KS, Hoyer A, Strassburger K, Bohnau NT, et al. Cognitive function is impaired in patients with recently diagnosed

type 2 diabetes, but not type 1 diabetes. *J Diabetes Res.* (2018) 2018:1470476. doi: 10.1155/2018/1470476
70. Williams MD, Nadler JL. Inflammatory mechanisms of diabetic complications. *Curr Diab Rep.* (2007) 7:242–8. doi: 10.1007/s11892-007-0038-y
71. Nguyen DV, Shaw LC, Grant MB. Inflammation in the pathogenesis of microvascular complications in diabetes. *Front Endocrinol.* (2012) 3:170. doi: 10.3389/fendo.2012.00170
72. Marioni RE, Strachan MW, Reynolds RM, Lowe GD, Mitchell RJ, Fowkes FG, et al. Association between raised inflammatory markers and cognitive decline in elderly people with type 2 diabetes: the Edinburgh Type 2 *Diabetes* Study. *Diabetes* (2010) 59:710–3. doi: 10.2337/db09-1163
73. Chung CC, Pimentel D, Jor'dan AJ, Hao Y, Milberg W, Novak V. Inflammation-associated declines in cerebral vasoreactivity and cognition in type 2 diabetes. *Neurology* (2015) 85:450–8. doi: 10.1212/WNL.0000000000001820
74. Gorska-Ciebiada M, Saryusz-Wolska M, Borkowska A, Ciebiada M, Loba J. Serum levels of inflammatory markers in depressed elderly patients with diabetes and mild cognitive impairment. *PLoS ONE* (2015) 10:e0120433. doi: 10.1371/journal.pone.0120433
75. Preston AR, Eichenbaum H. Interplay of hippocampus and prefrontal cortex in memory. *Curr Biol.* (2013) 23:R764–73. doi: 10.1016/j.cub.2013.05.041
76. Feng X, Valdearcos M, Uchida Y, Lutrin D, Maze M, Koliwad SK. Microglia mediate postoperative hippocampal inflammation and cognitive decline in mice. *JCI Insight* (2017) 2:e91229. doi: 10.1172/jci.insight.91229
77. Lin Y, Rajala MW, Berger JP, Moller DE, Barzilai N, Scherer PE. Hyperglycemia-induced production of acute phase reactants in adipose tissue. *J Biol Chem.* (2001) 276:42077–83. doi: 10.1074/jbc.M107101200
78. Korrapati MC, Shaner BE, Neely BA, Alge JL, Arthur JM, Schnellmann RG. Diabetes-induced renal injury in rats is attenuated by suramin. *J Pharmacol Exp Ther.* (2012) 343:34–43. doi: 10.1124/jpet.112.196964
79. Abdollahi M, Ng TS, Rezaeizadeh A, Aamidor S, Twigg SM, Min D, et al. Insulin treatment prevents wounding associated changes in tissue and circulating neutrophil MMP-9 and NGAL in diabetic rats. *PLoS ONE* (2017) 12:e0170951. doi: 10.1371/journal.pone.0170951
80. Gao M, Ma Y, Liu D. High-fat diet-induced adiposity, adipose inflammation, hepatic steatosis and hyperinsulinemia in outbred CD-1 mice. *PLoS ONE* (2015) 10:e0119784. doi: 10.1371/journal.pone.0119784
81. Zhang Y, Foncea R, Deis JA, Guo H, Bernlohr DA, Chen X. Lipocalin 2 expression and secretion is highly regulated by metabolic stress, cytokines, and nutrients in adipocytes. *PLoS ONE* (2014) 9:e96997. doi: 10.1371/journal.pone.0096997
82. Tan BK, Adya R, Shan X, Syed F, Lewandowski KC, O'Hare JP, et al. *Ex vivo* and *in vivo* regulation of lipocalin-2, a novel adipokine, by insulin. *Diabetes Care* (2009) 32:129–31. doi: 10.2337/dc08-1236
83. Pradhan AD, Manson JE, Rifai N, Buring JE, Ridker PM. C-reactive protein, interleukin 6, and risk of developing type 2 diabetes mellitus. *JAMA* (2001) 286:327–34. doi: 10.1001/jama.286.3.327
84. Pop-Busui R, Ang L, Holmes C, Gallagher K, Feldman EL. Inflammation as a therapeutic target for diabetic neuropathies. *Curr Diab Rep.* (2016) 16:29. doi: 10.1007/s11892-016-0727-5
85. Reemst K, Noctor SC, Lucassen PJ, Hol EM. The Indispensable roles of microglia and astrocytes during brain development. *Front Hum Neurosci.* (2016) 10:566. doi: 10.3389/fnhum.2016.00566
86. Becerra-Calixto A, Cardona-Gomez GP. The role of astrocytes in neuroprotection after brain stroke: potential in cell therapy. *Front Mol Neurosci.* (2017) 10:88. doi: 10.3389/fnmol.2017.00088
87. Nagayach A, Patro N, Patro I. Experimentally induced diabetes causes glial activation, glutamate toxicity and cellular damage leading to changes in motor function. *Front Cell Neurosci.* (2014) 8:355. doi: 10.3389/fncel.2014.00355
88. Lo W, O'Donnell M, Tancredi D, Orgain M, Glaser N. Diabetic ketoacidosis in juvenile rats is associated with reactive gliosis and activation of microglia in the hippocampus. *Pediatr Diabetes* (2016) 17:127–39. doi: 10.1111/pedi.12251
89. Jha MK, Jeon S, Jin M, Ock J, Kim JH, Lee WH, et al. The pivotal role played by lipocalin-2 in chronic inflammatory pain. *Exp Neurol.* (2014) 254:41–53. doi: 10.1016/j.expneurol.2014.01.009
90. Stranahan AM, Hao S, Dey A, Yu X, Baban B. Blood-brain barrier breakdown promotes macrophage infiltration and cognitive impairment in leptin receptor-deficient mice. *J Cereb Blood Flow Metab.* (2016) 36:2108–21. doi: 10.1177/0271678X16642233
91. Sima AA, Zhang W, Kreipke CW, Rafols JA, Hoffman WH. Inflammation in diabetic encephalopathy is prevented by C-Peptide. *Rev Diabet Stud.* (2009) 6:37–42. doi: 10.1900/RDS.2009.6.37
92. Hameed I, Masoodi SR, Mir SA, Nabi M, Ghazanfar K, Ganai BA. Type 2 diabetes mellitus: from a metabolic disorder to an inflammatory condition. *World J Diabetes* (2015) 6:598–612. doi: 10.4239/wjd.v6.i4.598
93. Li HY, Wang XC, Xu YM, Luo NC, Luo S, Hao XY, et al. Berberine improves diabetic encephalopathy through the SIRT1/ER stress pathway in db/db mice. *Rejuvenation Res.* (2018) 21:200–9. doi: 10.1089/rej.2017.1972
94. Shao S, Cao T, Jin L, Li B, Fang H, Zhang J, et al. Increased Lipocalin-2 Contributes to the Pathogenesis of Psoriasis by Modulating Neutrophil Chemotaxis and Cytokine Secretion. *J Invest Dermatol.* (2016) 136:1418–28. doi: 10.1016/j.jid.2016.03.002
95. Nam Y, Kim JH, Seo M, Kim JH, Jin M, Jeon S, et al. Lipocalin-2 protein deficiency ameliorates experimental autoimmune encephalomyelitis: the pathogenic role of lipocalin-2 in the central nervous system and peripheral lymphoid tissues. *J Biol Chem.* (2014) 289:16773–89. doi: 10.1074/jbc.M113.542282
96. Saijo K, Winner B, Carson CT, Collier JG, Boyer L, Rosenfeld MG, et al. A Nurr1/CoREST pathway in microglia and astrocytes protects dopaminergic neurons from inflammation-induced death. *Cell* (2009) 137:47–59. doi: 10.1016/j.cell.2009.01.038
97. Jha MK, Jo M, Kim JH, Suk K. Microglia-astrocyte crosstalk: an intimate molecular conversation. *Neuroscientist* (2018). doi: 10.1177/1073858418783959. [Epub ahead of print].
98. Simi A, Tsakiri N, Wang P, Rothwell NJ. Interleukin-1 and inflammatory neurodegeneration. *Biochem Soc Trans.* (2007) 35(Pt 5):1122–6. doi: 10.1042/BST0351122
99. McCoy MK, Tansey MG. TNF signaling inhibition in the CNS: implications for normal brain function and neurodegenerative disease. *J Neuroinflammation* (2008) 5:45. doi: 10.1186/1742-2094-5-45
100. Pistell PJ, Morrison CD, Gupta S, Knight AG, Keller JN, Ingram DK, et al. Cognitive impairment following high fat diet consumption is associated with brain inflammation. *J Neuroimmunol.* (2010) 219:25–32. doi: 10.1016/j.jneuroim.2009.11.010
101. Chen WW, Zhang X, Huang WJ. Role of neuroinflammation in neurodegenerative diseases (Review). *Mol Med Report.* (2016) 13:3391–6. doi: 10.3892/mmr.2016.4948
102. Ransohoff RM. How neuroinflammation contributes to neurodegeneration. *Science* (2016) 353:777–83. doi: 10.1126/science.aag2590
103. Law IK, Xu A, Lam KS, Berger T, Mak TW, Vanhoutte PM, et al. Lipocalin-2 deficiency attenuates insulin resistance associated with aging and obesity. *Diabetes* (2010) 59:872–82. doi: 10.2337/db09-1541
104. Rashad NM, El-Shal AS, Etewa RL, Wadea FM. Lipocalin-2 expression and serum levels as early predictors of type 2 diabetes mellitus in obese women. *IUBMB Life* (2017) 69:88–97. doi: 10.1002/iub.1594
105. Zhang J, Wu Y, Zhang Y, Leroith D, Bernlohr DA, Chen X. The role of lipocalin 2 in the regulation of inflammation in adipocytes and macrophages. *Mol Endocrinol.* (2008) 22:1416–26. doi: 10.1210/me.2007-0420
106. Bi F, Huang C, Tong J, Qiu G, Huang B, Wu Q, et al. Reactive astrocytes secrete lcn2 to promote neuron death. *Proc Natl Acad Sci USA.* (2013) 110:4069–74. doi: 10.1073/pnas.1218497110
107. Dong M, Xi G, Keep RF, Hua Y. Role of iron in brain lipocalin 2 upregulation after intracerebral hemorrhage in rats. *Brain Res.* (2013) 1505:86–92. doi: 10.1016/j.brainres.2013.02.008
108. Devireddy LR, Gazin C, Zhu X, Green MR. A cell-surface receptor for lipocalin 24p3 selectively mediates apoptosis and iron uptake. *Cell* (2005) 123:1293–305. doi: 10.1016/j.cell.2005.10.027

109. Choi J, Lee HW, Suk K. Increased plasma levels of lipocalin 2 in mild cognitive impairment. *J Neurol Sci.* (2011) 305:28–33. doi: 10.1016/j.jns.2011.03.023
110. Dekens DW, Naude PJ, Engelborghs S, Vermeiren Y, Van Dam D, Oude Voshaar RC, et al. Neutrophil Gelatinase-Associated Lipocalin and its Receptors in Alzheimer's Disease (AD) brain regions: differential findings in AD with and without depression. *J Alzheimers Dis.* (2017) 55:763–76. doi: 10.3233/JAD-160330
111. Ferreira AC, Da Mesquita S, Sousa JC, Correia-Neves M, Sousa N, Palha JA, et al. From the periphery to the brain: lipocalin-2, a friend or foe? *Prog Neurobiol.* (2015) 131:120–36. doi: 10.1016/j.pneurobio.2015.06.005
112. Mucha M, Skrzypiec AE, Schiavon E, Attwood BK, Kucerova E, Pawlak R. Lipocalin-2 controls neuronal excitability and anxiety by regulatingdendritic spine formation and maturation. *Proc Natl Acad Sci USA.* (2011) 108:18436–41. doi: 10.1073/pnas.1107936108

Conflict of Interest Statement: The authors declare that the research was conducted in the absence of any commercial or financial relationships that could be construed as a potential conflict of interest.

frontiers in Endocrinology

CORRECTION
published: 09 April 2019
doi: 10.3389/fendo.2019.00239

Corrigendum: Role of Hippocampal Lipocalin-2 in Experimental Diabetic Encephalopathy

Anup Bhusal[1†], *Md Habibur Rahman*[1†], *In-Kyu Lee*[2] *and Kyoungho Suk*[1,3*]

[1] BK21 Plus KNU Biomedical Convergence Program, Departments of Biomedical Science and Pharmacology, School of Medicine, Kyungpook National University, Daegu, South Korea, [2] Division of Endocrinology and Metabolism, Department of Internal Medicine, School of Medicine, Kyungpook National University, Daegu, South Korea, [3] Brain Science and Engineering Institute, Kyungpook National University, Daegu, South Korea

Keywords: Lipocalin-2, diabetic encephalopathy, hippocampus, glia, neuroinflammation, cognitive dysfunction

OPEN ACCESS

Approved by:
Frontiers in Endocrinology Editorial Office, Frontiers Media SA, Switzerland

***Correspondence:**
Kyoungho Suk
ksuk@knu.ac.kr

†These authors have contributed equally to this work

Specialty section:
This article was submitted to Experimental Endocrinology, a section of the journal Frontiers in Endocrinology

Received: *25 March 2019*
Accepted: *26 March 2019*
Published: *09 April 2019*

Citation:
Bhusal A, Rahman MH, Lee I-K and Suk K (2019) Corrigendum: Role of Hippocampal Lipocalin-2 in Experimental Diabetic Encephalopathy. Front. Endocrinol. 10:239. doi: 10.3389/fendo.2019.00239

A Corrigendum on

Role of Hippocampal Lipocalin-2 in Experimental Diabetic Encephalopathy
by Bhusal, A., Rahman, M. H., Lee, I.-K., and Suk, K. (2019). Front. Endocrinol. 10:25. doi: 10.3389/fendo.2019.00025

In the original article, there was a mistake in **Figure 1** as published. The *Gapdh* band image used in **Figure 1C** was from the pilot experiment. The corrected **Figure 1** appears below.

The authors apologize for this error and state that this does not change the scientific conclusions of the article in any way. The original article has been updated.

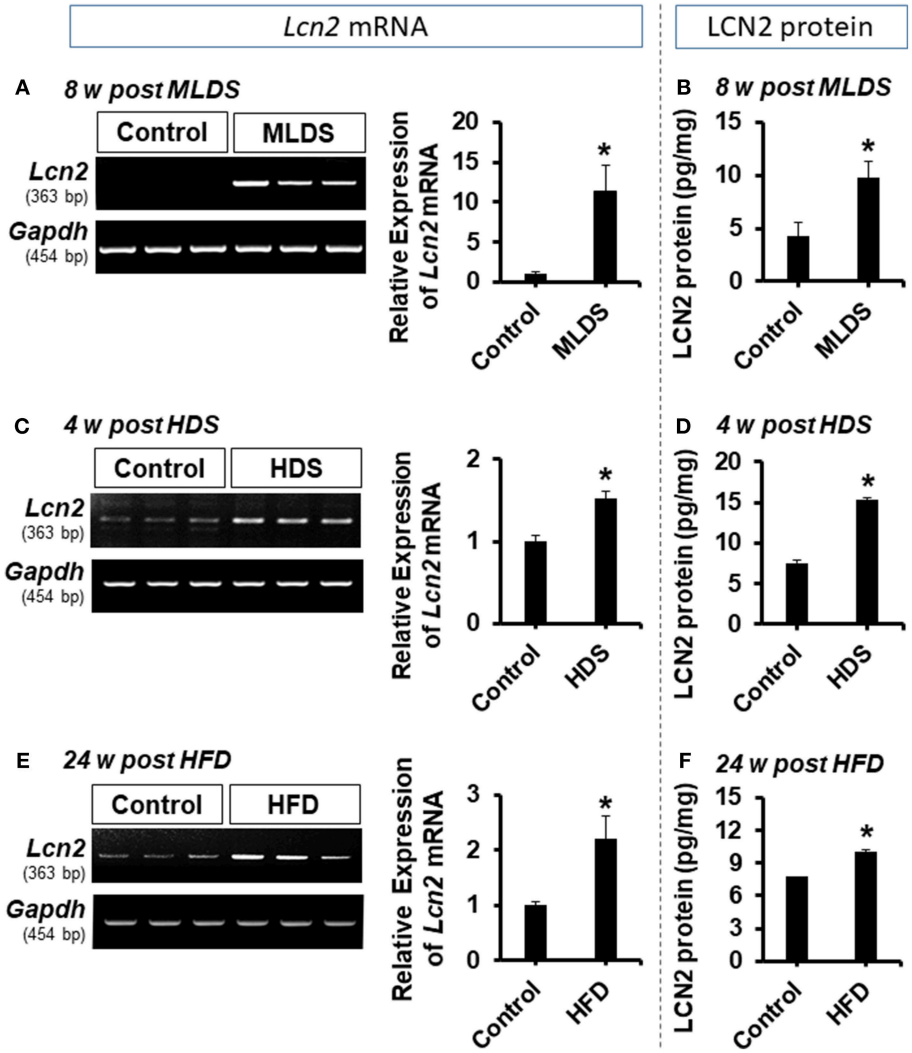

FIGURE 1 | Expression of LCN2 in the hippocampus of diabetic mice. The expression of *Lcn2* mRNA in the hippocampus at 8 w post MLDS and 4 w post HDS injection was assessed by conventional PCR **(A,C)**. Further, the expression level of LCN2 protein in the hippocampus of STZ-induced diabetic mice was estimated by ELISA assay **(B,D)**. Similar upregulation of *Lcn2* mRNA and LCN2 protein was detected in the hippocampus at 24 w post HFD feeding **(E,F)**. $^{*}p < 0.05$ vs. the vehicle-treated control animals; Student's *t*-test; $n = 3$ for each group; data are represented as mean ± SEM. STZ, streptozotocin; MLDS, multiple low dose of STZ; HDS, high dose of STZ; HFD, high fat diet; LCN2, Lipocalin-2; w, weeks; SEM, standard error of the mean.

frontiers in Endocrinology

ORIGINAL RESEARCH
published: 26 February 2019
doi: 10.3389/fendo.2019.00036

IL-33 Ameliorates the Development of MSU-Induced Inflammation Through Expanding MDSCs-Like Cells

Ke Shang[1†], Yingying Wei[2†], Qun Su[2†], Bing Yu[2], Ying Tao[2], Yan He[2], Youlian Wang[1], Guixiu Shi[2] and Lihua Duan[1,2*]*

[1] Department of Rheumatology and Clinical Immunology, Jiangxi Provincial People's Hospital, Nanchang, China,
[2] Department of Rheumatology and Clinical Immunology, The First Affiliated Hospital of Xiamen University, Xiamen, China

Interleukin-33 (IL-33), a member of the IL-1 superfamily, has been shown to play a critical role in many diseases through regulating the immune cell responses, including myeloid-derived suppressor cells (MDSCs). Our previous study demonstrated that IL-33 might play a protective role in kidney injury in gout patients by regulating the lipid metabolism. However, the role of IL-33in the development of MSU-induced inflammation remains elusive. In this study, an increased IL-33 expression was observed in gout patients, which was positively correlated with inflammatory marker CRP. To explore the effects and mechanisms of the increased IL-33 expression in the gout patients, the anti-ST2 antibody and exogenous recombinant IL-33 were used in MSU-induced peritonitis animal model that mimics human gout. Compared with control group, mice with exogenous recombinant IL-33 significantly ameliorated the inflammatory cells infiltration, while blockage of IL-33 signaling by anti-ST2 had no effect on the development of MSU-induced peritonitis. Furthermore, the crucial inflammatory cytokine IL-1β was markedly decreased in IL-33-treated mice. Besides that, a large number of anti-inflammatory MDSCs with $CD11b^{+}Gr1^{int}F4/80^{+}$ phenotype was observed in the IL-33-treated mice, and adoptive transfer of IL-33-induced MDSCs ($CD11b^{+}Gr1^{int}F4/80^{+}$) markedly inhibited the IL-1β production in MSU-induced peritonitis. In conclusion, our data provide clear evidences that the increased expression of IL-33 in the gout patients might be due to a cause of self-negative regulation, which inhibits the development of MSU-induced inflammation through expanding MDSCs. Thus, IL-33 might serve as a promising therapeutic target for gout.

Keywords: gout, MDSCs, IL-33, MSU, IL-1β

OPEN ACCESS

Edited by:
Wen Kong,
Wuhan Union Hospital, China

Reviewed by:
Hui Yin,
Guangdong Pharmaceutical University, China
Carlos Alfaro,
NavarraBiomed, Spain

***Correspondence:**
Lihua Duan
lh-duan@163.com
Guixiu Shi
gshi@xmu.edu.cn

†These authors have contributed equally to this work

Specialty section:
This article was submitted to Experimental Endocrinology, a section of the journal Frontiers in Endocrinology

Received: *20 November 2018*
Accepted: *16 January 2019*
Published: *26 February 2019*

Citation:
Shang K, Wei Y, Su Q, Yu B, Tao Y, He Y, Wang Y, Shi G and Duan L (2019) IL-33 Ameliorates the Development of MSU-Induced Inflammation Through Expanding MDSCs-Like Cells. Front. Endocrinol. 10:36. doi: 10.3389/fendo.2019.00036

INTRODUCTION

Gout is the most common inflammatory arthritis caused by inflammatory responses to the deposition of monosodium urate (MSU) crystals. The uric acid levels exceed the physiological saturation concentration, which will lead to monosodium urate crystal (MSU) formation (1). MSU is precipitated in a single crystalline form and deposited in synovial, cartilage, and other tissues around the joint. MSU crystals trigger an intense inflammatory response by activating the resident

tissue macrophages and promoting the recruitment of neutrophils to the joint (2). IL-1β is the most important pro-inflammatory regulatory cytokine from activated macrophage by MSU stimulation in the onset of acute gout (3). Likewise, it has also demonstrated that a high level of IL-1β can be detected in the sera of gout patients. During the development of MSU-induced inflammation, mature IL-1β production by macrophages induces activation of IL-l signaling pathways and medullary differentiation factor (MyD88)-dependent NF-κB pathway, resulting in a large number of chemokines and pro-inflammatory factors being produced, and inflammatory immune cells infiltration (4). An interesting character of acute gout is the self-limiting nature of the inflammatory flare. In the absence of clinical intervention, a gouty episode can spontaneously resolve within 7–10 days. However, the mechanism of inflammation self-resolution is still elusive (5, 6).

Interleukin-33 (IL-33), a member of the IL-1 family, is widely expressed in a variety of tissue cells, especially epithelial cells, endothelial cells, and fibroblast cells (7, 8). Numerous studies have shown the complex biological effects of IL-33 in human diseases (9). As an inflammatory factor, IL-33 can promote the pathological development of diseases like asthma, allergic rhinitis and rheumatoid arthritis by inducing type2-immune response and activating mast cells (10–13). In contrast, IL-33 also can act as an anti-inflammatory factor to suppress inflammation by promoting alternatively activated macrophage polarization and Tregs differentiation. Recent studies have shown that IL-33 prevents the development of parasitic infection, allogeneic allograft rejection and atherosclerosis (14, 15). However, the role of IL-33 in the development of MSU-induced inflammation remains unclear.

Myeloid-derived suppressor cells (MDSCs) are a group of heterogeneous cells discovered in recent years, including immature myeloid cells, immature granulocytes, monocytes-macrophages, dendritic cells, and myeloid precursor cells. MDSCs are commonly divided granular cell-like MDSC ($CD11b^{+}Gr\text{-}1^{high}$) and mononuclear cell-like MDSC ($CD11b^{+}Gr\text{-}1^{int}$) (16, 17). Numerous studies have shown that MDSCs play a role in the regulation of effector T cells by nitric oxide production, arginase I synthesis and reactive oxygen species (ROS) production, and promoting Treg cells expansion through indoleamine-2,3-dioxygenase (IDO) production (18). In addition, MDSCs also regulate macrophages and dendritic cells function by the production of IL-10 and TGF-β (16). It is known that varieties of factors could affect the induction and activation of MDSCs, such as IL-6, IL-4 and IL-13 (17, 19). In allogeneic transplantation and tumor environments, it has been shown that IL-33 can induce MDSCs expansion, which inhibits transplant rejection and promotes the progression of mouse breast cancer through inhibition of T cell responses (20–22). Recent literature reported that LPS can induce mononuclear cell-like MDSC, which can block the action of neutrophils causing tissue damage by phagocytose them, thereby alleviating bacterial septic shock (23).

In our study, we found that the expression of IL-33 in gout patients was significantly higher than that of the healthy control group, which was positively correlated with inflammatory indicator C-reactive protein (CRP). However, mice treated with exogenous recombinant IL-33 could significantly alleviate MSU-induced inflammation through expanding $CD11b^{+}Gr1^{int}F4/80^{+}$ MDSCs. However, blockage of endogenous IL-33 signaling by anti-ST2 had no effect on the development of MSU-induced peritonitis. Taken together, our data demonstrated that the increased levels of IL-33 may be a cause of self-negative regulation which inhibits the development of MSU-induced inflammation, and IL-33 might offer an alternative therapy to our current approaches of managing gout.

MATERIALS AND METHODS

Human Subjects and Animals

Fifty-two cases of acute gout patients were collected from the First Affiliated Hospital of Xiamen University in accordance with the diagnosis criteria of American Rheumatology Association &&(1977). Fifty-eighty healthy controls who matched their age and sex were also collected. The research program has been approved by the Ethics Committee of Xiamen University, and all subjects have signed an informed consent form in accordance with the Declaration of Helsinki. Male 6–8 week C57BL/6 were obtained from the Animal Laboratory Center of Xiamen University. All animal studies were conducted in accordance with the guidelines of the Animal Care and use committee of Xiamen University.

Culture of Human Synovial Fibroblasts

In sterile conditions, we isolated the synovial fibroblasts from the joint fluid of the acute gout patients. Cells were cultured in Dulbecco's modified Eagle's medium plus 10% Fetal Bovine Serum (Hyclone, United States) and seeded at the flask, fed after 48 and 72 h. When the cells grown to sub-confluence (85%) of the culture dishes, used trypsin (Hyclone, United States) to passage cell, rinsed with PBS and plated into the dish. We then collected non-adherent cells after 2 h culture in Dulbecco's modified Eagle's medium plus 10% Fetal Bovine Serum. Repeated passages to the third generation, fibroblast cells can be used for subsequent experiments.

Histological and Immunohistochemical Analysis

The synovial fibroblasts were put on cover slides in the 6-well plate and were treated with MSU, TNFα, or IL-1β for 24 h. Next, the cell slides were taken out for immunohistochemistry analysis. Cell slides were fixed for 5 min in 4% paraformaldehyde solution, rinsed twice with PBS, followed by 0.5% Triton-100 solution treatment. The slides were treated with 3% BSA (Sangon Biotech, Shanghai) for 30 min at 37°C for blocking non-specific staining. After that, the slides were then incubated with goat anti-human IL-33 Ab (Minneapolis, MN, United States) or control gout IgG at 4° overnight, and were then used hypersensitive two-step immunohistochemical detection reagent (ZSGB-BIO, China) to detect the IL-33 expression levels by microscope.

Establishment of Acute Gout Animal Model

Male C57BL/6 mice (6–8 weeks old) were grouped into PBS, MSU, IL-33, and IL-33 plus MSU. The mice of PBS group and MSU group were daily administered an intraperitoneal (IP) injection of PBS for 4 days; the mice of IL-33 group and IL-33 + MSU group were daily administered an intraperitoneal (IP) injection of 2 μg rIL-33 for 4 days. On the fourth day, the mice of MSU group and IL-33 plus MSU group were administered an intraperitoneal (IP) injection of 3 mg MSU after inoculation; the mice of PBS group and IL-33 group were administered an intraperitoneal (IP) injection of PBS after inoculation. Expression and purification of mouse recombinant IL-33 were carried out as previously described (24). For blockage of endogenous IL-33 activity, a neutralizing anti-ST2 antibody (DIH4; Biolegend, San Diego, CA, United States) or control IgG (200 μg/mouse) was given into MSU-treated mice 1 h before MSU administration. At 16 h after MSU stimulation, peritoneal exudate cells were harvested by lavage with 3 ml PBS. Cells were analyzed by flow cytometry and lavage fluids were retained for cytokine assay. In the MDSCs adoptive transfer experiments, the $CD11b^{+}Gr\text{-}1^{high}F4/80^{+}$, $CD11b^{+}Gr\text{-}1^{int}F4/80^{+}$, and $CD11b^{+}Gr\text{-}1^{int}F4/80^{-}$ were isolated from IL-33-treated mice, and then the 3 mg MSU per mouse were administered, the lavage fluids were harvested for cytokine assay after 16 h.

Flow Cytometry

1×10^{6} peritoneal exudate cells were obtained, and the cells were incubated with the fluorescent-conjugated monoclonal antibodies in the staining buffer. Antibodies used for flow cytometry are as follows: FITC anti-mouse F4/80, Percy5.5 anti-mouse CD11b and PE/Cy7 anti-mouse Gr-1. All antibodies are purchased from Biolegend (San Diego, CA, United States).

ELISA (Enzyme-Linked Immunosorbent Assay)

The gout patients and healthy volunteers were collected 3∼5 ml through elbow vein in the morning, and put into non-anticoagulant test tube, the serum samples were separated in 2 h. The concentration of IL-33 was determined by ELISA Kit according to the Manufacturer's instruction. IL-1β, IL-6, IL-10, IL-5, and IL-13 in the peritoneal lavage fluid of model mice were also determined by ELISA Kit. All kits were purchased from R&D (Minneapolis, MN, United States).

Quantitative Real-Time Reverse Transcriptase-Polymerase Chain Reaction

The total RNA was extracted from the collected human PBMC and mouse PECs by TRIzol lysis (Invitrogen) and used Reverse transcription kit (Roche) to acquire cDNA according to the manufacturer's protocol. Then the outcomes were used to analyze the expression level of the target gene arginine1. The sequences were used for the amplification of cDNA derived from mRNA transcripts of the arginine1 gene as shown below: (Forward: 5′-TTG GCA ATT GGA AGC ATC TCT GGC-3′; Reverse: 5′-TCC ACT TGT GGT TGT CAG TGG AGT-3′), and the primer sequences for β-actin gene (Forward: 5′-AGA AAA TCT GGC ACC ACA CC-3′; Reverse: 5′-AGA GGC GTA CAG GGA TAG CA-3′). The sequences were used for the amplification of cDNA derived from mouse PECs mRNA transcripts as shown below: mouse β-actin gene (Forward: 5′-ACC TTC TAC AAT GAG CTG CG-3′; Reverse: 5′-CTG GAT GGC TAC GTA CAT GG-3′), mouse IL-1β gene (Forward: 5′-ACG GAC CCC AAA AGA TGA AG-3′; Reverse: 5′-TTC TCC ACA GCC ACA ATG AG-3′), mouse IL-6 gene (Forward: 5′-AAA CCG CTA TGA AGT TCC TCT C-3′; Reverse: 5′-GTG GTA TCC TCT GTG AAG TCT C-3′), mouse nlrp3 gene (Forward: 5′-ACC TTT GCC CAT ACC TTC AG-3′; Reverse: 5′-TGC CAC AAA CCT TCC ATC TAG-3′), mouse caspase-1 gene (Forward: 5′-TCT GTA TTC ACG CCC TGT TG-3′; Reverse: 5′-GAT AAA TTG CTT CCT CTT TGC CC-3′). The obtained data were analyzed on the ABI7500. Relative expression levels for cytokines were normalized by β-actin and calculated by using the $2^{-\Delta\Delta Ct}$ method.

Statistical Analysis

Data are presented as mean ± SEM. Group comparisons were performed using Student's *t*-test by GraphPad Prism software; *p*-values (two-tailed) below 0.05 were considered as significant. The Mann-Whitney *U*-test and Spearman's correlation analysis were used to calculate the clinical sample significance. Statistical significance was accepted for $p < 0.05$.

RESULTS

Positive Correlation of Increased Serum IL-33 With Disease Activity Index CRP in Gout Patients

Our previous study has shown that the serum IL-33 level was predominantly increased in gout patients when compared to healthy controls, and the increased IL-33 expression might play a protective role in kidney injury by regulating lipid metabolism in gout (25). In this study, we recruited more participants to compare levels of IL-33 in gout patients and healthy volunteers. Consistent with our previous study, an increased expression of IL-33 was observed in the sera of gout patients compared with healthy control (data not shown). It has been reported that IL-33 was expressed in synovial fibroblasts from patients with rheumatoid arthritis (RA), and expression was markedly elevated *in vitro* by TNFα and IL-lβ stimulation (13, 26, 27). Deposition of MSU in the articular cavity can stimulate resident tissue macrophages to produce inflammatory factors TNFα and IL-lβ. Therefore, synovial fibroblasts from gout patients with gouty arthritis were separated and treated with MSU or TNFα/IL-lβ. Consistently, TNFα and IL-lβ also induced the up-regulation of IL-33 expression in the synovial fibroblasts from gout patients. In addition, we also found that MSU can directly induce the expression of IL-33 in synovial fibroblasts (**Figure 1A**). CRP was an acute time-phase reaction protein and the most common inflammatory marker for disease activity index in acute gout. Although a protective role of IL-33 in the kidney injury of gout was observed, we here found a positive correlation between the increased IL-33 expression and inflammatory indicator CRP ($r = 0.38$, $p = 0.005$; **Figure 1B**). Our data suggested that IL-33 might modulate MSU-induced inflammation.

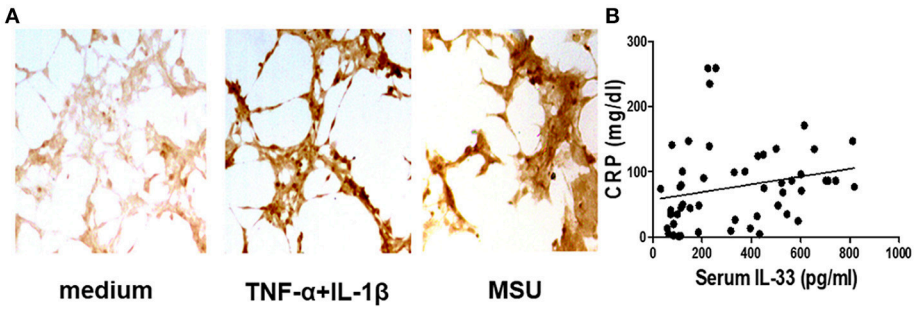

FIGURE 1 | Corrrelation of the increased IL-33 with CRP in gout patients **(A).** The synovial fibroblasts from synovial fluids were harvested to stimulate with TNF-α/IL-1β and MSU for 24 h, and then were stained with anti-IL-33 antibody by immunohistochemistry analysis. The results shown are from one of three independent experiments **(B).** The sera collected from gout patients were used to analyze IL-33 levels by ELISA. The determination of linear relationships between IL-33 expression and CRP in gout patients was performed by Spearman correlation coefficient ($r = 0.38$, $p = 0.005$).

IL-33 Reduces the Development of Experimental Gout in Mice

Next, we sought to determine the role of increased expression of IL-33 in gout by using MSU-induced peritonitis experimental model. The exogenous IL-33 was given intraperitoneally daily before MSU treatment for 4 continuous days. The infiltrated leukocytes in the peritoneal cavity were harvested to analyze after MSU administration. Because neutrophils are the important effector cells in MSU-induced inflammation, the peritoneal exudate cells were subjected to analyze the neutrophils by flow cytometry. The $CD11b^{+}Gr\text{-}1^{high}F4/80^{-}$ cells were considered as neutrophils (**Figure 2A**). The percentage of neutrophils in mice treated with PBS was very low, and exogenous IL-33 treatment slightly elevated the percentage of neutrophils. As expected, the percentage of neutrophils was significantly increased after MSU treatment. However, the percentage of neutrophils induced by MSU administration was significantly decreased in the mice with IL-33 treatment (**Figure 2B**). In addition, we also analyzed the absolute number of neutrophils in these mice. In keeping with the percentage, the absolute number of neutrophils in the MSU-treated mice was also significantly decreased in the mice with IL-33 administration (**Figure 2C**). Collectively, these results indicated that IL-33 can prevent the recruitment of neutrophils in MSU-induced acute inflammation.

IL-33 Shapes the Cytokines Profiles in MSU-Induced Inflammation

The above data showed that IL-33 played a protective role in the development of gout, we here further explored whether exogenous IL-33-induced amelioration of MSU-induced inflammation correlated with reduction of IL-1β, which is the critical cytokine in the development of MSU-induced inflammation. The levels of IL-1β in the peritoneal cavity lavage were analyzed in our study. As expected, the expression of IL-1β was significantly decreased in the gout model mice with IL-33 treatment (**Figure 3A**). Besides, the inflammatory cytokine IL-6 was also inhibited by IL-33 treatment in the gout animal model (**Figure 3B**). IL-10 is an anti-inflammatory cytokine and plays a role in regulating inflammatory response. Here, we found that IL-33 administration evidently up-regulated the anti-inflammatory cytokine IL-10 production when compared with the PBS group (**Figure 3C**). In consistent with previous studies, we also observed an increased level of IL-5 and IL-13 in the peritoneal cavity after exogenous IL-33 treatment (**Figures 3D,E**). Taken together, IL-33 could up-regulate the expression of anti-inflammatory cytokines and inhibit the pro-inflammatory cytokines production in MSU-induced inflammation.

Blockage of Endogenous IL-33 Signaling Has No Effect on MSU-Induced Inflammation

Exogenous recombinant IL-33 treatment significantly inhibited the development of MSU-induced inflammation. To investigate the functional effects of endogenous increased IL-33 production in MSU-induced inflammation, the endogenous IL-33 signaling was blocked by the administration of anti-ST2 antibodies. However, mice treated with anti-ST2 antibody were unaffected by the neutrophils infiltration and MDSCs expansion in the MSU-induced inflammation. Furthermore, the expressions of IL-1β, IL-6, NLRP3, Caspase-1 were detected by RT-PCR, while no significant difference was observed between control group and anti-ST2 group (**Figure 4**). Therefore, we speculate that an increased expression of IL-33 in the gout patients might be due to a cause of self-negative regulation, while the increased amount of IL-33 expression was inadequate to induce a potent protective effect to reduce the development of gout.

IL-33 Inhibits MSU-Induced Inflammation Through Expanding MDSCs

MDSCs are a group of heterogeneous cells, which consist of granular cell-like MDSCs and mononuclear cell-like MDSCs. By flow cytometry analysis of the collective peritoneal cells, we observed a large number of MDSCs in the PECs of the mice with IL-33 treatment. Specially, the increased number of MDSCs induced by IL-33 in the animal gout model was characterized by surface markers $CD11b^{+}Gr\text{-}1^{int}F4/80^{+}$ (**Figures 5A–C**). Arginine1 was also recognized as an important

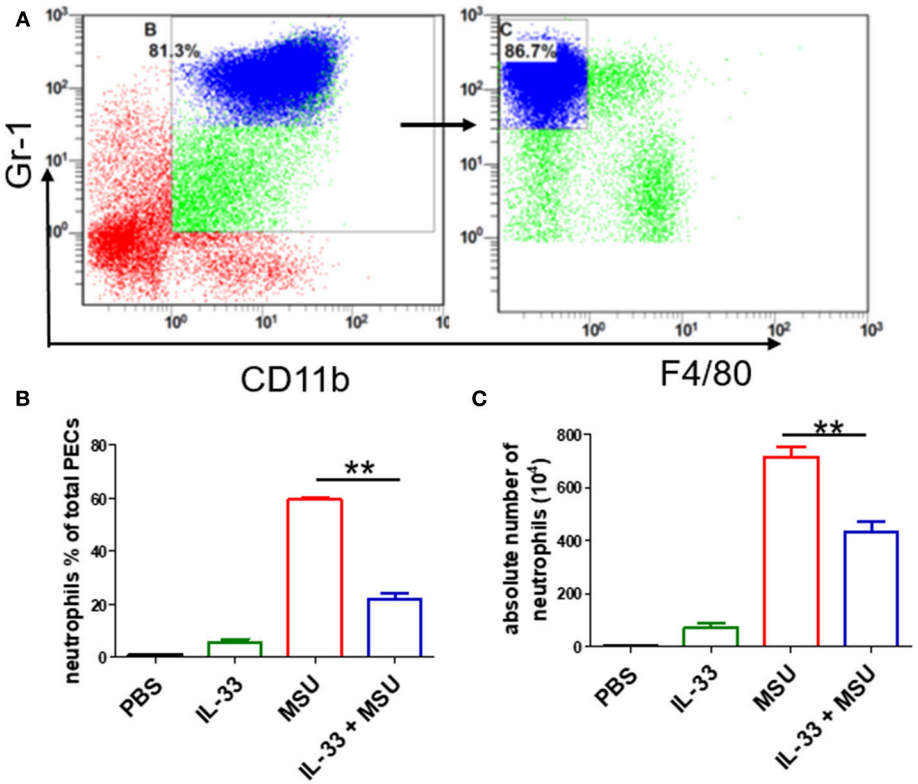

FIGURE 2 | IL-33 reduces the neutrophils recruitment in gout animal model. Mice treated with IL-33 or PBS for 4 consecutive days, then injected with MSU or PBS. The mice were sacrificed after 16 h, and the cells in the peritoneal cavity were harvested and analyzed by flow cytometry **(A)**. Neutrophils are defined as cells with $CD11b^{+}Gr\text{-}1^{+}F4/80^{-}$ surface marker **(B,C)**. The infiltrated inflammatory cells in the peritoneal cavity were analyzed by flow cytometry for neutrophils. Data represent mean ± SEM per group ($n = 7$/group). $^{**}p < 0.001$.

marker for MDSCs, we detected the expression of arginine1 in the gout and healthy control PBMCs at the mRNA level by RT-PCR. We observed an increased expression of arginine1 in the gout patients when compared with healthy controls (**Figure 5D**). These results demonstrated that IL-33 can induce MDSCs recruitment, which might be involved in the self-limiting of the MSU-induced inflammation in the gout patients. Furthermore, three groups of cells induced by IL-33 were isolated and adoptively transferred to the gout model mice (**Figure 6A**). The expression levels of cytokines IL-1β in the peritoneal cavity were analyzed. Compared to other groups, the expression of IL-1β cytokine in the MSU-inflammation was decreased by $CD11b^{+}Gr\text{-}1^{int}F4/80^{+}$ cells transfusion (**Figure 6B**). Thus, the $CD11b^{+}Gr\text{-}1^{int}F4/80^{+}$ expansion induced by IL-33 exerts an important role in the resolution of MSU-induced inflammation.

DISCUSSION

In this study, we found an increased level of IL-33 in gout patients, which was positively correlated with inflammatory marker CRP. However, exogenous recombinant IL-33 significantly ameliorated the development of animal gout model. Interestingly, a large number of $CD11b^{+}Gr1^{int}F4/80^{+}$ MDSCs was detected in the IL-33-treated mice, and adoptive transfer of IL-33-induced MDSCs markedly inhibited the IL-1β production in MSU-induced peritonitis. This is the first to document the role of IL-33 in a mouse model of human gout. Current results provide evidences for a novel mechanism by which IL-33 ameliorates the MSU-induced inflammation via expanding $CD11b^{+}Gr1^{int}F4/80^{+}$ MDSCs.

IL-33 is a cytokine that is widely expressed in a variety of tissue cells, especially fibroblasts (8). Its production can be upregulated by inflammatory cytokines, such as such as IL-1β and TNF-α. Unlike conventional cytokines, IL-33 might be also secreted via unconventional pathways, and can be released upon cell injury as an alarmin. Here, we also observed an increased production of IL-33 in fibroblasts from gout patients, which were stimulated by inflammatory cytokines or MSU. Recent studies have shown that IL-33 played a complex effect in many diseases by interacting with its specific receptor ST2 (7). It has been reported that IL-33 plays a deleterious role in Th2-type immune mediated asthma and Th17-mediated autoimmune arthritis (11, 13). Conversely, a protective role of IL-33 was observed in atherosclerosis, sepsis, allograft transplant and parasite infection (9). Indeed, the IL-33/ST2 signaling also played a dichotomous role in inflammatory bowel disease pathogenesis (28). Our previous studies showed that IL-33 was markedly increased in

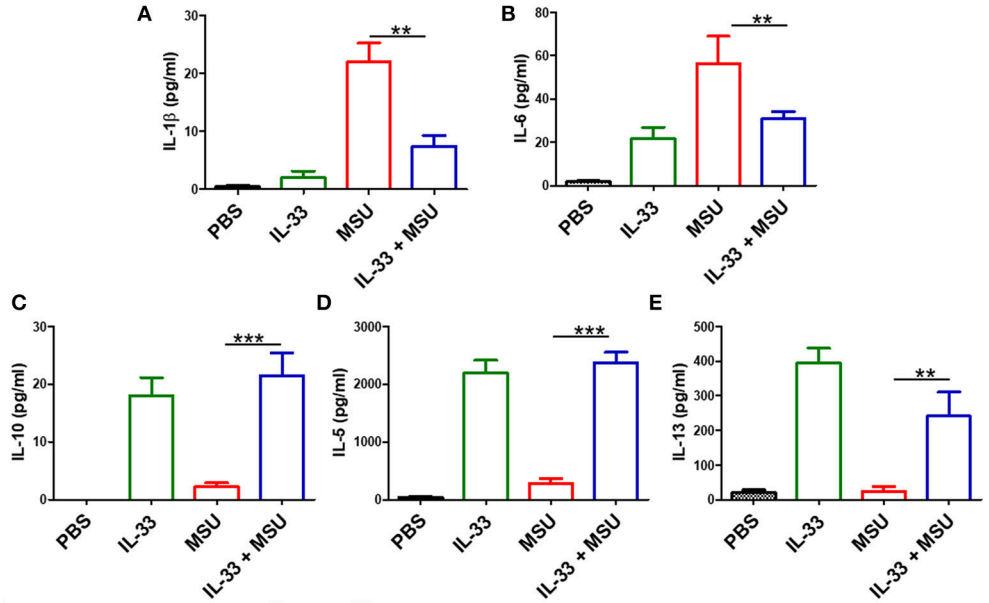

FIGURE 3 | IL-33 administration affects cytokines profile in MSU-induced inflammation. The peritoneal cavity gavage fluids were harvested after MSU treatment 16 h, and performed to detect the IL-1β, IL-6, IL-10, IL-5, and IL-13 cytokines levels by ELISA **(A,B)**. The expression of IL-1β and IL-6 in the MSU-inflammation was decreased by IL-33 treatment **(C–E)**. The expressions of IL-10, IL-5, and IL-13 in mice after IL-33 and MSU pretreatment were also analyzed by ELISA. Data are shown as the mean ± SEM ($n = 7$/group) and are representative of three independent experiments; $^{**}p < 0.001$, $^{***}p < 0.0001$.

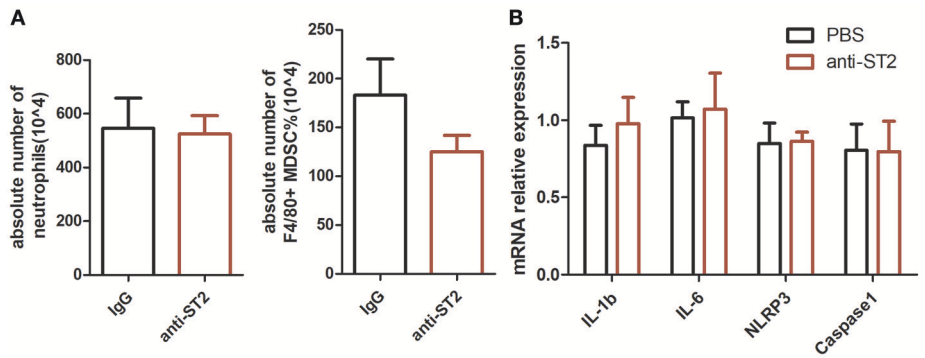

FIGURE 4 | Inhibition of endogenous interleukin-33 signaling has no effect on the development of MSU-induced peritonitis. Mice were pretreated with a neutralizing anti-ST2 antibody or control IgG 1 h before the injection of MSU. The mice were sacrificed after 16 h of MSU treatment, and the peritoneal exudate cells were harvested. The peritoneal cells were stained with anti-CD11b, anti-Gr-1, and anti-F4/80 antibodies **(A)**. The absolute number of neutrophils and MDSCs were analyzed by performing flow cytometry. Data represent mean ± SEM per group ($n = 5$/group). $p > 0.05$ **(B)**. The RNA of peritoneal cells were harvest and performed to detect the IL-1β, IL-6, NLRP3, and caspase-1 mRNA expression by RT-PCR method. $p > 0.05$.

the mice with TNBS-induced colitis, while rIL-33 treatment had a significant beneficial effect on Th1/Th17-mediated experimental colitis through promoting alternatively activated macrophage polarization and Tregs differentiation (24, 29). Interestingly, in our present study, although the level of IL-33 expression was increased in the gout patients and positively correlated with inflammatory marker CRP, the exogenous IL-33 treatment significantly inhibited the development of inflammation induced by MSU administration. In addition, blockage of IL-33 signaling by anti-ST2 antibody had no effect on the development of MSU-induced peritonitis. An interesting character of acute gout is the self-limiting nature of the inflammatory flare. In the absence of clinical intervention, a gouty episode can spontaneously resolve within 7–10 days. However, the mechanism of inflammation self-resolution is still elusive. Here, we speculate that an increased expression of IL-33 in the gout patients might due to a cause of self-negative regulation, which inhibits the development of MSU-induced inflammation, while the increased amount of IL-33 expression was inadequate to induce a potent protective effect to reduce the development of gout.

Acute gouty attacks are by nature self-limiting, and multiple mechanisms have been proposed for the spontaneous resolution

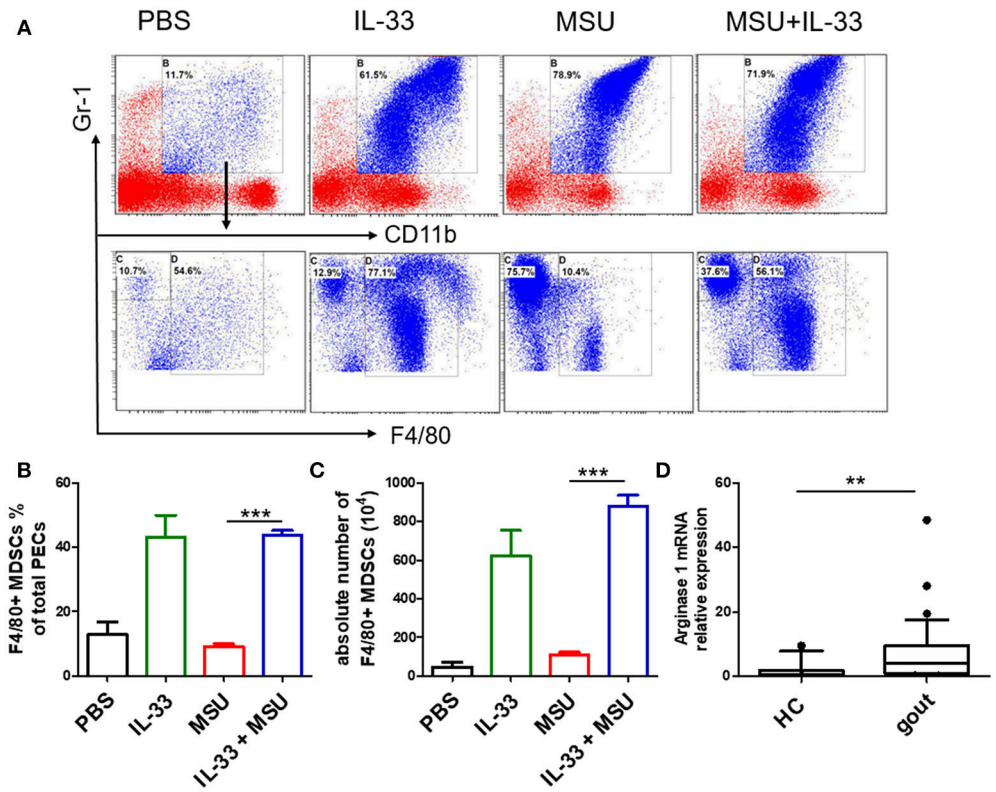

FIGURE 5 | IL-33 promoted MDSCs expansion in gout animal model. Mice were pretreated with IL-33 or PBS for 4 consecutive days prior to injection of MSU. The mice were sacrificed after 16 h of MSU treatment, and the cells from the peritoneal cavity were harvested **(A)**. The peritoneal cells were stained with anti-CD11b, anti-Gr-1, and anti-F4/80 antibodies. $CD11b^{+}Gr\text{-}1^{+}F4/80^{-}$ cells were considered to be neutrophils, while $CD11b^{+}Gr\text{-}1^{+}F4/80^{+}$ cells represent MDSCs **(B)**. Data are presented as the percentage of $CD11b^{+}Gr\text{-}1^{+}F4/80^{+}$ cells in $CD11b^{+}Gr\text{-}1^{+}$ cells **(C)**. The absolute number of $CD11b^{+}Gr\text{-}1^{+}F4/80^{+}$ cell was also quantified. The results shown are from one of three independent experiments. $^{***}p < 0.0001$ **(D)**. The PBMCs collected from gout patients and healthy control (HC) were subjected to analyze the Arginase-1 expression by RT-PCR method. The Mann-Whitney *U* test was used to calculate the significance. $^{**}p < 0.001$.

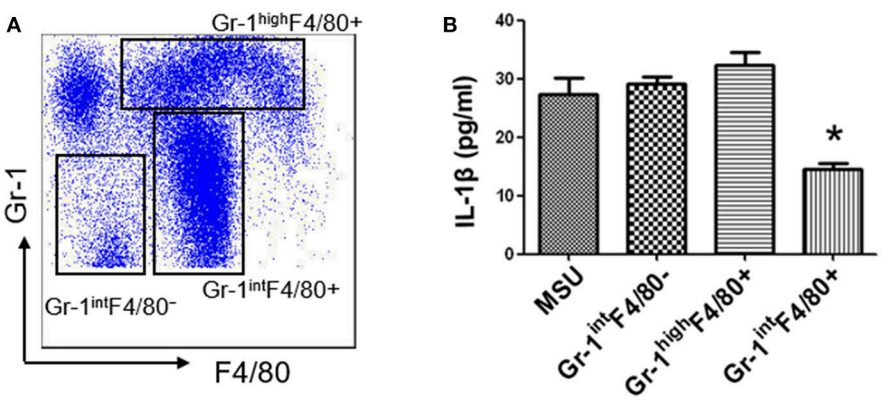

FIGURE 6 | IL-33 suppresses IL-1β production through expanding $CD11b^{+}Gr\text{-}1^{int}F4/80^{+}$ MDSCs **(A)**. Subpopulation ($CD11b^{+}Gr\text{-}1^{high}F4/80^{+}$, $CD11b^{+}Gr\text{-}1^{int}F4/80^{+}$, and $CD11b^{+}Gr\text{-}1^{int}F4/80^{-}$) induced by IL-33 in wild type mice were sorted by flow cytometry. The dot plots were gated from $CD11b^{+}$ cells **(B)**. Three groups of cells were successively adoptive transfer to the MSU-induced gout model mice. Four groups of mice (including a group of control mice treated with MSU only) were sacrificed and peritoneal lavage fluids were subjected to analyze the IL-1β production. Data are shown as the mean ± SEM ($n = 7$/group) and are representative of three independent experiments. $^{*}p < 0.05$.

of acute gout. Previous studies have shown that activated neutrophil impedes the interaction between immunoglobulin G (IgG) and MSU, leading to decrease the inflammation response. Besides that, ApoB and ApoE also exerts a key role in the resolution of acute gout through coating MSU crystal (30). Recently, the formation of neutrophil extracellular traps

(NETs) has gained increased attention in self-limiting gout inflammation. NETs can neutralize bacteria as well as other danger signals such as MSU crystals by the rapid extrusion of DNA, and can cleave inflammatory cytokines within minutes (5). Numerous studies have showed that MDSCs play an important role in regulating immune responses through producing arginase I, IL-10, and TGF-β (16). In allogeneic transplantation and tumor environments, IL-33 could regulate the induction and migration of MDSCs to inhibit transplant rejection and promotes the progression of mouse breast cancer, the mechanism of which is related to its inhibition of T cell responses (31). Here, we observed a large number of MDSCs ($CD11b^{+}Gr1^{int}F4/80^{+}$) in MSU-treated mice, which was different from neutrophil ($CD11b^{+}Gr1^{high}F4/80^{-}$) phenotype. Furthermore, adoptive transfer of IL-33-induced MDSCs ($CD11b^{+}Gr1^{int}F4/80^{+}$) markedly inhibited IL-1β production in MSU-induced peritonitis. Our study here presented a new clue for the self-limiting acute gout, and the increased IL-33 expression in gout patients might be a negative feedback mechanism on MSU-induced inflammation. Consistently, a recent study reported that LPS induces mononuclear cell-like MDSCs which can prevent tissue damage in acute lung injury through clearing apoptotic neutrophils (23). The clearance of apoptotic neutrophils by MDSCs was dependent on IL-10. In MSU crystal-induced inflammation, the IL-10 expression was increased after IL-33 treatment. We speculate that IL-33-induced MDSCs might alleviate the development of gout inflammation through phagocytosing neutrophils.

Our data demonstrated that increased IL-33 expression in gout patients might be a negative feedback mechanism on the MSU-induced inflammation response, because the inflammatory cytokine IL-1β production and the number of neutrophils were both markedly decreased in IL-33-treated mice. Furthermore, we reveal a requirement for MDSCs ($CD11b^{+}Gr1^{int}F4/80^{+}$) in resolution of MSU-induced inflammation. In conclusion, our data provide clear evidences that the increased expression of IL-33 in gout patients was involved in the self-resolution of MSU-induced inflammation, and IL-33 might be a promising therapeutic target for gout.

AUTHOR CONTRIBUTIONS

KS, YYW, and LD analyzed data and wrote the manuscript. YYW, KS, QS, and BY performed the experiments. KS and YT contributed to the clinical patients' sample collection. YH provided technical support. KS, YLW, and GS provided critical revision of the manuscript. LD and GS designed the research and revised the article. All authors have read and approved the final manuscript.

FUNDING

This research was supported by grants from the National Natural Science Foundation of China (NSFC 81671544 and 81871286 to LD, 81701556 to YH, 81471534 to GS), Fujian Province health planning of young outstanding talents training project no.2016-ZQN-82 to Lihua Duan, Natural Science Foundation of Fujian Provincial Department of Science and Technology 2017J01356 to LD.

ACKNOWLEDGMENTS

We thank all the volunteers who participated in this study.

REFERENCES

1. Richette P, Bardin T. Gout. *Lancet* (2010) 375:318–28. doi: 10.1016/S0140-6736(09)60883-7
2. Choi HK, Mount DB, Reginato AM, American College of Physicians, American Physiological Society. Pathogenesis of gout. *Ann Intern Med.* (2005) 143:499–516. doi: 10.7326/0003-4819-143-7-200510040-00009
3. Martinon F, Petrilli V, Mayor A, Tardivel A, Tschopp J. Gout-associated uric acid crystals activate the NALP3 inflammasome. *Nature* (2006) 440:237–41. doi: 10.1038/nature04516
4. Chen CJ, Shi Y, Hearn A, Fitzgerald K, Golenbock D, Reed G, et al. MyD88-dependent IL-1 receptor signaling is essential for gouty inflammation stimulated by monosodium urate crystals. *J Clin Invest.* (2006) 116:2262–71. doi: 10.1172/JCI28075
5. Schett G, Schauer C, Hoffmann M, Herrmann M. Why does the gout attack stop? A roadmap for the immune pathogenesis of gout. *RMD Open* (2015) 1(Suppl. 1):e000046. doi: 10.1136/rmdopen-2015-000046
6. Cronstein BN, Terkeltaub R. The inflammatory process of gout and its treatment. *Arthritis Res Ther.* (2006) 8 (Suppl. 1):S3. doi: 10.1186/ar1908
7. Schmitz J, Owyang A, Oldham E, Song Y, Murphy E, McClanahan TK, et al. IL-33, an interleukin-1-like cytokine that signals via the IL-1 receptor-related protein ST2 and induces T helper type 2-associated cytokines. *Immunity* (2005) 23:479–90. doi: 10.1016/j.immuni.2005.09.015
8. Liew FY, Pitman NI, McInnes IB. Disease-associated functions of IL-33: the new kid in the IL-1 family. *Nat Rev Immunol.* (2010) 10:103–10. doi: 10.1038/nri2692
9. Liew FY. IL-33: a Janus cytokine. *Ann Rheum Dis.* (2012) 71 (Suppl. 2):i101–4. doi: 10.1136/annrheumdis-2011-200589
10. Arend WP, Palmer G, Gabay C. IL-1, IL-18, and IL-33 families of cytokines. *Immunol Rev.* (2008) 223:20–38. doi: 10.1111/j.1600-065X.2008.00624.x
11. Liu X, Li M, Wu Y, Zhou Y, Zeng L, Huang T. Anti-IL-33 antibody treatment inhibits airway inflammation in a murine model of allergic asthma. *Biochem Biophys Res Commun.* (2009) 386:181–5. doi: 10.1016/j.bbrc.2009.06.008
12. Haenuki Y, Matsushita K, Futatsugi-Yumikura S, Ishii KJ, Kawagoe T, Imoto Y, et al. A critical role of IL-33 in experimental allergic rhinitis. *J Allergy Clin Immunol.* (2012) 130:184–94 e11. doi: 10.1016/j.jaci.2012.02.013
13. Palmer G, Talabot-Ayer D, Lamacchia C, Toy D, Seemayer CA, Viatte S, et al. Inhibition of interleukin-33 signaling attenuates the severity of experimental arthritis. *Arthritis Rheum.* (2009) 60:738–49. doi: 10.1002/art.24305
14. Yin H, Li XY, Jin XB, Zhang BB, Gong Q, Yang H, et al. IL-33 prolongs murine cardiac allograft survival through induction of TH2-type immune deviation. *Transplantation* (2010) 89:1189–97. doi: 10.1097/TP.0b013e3181d720af
15. Miller AM, Xu D, Asquith DL, Denby L, Li Y, Sattar N, et al. IL-33 reduces the development of atherosclerosis. *J Exp Med.* (2008) 205:339–46. doi: 10.1084/jem.20071868
16. Gabrilovich DI, Nagaraj S. Myeloid-derived suppressor cells as regulators of the immune system. *Nat Rev Immunol.* (2009) 9:162–74. doi: 10.1038/nri2506
17. Highfill SL, Rodriguez PC, Zhou Q, Goetz CA, Koehn BH, Veenstra R, et al. Bone marrow myeloid-derived suppressor cells (MDSCs) inhibit graft-versus-host disease (GVHD) via an arginase-1-dependent mechanism that is up-regulated by interleukin-13. *Blood* (2010) 116:5738–47. doi: 10.1182/blood-2010-06-287839

18. Zoso A, Mazza EM, Bicciato S, Mandruzzato S, Bronte V, Serafini P, et al. Human fibrocytic myeloid-derived suppressor cells express IDO and promote tolerance via Treg-cell expansion. *Eur J Immunol.* (2014) 44:3307–19. doi: 10.1002/eji.201444522
19. Marigo I, Bosio E, Solito S, Mesa C, Fernandez A, Dolcetti L, et al. Tumor-induced tolerance and immune suppression depend on the C/EBPbeta transcription factor. *Immunity* (2010) 32:790–802. doi: 10.1016/j.immuni.2010.05.010
20. Brunner SM, Schiechl G, Falk W, Schlitt HJ, Geissler EK, Fichtner-Feigl S. Interleukin-33 prolongs allograft survival during chronic cardiac rejection. *Transpl Int.* (2011) 24:1027–39. doi: 10.1111/j.1432-2277.2011.01306.x
21. Lu B, Yang M, Wang Q. Interleukin-33 in tumorigenesis, tumor immune evasion, and cancer immunotherapy. *J Mol Med.* (2016) 94:535–43. doi: 10.1007/s00109-016-1397-0
22. Turnquist HR, Zhao Z, Rosborough BR, Liu Q, Castellaneta A, Isse K, et al. IL-33 expands suppressive CD11b+ Gr-1(int) and regulatory T cells, including ST2L+ Foxp3+ cells, and mediates regulatory T cell-dependent promotion of cardiac allograft survival. *J Immunol.* (2011) 187:4598–610. doi: 10.4049/jimmunol.1100519
23. Poe SL, Arora M, Oriss TB, Yarlagadda M, Isse K, Khare A, et al. STAT1-regulated lung MDSC-like cells produce IL-10 and efferocytose apoptotic neutrophils with relevance in resolution of bacterial pneumonia. *Mucosal Immunol.* (2013) 6:189–99. doi: 10.1038/mi.2012.62
24. Duan L, Chen J, Zhang H, Yang H, Zhu P, Xiong A, et al. Interleukin-33 ameliorates experimental colitis through promoting Th2/Foxp3(+) regulatory T-cell responses in mice. *Mol Med.* (2012) 18:753–61. doi: 10.2119/molmed.2011.00428
25. Duan L, Huang Y, Su Q, Lin Q, Liu W, Luo J, et al. Potential of IL-33 for preventing the kidney injury via regulating the lipid metabolism in gout patients. *J Diabetes Res.* (2016) 2016:1028401. doi: 10.1155/2016/1028401
26. Kunisch E, Chakilam S, Gandesiri M, Kinne RW. IL-33 regulates TNF-alpha dependent effects in synovial fibroblasts. *Int J Mol Med.* (2012) 29:530–40. doi: 10.3892/ijmm.2012.883
27. Xu D, Jiang HR, Kewin P, Li Y, Mu R, Fraser AR, et al. IL-33 exacerbates antigen-induced arthritis by activating mast cells. *Proc Natl Acad Sci USA.* (2008) 105:10913–8. doi: 10.1073/pnas.0801898105
28. Hodzic Z, Schill EM, Bolock AM, Good M. IL-33 and the intestine: the good, the bad, and the inflammatory. *Cytokine* (2017) 100:1–10. doi: 10.1016/j.cyto.2017.06.017
29. Tu L, Chen J, Xu D, Xie Z, Yu B, Tao Y, et al. IL-33-induced alternatively activated macrophage attenuates the development of TNBS-induced colitis. *Oncotarget* (2017) 8:27704–14. doi: 10.18632/oncotarget.15984
30. Scanu A, Oliviero F, Gruaz L, Sfriso P, Pozzuoli A, Frezzato F, et al. High-density lipoproteins downregulate CCL2 production in human fibroblast-like synoviocytes stimulated by urate crystals. *Arthritis Res Ther.* (2010) 12:R23. doi: 10.1186/ar2930
31. Nagaraj S, Gabrilovich DI. Myeloid-derived suppressor cells in human cancer. *Cancer J.* (2010) 16:348–53. doi: 10.1097/PPO.0b013e3181eb3358

Conflict of Interest Statement: The authors declare that the research was conducted in the absence of any commercial or financial relationships that could be construed as a potential conflict of interest.

frontiers in Endocrinology

ORIGINAL RESEARCH
published: 18 April 2019
doi: 10.3389/fendo.2019.00252

IgG Anti-ghrelin Immune Complexes Are Increased in Rheumatoid Arthritis Patients Under Biologic Therapy and Are Related to Clinical and Metabolic Markers

Mildren Porchas-Quijada[1], Zyanya Reyes-Castillo[1], José Francisco Muñoz-Valle[2], Sergio Durán-Barragán[3,4], Virginia Aguilera-Cervantes[1], Antonio López-Espinoza[1], Mónica Vázquez-Del Mercado[4], Mónica Navarro-Meza[1] and Patricia López-Uriarte[1]*

[1] Instituto de Investigaciones en Comportamiento Alimentario y Nutrición, Centro Universitario del Sur, Universidad de Guadalajara, Ciudad Guzmán, Mexico, [2] Instituto de Investigaciones en Ciencias Biomédicas, Centro Universitario de Ciencias de la Salud, Universidad de Guadalajara, Guadalajara, Mexico, [3] Departamento de Reumatología, Clínica de Investigación en Reumatología y Obesidad, Guadalajara, Mexico, [4] Instituto de Investigación en Reumatología y del Sistema Músculo Esquelético, Centro Universitario de Ciencias de la Salud, Universidad de Guadalajara, Guadalajara, Mexico

OPEN ACCESS

Edited by:
Wen Kong,
Wuhan Union Hospital, China

Reviewed by:
Giulia Ricci,
Università degli Studi della Campania Luigi Vanvitelli Caserta, Italy
Xue Xu,
The Affiliated Drum Tower Hospital of Nanjing University Medical School, China

***Correspondence:**
Zyanya Reyes-Castillo
zyanya.reyes@cusur.udg.mx

Specialty section:
This article was submitted to Experimental Endocrinology, a section of the journal Frontiers in Endocrinology

Received: *20 August 2018*
Accepted: *01 April 2019*
Published: *18 April 2019*

Citation:
Porchas-Quijada M, Reyes-Castillo Z, Muñoz-Valle JF, Durán-Barragán S, Aguilera-Cervantes V, López-Espinoza A, Vázquez-Del Mercado M, Navarro-Meza M and López-Uriarte P (2019) IgG Anti-ghrelin Immune Complexes Are Increased in Rheumatoid Arthritis Patients Under Biologic Therapy and Are Related to Clinical and Metabolic Markers. Front. Endocrinol. 10:252. doi: 10.3389/fendo.2019.00252

Rheumatoid arthritis (RA) is a systemic autoimmune disease associated with increased risk of cardiovascular disease and metabolic alterations. The mechanisms underlying these alterations remain unclear. Ghrelin is a gastrointestinal hormone with potent effects on food intake, body weight, metabolism, and immune response. Recent studies reported the presence of anti-ghrelin autoantibodies in healthy subjects and the levels and affinity of these autoantibodies were altered in anorectic and obese individuals. In this cross-sectional study we analyzed anti-ghrelin autoantibodies in RA patients and evaluated its relationship with clinical, body-composition and metabolic parameters. Clinical measurements of RA patients included the disease activity score-28 (DAS-28), inflammatory biomarkers, autoantibodies (RF and anti-CCP), body composition, glucose and lipid profile. Serum ghrelin levels were measured by enzyme-linked immunosorbent assay (ELISA). Free and total anti-ghrelin autoantibodies quantification (IgG and IgA isotypes) was performed by in-house ELISA. RA patients had lower IgG anti-ghrelin autoantibodies levels and higher immune complexes percentage (IgG+ghrelin) compared to the control group, while the IgA anti-ghrelin autoantibodies showed no significant differences. In the bivariate analysis, the percentage of IgG anti-ghrelin immune complexes positively correlated with BMI and ghrelin whereas in the multivariate regression model, the variables associated were DAS-28, body weight, visceral fat, LDL-C and TG (R^2 = 0.72). The percentage of IgA anti-ghrelin immune complexes positively correlated with RF and anti-CCP and the multivariate regression model showed an association with RF and body fat percentage (R^2 = 0.22). Our study shows an increased percentage of IgG anti-ghrelin immune complexes in RA patients despite ghrelin levels were similar in both groups, suggesting an increase in the affinity of these autoantibodies toward ghrelin. The associations found in the multiple regression analysis

for anti-ghrelin immune complexes support the previously reported functions of these natural autoantibodies as carriers and modulators of the stability and physiological effect of the hormone. However, in RA both the disease activity and the RF appear to influence the formation of these anti-ghrelin immune complexes.

Keywords: ghrelin, rheumatoid arthritis, metabolic alterations, clinical activity, body composition

INTRODUCTION

Rheumatoid arthritis (RA) is a systemic inflammatory autoimmune disease, associated with high incidence of cardiovascular disease (CVD) and metabolic alterations, reporting an increase of 50% in deaths related to CVD in RA patients compared to the general population (1). This elevated risk is not only related to the classical CV risks like hypertension and dyslipidemias, but also to the chronic systemic inflammation occurring in the patients (2, 3). In addition, the inflammatory status in RA is associated with modifications of body composition, specifically an increase of body fat mass and depletion of lean mass, known as rheumatoid cachexia that can be present simultaneously with obesity (4, 5). Both, cachexia and obesity have been associated with higher disability scores and elevated risk of progressive disability (6–9). It has been recognized that the treatment of RA patients with disease-modifying anti-rheumatic drugs (DMARDs) such as methotrexate (MTX) and biological drugs including TNF-α and IL-6 blockers, as well as co-stimulation inhibitors such abatacept exert beneficial effects on the metabolic profile (10). Nevertheless, the precise mechanisms underlying the body-composition and metabolic alterations in RA as well as its relationship with the pharmacological therapy remain poorly understood.

Research on appetite and metabolism regulating hormones has increased substantially in rheumatic autoimmune diseases such as RA during the last years. Accumulating data strongly indicate that these hormones also exhibit potent actions on the regulation of immune and inflammatory responses and may play a role both in the pathogenesis and development of comorbidities in RA (11–13). Ghrelin is a 28 amino acid gastrointestinal peptide with potent orexigenic effects as well as anti-inflammatory properties including the inhibition of cytokines such as TNF-α, IL-1β, and IL-6 produced by T lymphocytes and monocytes (14–17). It has been shown that ghrelin increases the expression of adhesion molecules and exerts anti-proliferative effects on microvascular endothelial cells (18, 19). Also, ghrelin has demonstrated regulatory effects on bone metabolism, as it promotes osteoblast differentiation and proliferation and inhibits apoptosis (20, 21). Nevertheless, the concentrations and clinical relevance of ghrelin in RA are still controversial considering that some investigations reported lower (15), higher (22) or even similar (23, 24) levels of this hormone in patients under DMARDs and/or biological therapy in comparison to healthy controls.

Recent studies described the presence of autoantibodies directed against ghrelin in healthy subjects, and altered levels and affinity of these natural autoantibodies were reported in anorectic and obese individuals sera; suggesting that anti-ghrelin autoantibodies, specifically immunoglobulins of the G isotype (IgG) may affect the hormone transport and function according to its affinity, as well as regulate its stability by protecting the hormone from degradation (25–28). Co-administration of ghrelin and ghrelin-reactive IgG extracted from plasma of *ob/ob* mice to male lean C57B16 mice, increased their daily food intake and induced a tendency to increase their body weight (28). This may indicate that the presence of these natural autoantibodies directed against ghrelin and other appetite-regulating peptide hormones are associated with metabolism and body weight alterations (29). However, the presence and the possible role of these autoantibodies in autoimmune diseases have not been addressed, especially in RA where the occurring metabolic and body-composition alterations are prominent and the underlying mechanisms remain barely explored. Therefore, in this study we analyzed serum samples of RA patients and controls to characterize the circulating anti-ghrelin autoantibodies of IgG and IgA isotypes and evaluate its relationship with metabolic profile, body-composition and clinical parameters in RA patients undergoing biological therapy.

MATERIALS AND METHODS

Subjects

A cross-sectional study of RA patients and control subjects was performed. RA patients were previously classified according to the American College Rheumatism (ACR)/European League Against Rheumatism (EULAR) 2010 criteria (30). Those who had known history of other autoimmune, diabetes mellitus, renal, hepatic or CV disease, as well as those under 18 years of age or pregnant were excluded. Control subjects reported not having any diagnosed autoimmune, cardiovascular, hepatic, renal, infectious, or thyroid disease as well as not being under lipid-lowering medication. Patients were recruited from the Obesity and Rheumatology Research Center, located at Guadalajara, Jalisco, Mexico.

The study was approved by the Ethics Research Committee of University of Guadalajara (CEICUC, Review Board registry number CONBIOETICA14CEI03420150130) and was conducted according to the principles of the declaration of Helsinki. All participants were adults and voluntarily signed an informed consent before their inclusion in the study.

Methods

Clinical Data

All patients and controls answered a demographic and clinical interview at the moment of the blood sample collection.

Patients were evaluated by a rheumatologist that performed a general physical examination and assessed the number of painful and swollen joints for determining the RA clinical activity index by the disease activity score 28 (DAS-28) (31). The functional disability was assessed through the Health Assessment Questionnaire-Disability Index (HAQ-DI, Spanish version) (32). The erythrocyte sedimentation rate (ESR) was assessed through the Wintrobe method. C-reactive protein (CRP) and rheumatoid factor (RF) were measured by turbidimetric assays (Cat. No. COD31029 and COD31030A25, respectively, A25 Biosystems, Barcelona, Spain) using automatized equipment (BS-10; Mindray, Shenzhen, China). The cutoff value for RF positivity was 30 IU/mL, with a 95% specificity. Anti-cyclic citrullinated peptide antibodies (anti-CCP) were assessed using an ELISA kit (Cat. No. COD-FCCP600; Axis-Shield Diagnostics, Dundee, UK) following the instructions provided by the manufacturer; 5 U/mL were set as the cut-off point for positivity, with a 100 % specificity.

Body Composition and Anthropometry

All body-composition and anthropometric measurements were made by certified nutritionists. Body weight, musculoskeletal mass, body fat percentage (BF%) and visceral fat were measured by a bioelectrical impedance equipment (HBF-514C Omron Healthcare, Inc. Lakeside Drive Bannockburn, Illinois, USA) following the manufacturer instructions.

The participant's height was measured using a 2.05 m ± 1 mm scale portable stadiometer (Holtain Limited, Crynich, Difed, Britain Ltd. UK) following the technique described by Jellife and Jellife (33). The body mass index (BMI) was calculated by dividing weight in kg by the square of height in m. The waist circumference (WC) was measured midway between the lower rib and the iliac crest, at the end of a normal expiration to the nearest 0.1 cm.

Glucose and Lipid Profile

The blood samples were taken after an 8–12 h overnight fasting and centrifuged at 3,500 rpm during 15 min for serum separation. Samples were aliquoted and stored at −20°C until the day of the assay. Fasting glucose (Cat. No .1001190), total cholesterol (TC, Cat. No. 41022), low-density lipoprotein cholesterol (LDL-C, Cat. No. BSIS51-E), high-density lipoprotein cholesterol (HDL-C, Cat. No. BSIS37-E) and triglycerides (TG, Cat. No.1001313) were determined by colorimetric enzymatic methods using commercial kits (all reagents by Spinreact, Girona, Spain). Dyslipidemias and impaired fasting glucose were defined according to the Adult Treatment Panel III (ATPIII) guidelines (34) as TC ≥240 mg/dL, LDL-C ≥160 mg/dL, TG ≥200 mg/dL, HDL-C <40 mg/dL, and glucose ≥110 mg/dL.

Quantification of Ghrelin and Anti-ghrelin Autoantibodies

The fasting total ghrelin concentrations were assessed using an ELISA kit (Cat. No. EZGRT-89K, Upstate Chemicon Linco, Millipore), according to the manufacturer's instructions. A subsample of the RA patients ($n = 25$) was used to assess the serum ghrelin levels since not all were fasting.

To measure the autoantibodies against ghrelin of both IgA and IgG isotypes, an in-house ELISA test was performed based on a published protocol (35). This test allows the quantification of free (autoantibodies unbound to ghrelin) and total (autoantibodies forming immune complexes with ghrelin plus the free form) using two types of sample dilution buffers that create normal (pH 7.4) or dissociative conditions (pH 8.9), respectively, giving information about relative autoantibodies levels and affinities. Slight modifications were made to the method after thorough standardization; including the RA patients and controls serum dilution (1:1,000), the time of serum incubation (2 h) on ELISA plate, and the detection antibody dilution (1:8,000 for IgG and 1:15,000 for IgA). Both detection antibodies were conjugated to horseradish peroxidase (Cat. No. MBS674609 and Cat. No. MBS176676 for anti-human IgG and IgA, both from MyBioSource, California, USA) and incubated for 2 h. Subsequently, the plates were washed 4 times and 100 µl of the substrate tetramethylbenzidine (TMB, Sigma Aldrich) were added to the plate and incubated for 15 min for color development. Finally, 50 µl of stop solution was added and the optical density (OD) was read at 450 nm on a plate spectrophotometer (Bio-Rad, California, USA). For each ELISA plate, 2 wells were set as blank and the mean OD values were subtracted from the mean OD values of samples. Blank OD values in ELISA tests were all below 0.1, indicating that there was no unspecific binding of the detection antibody. Patient and control samples were run in duplicate, obtaining values with a mean variation <5% between duplicates for both IgA and IgG. IgG and IgA anti-ghrelin autoantibodies serum levels were expressed as OD, whereas IgG- and IgA-ghrelin immune complexes percentage were calculated using a ratio between free and total immunoglobulins by the following formula:

$$\text{Immune complexes percentage} = \mathbf{100} - \left(\frac{\textbf{Free OD}}{\textbf{Total OD}} \right) \times \mathbf{100}$$

Statistical Analyses

The data distribution was verified by D'Agostino-Pearson normality test and were reported as mean ± standard deviation (s.d.) for parametric data, and median (25–75th centiles) for variables with non-parametric distribution. Categorical variables were expressed as percentage and absolute frequency. Differences between two groups were assessed using Student's *t*-test or Mann-Whitney *U*-test for independent samples, according to data normality. To evaluate the relationship between clinical and metabolic variables with the anti-ghrelin autoantibodies a correlation analysis was carried out using Pearson's or Spearman's correlation tests in accordance with the data normality. Multivariate linear regression analysis was performed to analyze the association of clinical, biochemical and body-composition variables with the IgG and IgA anti-ghrelin immune complexes. Analyses were carried out using GraphPad Prism 6.0 (GraphPad Software, USA) and NCSS 2007 software (Number Cruncher Statistical System for Window, USA). The significance level was set at $p \leq 0.05$.

RESULTS

Patients Characteristics

Forty-nine RA patients and 32 control subjects were included in the study. The demographic, body composition, biochemical and clinical characteristics of both groups are shown in **Table 1**. The RA patients had a mean age of 50 ± 15 years, of which 87.7% were females. Controls had a mean age of 43 ± 8 years, of which 93.7% were females. The 30.6% of the RA patients reported past, and 8.2% current smoking habits while 9.4% of the control group reported past and 9.4% current smoking habits. Mean disease duration among patients was 8.5 ± 8.46 years, the ESR levels were higher in patients than in controls. The CRP levels in patients were found within normal values, whereas positivity for RF was 75 and 95% for anti-CCP. According to the DAS-28 score and the HAQ-DI questionnaire, on average, patients had moderate activity (3.43 ± 1.23) and low disability (0.54 ± 0.51). Most patients (91.8 %) were treated with politherapy, incorporating biological DMARDs (DMARDb).

The body-composition parameters were similar between RA patients and controls, except the visceral fat level which was higher ($p < 0.01$) among controls. On average, both groups were overweight (>25 kg/m^2) (36) according to the BMI (26.69 ± 4.05 kg/m^2 for RA patients and 27.92 ± 5.26 kg/m^2 for controls). The WC mean value was 89 cm in both groups, indicating abdominal obesity according to the ATP III WC cutoff point for women (>88 cm) (37). Both groups showed an excess of body fat (>30%) (38). Alike, the lipid profile and glucose levels were similar between RA patients and controls being within the normality ranges, excluding the LDL-C median levels which were higher among controls (141.50 mg/dL) than patients (113.50 mg/dL). The median total ghrelin levels were 636.20 pg/mL for RA patients and 642 pg/mL for controls, showing no significant differences.

TABLE 1 | Demographic, body composition, biochemical, and clinical characteristics.

	RA	Controls	*p*-value
Characteristics			
Demographics			
n	49	32	–
Age (years)	50 ± 15	43 ± 8	–
Female, % (*n*)	87.7 (43)	93.7 (30)	–
Smoking			–
Never, % (*n*)	61.2 (30)	81.2 (26)	–
Former, % (*n*)	30.6 (15)	9.4 (3)	–
Current, % (*n*)	8.2 (4)	9.4 (3)	–
Clinical Parameters			
RA duration (years)	8.50 ± 8.46	–	–
ESR (mm/h)	34.92 ± 13.93	27.53 ± 13.04	**0.021**
CRP (mg/dL)	3.40 (1.6–9.0)	–	–
RF (IU/mL)	80.05 (34.9–94.3)	–	–
Positives, % (n)	75.5 (37)	–	–
Anti-CCP (U/mL)	129.60 (35.1–412.8)	–	–
Positives, % (n)	95.9 (47)	–	–
DAS-28	3.43 ± 1.23	–	–
HAQ-DI	0.54 ± 0.51	–	–
Drug Treatment			
MTX + DMARDb[a], %	71.4	–	–
MTX + Baricitinib, %	8.2	–	–
DMARDb[a], %	20.4	–	–
Body Composition			
Weight	66.50 (57.3–71.8)	73.45 (63.3–79.6)	0.081
BMI (kg/m^2)	26.69 ± 4.05	27.92 ± 5.26	0.245
WC (cm)	89.28 ± 11.69	89.13 ± 14.09	0.957
BF (%)	39.55 (33.8–44.4)	41.60 (33.5–45)	0.468
Visceral fat level	8.30 ± 3.10	11.90 ± 5.40	**0.000**
Biochemical Parameters			
TC (mg/dL)	198.5 (174.3–240)	214.5 (186–243)	0.794
HDL-C (mg/dL)	40.92 ± 16.82	48.09 ± 14.80	0.089
LDL-C (mg/dL)	113.50 (102.5–149.3)	141.50 (102.3–201.8)	**0.030**
TG (mg/dL)	123.50 (94.7–191.3)	143.50 (102.3–201.8)	0.403
Glucose (mg/dL)	87.75 (79.8–97.6)	93.25 (83.25–104)	0.137
Ghrelin (pg/mL)	636.20 (503–761.1)	642 (480.5–1063)	0.634

Data are shown as mean ± s.d. or median (25–75th centile). TC, total cholesterol; HDL-C, high density lipoprotein cholesterol; LDL-C, low density lipoprotein cholesterol; TG, triglycerides; BMI, body mass index; WC, waist circumference; BF, body fat; ESR, erythrocyte sedimentation rate; RF, rheumatoid factor; Anti-CCP, anti-cyclic citrullinated peptide antibodies; CRP, C-reactive protein; DAS-28, disease activity score 28; HAQ-DI, health assessment questionnaire-disability index (Spanish version); MTX, methotrexate; DMARDb, biological disease-modifying anti-rheumatic drugs. Difference between groups was assessed by Student's t-test or Mann-Whitney U-test, p ≤ 0.05 values are highlighted in bold. [a] Including TNF, CD20, and IL-6 receptor inhibitors.

Anti-ghrelin Autoantibodies Analysis

Anti-ghrelin autoantibodies levels of both IgG and IgA isotypes are shown in **Figure 1**. Both free and total IgG anti-ghrelin autoantibodies were significantly higher in controls than in RA patients ($p < 0.05$) and on the contrary, the IgG immune complexes percentage was lower in controls than in RA patients ($p < 0.05$). While the IgA free and total anti-ghrelin autoantibodies levels, as well as the immune complexes percentage, showed no significant differences between controls and RA patients.

Correlations Between Anti-ghrelin Autoantibodies With Clinical Parameters and Metabolic Profile in RA

We assessed the correlation between the clinical parameters in RA with the free and total fractions of IgG and IgA anti-ghrelin autoantibodies. Anti-CCP antibodies were positively correlated with total IgA anti-ghrelin autoantibodies ($r = 0.326$, $p = 0.022$) and the DAS-28 activity score showed a positive correlation with free IgA anti-ghrelin autoantibodies ($r = 0.296$, $p = 0.050$).When addressing the relationship between metabolic profile in RA with free and total fractions of anti-ghrelin, we detected a negative correlation between visceral fat level and total IgG anti-ghrelin autoantibodies ($r = -0.519$, $p = 0.000$). LDL-C levels were found positively correlated with free IgA anti-ghrelin autoantibodies ($r = 0.404$, $p = 0.040$). Ghrelin levels showed a negative correlation with free IgG anti-ghrelin autoantibodies ($r = -0.534$, $p = 0.006$).

The percentage of ghrelin-immune complexes also displayed significant correlations with both the clinical and metabolic parameters in RA (**Figure 2**); the RF and anti-CCP antibodies

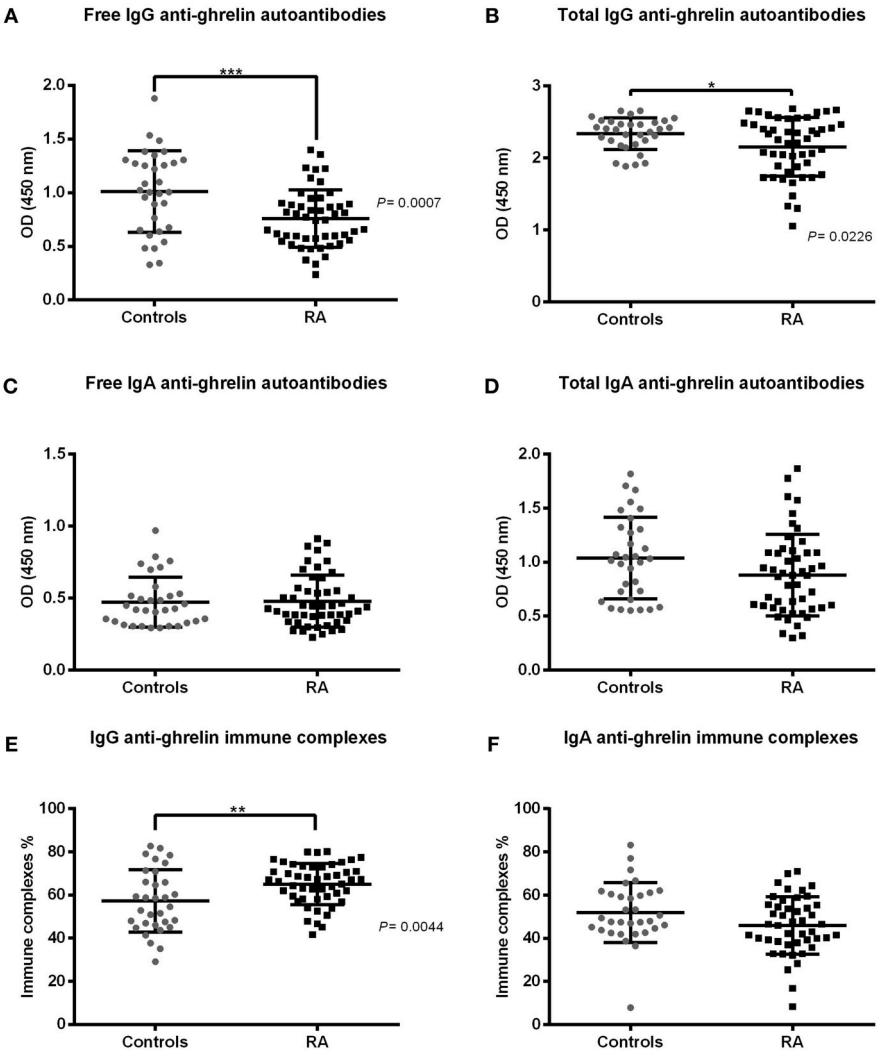

FIGURE 1 | IgG and IgA anti-ghrelin autoantibodies levels in rheumatoid arthritis (RA) patients and controls. IgG and IgA anti-ghrelin autoantibodies serum levels are expressed in optical density (OD). **(A,C)** Free IgG and IgA autoantibodies. **(B,D)** Total IgG and IgA anti-ghrelin autoantibodies. **(E,F)** IgG and IgA immune complexes percentage. Controls n=32, RA n=49. Horizontal lines indicate mean and standard deviation. Difference between groups was assessed by Student's *t*-test or Mann-Whitney *U*-test, as appropriate. *P*-values ≤0.05 were considered statistically significant (*p <0.05, **p <0.01, ***p <0.001).

showed positive correlations with the IgA anti-ghrelin immune complexes percentage ($r = 0.300$, $p = 0.042$ and $r = 0.372$, $p = 0.008$, respectively) while the BMI was negatively correlated with IgG anti-ghrelin immune complexes percentage ($r = -0.307$, $p = 0.035$). Ghrelin levels were found positively correlated with the IgG anti-ghrelin immune complexes percentage ($r = 0.432$, $p = 0.030$).

Multiple Regression Analyses of the Clinical, Biochemical, and Body-Composition Variables Associated With Anti-ghrelin Immune Complexes in RA

The IgG and IgA anti-ghrelin immune complexes percentage were further analyzed in a multiple regression model. We focused on the analysis of these complexes as they were significantly increased in RA patients and are likely implicated in the transport and modulation of biological effects of ghrelin (28). Thus, once we analyzed the simple correlations between the clinical, biochemical and body-composition parameters with both IgG and IgA anti-ghrelin autoantibodies levels, we selected the variables showing a significance of $p < 0.20$ as well as those previously reported to affect ghrelin concentrations.

The IgG anti-ghrelin immune complexes percentage was found associated with the DAS-28 score, weight, visceral fat level, LDL-C and TG concentrations explaining in a 72% its variance. While the IgA anti-ghrelin immune complexes were associated with RF and the BF percentage which explained a 22% of its variance (**Table 2**).

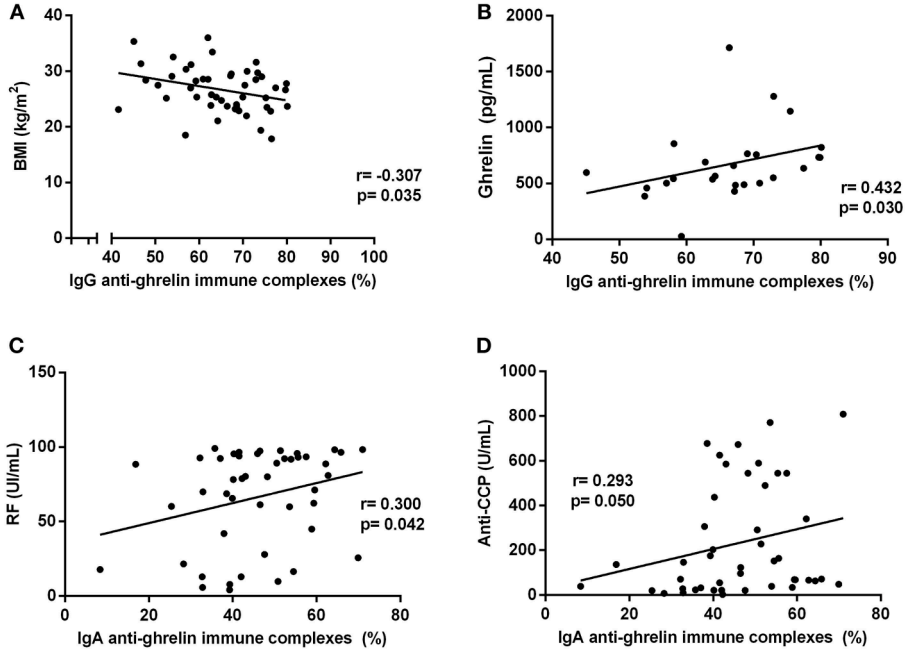

FIGURE 2 | Correlations analysis of IgG and IgA anti-ghrelin immune complexes percentage with clinical and metabolic parameters in rheumatoid arthritis patients. **(A)** Correlation between IgG immune complexes % and BMI. **(B)** Correlation between IgG immune complexes % and ghrelin levels. **(C)** Correlation between IgA immune complexes % and RF. **(D)** Correlation between IgA immune complexes % and anti-CCP antibodies. BMI, body mass index; RF, rheumatoid factor; Anti-CCP, anti-cyclic citrullinated peptide antibodies. R, Spearman's or Pearson's coefficient, as appropriate. Statistical significance was considered at $p \leq 0.05$.

TABLE 2 | Clinical, body composition, and biochemical parameters associated with IgG and IgA anti-ghrelin immune complexes in rheumatoid arthritis patients.

Parameters	IgG immune complexes (%)[a]		IgA immune complexes (%)[b]	
	β	*p*	β	*p*
DAS-28 (score)	−3.385	0.006		
Weight (kg)	−0.588	0.000		
Visceral fat	4.255	0.000		
LDL-C (mg/dL)	−0.121	0.003		
TG (mg/dL)	−0.086	0.003		
RF (IU/mL)			0.119	0.041
Body fat (%)			−0.503	0.028

DAS-28, disease activity score 28; RF, rheumatoid factor; LDL-C, low density lipoprotein cholesterol; TG, triglycerides. Multivariate analysis results from multiple linear regression analysis. The total explained variance of the model was $^{a}R^2 = 0.72$, $^{b}R^2 = 0.22$.

DISCUSSION

RA is associated with metabolic alterations, changes in body composition as well as increased risk of developing CV diseases (1, 2). Ghrelin, the main orexigenic hormone, is a gastrointestinal peptide with regulatory effects on metabolism and anti-inflammatory properties (15, 16). Recent studies reported the presence of natural autoantibodies directed against ghrelin in healthy individuals and altered levels and affinity of these autoantibodies in appetite-related pathologies including obesity and anorexia nervosa, suggesting a physiological role of these autoantibodies in ghrelin regulation (25, 27). In the present study, we evaluated for the first time the presence of anti-ghrelin autoantibodies of both IgG and IgA isotypes in RA patients under biological therapy and analyzed its relationship with body composition, metabolic profile and clinical activity parameters.

Analysis of ghrelin serum levels showed no significant differences in our cohort of RA patients in comparison to controls. Similarly to our findings, no significant differences in ghrelin levels were found among patients with established RA receiving traditional DMARDs treatment (17, 18) neither in patients under anti-TNF-α therapy (39) when compared to healthy controls. Conversely, a decrease in acyl-ghrelin levels in RA patients under DMARDs and/or biologics was reported in comparison to controls (15, 22), whereas higher levels of total ghrelin were observed after treatment with a TNF-α blocker in comparison to controls (22, 40). These apparently conflicting results may be explained by differences in the form of ghrelin measured in the studies (acyl, des-acyl, or total hormone levels), the patient's clinical characteristics as well as the treatment scheme.

Despite the lack of differences in ghrelin serum levels, we found that free and total IgG anti-ghrelin autoantibodies were decreased in our cohort of RA patients compared to controls. This decrease is probably an effect of the patient's immunosuppressive therapy as all of them were under MTX and/or biological therapy. MTX and abatacept have potent anti-inflammatory properties, and several clinical studies have demonstrated its effects on reducing serum immunoglobulins

(41–44). Furthermore, MTX has demonstrated to lower total and transitional B cells as well as total T cell numbers in peripheral blood (41, 42, 45). Similarly, a decrement in both free and total IgG anti-ghrelin autoantibodies levels, as well as a decrease on their binding affinity with ghrelin, were observed in a rat model of methotrexate chemotherapy-induced anorexia (46). To support and extend the data obtained in this cross-sectional study it will be important to conduct longitudinal studies to further determine the effects of different RA treatment schemes on these natural anti-ghrelin autoantibodies.

In contrast to the decrease in free and total IgG anti-ghrelin autoantibodies in RA, we detected a higher percentage of IgG-ghrelin immune complexes in the patients as compared to controls. This is indicative of an increase on the affinity these autoantibodies toward ghrelin, probably as an adaptive mechanism in response to the reduction of the total fraction of anti-ghrelin autoantibodies among treated patients. We speculate that such affinity-mediated augment in the formation of anti-ghrelin immune complexes in RA, favor the stability and transport of ghrelin thereby enhancing its biological effects. Despite in the present study we did not measured the kinetic affinities of these autoantibodies in RA, previous studies performed by Fetissov and co-workers in other pathologies including obesity and anorexia nervosa can support our theory (28, 47). They demonstrated that ghrelin-reactive antibodies of the IgG isotype present a very variable Fab region showing distinctive affinities in the context of different pathologies (28). In obese individuals, increased kinetics affinities of IgG antibodies for the orexigenic hormone ghrelin were found and the transfer of these antibodies to mice promoted food intake and body weight gain. Similarly, IgG antibodies directed to the anorexigenic hormone leptin showed decreased affinity in obese humans (28, 48). It is worth mentioning that although there can be changes in the affinity of these ghrelin-reactive autoantibodies its affinity remains at the micromolar range and these can be classified as low-affinity, not being capable of neutralizing the hormone, but instead modulate its transport and/or protect it from degradation by serum enzymes (28). Even though the precise mechanisms fine-tuning the affinity of these natural autoantibodies remain unknown, these findings provide evidence that IgG anti-ghrelin autoantibodies undergo affinity modification in the context of metabolic pathologies as well as in immune-mediated diseases such as RA.

The IgG anti-ghrelin immune complexes percentage correlated with BMI and ghrelin levels in the bivariate analysis. This positive correlation with total ghrelin levels is reasonable, since it suggests that an increase in serum ghrelin levels cause more availability for the ghrelin-reactive antibodies to bound and form immune complexes. While in the multivariate regression model we found an interaction between DAS-28 score, body weight, visceral fat level, LDL-C, and TG concentrations, which explained a 72% of the variation in the percentage of these complexes. It should be noted that body weight, visceral fat level, LDL-C and TG have been previously correlated with ghrelin levels in several studies. The BMI and visceral fat mass were reported negatively correlated with plasma ghrelin (49, 50), which may indicate that the secretion of this hormone is reduced as a physiological adjustment in response to the positive energetic balance. In addition, it is recognized that ghrelin participates in lipid metabolism as it enhances adiposity by promoting the expression of several fat storage-related proteins in adipocytes (51). In concordance with our multivariate model, LDL-C and TG concentrations were reported negatively correlated with ghrelin in a study in obese children (52). In addition, Beaumont et al. (53) described that HDL-C particles may directly interact with ghrelin serving as a circulatory carrier, however, in our model HDL-C did not show an association with the percentage of ghrelin-immune complexes, suggesting that these antibodies are an independent carrier of the hormone.

The association of anti-ghrelin immune complexes with the DAS-28 in the multivariate analysis was striking, considering the fact that serum ghrelin levels alone were not associated with the disease activity nor with other clinical biomarkers in RA (data not shown); this suggests that anti-ghrelin autoantibodies but not ghrelin, are affected by the disease activity of the patients. Taken together, our results show that IgG-ghrelin immune complexes percentage exhibit the same associations previously reported for ghrelin and strongly support the idea of these autoantibodies as low-affinity carriers modulating the stability and biological effects of the hormone. However, in RA the IgG-ghrelin immune complexes formation appears to be negatively influenced by the disease activity. According to the multiple regression model it can be predicted that an increase on the disease activity as well as a rise in LDL-C and TG concentrations could affect the formation of IgG-ghrelin immune complexes. Based on the observation that patients in our study had an overall controlled RA (showing low to moderate activity according to DAS-28 score and low inflammatory biomarkers) this model may also explain the significant increase observed in the IgG anti-ghrelin immune complexes percentage in the patients, besides the previously discussed affinity-mediated compensatory mechanism that may promote ghrelin immune complexes formation.

While for the IgA anti-ghrelin autoantibodies levels, no differences were found between controls and patients. We hypothesize that this is related to the sample type used to quantify these isotype because IgA is not predominant in serum (in contrast to the IgG class), but is rather predominantly secreted in mucous membranes (54). Furthermore, the presence of IgA anti-ghrelin autoantibodies in serum, may indicate that these autoantibodies are triggered by antigens present in the intestinal lumen either under physiological or pathological conditions (27, 55). Since the gastrointestinal microbiota is a major physiological source of antigens, there has been suggested that bacterial epitopes can trigger cross-reactivity to regulatory peptides such as ghrelin, which displays sequence homology with commensal bacteria and viruses (27).

An interesting finding was the positive correlation observed between IgA anti-ghrelin immune complexes with RF and anti-CCP autoantibodies. The role of rheumatoid factors in the formation of immune complexes has been widely acknowledged in RA; this mechanism can enhance the inflammatory status through the release of inflammatory cytokines such as TNF-α and IL-6 via activation of Fc receptors expressed by innate immune cells such as macrophages. Nevertheless, this observation does

not imply that anti-ghrelin complexes are considered pathogenic but rather regulatory, as these are detected in healthy individuals. In addition, autoantibody systems in RA are frequently correlated with each other; as described previously for anti-CCP and RF, and for RF and anti-PAD4 antibodies (56). Similarly, the multivariate regression model showed an association of the IgA anti-ghrelin immune complexes with RF and body fat percentage but only explained a 22 % of its variance. The negative association with body fat percentage again supports the hypothesis that the secretion of this hormone is reduced as a physiological adjustment in response to the positive energetic balance.

In summary, we evaluated for the first time the presence of IgG and IgA anti-ghrelin autoantibodies in RA patients and confirmed the previously reported presence of these natural autoantibodies in healthy individuals (26). Increased percentage of IgG anti-ghrelin immune complexes was found in RA patients under biological therapy with a low to moderate disease activity. This is indicative of an increase in the affinity of these autoantibodies toward ghrelin, probably as an adaptive mechanism in response to the reduction of the total fraction of anti-ghrelin autoantibodies among treated patients. In the multivariate regression analyses, the IgG-ghrelin immune complexes were associated with DAS-28, body weight, visceral fat, LDL-C, and TG while the IgA-ghrelin immune complexes were only associated to RF and body fat percentage, supporting the idea of these anti-ghrelin natural autoantibodies acting as carriers and modulators of the stability and physiological effect of the hormone. However, in RA both the disease activity and the hallmark autoantibody (RF) appear to influence the formation of these anti-ghrelin immune complexes. Future longitudinal studies should address the effects of different treatment schemes on these natural antibodies as well as monitor its changes in relation to clinical activity and metabolic changes in RA. In addition, analysis of autoantibodies directed to acyl-ghrelin or des-acyl ghrelin specific forms would be also informative.

ETHICS STATEMENT

The study was approved by the Ethics Research Committee of University of Guadalajara (CEICUC, Review Board registry number CONBIOETICA14CEI03420150130) and was conducted according to the principles of the declaration of Helsinki. All participants were adults and voluntarily signed an informed consent before their inclusion in the study.

AUTHOR CONTRIBUTIONS

ZR-C was involved in the conception, design and performance of experiments, interpretation of data, and revision of the manuscript. MP-Q performed experiments, analyzed and interpreted the data, and wrote the article. JFM-V and SD-B aided in the design of the study, interpretation of data, and critical revision of the manuscript. MN-M provided help on data acquisition and interpretation. VA-C, AL-E, MV-D, and PL-U helped with the interpretation of data and critical revision of the paper. All authors read and approved the submitted version of the manuscript.

FUNDING

This study was supported by Instituto de Nutrición y Salud Kellogg's (INSK) by the funding program Apoyo a Proyectos de Investigación en Nutrición (APIN-2016) granted to ZR-C. The funding source had no involvement on the design nor any steps of the study.

ACKNOWLEDGMENTS

The authors would like to thank Instituto de Investigación en Ciencias Biomédicas and Centro de Investigación en Biología Molecular de las Enfermedades Crónicas, for kindly providing the facilities for performing some of the experiments of the study.

REFERENCES

1. Avina-Zubieta JA, Thomas J, Sadatsafavi M, Lehman AJ, Lacaille D. Risk of incident cardiovascular events in patients with rheumatoid arthritis: a meta-analysis of observational studies. *Ann Rheum Dis.* (2012) 71:1524–9. doi: 10.1136/annrheumdis-2011-200726
2. Dessein PH, Joffe BI, Veller MG, Stevens BA, Tobias M, Reddi K, et al. Traditional and nontraditional cardiovascular risk factors are associated with atherosclerosis in rheumatoid arthritis. *J Rheumatol.* (2005) 32:435–42. Available online at: http://www.jrheum.org/content/jrheum/32/3/435.full.pdf
3. Graf J, Scherzer R, Grunfeld C, Imboden J. Levels of C-reactive protein associated with high and very high cardiovascular risk are prevalent in patients with rheumatoid arthritis. *PLoS ONE.* (2009) 4:e6242. doi: 10.1371/journal.pone.0006242
4. Elkan A-C, Engvall I-L, Cederholm T, Hafström I. Rheumatoid cachexia, central obesity and malnutrition in patients with low-active rheumatoid arthritis: feasibility of anthropometry, Mini Nutritional Assessment and body composition techniques. *Eur J Nutr.* (2009) 48:315–22. doi: 10.1007/s00394-009-0017-y
5. Rall LC. Rheumatoid cachexia: metabolic abnormalities, mechanisms and interventions. *Rheumatology.* (2004) 43:1219–23. doi: 10.1093/rheumatology/keh321
6. Feng J, Chen Q, Yu F, Wang Z, Chen S, Jin Z, et al. Body mass index and risk of rheumatoid arthritis: a meta-analysis of observational studies. *Medicine.* (2016) 95:e2859. doi: 10.1097/MD.0000000000002859
7. Baker JF, England BR, Mikuls TR, Sayles H, Cannon GW, Sauer BC, et al. Obesity, weight loss, and progression of disability in rheumatoid arthritis. *Arthr Care Res.* (2018) 70:1740–7. doi: 10.1002/acr.23579
8. Engvall I, Elkan A, Tengstrand B, Cederholm T, Brismar K, Hafström I. Cachexia in rheumatoid arthritis is associated with inflammatory activity, physical disability, and low bioavailable insulin-like growth factor. *Scand J Rheumatol.* (2008) 37:321–8. doi: 10.1080/03009740802055984
9. Masuko K. Rheumatoid cachexia revisited: a metabolic co-morbidity in rheumatoid arthritis. *Front Nutr.* (2014) 1:20. doi: 10.3389/fnut.2014.00020
10. Lee JL, Sinnathurai P, Buchbinder R, Hill C, Lassere M, March L. Biologics and cardiovascular events in inflammatory arthritis: a prospective national cohort study. *Arthr ResTher.* (2018) 20:171. doi: 10.1186/s13075-018-1669-x
11. Morton GJ, Cummings DE, Baskin DG, Barsh GS, Schwartz MW. Central nervous system control of food intake and body weight. *Nature.* (2006) 443:289–95. doi: 10.1038/nature05026

12. Stensel D. Exercise, appetite and appetite-regulating hormones: implications for food intake and weight control. *Ann Nutr Metabol.* (2010) 57:36–42. doi: 10.1159/000322702
13. Francisco V, Pino J, Campos-Cabaleiro V, Ruiz-Fernández C, Mera A, Gonzalez-Gay MA, et al. Obesity, fat mass and immune system: role for leptin. *Front Physiol.* (2018) 9:640. doi: 10.3389/fphys.2018.00640
14. Wren AM, Seal LJ, Cohen MA, Brynes AE, Frost GS, Murphy KG, et al. Ghrelin enhances appetite and increases food intake in humans. *J Clin Endocrinol Metab.* (2001) 86:5992. doi: 10.1210/jcem.86.12.8111
15. Otero M, Nogueiras R, Lago F, Dieguez C, Gomez-Reino JJ, Gualillo O. Chronic inflammation modulates ghrelin levels in humans and rats. *Rheumatology*. (2004) 43:306–10. doi: 10.1093/rheumatology/keh055
16. Li WG. Ghrelin inhibits proinflammatory responses and nuclear factor-B activation in human endothelial cells. *Circulation.* (2004) 109:2221–6. doi: 10.1161/01.CIR.0000127956.43874.F2
17. Dixit VD, Schaffer EM, Pyle RS, Collins GD, Sakthivel SK, Palaniappan R, et al. Ghrelin inhibits leptin- and activation-induced proinflammatory cytokine expression by human monocytes and T cells. *J Clin Investig.* (2004) 114:57–66. doi: 10.1172/JCI200421134
18. Kumpers P, Horn R, Brabant G, Woywodt A, Schiffer M, Haller H, et al. Serum leptin and ghrelin correlate with disease activity in ANCA-associated vasculitis. *Rheumatology.* (2007) 47:484–7. doi: 10.1093/rheumatology/ken023
19. Skilton MR, Nakhla S, Sieveking DP, Caterson ID, Celermajer DS. Pathophysiological levels of the obesity related peptides resistin and ghrelin increase adhesion molecule expression on human vascular endothelial cells. *Clin Exp Pharmacol Physiol.* (2005) 32:839–44. doi: 10.1111/j.1440-1681.2005.04274.x
20. Delhanty PJD, van der Eerden BCJ, van Leeuwen JPTM. Ghrelin and bone: ghrelin and bone. *BioFactors.* (2014) 40:41–8. doi: 10.1002/biof.1120
21. Kim SW, Her SJ, Park SJ, Kim D, Park KS, Lee HK, et al. Ghrelin stimulates proliferation and differentiation and inhibits apoptosis in osteoblastic MC3T3-E1 cells. *Bone.* (2005) 37:359–69. doi: 10.1016/j.bone.2005.04.020
22. Magiera M, Kopec-Medrek M, Widuchowska M, Kotulska A, Dziewit T, Ziaja D, et al. Serum ghrelin in female patients with rheumatoid arthritis during treatment with infliximab. *Rheumatol Int.* (2013) 33:1611–3. doi: 10.1007/s00296-011-2262-7
23. Toussirot É. Serum adipokines and adipose tissue distribution in rheumatoid arthritis and ankylosing spondylitis. A comparative study. *Front Immunol.* (2013) 4:453. doi: 10.3389/fimmu.2013.00453
24. Koca SS, Ozgen M, Aydin S, Dag S, Evren B, Isik A. Ghrelin and obestatin levels in rheumatoid arthritis. *Inflammation.* (2008) 31:329–35. doi: 10.1007/s10753-008-9082-2
25. Fetissov SO, Lucas N, Legrand R. Ghrelin-reactive immunoglobulins in conditions of altered appetite and energy balance. *Front Endocrinol.* (2017) 8:10. doi: 10.3389/fendo.2017.00010
26. Fetissov SO, Hamze Sinno M, Coquerel Q, Do Rego JC, Coëffier M, Gilbert D, et al. Emerging role of autoantibodies against appetite-regulating neuropeptides in eating disorders. *Nutrition.* (2008) 24:854–9. doi: 10.1016/j.nut.2008.06.021
27. Fetissov SO, Hamze Sinno M, Coëffier M, Bole-Feysot C, Ducrotté P, Hökfelt T, et al. Autoantibodies against appetite-regulating peptide hormones and neuropeptides: Putative modulation by gut microflora. *Nutrition*. (2008) 24:348–59. doi: 10.1016/j.nut.2007.12.006
28. Takagi K, Legrand R, Asakawa A, Amitani H, François M, Tennoune N, et al. Anti-ghrelin immunoglobulins modulate ghrelin stability and its orexigenic effect in obese mice and humans. *Nat Commun.* (2013) 4:2685. doi: 10.1038/ncomms3685
29. Fetissov SO, Déchelotte P. The putative role of neuropeptide autoantibodies in anorexia nervosa. *Curr Opin Clin Nutr Metabol Care.* (2008) 11:428–34. doi: 10.1097/MCO.0b013e3282fcec2e
30. Aletaha D, Neogi T, Silman AJ, Funovits J, Felson DT, Bingham CO, et al. Rheumatoid arthritis classification criteria: an American college of rheumatology/european league against rheumatism collaborative initiative. *Ann Rheum Dis.* (2010) 69:1892. doi: 10.1136/ard.2010.138461
31. Prevoo ML, van 't Hof MA, Kuper HH, van Leeuwen MA, van de Putte LB, van Riel PL. Modified disease activity scores that include twenty-eight-joint counts. Development and validation in a prospective longitudinal study of patients with rheumatoid arthritis. *Arthritis Rheum.* (1995) 38:44–8. doi: 10.1002/art.1780380107
32. Cardiel MH, Abello-Banfi M, Ruiz-Mercado R, Alarcon-Segovia D. How to measure health status in rheumatoid arthritis in non-English speaking patients: validation of a Spanish version of the Health Assessment Questionnaire Disability Index (Spanish HAQ-DI). *Clin Exp Rheumatol.* (1993) 11:117–21.
33. Jelliffe DB, Jelliffe EFP. *Community Nutritional Assessment: With Special Reference to Less Technically Developed Countries.* Oxford; New York, NY: Oxford University Press (1989). p. 633.
34. National Cholesterol Education Program (NCEP) expert panel on detection, evaluation, and treatment of high blood cholesterol in adults (adult treatment panel III). Third report of the national cholesterol education program (NCEP) expert panel on detection, evaluation, and treatment of high blood cholesterol in adults (adult treatment panel III) final report. *Circulation*. (2002) 106:3143–421. doi: 10.1161/circ.106.25.3143
35. Fetissov SO. Neuropeptide Autoantibodies Assay. In: Merighi A, editor. *Neuropeptides [Internet].* Totowa, NJ: Humana Press (2011) p. 253.
36. World Health Organization. *Obesity: Preventing and Managing the Global Epidemic: Report of a WHO Consultation.* Geneva: World Health Organization (2000). p. 253
37. World Health Organization. *Waist Circumference and Waist-Hip Ratio: Report of a WHO Expert Consultation, Geneva, 8-11 December 2008*. Geneva: World Health Organization (2011).
38. Bray GA. *Contemporary Diagnosis and Management of Obesity*. Newton, PA: Handbooks in Health Care Co (1998).
39. Ferraz-Amaro I, Arce-Franco M, Mu-iz J, López-Fernández J, Hernández-Hernández V, Franco A, et al. Systemic blockade of TNF-α does not improve insulin resistance in humans. *Hormone Metabol Res.* (2011) 43:801–8. doi: 10.1055/s-0031-1287783
40. Gonzalez-Gay MA, Gonzalez-Juanatey C, Miranda-Filloy JA, Martin J, Garcia-Unzueta MT, Llorca J. Response to "Infliximab therapy increases body fat mass in early rheumatoid arthritis independently of changes in disease activity and levels of leptin and adiponectin: a randomized study over 21 months." *Arthr Res Ther.* (2011) 13:404. doi: 10.1186/ar3301
41. Glaesener S, Quách TD, Onken N, Weller-Heinemann F, Dressler F, Huppertz H-I, et al. Distinct effects of methotrexate and etanercept on the B cell compartment in patients with juvenile idiopathic arthritis: MTX and etanercept differentially affect B cells in JIA. *Arthr Rheumatol.* (2014) 66:2590–600. doi: 10.1002/art.38736
42. Böhm I. Decrease of B-cells and autoantibodies after low-dose methotrexate. *Biomed Pharmacother.* (2003) 57:278–81. doi: 10.1016/S0753-3322(03)00086-6
43. Scarsi M, Paolini L, Ricotta D, Pedrini A, Piantoni S, Caimi L, et al. Abatacept reduces levels of switched memory b cells, autoantibodies, and immunoglobulins in patients with rheumatoid arthritis. *J Rheumatol.* (2014) 41:666–72. doi: 10.3899/jrheum.130905
44. Conigliaro P, Triggianese P, Giampà E, Sole Chimenti M, Kroegler B, Perricone R. Effects of abatacept on T-lymphocyte sub-populations and immunoglobulins in patients affected by rheumatoid arthritis. *Isr Med Assoc J.* (2017) 19:406–10. Available online at: https://www.ima.org.il/MedicineIMAJ/viewarticle.aspx?year=2017&month=07&page=406
45. Wascher TC, Hermann J, Brezinschek HP, Brezinschek R, Wilders-Truschnig M, Rainer F, et al. Cell-type specific response of peripheral blood lymphocytes to methotrexate in the treatment of rheumatoid arthritis. *Clin Investig.* (1994) 72:535–40. doi: 10.1007/BF00207484
46. François M, Takagi K, Legrand R, Lucas N, Beutheu S, Bôle-Feysot C, et al. Increased ghrelin but low ghrelin-reactive immunoglobulins in a rat model of methotrexate chemotherapy-induced anorexia. *Front Nutr.* (2016) 3:23. doi: 10.3389/fnut.2016.00023
47. Lucas N, Legrand R, Breton J, Déchelotte P, Fetissov SO. Increased affinity of ghrelin-reactive immunoglobulins in obese Zucker rats. *Nutrition.* (2017) 39–40:98–9. doi: 10.1016/j.nut.2016.11.007
48. Bouhajja H, Bougacha-Elleuch N, Lucas N, Legrand R, Marrakchi R, Kaveri SV, et al. Affinity kinetics of leptin-reactive immunoglobulins are associated

with plasma leptin and markers of obesity and diabetes. *Nutr Diabet.* (2018) 8:32. doi: 10.1038/s41387-018-0044-y
49. Monti V, Carlson JJ, Hunt SC, Adams TD. Relationship of ghrelin and leptin hormones with body mass index and waist circumference in a random sample of adults. *J Am Diet Assoc.* (2006) 106:822–8. doi: 10.1016/j.jada.2006.03.015
50. Sondergaard E, Gormsen LC, Nellemann B, Vestergaard ET, Christiansen JS, Nielsen S. Visceral fat mass is a strong predictor of circulating ghrelin levels in premenopausal women. *Eur J Endocrinol.* (2009) 160:375–9. doi: 10.1530/EJE-08-0735
51. Rodríguez A. Novel molecular aspects of ghrelin and leptin in the control of adipobiology and the cardiovascular system. *Obesity Facts.* (2014) 7:82–95. doi: 10.1159/000360837
52. Razzaghy-Azar M, Nourbakhsh M, Pourmoteabed A, Nourbakhsh M, Ilbeigi D, Khosravi M. An evaluation of acylated ghrelin and obestatin levels in childhood obesity and their association with insulin resistance, metabolic syndrome, and oxidative stress. *J Clin Med.* (2016) 5:61. doi: 10.3390/jcm5070061
53. Beaumont NJ, Skinner VO, Tan TM-M, Ramesh BS, Byrne DJ, MacColl GS, et al. Ghrelin can bind to a species of high density lipoprotein associated with paraoxonase. *J Biol Chem.* (2003) 278:8877–80. doi: 10.1074/jbc.C200575200
54. Underdown BJ. IgA. In: *Encyclopedia of Immunology [Internet]*, eds J. D. Peter and I. M. Roitt (San Diego, CA: Elsevier) (1998) p. 1021–35.
55. Macpherson AJ, Hunziker L, McCoy K, Lamarre A. IgA responses in the intestinal mucosa against pathogenic and non-pathogenic microorganisms. *Microb Infect.* (2001) 3:1021–35. doi: 10.1016/S1286-4579(01)01460-5
56. Reyes-Castillo Z, Palafox-Sánchez CA, Parra-Rojas I, Martínez-Bonilla GE, del Toro-Arreola S, Ramírez-Due-as MG, et al. Comparative analysis of autoantibodies targeting peptidylarginine deiminase type 4, mutated citrullinated vimentin and cyclic citrullinated peptides in rheumatoid arthritis: associations with cytokine profiles, clinical and genetic features: anti-PAD4, anti-MCV and anti-CCP autoantibodies in RA. *Clin Exp Immunol.* (2015) 182:119–31. doi: 10.1111/cei.12677

Conflict of Interest Statement: The authors declare that the research was conducted in the absence of any commercial or financial relationships that could be construed as a potential conflict of interest.

frontiers in Endocrinology

MINI REVIEW
published: 04 June 2019
doi: 10.3389/fendo.2019.00350

Thyroid Hormone Action on Innate Immunity

*María del Mar Montesinos and Claudia Gabriela Pellizas**

Facultad de Ciencias Químicas, Centro de Investigaciones en Bioquímica Clínica e Inmunología (CIBICI-CONICET) and Departamento de Bioquímica Clínica, Universidad Nacional de Córdoba, Córdoba, Argentina

The interplay between thyroid hormone action and the immune system has been established in physiological and pathological settings. However, their connection is complex and still not completely understood. The thyroid hormones (THs), 3,3′,5,5′ tetraiodo-L-thyroxine (T4) and 3,3′,5-triiodo-L-thyronine (T3) play essential roles in both the innate and adaptive immune responses. Despite much research having been carried out on this topic, the available data are sometimes difficult to interpret or even contradictory. Innate immune cells act as the first line of defense, mainly involving granulocytes and natural killer cells. In turn, antigen presenting cells, macrophages and dendritic cells capture, process and present antigens (self and foreign) to naïve T lymphocytes in secondary lymphoid tissues for the development of adaptive immunity. Here, we review the cellular and molecular mechanisms involved in T4 and T3 effects on innate immune cells. An overview of the state-of-the-art of TH transport across the target cell membrane, TH metabolism inside these cells, and the genomic and non-genomic mechanisms involved in the action of THs in the different innate immune cell subsets is included. The present knowledge of TH effects as well as the thyroid status on innate immunity helps to understand the complex adaptive responses achieved with profound implications in immunopathology, which include inflammation, cancer and autoimmunity, at the crossroads of the immune and endocrine systems.

Keywords: thyroid hormones, innate immunity, neutrophils, natural killer cells, macrophages, dendritic cells

OPEN ACCESS

Edited by:
Wen Kong,
Wuhan Union Hospital, China

Reviewed by:
Lan Wu,
Vanderbilt University Medical Center, United States
Taisen Iguchi,
National Institute for Basic Biology, Japan

***Correspondence:**
Claudia Gabriela Pellizas
claudia@fcq.unc.edu.ar

Specialty section:
This article was submitted to Experimental Endocrinology, a section of the journal Frontiers in Endocrinology

Received: *08 January 2019*
Accepted: *15 May 2019*
Published: *04 June 2019*

Citation:
Montesinos MM and Pellizas CG (2019) Thyroid Hormone Action on Innate Immunity. Front. Endocrinol. 10:350. doi: 10.3389/fendo.2019.00350

INTRODUCTION

Growing evidence compiled over recent decades has revealed a bidirectional crosstalk between thyroid hormones (THs) and the immune system. This interplay has been demonstrated for several pathophysiological conditions of the thyroid functioning and the innate and adaptive immunity. Many situations primarily affecting the action of THs have an impact on the characteristics and/or functions of immune cells, and are translated to host defense status and related disorders. In turn, immune-related disorders conduct to the most frequent thyroid dysfunctions, which have an autoimmune origin. The connection between these systems is complex and not well-understood. This article reviews the current evidence supporting the contribution of THs to the modulation of innate immunity at the cellular level.

Thyroid Hormone Action

THs exert a pivotal role for normal development and function. The thyroid produces 3,3′,5,5′ tetraiodo-L-thyroxine (T4) and 3,3′,5-triiodo-L-thyronine (T3), mainly under thyrotropin (TSH) regulation. While this gland secretes 100% of circulating T4, it provides only a low percentage of serum levels of the most physiologically active TH: T3, which for the major part derives from peripheral 5′ deiodination of T4 (1). At the target cell level, the action of THs is genomic (nuclear) and non-genomic. The former requires T3 and the specific nuclear receptors (TRs): TRα1, TRβ1, TRβ2, and TRβ3 (2) and is controlled by a multiprotein complex comprising both corepressors and coactivators (3).

Translocation of TRs from their synthesis in the cytosol to the nucleus is a functionally active process (4). In this regard, non-genomic effects exerted intracellularly by TRs and truncated variants occur rapidly, can be observed in the cytoplasm, mitochondria and other organelles, and are independent of nuclear receptor activity and protein synthesis. Many effects conducted by cytoplasmic TRs involve PI3K-dependent Akt activation (5). Furthermore, non-genomic actions of THs are also initiated at the plasma membrane through different proteins. The best studied is the integrin αvβ3, which binds mainly T4 and tetraiodothyroacetic acid (tetrac), a derivative of T4, inducing activation of AMPK, PI3K/Akt, and MAPK (6, 7). Overall, THs interact with a wide variety of signaling pathways that are not yet fully deciphered.

Circulating levels of THs are not representative of what each cell type detects. Instead, the action of THs requires an appropriate interplay among membrane TH transporters, TH deiodinases and TR expression, and thus there is a fine-tuned cellular TH responsiveness. The main TH transporters include monocarboxylate transporters (MCT) 8 and 10, organic anion transporter polypeptides (OATPs) and large neutral amino acid transporters (LATs), with MCT8, MCT10, and LATs having a higher affinity for T3 than T4 uptake. Additionally, the cellular concentrations of THs are regulated by the activity of the 1, 2, and 3 iodothyronine deiodinases: D1, 2, and 3. D2 is an "activating" enzyme, responsible for the peripheral production of 50–80% of the body pool of T3 from T4. In contrast, D3 restrains T3 action, converting T4 and T3 into inactive metabolites. TH transporters and deiodinases exhibit a particular expression profile that is cellular and metabolic state specific (8, 9). Newly discovered actions of T4 and T3 metabolites, such as 3,5-diiodothyronine (3,5-T2), and 3-iodothyronamine (T1AM) are emerging (10).

Innate Immunity

The immune system includes cells that protect the organism from foreign antigens, such as microbes, cancer cells, toxins, and damage signals. It is simplistically referred to as innate and adaptive immunity. The former offers immediate protection against intruders, with specific cells being able to fight a wide range of pathogens, with the latter being specific and antigen-dependent (11). Moreover, adaptive immunity is orchestrated and directed by its innate counterpart.

The main innate cells are polymorphonuclear leukocytes (PMNL, mainly neutrophils), innate lymphoid cells (ILCs) including natural killer (NK) cells and cytokine-producing helper-like ILCs, innate T-like cells comprising NKT and γδ T cells, monocytes, macrophages and dendritic cells (DCs). Their complete classification and plethora of functions have been extensively reviewed (12–15).

The belief that innate immunity is non-specific was challenged after the description of pattern-recognition receptors and molecules that recognize pathogen and damage-associated molecular patterns from intruders (16, 17). Furthermore, the concept of exclusive memory for adaptive responses was weakened after the description of "trained innate memory," involving a heightened response upon re-exposure to a certain stimulus (16, 18) under the control of the cellular metabolism (19). Moreover, innate immune tolerance has also been demonstrated (20).

This review article focuses on the state-of-the-art of the TH mechanism of action and its effects on innate immunity at cellular level, with the pathophysiological role of the reported findings also discussed. The main effects of T3 and/or T4 in Neutrophils, NK cells, Macrophages and DCs are depicted in **Figure 1** and considered below.

Neutrophils

Neutrophils are the first line of defense against bacteria and fungi, and also help to combat parasites and viruses (21). They travel from the blood to the inflammatory site where they engage and kill microorganisms and clear infections through chemotaxis, phagocytosis, and cytokine synthesis, and the release of reactive oxygen species (ROS) and granular proteins such as myeloperoxidase (MPO) (22). Classical concepts of neutrophil biology are being increasingly challenged by recent findings (23, 24).

Administration of T3 to rats increased the respiratory burst activity of isolated PMNLs with enhanced NADPH oxidase and MPO activities (25, 26). Accordingly, increased mitochondrial oxygen consumption and ROS production were reported in PMNLs from both Graves' disease and toxic adenoma patients (27). Moreover, T3 administration to euthyroid subjects induced ROS generation by PMNLs (28). However, a decrease in oxidative metabolism was registered in human PMNLs during hypothyroidism, which was reversed upon L-T4 substitution therapy (29). The authors suggest that this effect was unlikely to result from direct actions of THs on PMNLs, considering that T3 showed no appreciable effect on superoxide anion (O_2^-) generation in *in vitro* experiments with PMNLs from healthy donors. In addition, hypothyroidism causes changes in the lipid composition of PMNLs' membranes that may be involved in their impaired function (30). To note, human neutrophils express TR (31).

T4 and the TH metabolite 3,5-T2 as well as T3 induced respiratory-burst activity and stimulated MPO activity in human PMNLs. These effects were mediated by a non-genomic mechanism initiated at the plasma membrane, dependent on PKC and Ca^+ levels. Moreover, O_2^- production in resting PMNLs of hyperthyroid patients was elevated compared with either controls or hypothyroid subjects (32). Furthermore, PMNLs

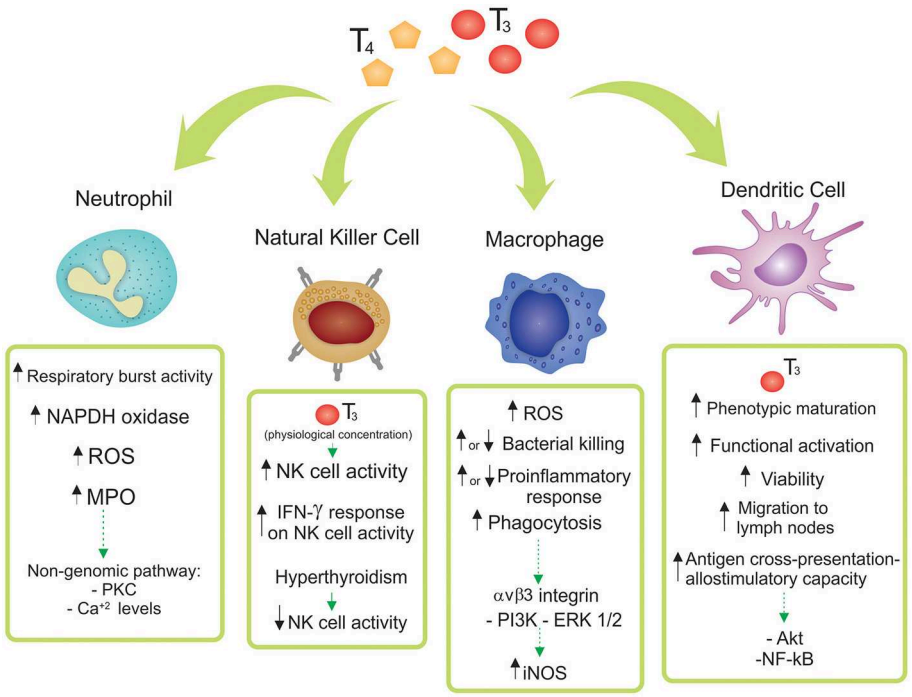

FIGURE 1 | Effects of thyroid hormones 3,3′,5,5′ tetraiodo-L-thyroxine (T4) and 3,3′,5-triiodo-L-thyronine (T3) on innate immune cell subsets. The main reported effects of T3 and/or T4 in Neutrophils, Natural Killer (NK) cells, Macrophages and Dendritic Cells are depicted. Particular differences among the diverse origins of the cells (human, mice, cell lines, and/or tissue source) are shown and discussed in the main text.

express receptors for T1AM, a T4 derivative, involved in the chemosensory migration toward T1AM (33).

TH metabolism plays an important role in neutrophil function during infection. It has been demonstrated that D3 is strongly expressed in murine neutrophils during chronic chemical inflammation and in acute bacterial infection. Accordingly, human neutrophils express D3, D1, MCT10, and TRα1, which could therefore be involved in TH action in this cell type. Furthermore, evidence has supported the notion that D3 plays a role in the bacterial killing capacity of neutrophils, either through generation of iodide for the MPO system or through modulation of intracellular TH bioavailability (34). Recent results have demonstrated that intracellular TH levels are regulated by D3, playing a key role in neutrophil function in zebrafish, mice and humans (35).

Natural Killer Cells

NK cells mediate cytolytic activities against tumor and virus-infected targets. Of note, NK cells also possess traits of adaptive immunity and can acquire functional qualities associated with immunological memory (36). The studies of the effects of THs on these cells have produced conflicting results. A positive correlation between serum T3 concentration and NK cell activity in healthy elderly subjects was recorded but exogenous T3 administration increased NK cell activity only in old individuals who had T3 concentrations at the lower end of the reference range (37). Although NK cell functionality was impaired in Graves' patients and restored in the euthyroid state (38, 39), *in vitro* treatment with T4 to peripheral blood lymphocytes from these patients did not show any increase in NK cell activity (40). In agreement, hyperthyroxinemia induced in mice reduced NK cell capacity to lyse target cells (41) whereas exogenous T4 or T3 administered to mice increased NK cell lytic activity (42), as well as during protein starvation (43), or aging (44).

Endogenous IFN-γ plays a relevant role in the host defense against infectious and neoplastic diseases by mechanisms that involve modulation of the NK cell function (45, 46). Both T3 and T4 boosted IFNγ-response in murine NK cells (44, 47), while T4 amplified the effect induced by both IFN-γ and IL-2 (48). These findings suggest a role for THs in the modulation of NK cell sensitivity to IFN-γ.

A recent study linked uterine NK cells (the most prominent leukocytes at the maternal-fetal interface) with THs. These cells express MCT8 and MCT10, as well as TRα1 and β1 in the first trimester of human pregnancy. An increase of IL-6 secretion after T3 exposure *in vitro* was also reported (49).

Monocytes—Macrophages

Macrophages are strategically positioned in all tissues of the body and can recognize and remove pathogens, toxins, cellular debris, and apoptotic cells. Tissue-resident macrophages in adulthood rely on replenishment by bone marrow (BM)-derived blood monocytes, with circulating monocytes being recruited to tissues by specific chemotactic factors. Among

other names, tissue-resident macrophages are referred to as "microglia" in the central nervous system and "Kupffer cells" in the liver (50–52). Depending on the signal and the dose, a second stimulation can result in tolerance or trained immunity (53, 54). In response to stimuli, differentiated macrophages polarize to classically activated M1 or alternatively activated M2 macrophages, although a spectrum of phenotypes across the M1/M2 continuum is recognized. M1 macrophages phagocytize and destroy microbes, eliminate tumor cells, and present antigens to T cells through ROS production, expression of inducible nitric oxide synthase (iNOS) and release of proinflammatory cytokines, thereby promoting T helper (Th) 1 responses (55). In contrast, M2 macrophages show an immunosuppressive phenotype characterized by a decreased antigen presentation to T cells and production of cytokines that stimulate Th2 responses. These regulatory cells are involved in tissue repair, promote tumor growth and exert antiparasitic effects (56).

In spite of controversial results concerning the expression of TR isoforms, macrophages express TRα and β (57–61). In addition, murine and human macrophage cell lines express D2, MCT10, and MCT8 (59). Over the past decade, it has become clear that shifts in cellular metabolism are determinants of macrophage function and phenotype (62). The activities of key enzymes of glycolysis are regulated by THs in these cells, affecting macrophage metabolism and function (63). Stimulation of the immune system in hyperthyroid rats revealed that monocyte migration and ROS production by macrophages were suppressed. In contrast, hypothyroidism enhanced ROS release, whereas monocyte migration was not affected (64).

THs enhanced the phagocytic activity of intraperitoneal macrophages from hypothyroid rats (64). Moreover, T4 administration to old mice also increased their phagocytic capacity (65). In agreement, a stimulatory effect of T4 (but not T3) on the phagocytosis process of cultured peritoneal mouse macrophages was reported (66). However, both THs enhanced bacteria-cell interaction and intracellular killing in mice RAW 264.7 and human THP-1 monocyte-derived macrophage cell lines (67). This mechanism involved the integrin αvβ3, TH-induced iNOS expression, generation of NO and triggering of the PI3K and ERK1/2 signaling pathways.

The inflammatory response exerted by macrophages was stimulated during hypothyroid condition and inhibited in the course of hyperthyroidism (68). T4 inhibited the migration inhibitory factor (MIF) in macrophages (67, 69), and in agreement, low plasma T4 concentrations augmented plasma MIF levels in both patients and rats with severe sepsis (69). Although T4 attenuated proinflammatory responses *in vivo*, no significant changes in IL-6 and TNFα levels could be detected in T4-treated peritoneal macrophages from mice, or in mouse and human cell lines (67).

The "euthyroid sick syndrome" (or "nonthyroidal illness") is distinctive of critically ill patients with severe infections or sepsis, being characterized by low serum T3 and in serious cases by also low serum T4 without the expected increase in TSH (70). Interestingly, supplementation of T4 to rats and mice in bacterial infectious models enhanced animal survival and attenuated septicemia and inflammatory responses (67, 71). In agreement, hypothyroid mice exhibited increased mortality during inflammation induced by LPS, whereas circulating T3, through TRβ1 signaling, protected animals from endotoxemia (57). However, it was reported that hyperthyroidism increased mice mortality in response to LPS. Noteworthy, Signal Transducer and Activator of Transcription 3 (STAT3) activation induced by LPS or IL-6 was inhibited by T3 through TR signaling in RAW 264.7 cells and in primary cultures of BM-derived macrophages. These authors suggested that inhibition of IL-6 signaling induced by T3 has potent regulatory functions during infection and inflammation (72).

Switching from M1 to the M2 phenotype protects the organism from excessive inflammation, whereas switching from M2 to M1 prevents allergic and asthmatic Th2 reactions, decreases the bactericidal properties of macrophages and favors the resolution of inflammation (63). In this regard, T3 reduced monocyte differentiation into macrophages and induced a M1 signature. In agreement, T3 decreased the expression of genes regulated by M2-activated macrophages through a TRβ1-mediated mechanism (58). Although comparable results were registered in RAW264.7 macrophages, a TRα-dependence was revealed (73). In contrast, in a model of kidney obstruction, ligand-bound TRα inhibited the NF-κB pathway and proinflammatory cytokines in macrophages isolated at the inflammatory site (61).

The role of intracellular TH metabolism in macrophages has been extensively reported and reviewed by Boelen group (34), and is therefore not covered in this review. More recently, a reduction of intracellular T3 concentration due to a lack of D2 activity with impaired macrophage function was reported. Also, primary BM-derived macrophages treated with LPS decreased phagocytosis and proinflammatory cytokines in D2 KO mice (73), consistent with earlier results in RAW264.7 cells (59).

Modifications in the homeostatic conditions of the nervous tissue promote microglia activation, release of inflammatory mediators and phagocytosis of degenerating cells (74). Lima et al. (75) reported that rat microglial cells in culture express TRα and TRβ, whereas other authors did not observe the latter (76). αVβ3 integrin has also been described in these cells (77), and in mice microglia, the TH transporters OATP4A1, LAT2, and MCT10 were also found (78, 79). It is known that T3 modulates microglial development (75) and functions such as migration and phagocytosis by genomic and non-genomic pathways (80). The molecular mechanism involves T3 uptake by TH transporters and binding to TRs, thus triggering multiple signaling pathways (80, 81). Moreover, T3 increased the release of soluble factors by the microglia through STAT3 activation, promoting glioma growth (82).

Liver is one of the most relevant TH target tissues. T3 induced acceleration of cellular O_2^- consumption, resulting in elevated ROS and NO (83). In agreement, T3-stimulated free radical activity reduced the cellular antioxidant defenses leading to oxidative stress in rats, a phenomenon also observed in human hyperthyroidism (84, 85). Kupffer cells are main scavengers constantly clearing gut-derived pathogens from the blood,

preventing liver diseases (86). T3 promoted hyperplasia and hypertrophy of these cells, with a resulting enhancement in the respiratory burst activity. Furthermore, T3-induced calorigenesis resulted in transient elevations in serum TNF-α, determined by actions exerted in Kupffer cells and involving activation of NF-kB (87). The hepatic response induced by T3 involved cell proliferation associated with TNF-α generation by Kupffer cells (88).

Dendritic Cells

DCs are the main antigen presenting cells in the interface between innate and adaptive immunity. They integrate signals derived from infection or damage, and present processed antigen to naive T cells to tailor the appropriate T cell program. Recent advances in DC immunobiology have led to a clearer understanding of how T cell responses are shaped (89). The main DCs include conventional (classical or myeloid) DCs (cDCs, referred as DCs from now on) and plasmacytoid DCs (pDCs). The genetic signature of DCs from different tissues is similar, but differs from that of pDCs, monocytes and macrophages. To note, DCs are functionally different to macrophages (89, 90). Immature DCs (iDCs) have substantial endocytic activity but lower surface expression of major histocompatibility complex (MHC) class I and II proteins. After encountering any stimulus, DCs mature to undergo considerable cytoplasmic reorganization, transporting peptide-MHC complexes to the cell surface and upregulating costimulatory molecules (90). Recent studies highlighted the relevance of DC migration in the maintenance of immune surveillance. Immature DCs are rather immotile, and after processing foreign and self-antigens or damage signals undergo an activation process, leading to an increase in motility corresponding to upregulation of CC-chemokine receptor 7 (CCR7). The interaction of CCR7 with its ligand guides DCs toward secondary lymphoid organs (91).

The role of THs in the initiation of adaptive immunity remained uncertain for many years, with Mooij et al. providing the earliest clues that THs and other iodinated derivatives, mainly T3, favored the maturation of human peripheral blood monocytes into functional DCs (92). Many years later, our laboratory initiated a study on the effects of THs at the DC level (**Figure 2**). We observed the expression of TRs in BM-derived mouse DCs, principally the TRβ1 isoform, and mainly in the cytoplasm of both iDCs and LPS-matured DCs. The ability of physiological concentrations of T3 to induce phenotypic and functional activation of DCs and to drive a Th1 profile was also demonstrated (93). Mechanistically, this effect involved activation of the Akt and NF-kB pathways (94) and was counteracted by glucocorticoids (95). The requirement for an intact TRβ-T3 signaling in T3-induced DC activation was confirmed by *in vitro* and *in vivo* studies (94, 96).

Interestingly, we showed that T4, the main circulating TH, did not reproduce T3-dependent effects in DCs. The characterization of the mechanisms of TH transport and metabolism in DCs supports the notion of a homeostatic balance to prevent unspecific systemic activation of DCs. In this regard, DCs express MCT10 and LAT2 TH transporters, and mainly transport T3 with a favored involvement of MCT10, as its inhibition almost prevented T3 saturable uptake mechanism and reduced T3-induced IL-12 production. In addition, DCs express D2 and D3, and exhibit both enzymatic activities with a prevalence toward TH inactivation (97).

Immunotherapy has become the fourth pillar of cancer care, complementing surgery, cytotoxic therapy, and radiotherapy (98). In this context, DCs have been the subject of numerous studies seeking new immunotherapeutic strategies against cancer. However, despite initial enthusiasm, disappointing results including a short half-life of DCs in circulation and induction of tolerogenic responses by death cells, have raised doubts regarding these approaches. Nevertheless, the increased understanding of DC immunobiology and the search for optimization strategies are allowing a more rational development of DC-based immunotherapies (99, 100). A new role for THs in this field has arisen, with T3 binding to TRβ increasing mice DC viability and augmenting CCR7 expression, thereby driving migration of DCs to lymph nodes. Moreover, T3 stimulated the antigen cross-presentation ability of DCs, boosting antigen-specific cytotoxic T-cell responses. Also, vaccination with T3-stimulated DCs in mice bearing B16 melanoma inhibited tumor growth and prolonged host survival (96, 101). Overall, these results established the adjuvant effect of T3-TRβ signaling in DCs, identifying a DC vaccination approach in cancer immunotherapy.

Further recent *in vitro* and *in vivo* evidence has shed light on the molecular and cellular mechanisms driven by T3-conditioned murine DCs (102). Findings revealed an induction of a proinflammatory cytokine profile and a down-modulation of PDL expression in DCs. In co-cultures, these cells increased the frequency of IL-17-producing splenocytes, mainly by the γδ-T population. Thus, down-regulation of tolerogenic T regulatory (Treg) cells and PD1 expression were induced, limiting the inhibitory signals and emphasizing the relevance of T3 as an additional immune-endocrine checkpoint.

The understanding of the effect of THs in human DCs is still limited. Dedecjus et al. (103) reported that the thyrometabolic state influenced the major human peripheral blood DCs, pDCs, and cDCs, with T4 substitution to thyroid cancer patients after surgery increasing the frequency of these cells and the expression of CD86 and HLA-DR (activation markers). In hypothyroid patients with Hashimoto's Thyroiditis, T4 supplementation exerted changes of peripheral blood DC subpopulations, with increased expression of costimulatory molecules (104). Although TRs in human DC populations have not yet been found, increased expression of CD86 by T3 addition to cell cultures of human peripheral blood pDCs was reported (103). Also, T3 increased the ability of human DCs to upregulate the proliferative response and secretion of IL-12 by peripheral blood mononuclear cells, similar to our findings in mice splenocytes co-cultured with T3-stimulated DCs (93).

The proinflammatory role of IL-12 and its involvement in Th1-mediated organ-specific autoimmune diseases (105) confer potential clinical relevance of the aforementioned studies. An increased synthesis of IL-12 by DCs obtained from hyperthyroid mice has been reported (106). Furthermore, patients with

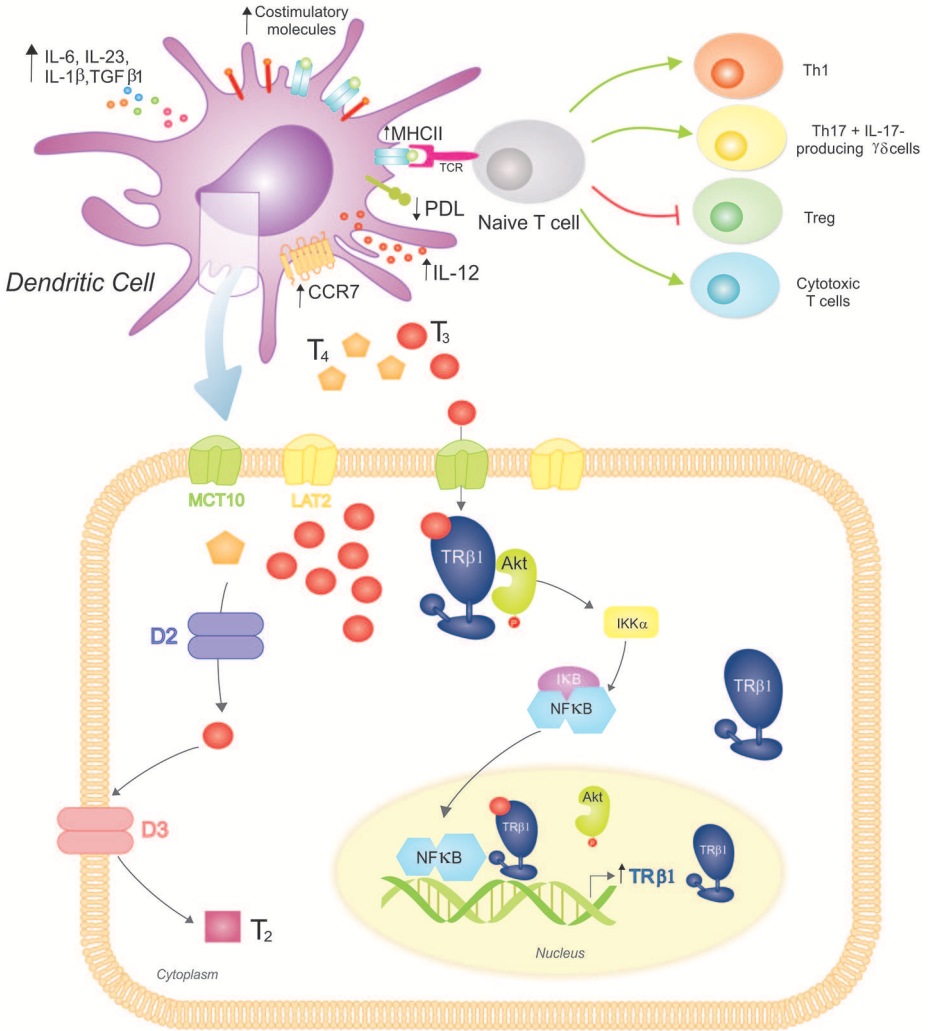

FIGURE 2 | 3,3′,5-triiodo-L-thyronine (T3) promotes Dendritic Cell (DC) maturation and function, driving proinflammatory and cytotoxic adaptive responses. **(Top)** T3 promotes DC phenotypic maturation upregulating MHCII and costimulatory molecules. The functional DC activation promotes a proinflammatory cytokine phenotype (increased production of IL-12, IL-6, IL-23, IL-1β, and TGFβ1) that drives adaptive responses favoring the development of Th1 and Th17 T cells, IL-17-producing γδ T cells, and cytotoxic T cells. In contrast, the Treg population is restrained. T3-conditioned DCs also augment CCR7 expression, which favors their migration to lymph nodes, where they present processed antigens in the context of MHCII to specific T cell receptors (TCR) from naïve T cells. T3 also modulates the immune checkpoint, reducing PDL expression on DCs and triggering the down-regulation of PD-1-expressing T cells (not shown). **(Bottom)** DCs take up T3 more effectively than T4 through MCT10 and LAT2. Inside DCs, D2 catalyzes the conversion of T4 to T3, whereas D3 inactivates T3 resulting in T2. These cells mainly express TRβ1 with a preferred cytoplasmic localization, where it co-localizes with Akt. Upon T3 binding to TRβ1, Akt is activated and translocated to the nucleus. This mechanism includes IκB degradation and thus NF-κB cytoplasmic-nuclear shuttling that acts as a transcription factor upregulating TRβ1 expression. An intact T3-TRβ1 signaling is essential for T3-dependent DC induced effects.

Graves' disease exhibited elevated IL-12 circulating levels (107). Considering that DCs are involved in the pathogenesis of autoimmune thyroid diseases (108) and also their potential application for the treatment of these pathologies (109), further research should shed light in this field.

CONCLUDING REMARKS

The relationship between THs and innate immune cells is complex, with an improved knowledge still necessary. Cellular and molecular signaling pathways involved in the crosstalk between THs and innate immune functions, and their role directing adaptive immunity have profound implications in immunopathology, including cancer and autoimmune manifestations of the thyroid gland, at the crossroads of the immune and endocrine systems. The etiopathogenic mechanism involved in both immune-related thyroid pathologies and immune disorders due to thyroid dysfunctions are now better understood. With a focus on particular cell subsets, further research will provide valuable

tools for manipulating the immunogenic potential of innate immune cells to positively regulate the development of protective immunity, or negatively control the generation of autoimmune thyroid inflammation.

AUTHOR CONTRIBUTIONS

MM and CP: conception and design, analysis and interpretation of available data, writing, review, and revision of the manuscript. MM: design of figures. CP: general supervision.

FUNDING

This study was supported by grants from Agencia Nacional de Promoción Científica y Tecnológica (ANPCyT, PICT-2016-0254 y PICT-2016-0037), Secretaría de Ciencia y Tecnología de la Universidad Nacional de Córdoba (SeCyT, 2018-2020), and Fundación Sales.

ACKNOWLEDGMENTS

The authors are extremely grateful to Isabel Maria Montesinos for her excellent assistance in the design and drawing of the figures.

REFERENCES

1. Williams GR, Bassett JH. Deiodinases: the balance of thyroid hormone: local control of thyroid hormone action: role of type 2 deiodinase. *J Endocrinol*. (2011) 209:261–72. doi: 10.1530/JOE-10-0448
2. Bernal J, Guadano-Ferraz A, Morte B. Thyroid hormone transporters-functions and clinical implications. *Nat Rev Endocrinol*. (2015) 11:690. doi: 10.1038/nrendo.2015.113
3. Astapova I. Role of co-regulators in metabolic and transcriptional actions of thyroid hormone. *J Mol Endocrinol*. (2016) 56:73–97. doi: 10.1530/JME-15-0246
4. Anyetei-Anum CS, Roggero VR, Allison LA. Thyroid hormone receptor localization in target tissues. *J Endocrinol*. (2018) 237:R19–34. doi: 10.1530/JOE-17-0708
5. Cao X, Kambe F, Moeller LC, Refetoff S, Seo H. Thyroid hormone induces rapid activation of Akt/protein kinase B-mammalian target of rapamycin-p70S6K cascade through phosphatidylinositol 3-kinase in human fibroblasts. *Mol Endocrinol*. (2005) 19:102–12. doi: 10.1210/me.2004-0093
6. Kalyanaraman H, Schwappacher R, Joshua J, Zhuang S, Scott BT, Klos M, et al. Nongenomic thyroid hormone signaling occurs through a plasma membrane-localized receptor. *Sci Signal*. (2014) 7:ra48. doi: 10.1126/scisignal.2004911
7. Davis PJ, Goglia F, Leonard JL. Nongenomic actions of thyroid hormone. *Nat Rev Endocrinol*. (2016) 12:111–21. doi: 10.1038/nrendo.2015.205
8. Ortiga-Carvalho TM, Chiamolera MI, Pazos-Moura CC, Wondisford FE. Hypothalamus-pituitary-thyroid axis. *Compr Physiol*. (2016) 6:1387–428. doi: 10.1002/cphy.c150027
9. Mendoza A, Hollenberg AN. New insights into thyroid hormone action. *Pharmacol Ther*. (2017) 173:135–45. doi: 10.1016/j.pharmthera.2017.02.012
10. Louzada RA, Carvalho DP. Similarities and differences in the peripheral actions of thyroid hormones and their metabolites. *Front Endocrinol.* (2018) 9:394. doi: 10.3389/fendo.2018.00394
11. Yatim KM, Lakkis FG. A brief journey through the immune system. *Clin J Am Soc Nephrol*. (2015) 10:1274–81. doi: 10.2215/CJN.10031014
12. Diefenbach A, Colonna M, Koyasu S. Development, differentiation, and diversity of innate lymphoid cells. *Immunity*. (2014) 41:354–65. doi: 10.1016/j.immuni.2014.09.005
13. Woo SR, Corrales L, Gajewski TF. Innate immune recognition of cancer. *Annu Rev Immunol*. (2015) 33:445–74. doi: 10.1146/annurev-immunol-032414-112043
14. Dadi S, Chhangawala S, Whitlock BM, Franklin RA, Luo CT, Oh SA, et al. Cancer immunosurveillance by tissue-resident innate lymphoid cells and innate-like T cells. *Cell*. (2016) 164:365–77. doi: 10.1016/j.cell.2016.01.002
15. Ebbo M, Crinier A, Vely F, Vivier E. Innate lymphoid cells: major players in inflammatory diseases. *Nat Rev Immunol*. (2017) 17:665–78. doi: 10.1038/nri.2017.86
16. Netea MG, Latz E, Mills KH, O'Neill LA. Innate immune memory: a paradigm shift in understanding host defense. *Nat Immunol*. (2015) 16:675–9. doi: 10.1038/ni.3178
17. Herwald H, Egesten A. On PAMPs and DAMPs. *J Innate Immun*. (2016) 8:427–8. doi: 10.1159/000448437
18. Netea MG, Quintin J, van der Meer JW. Trained immunity: a memory for innate host defense. *Cell Host Microbe*. (2011) 9:355–61. doi: 10.1016/j.chom.2011.04.006
19. Penkov S, Mitroulis I, Hajishengallis G, Chavakis T. Immunometabolic crosstalk: an ancestral principle of trained immunity? *Trends Immunol*. (2019) 40:1–11. doi: 10.1016/j.it.2018.11.002
20. Dominguez-Andres J, Novakovic B, Li Y, Scicluna BP, Gresnigt MS, Arts RJW, et al. The itaconate pathway is a central regulatory node linking innate immune tolerance and trained immunity. *Cell Metab*. (2019) 29:211–20.e5. doi: 10.1016/j.cmet.2018.09.003
21. Ley K, Hoffman HM, Kubes P, Cassatella MA, Zychlinsky A, Hedrick CC, et al. Neutrophils: new insights and open questions. *Sci Immunol*. (2018) 3:eaat4579. doi: 10.1126/sciimmunol.aat4579
22. Mortaz E, Alipoor SD, Adcock IM, Mumby S, Koenderman L. Update on neutrophil function in severe inflammation. *Front Immunol*. (2018) 9:2171. doi: 10.3389/fimmu.2018.02171
23. Silvestre-Roig C, Hidalgo A, Soehnlein O. Neutrophil heterogeneity: implications for homeostasis and pathogenesis. *Blood*. (2016) 127:2173–81. doi: 10.1182/blood-2016-01-688887
24. Jablonska J, Granot Z. Neutrophil, quo vadis? *J Leukoc Biol*. (2017) 102:685–8. doi: 10.1189/jlb.3MR0117-015R
25. Videla LA, Correa L, Rivera M, Sir T. Zymosan-induced luminol-amplified chemiluminescence of whole blood phagocytes in experimental and human hyperthyroidism. *Free Radic Biol Med*. (1993) 14:669–75. doi: 10.1016/0891-5849(93)90149-O
26. Fernandez V, Videla LA. On the mechanism of thyroid hormone-induced respiratory burst activity in rat polymorphonuclear leukocytes. *Free Radic Biol Med*. (1995) 19:359–63. doi: 10.1016/0891-5849(95)00016-Q
27. Szabo J, Foris G, Mezosi E, Nagy EV, Paragh G, Sztojka I, et al. Parameters of respiratory burst and arachidonic acid metabolism in polymorphonuclear granulocytes from patients with various thyroid diseases. *Exp Clin Endocrinol Diabetes*. (1996) 104:172–6. doi: 10.1055/s-0029-1211440
28. Magsino CH Jr., Hamouda W, Ghanim H, Browne R, Aljada A, Dandona P. Effect of triiodothyronine on reactive oxygen species generation by leukocytes, indices of oxidative damage, and antioxidant reserve. *Metabolism*. (2000) 49:799–803. doi: 10.1053/meta.2000.6263
29. Marino F, Guasti L, Cosentino M, De Piazza D, Simoni C, Piantanida E, et al. Thyroid hormone regulation of cell migration and oxidative metabolism in polymorphonuclear leukocytes: clinical evidence in thyroidectomized subjects on thyroxine replacement therapy. *Life Sci*. (2006) 78:1071–7. doi: 10.1016/j.lfs.2005.06.016
30. Coria MJ, Carmona Viglianco YV, Marra CA, Gomez-Mejiba SE, Ramirez DC, Anzulovich AC, et al. Hypothyroidism modifies lipid composition of polymorphonuclear leukocytes. *Cell Physiol Biochem*. (2012) 29:713–24. doi: 10.1159/000170987
31. Brisson-Lougarre A, Blum CJ. [Specific receptors for triiodothyronine in nuclei isolated from normal human polynuclear neutrophils]. *C R Acad Sci III*. (1985) 300:287–92.
32. Mezosi E, Szabo J, Nagy EV, Borbely A, Varga E, Paragh G, et al. Nongenomic effect of thyroid hormone on free-radical production in

human polymorphonuclear leukocytes. *J Endocrinol*. (2005) 185:121–9. doi: 10.1677/joe.1.05968
33. Babusyte A, Kotthoff M, Fiedler J, Krautwurst D. Biogenic amines activate blood leukocytes via trace amine-associated receptors TAAR1 and TAAR2. *J Leukoc Biol*. (2013) 93:387–94. doi: 10.1189/jlb.0912433
34. van der Spek AH, Fliers E, Boelen A. Thyroid hormone metabolism in innate immune cells. *J Endocrinol*. (2017) 232:R67–81. doi: 10.1530/JOE-16-0462
35. van der Spek AH, Jim KK, Karaczyn A, van Beeren HC, Ackermans MT, Darras VM, et al. The thyroid hormone inactivating type 3 deiodinase is essential for optimal neutrophil function: observations from three species. *Endocrinology*. (2018) 159:826–35. doi: 10.1210/en.2017-00666
36. O'Sullivan TE, Sun JC, Lanier LL. Natural killer cell memory. *Immunity*. (2015) 43:634–45. doi: 10.1016/j.immuni.2015.09.013
37. Kmiec Z, Mysliwska J, Rachon D, Kotlarz G, Sworczak K, Mysliwski A. Natural killer activity and thyroid hormone levels in young and elderly persons. *Gerontology*. (2001) 47:282–8. doi: 10.1159/000052813
38. Papic M, Stein-Streilein J, Zakarija M, McKenzie JM, Guffee J, Fletcher MA. Suppression of peripheral blood natural killer cell activity by excess thyroid hormone. *J Clin Invest*. (1987) 79:404–8. doi: 10.1172/JCI112826
39. Wang PW, Luo SF, Huang BY, Lin JD, Huang MJ. Depressed natural killer activity in Graves' disease and during antithyroid medication. *Clin Endocrinol*. (1988) 28:205–14. doi: 10.1111/j.1365-2265.1988.tb03657.x
40. Lee MS, Hong WS, Hong SW, Lee JO, Kang TW. Defective response of natural killer activity to thyroxine in Graves' disease. *Korean J Intern Med*. (1990) 5:93–6. doi: 10.3904/kjim.1990.5.2.93
41. Stein-Streilein J, Zakarija M, Papic M, McKenzie JM. Hyperthyroxinemic mice have reduced natural killer cell activity. Evidence for a defective trigger mechanism. *J Immunol*. (1987) 139:2502–7.
42. Sharma SD, Tsai V, Proffitt MR. Enhancement of mouse natural killer cell activity by thyroxine. *Cell Immunol*. (1982) 73:83–97. doi: 10.1016/0008-8749(82)90437-3
43. Ingram KG, Crouch DA, Douez DL, Croy BA, Woodward B. Effects of triiodothyronine supplements on splenic natural killer cells in malnourished weanling mice. *Int J Immunopharmacol*. (1995) 17:21–32. doi: 10.1016/0192-0561(94)00079-4
44. Provinciali M, Muzzioli M, Di Stefano G, Fabris N. Recovery of spleen cell natural killer activity by thyroid hormone treatment in old mice. *Nat Immun Cell Growth Regul*. (1991) 10:226–36.
45. Vivier E, Ugolini S. Natural killer cells: from basic research to treatments. *Front Immunol*. (2011) 2:18. doi: 10.3389/fimmu.2011.00018
46. Vivier E, Ugolini S, Blaise D, Chabannon C, Brossay L. Targeting natural killer cells and natural killer T cells in cancer. *Nat Rev Immunol*. (2012) 12:239–52. doi: 10.1038/nri3174
47. Provinciali M, Fabris N. Modulation of lymphoid cell sensitivity to interferon by thyroid hormones. *J Endocrinol Invest*. (1990) 13:187–91. doi: 10.1007/BF03349536
48. Provinciali M, Muzzioli M, Fabris N. Thyroxine-dependent modulation of natural killer activity. *J Exp Pathol*. (1987) 3:617–22.
49. Vasilopoulou E, Loubiere LS, Lash GE, Ohizua O, McCabe CJ, Franklyn JA, et al. Triiodothyronine regulates angiogenic growth factor and cytokine secretion by isolated human decidual cells in a cell-type specific and gestational age-dependent manner. *Hum Reprod*. (2014) 29:1161–72. doi: 10.1093/humrep/deu046
50. Varol C, Mildner A, Jung S. Macrophages: development and tissue specialization. *Annu Rev Immunol*. (2015) 33:643–75. doi: 10.1146/annurev-immunol-032414-112220
51. Ginhoux F, Guilliams M. Tissue-resident macrophage ontogeny and homeostasis. *Immunity*. (2016) 44:439–49. doi: 10.1016/j.immuni.2016.02.024
52. Stocks CJ, Schembri MA, Sweet MJ, Kapetanovic R. For when bacterial infections persist: toll-like receptor-inducible direct antimicrobial pathways in macrophages. *J Leukoc Biol*. (2018) 103:35–51. doi: 10.1002/JLB.4RI0917-358R
53. Hoeksema MA, Glass CK. Nature and nurture of tissue-specific macrophage phenotypes. *Atherosclerosis*. (2019) 281:159–67 doi: 10.1016/j.atherosclerosis.2018.10.005
54. Lo CH, Lynch CC. Multifaceted roles for macrophages in prostate cancer skeletal metastasis. *Front Endocrinol*. (2018) 9:247. doi: 10.3389/fendo.2018.00247
55. Ruytinx P, Proost P, Van Damme J, Struyf S. Chemokine-induced macrophage polarization in inflammatory conditions. *Front Immunol*. (2018) 9:1930. doi: 10.3389/fimmu.2018.01930
56. Braga TT, Agudelo JS, Camara NO. Macrophages during the fibrotic process: M2 as friend and foe. *Front Immunol*. (2015) 6:602. doi: 10.3389/fimmu.2015.00602
57. Barish GD, Downes M, Alaynick WA, Yu RT, Ocampo CB, Bookout AL, et al. A Nuclear Receptor Atlas: macrophage activation. *Mol Endocrinol*. (2005) 19:2466–77. doi: 10.1210/me.2004-0529
58. Perrotta C, Buldorini M, Assi E, Cazzato D, De Palma C, Clementi E, et al. The thyroid hormone triiodothyronine controls macrophage maturation and functions: protective role during inflammation. *Am J Pathol*. (2014) 184:230–47. doi: 10.1016/j.ajpath.2013.10.006
59. Kwakkel J, Surovtseva OV, de Vries EM, Stap J, Fliers E, Boelen A. A novel role for the thyroid hormone-activating enzyme type 2 deiodinase in the inflammatory response of macrophages. *Endocrinology*. (2014) 155:2725–34. doi: 10.1210/en.2013-2066
60. Billon C, Canaple L, Fleury S, Deloire A, Beylot M, Dombrowicz D, et al. TRalpha protects against atherosclerosis in male mice: identification of a novel anti-inflammatory property for TRalpha in mice. *Endocrinology*. (2014) 155:2735–45. doi: 10.1210/en.2014-1098
61. Furuya F, Ishii T, Tamura S, Takahashi K, Kobayashi H, Ichijo M, et al. The ligand-bound thyroid hormone receptor in macrophages ameliorates kidney injury via inhibition of nuclear factor-kappaB activities. *Sci Rep*. (2017) 7:43960. doi: 10.1038/srep43960
62. Artyomov MN, Sergushichev A, Schilling JD. Integrating immunometabolism and macrophage diversity. *Semin Immunol*. (2016) 28:417–24. doi: 10.1016/j.smim.2016.10.004
63. Curi R, de Siqueira Mendes R, de Campos Crispin LA, Norata GD, Sampaio SC, Newsholme P. A past and present overview of macrophage metabolism and functional outcomes. *Clin Sci*. (2017) 131:1329–42. doi: 10.1042/CS20170220
64. Rosa LF, Safi DA, Curi R. Effect of hypo- and hyperthyroidism on the function and metabolism of macrophages in rats. *Cell Biochem Funct*. (1995) 13:141–7. doi: 10.1002/cbf.290130211
65. El-Shaikh KA, Gabry MS, Othman GA. Recovery of age-dependent immunological deterioration in old mice by thyroxine treatment. *J Anim Physiol Anim Nutr*. (2006) 90:244–54. doi: 10.1111/j.1439-0396.2005.00602.x
66. Forner MA, Barriga C, Ortega E. Exercise-induced stimulation of murine macrophage phagocytosis may be mediated by thyroxine. *J Appl Physiol*. (1996) 80:899–903. doi: 10.1152/jappl.1996.80.3.899
67. Chen Y, Sjolinder M, Wang X, Altenbacher G, Hagner M, Berglund P, et al. Thyroid hormone enhances nitric oxide-mediated bacterial clearance and promotes survival after meningococcal infection. *PLoS ONE*. (2012) 7:e41445. doi: 10.1371/journal.pone.0041445
68. De Vito P, Incerpi S, Pedersen JZ, Luly P, Davis FB, Davis PJ. Thyroid hormones as modulators of immune activities at the cellular level. *Thyroid*. (2011) 21:879–90. doi: 10.1089/thy.2010.0429
69. Al-Abed Y, Metz CN, Cheng KF, Aljabari B, VanPatten S, Blau S, et al. Thyroxine is a potential endogenous antagonist of macrophage migration inhibitory factor. (MIF) activity. *Proc Natl Acad Sci USA*. (2011) 108:8224–7. doi: 10.1073/pnas.1017624108
70. Ganesan K, Wadud K. *Euthyroid Sick Syndrome*. Treasure Island, FL: StatPearls (2018).
71. Little JS. Effect of thyroid hormone supplementation on survival after bacterial infection. *Endocrinology*. (1985) 117:1431–5. doi: 10.1210/endo-117-4-1431
72. Contreras-Jurado C, Alonso-Merino E, Saiz-Ladera C, Valino AJ, Regadera J, Alemany S, et al. The thyroid hormone receptors inhibit hepatic interleukin-6 signaling during endotoxemia. *Sci Rep*. (2016) 6:30990. doi: 10.1038/srep30990
73. van der Spek AH, Surovtseva OV, Jim KK, van Oudenaren A, Brouwer MC, Vandenbroucke-Grauls C, et al. Regulation of intracellular triiodothyronine is essential for optimal macrophage function. *Endocrinology*. (2018) 159:2241–52. doi: 10.1210/en.2018-00053
74. Lenz KM, Nelson LH. Microglia and beyond: innate immune cells as regulators of brain development and behavioral function. *Front Immunol*. (2018) 9:698. doi: 10.3389/fimmu.2018.00698

75. Lima FR, Gervais A, Colin C, Izembart M, Neto VM, Mallat M. Regulation of microglial development: a novel role for thyroid hormone. *J Neurosci*. (2001) 21:2028–38. doi: 10.1523/JNEUROSCI.21-06-02028.2001
76. Lourbopoulos A, Mourouzis I, Karapanayiotides T, Nousiopoulou E, Chatzigeorgiou S, Mavridis T, et al. Changes in thyroid hormone receptors after permanent cerebral ischemia in male rats. *J Mol Neurosci*. (2014) 54:78–91. doi: 10.1007/s12031-014-0253-3
77. Jin YC, Lee H, Kim SW, Kim ID, Lee HK, Lee Y, et al. Intranasal delivery of RGD motif-containing osteopontin icosamer confers neuroprotection in the postischemic brain via alphavbeta3 integrin binding. *Mol Neurobiol*. (2016) 53:5652–63. doi: 10.1007/s12035-015-9480-z
78. Wirth EK, Roth S, Blechschmidt C, Holter SM, Becker L, Racz I, et al. Neuronal 3′,3,5-triiodothyronine. (T3) uptake and behavioral phenotype of mice deficient in Mct8, the neuronal T3 transporter mutated in Allan-Herndon-Dudley syndrome. *J Neurosci*. (2009) 29:9439–49. doi: 10.1523/JNEUROSCI.6055-08.2009
79. Braun D, Kinne A, Brauer AU, Sapin R, Klein MO, Kohrle J, et al. Developmental and cell type-specific expression of thyroid hormone transporters in the mouse brain and in primary brain cells. *Glia*. (2011) 59:463–71. doi: 10.1002/glia.21116
80. Mori Y, Tomonaga D, Kalashnikova A, Furuya F, Akimoto N, Ifuku M, et al. Effects of 3,3',5-triiodothyronine on microglial functions. *Glia*. (2015) 63:906–20. doi: 10.1002/glia.22792
81. Noda M. Thyroid hormone in the CNS: contribution of neuron-glia interaction. *Vitam Horm*. (2018) 106:313–31. doi: 10.1016/bs.vh.2017.05.005
82. Perrotta C, De Palma C, Clementi E, Cervia D. Hormones and immunity in cancer: are thyroid hormones endocrine players in the microglia/glioma cross-talk? *Front Cell Neurosci*. (2015) 9:236. doi: 10.3389/fncel.2015.00236
83. Kowalik MA, Columbano A, Perra A. Thyroid hormones, thyromimetics and their metabolites in the treatment of liver disease. *Front Endocrinol*. (2018) 9:382. doi: 10.3389/fendo.2018.00382
84. Videla LA. Energy metabolism, thyroid calorigenesis, and oxidative stress: functional and cytotoxic consequences. *Redox Rep*. (2000) 5:265–75. doi: 10.1179/135100000101535807
85. Varela P, Tapia G, Fernandez V, Videla LA. The role of thyroid hormone calorigenesis in the redox regulation of gene expression. *Biol Res*. (2006) 39:611–7. doi: 10.4067/S0716-97602006000500004
86. Krenkel O, Tacke F. Liver macrophages in tissue homeostasis and disease. *Nat Rev Immunol*. (2017) 17:306–21. doi: 10.1038/nri.2017.11
87. Videla LA, Fernandez V, Tapia G, Varela P. Thyroid hormone calorigenesis and mitochondrial redox signaling: upregulation of gene expression. *Front Biosci*. (2007) 12:1220–8. doi: 10.2741/2140
88. Fernandez V, Reyes S, Bravo S, Sepulveda R, Romanque P, Santander G, et al. Involvement of Kupffer cell-dependent signaling in T3-induced hepatocyte proliferation *in vivo*. *Biol Chem*. (2007) 388:831–7. doi: 10.1515/BC.2007.101
89. Eisenbarth SC. Dendritic cell subsets in T cell programming: location dictates function. *Nat Rev Immunol*. (2019) 19:89–103. doi: 10.1038/s41577-018-0088-1
90. Satpathy AT, Kc W, Albring JC, Edelson BT, Kretzer NM, Bhattacharya D, et al. Zbtb46 expression distinguishes classical dendritic cells and their committed progenitors from other immune lineages. *J Exp Med*. (2012) 209:1135–52. doi: 10.1084/jem.20120030
91. Worbs T, Hammerschmidt SI, Forster R. Dendritic cell migration in health and disease. *Nat Rev Immunol*. (2017) 17:30–48. doi: 10.1038/nri.2016.116
92. Mooij P, Simons PJ, de Haan-Meulman M, de Wit HJ, Drexhage HA. Effect of thyroid hormones and other iodinated compounds on the transition of monocytes into veiled/dendritic cells: role of granulocyte-macrophage colony-stimulating factor, tumour-necrosis factor-alpha and interleukin-6. *J Endocrinol*. (1994) 140:503–12. doi: 10.1677/joe.0.1400503
93. Mascanfroni I, Montesinos Mdel M, Susperreguy S, Cervi L, Ilarregui JM, Ramseyer VD, et al. Control of dendritic cell maturation and function by triiodothyronine. *FASEB J*. (2008) 22:1032–42. doi: 10.1096/fj.07-8652com
94. Mascanfroni ID, Montesinos Mdel M, Alamino VA, Susperreguy S, Nicola JP, Ilarregui JM, et al. Nuclear factor. (NF)-kappaB-dependent thyroid hormone receptor beta1 expression controls dendritic cell function via Akt signaling. *J Biol Chem*. (2010) 285:9569–82. doi: 10.1074/jbc.M109.071241
95. Montesinos MM, Alamino VA, Mascanfroni ID, Susperreguy S, Gigena N, Masini-Repiso AM, et al. Dexamethasone counteracts the immunostimulatory effects of triiodothyronine. (T3) on dendritic cells. *Steroids*. (2012) 77:67–76. doi: 10.1016/j.steroids.2011.10.006
96. Alamino VA, Mascanfroni ID, Montesinos MM, Gigena N, Donadio AC, Blidner AG, et al. Antitumor responses stimulated by dendritic cells are improved by triiodothyronine binding to the thyroid hormone receptor beta. *Cancer Res*. (2015) 75:1265–74. doi: 10.1158/0008-5472.CAN-14-1875
97. Gigena N, Alamino VA, Montesinos MD, Nazar M, Louzada RA, Wajner SM, et al. Dissecting thyroid hormone transport and metabolism in dendritic cells. *J Endocrinol*. (2017) 232:337–50. doi: 10.1530/JOE-16-0423
98. Emens LA, Ascierto PA, Darcy PK, Demaria S, Eggermont AMM, Redmond WL, et al. Cancer immunotherapy: opportunities and challenges in the rapidly evolving clinical landscape. *Eur J Cancer*. (2017) 81:116–29. doi: 10.1016/j.ejca.2017.01.035
99. Constantino J, Gomes C, Falcao A, Cruz MT, Neves BM. Antitumor dendritic cell-based vaccines: lessons from 20 years of clinical trials and future perspectives. *Transl Res*. (2016) 168:74–95. doi: 10.1016/j.trsl.2015.07.008
100. Veglia F, Gabrilovich DI. Dendritic cells in cancer: the role revisited. *Curr Opin Immunol*. (2017) 45:43–51. doi: 10.1016/j.coi.2017.01.002
101. Alamino VA, Montesinos MM, Rabinovich GA, Pellizas CG. The thyroid hormone triiodothyronine reinvigorates dendritic cells and potentiates anti-tumor immunity. *Oncoimmunology*. (2016) 5:e1064579. doi: 10.1080/2162402X.2015.1064579
102. Alamino VA, Montesinos MDM, Soler MF, Giusiano L, Gigena N, Fozzatti L, et al. Dendritic cells exposed to triiodothyronine deliver pro-inflammatory signals and amplify IL-17-driven immune responses. *Cell Physiol Biochem*. (2019) 52:354–67. doi: 10.33594/000000025
103. Dedecjus M, Stasiolek M, Brzezinski J, Selmaj K, Lewinski A. Thyroid hormones influence human dendritic cells' phenotype, function, and subsets distribution. *Thyroid*. (2011) 21:533–40. doi: 10.1089/thy.2010.0183
104. Stasiolek M, Dedecjus M, Adamczewski Z, Sliwka PW, Brzezinski J, Lewinski A. Effect of L-thyroxine treatment on peripheral blood dendritic cell subpopulations in patients with Hashimoto's thyroiditis. *Folia Histochem Cytobiol*. (2014) 52:138–43. doi: 10.5603/FHC.2014.0013
105. Trinchieri G. Interleukin-12 and the regulation of innate resistance and adaptive immunity. *Nat Rev Immunol*. (2003) 3:133–46. doi: 10.1038/nri1001
106. Tamura M, Matsuura B, Miyauchi S, Onji M. Dendritic cells produce interleukin-12 in hyperthyroid mice. *Eur J Endocrinol*. (1999) 141:625–9. doi: 10.1530/eje.0.1410625
107. Tamaru M, Matsuura B, Onji M. Increased levels of serum interleukin-12 in Graves' disease. *Eur J Endocrinol*. (1999) 141:111–6. doi: 10.1530/eje.0.1410111
108. Ganesh BB, Cheatem DM, Sheng JR, Vasu C, Prabhakar BS. GM-CSF-induced CD11c+CD8a–dendritic cells facilitate Foxp3+ and IL-10+ regulatory T cell expansion resulting in suppression of autoimmune thyroiditis. *Int Immunol*. (2009) 21:269–82. doi: 10.1093/intimm/dxn147
109. Liu J, Cao X. Regulatory dendritic cells in autoimmunity: a comprehensive review. *J Autoimmun*. (2015) 63:1–12. doi: 10.1016/j.jaut.2015.07.011

Conflict of Interest Statement: The authors declare that the research was conducted in the absence of any commercial or financial relationships that could be construed as a potential conflict of interest.

frontiers in Endocrinology

CORRECTION
published: 19 July 2019
doi: 10.3389/fendo.2019.00486

Corrigendum: Thyroid Hormone Action on Innate Immunity

*María del Mar Montesinos and Claudia Gabriela Pellizas**

Facultad de Ciencias Químicas, Centro de Investigaciones en Bioquímica Clínica e Inmunología (CIBICI-CONICET) and Departamento de Bioquímica Clínica, Universidad Nacional de Córdoba, Córdoba, Argentina

Keywords: thyroid hormones, innate immunity, neutrophils, natural killer cells, macrophages, dendritic cells

OPEN ACCESS

Approved by:
Frontiers Editorial Office, Frontiers Media SA, Switzerland

***Correspondence:**
Claudia Gabriela Pellizas
claudia@fcq.unc.edu.ar

Specialty section:
This article was submitted to Experimental Endocrinology, a section of the journal Frontiers in Endocrinology

Received: *02 July 2019*
Accepted: *04 July 2019*
Published: *19 July 2019*

Citation:
Montesinos MM and Pellizas CG (2019) Corrigendum: Thyroid Hormone Action on Innate Immunity. Front. Endocrinol. 10:486. doi: 10.3389/fendo.2019.00486

A Corrigendum on

Thyroid Hormone Action on Innate Immunity
by Montesinos, M. M., and Pellizas, C. G. (2019). Front. Endocrinol. 10:350. doi: 10.3389/fendo.2019.00350

An author name was incorrectly spelled as "Claudia Pellizas." The correct spelling is "Claudia Gabriela Pellizas."

The authors apologize for this error and state that this does not change the scientific conclusions of the article in any way. The original article has been updated.

frontiers in Endocrinology

ORIGINAL RESEARCH
published: 18 June 2019
doi: 10.3389/fendo.2019.00369

"Beige" Cross Talk Between the Immune System and Metabolism

*Krisztina Banfai[1,2], David Ernszt[2,3], Attila Pap[4], Peter Bai[5,6,7,8], Kitti Garai[1,2], Djeda Belharazem[9], Judit E. Pongracz[1,2] and Krisztian Kvell[1,2]**

[1] Department of Pharmaceutical Biotechnology, Faculty of Pharmacy, University of Pécs, Pécs, Hungary, [2] Szentagothai Research Center, University of Pécs, Pécs, Hungary, [3] Department of Physiology, Medical School, University of Pécs, Pécs, Hungary, [4] Department of Biochemistry and Molecular Biology, Faculty of Medicine, University of Debrecen, Debrecen, Hungary, [5] Medical Chemistry, Faculty of Medicine, University of Debrecen, Debrecen, Hungary, [6] MTA-DE Cell Biology and Signaling Research Group, Debrecen, Hungary, [7] MTA-DE Lendulet Laboratory of Cellular Metabolism, Debrecen, Hungary, [8] Research Center for Molecular Medicine, University of Debrecen, Debrecen, Hungary, [9] Department of Pathology, University Hospital of Mannheim, Mannheim, Germany

With thymic senescence the epithelial network shrinks to be replaced by adipose tissue. Transcription factor TBX-1 controls thymus organogenesis, however, the same TBX-1 has also been reported to orchestrate beige adipose tissue development. Given these different roles of TBX-1, we have assessed if thymic TBX-1 expression persists and demonstrates this dualism during adulthood. We have also checked whether thymic adipose involution could yield beige adipose tissue. We have used adult mouse and human thymus tissue from various ages to evaluate the kinetics of TBX-1 expression, as well as mouse (TEP1) and human (1889c) thymic epithelial cells (TECs) for our studies. Electron micrographs show multi-locular lipid deposits typical of beige adipose cells. Histology staining shows the accumulation of neutral lipid deposits. qPCR measurements show persistent and/or elevating levels of beige-specific and beige-indicative markers (TBX-1, EAR-2, UCP-1, PPAR-gamma). We have performed miRNome profiling using qPCR-based QuantStudio platform and amplification-free NanoString platform. We have observed characteristic alterations, including increased miR21 level (promoting adipose tissue development) and decreased miR34a level (bias toward beige adipose tissue differentiation). Finally, using the Seahorse metabolic platform we have recorded a metabolic profile (OCR/ECAR ratio) indicative of beige adipose tissue. In summary, our results support that thymic adipose tissue emerging with senescence is *bona fide* beige adipose tissue. Our data show how the borders blur between a key immune tissue (the thymus) and a key metabolic tissue (beige adipose tissue) with senescence. Our work contributes to the understanding of cross talk between the immune system and metabolism.

Keywords: thymus senescence, beige adipose tissue, TBX-1, UCP-1, PPARgamma

OPEN ACCESS

Edited by:
Jie Chen,
Xiamen University, China

Reviewed by:
Lluis Tort,
Autonomous University of Barcelona, Spain
Mark Klitgaard Nøhr,
University of Copenhagen, Denmark

****Correspondence:***
Krisztian Kvell
kvell.krisztian@pte.hu

Specialty section:
This article was submitted to Experimental Endocrinology, a section of the journal Frontiers in Endocrinology

Received: *11 March 2019*
Accepted: *24 May 2019*
Published: *18 June 2019*

Citation:
Banfai K, Ernszt D, Pap A, Bai P, Garai K, Belharazem D, Pongracz JE and Kvell K (2019) "Beige" Cross Talk Between the Immune System and Metabolism. Front. Endocrinol. 10:369. doi: 10.3389/fendo.2019.00369

INTRODUCTION

In human the degenerative process of thymic adipose involution is already detectable in childhood and accelerates with puberty due to hormonal (sex-steroid) induction (1–3). The process shows identical kinetics in mouse. Also, we have developed a model whereby TECs are treated by a steroid (using Dx or dexamethasone) thus both *in vivo* and *in vitro* model systems are readily available (4) As for all adipose tissues subtypes, thymic adipose involution is orchestrated by transcription

factor PPARgamma (5–7). It is estimated that by the age of 50 years in human (approx. 12 months in mouse), the thymus loses approx. Ninety percent of its function: naïve T-cell production (8, 9). The consequences of impaired thymus function are profound: elevated incidence of infections, cancer and autoimmune disorders observed at senior ages (10, 11). This poses a significant burden on health-care and health-insurance systems, while simultaneously lowering the quality of life in the elderly.

Transcription factor TBX-1 is a key molecular player in the formation of the third pharyngeal pouch involved in thymus organogenesis during embryonic development (12). Human patients with 22q11.2DS impairing TBX-1 often have thymus hypoplasia or aplasia. In accordance, Tbx-1^{null} mice develop severe pathologies in tissues derived from the third pharyngeal pouch, including hypoplasia of the thymus (13, 14). In these cases, impaired thymus organogenesis leads to deficient thymocyte development, naive T-cell production, and immune functions (15). However, recently it has also been reported that the role of TBX-1 in thymus organogenesis is more complex. Ectopic expression of TBX-1 may suppress transcription factor FoxN1, the mastermind of thymic epithelial identity (16). The issue was investigated in the embryonic setting, but the potential role of persistent TBX-1 expression during adulthood has not been addressed.

TBX-1 has another pivotal role in the development and function of a recently described subtype of adipose tissue: beige adipose tissue (17–20). White adipose tissue stores energy, brown adipose tissue generates heat (via NST or non-shivering thermogenesis), while beige adipocytes act as intermediates. Beige adipocytes respond to adrenergic stimuli by thermogenesis (21). TBX-1 is considered as a beige-specific marker, but other beige-indicative markers have also been described. Mitochondrial uncoupling proteins (mostly UCP-1) have been reported to be expressed by brown / beige adipose tissue. EAR2 (also known as Nr2f6) was reported to efficiently promote adipose tissue development with beige bias, while CD137 (also known as Tnfrsf9) is an acknowledged beige adipocyte surface marker (22).

The adult thymus expresses TBX-1 and UCP-1 in the stromal compartment, both known to promote beige adipose tissue development. Yet to date thymic adipose tissue that develops with age has not been accurately positioned on this white-beige-brown continuum of adipose tissue subtypes, despite recent cellular analysis from an adipocyte perspective (23–26). For this reason, we have characterized senescence-related thymic adipose tissue using molecular, cellular and histological markers, at structural and ultra-structural levels, using both mouse and human samples. Additionally, we have also performed metabolic profiling and complete miRNome analysis using both PCR-based and amplification-free platforms.

METHODS

Cell Cultures

For *in vitro* experiments primary-derived (BALB/c) thymic epithelial cells were used (TEP1) as reported previously (cell source: Prof. G. Anderson, University of Birmingham, UK) (27). Briefly, the cells were cultured in DMEM (Dulbecco's Modified Eagle's medium Lonza) supplemented with 10% FCS, penicillin, streptomycin and β-mercapto-ethanol. Human thymus-derived 1889c thymic carcinoma cells were cultured in RPMI 1640 (Roswell Park Memorial Institute medium, Lonza) containing 10% FCS, penicillin, streptomycin, L-Glutamine and Hepes (28, 29). Adipose differentiation of TEP1 and 1889c cells was induced by steroid treatment. Briefly, experiments differentiation was induced by dexamethasone alone (Dx) as added to complete DMEM and RPMI medium. Cells were treated with Dx at a final concentration of 1 μM for 1 week.

Animal Samples

Thymus lobes were used from C57BL/6J mice at 1, 6, 8, 12, 14, 18, and 21 months of age. Mice were housed under minimal disease (MD) conditions. Animal rooms were ventilated 15 times/h with filtered air, mice received autoclaved pellet diet (Altromin VRF1) and tap water *ad libitum*. The cages contained sterilized bedding. Room lighting was automated with 12 h light and 12 h dark periods. Room temperature was 21 ± 2°C, relative humidity was between 30 and 60%. Mice were kept in the Laboratory Animal Core Facility of the University. Experimental procedures were carried out according to the "1988/XXVIII act of the Hungarian Parliament on Animal Protection (243/1988)" which complies with recommendations of the Helsinki Declaration. All animal experiments were performed with the consent of the Ethics Committee on Animal Research of the University (ref. no.: #BA02/2000-46/2016).

Enrichment of Primary Cells

Mouse thymic epithelial cells were isolated by MACS cell separation. Briefly, mouse thymic lobes (1 month-old or 12 month-old) were digested with type F collagenase from C. hystolyticum (3mg/ml, Sigma-Aldrich) for 2 h, with stirring in every 20 min, then washed with DMEM. Cell suspensions were then labeled with anti-EpCAM1 antibody (1:100, rat monoclonal antibody clone: G8.8) and washed with MACS-buffer (2% FCS, 1mM EDTA in PBS) followed by incubation with Dynabeads sheep anti-rat IgG-coated beads (Invitrogen) The EpCAM+-cells were separated with EasySep column-free cell isolation platform (Stemcell Technologies) according to the manufacturer's instructions. Isolated cells were used for total RNA isolation and subsequent qPCR analysis.

Human Thymus Samples

Formalin-fixed, paraffin-embedded (FFPE) human thymus samples from 18, 23, 42, 44, and 58 years of age were provided by the Department of Pathology, Faculty of Medicine, University of Pecs, Hungary. Experiments involving human samples were performed with the consent of the Regional and Local Ethics Committee of Clinical Center of the University (ref. no.: 6069/2016) according to their guidelines. All subjects gave written informed consent in accordance with the Declaration of Helsinki.

Transmission Electron Microscopy

Cells were harvested and pelleted then fixed with PBS containing 2.5% glutaraldehyde overnight at 4°C. Following fixation, pellets were mixed in 3% porcine gelatin (Sigma-Aldrich). Hardened small blocks of approximately 1 mm^3 were cut. Blocks were post-fixed in 1% osmium-tetroxide in PBS for 1 h at 4°C and dehydrated with increasing concentration of ethanol. Uranyl-acetate (1%) was added in 70% ethanol to increase contrast. After complete dehydration in ascending ethanol series, blocks were transferred to propylene-oxide twice for 4 min. Then blocks were immersed in the mixture of propylene-oxide and Durcupan resin (Sigma-Aldrich) for 30 min. Later blocks were placed into Durcupan-containing tin-foil boats overnight, and embedded into gelatin capsule filled with Durcupan resin (Sigma-Aldrich). Following polymerization and hardening of the resin at 56 °C for 72 h, semi thin sections were cut with Leica Ultracut ultramicrotom, mounted on glass slides, stained with toluidine-blue and examined with Olympus BX50 light microscope. Then serial ultra-thin sections were cut by ultramicrotom, and mounted on mesh grids. Ultra-thin sections were contrasted by uranyl-acetate and lead-citrate, and examined using JEOL 1200EX-II electron microscope.

Immune-Histochemistry

Human thymus lobes were fixed in paraformaldehyde (4% PFA in PBS) then paraffin embedded. 5μm thick sections were stained with immunohistochemistry method as described earlier (30). First, slides were rinsed in heated xylene then washed with a descending series of alcohol. After deparaffinization slides were rehydrated and antigen retrieval was performed in Target Retrieval Solution (pH 6 DAKO) at 97°C for 20–30 min. Following wash in dH_2O and endogenous peroxidase activity was blocked with 3% H_2O_2 in TBS (pH 7.4) for 15 min. Then slides were washed with TBS containing Tween (0.05%, pH 7.4). Pre-blocking was carried out with 3% BSA in TBS for 20 min followed by overnight incubation with a-TBX-1 (1:100, rabbit polyclonal antibody, Sigma-Aldrich) primary antibody at 4°C. After the incubation slides were washed with TBS then incubated with peroxidase conjugated secondary antibody (1:100, Polyclonal Goat Anti-Rabbit IgG, DAKO) for 90 min. Labeling was visualized with liquid DAB Substrate Chromogen System (DAKO). Hematoxylin served for nuclear counterstaining. Slides were mounted with Faramount Aqueous Mounting Medium (DAKO). Histological evaluation was performed with Panoramic MIDI digital slide scanner (3DHistech) and images were captured with CaseViewer. Image analysis was made with ImageJ / IHC toolbox.

Immune-Fluorescent Staining

Immune-fluorescent staining was performed on 8μm cryostat thymus sections. Cytospin technique was used to spin TEP1 and 1889c cells onto glass slides (4). Slides were fixed in cold acetone, then dried and blocked using 5% BSA in PBS for 20 min before staining with fluorochrome conjugated or primary antibodies: a-EpCAM-FITC (1:100, clone: G8.8,), a-UCP-1 (1:100, rabbit polyclonal antibody, Abcam) a-TBX-1 (1:100, rabbit polyclonal antibody, Sigma-Aldrich), a-PPAR-gamma (1:100, rabbit monoclonal antibody, Cell Signaling Technology). For secondary antibody Alexa-555 conjugated a-rabbit goat IgG (1:200, Life Technologies) was used. Fluorescent lipid staining was performed on paraformaldehyde (4%) fixed TEP1 and 1889c cytospin slides with LipidTOX Red dye (1:200, Invitrogen). For nuclear counterstain DAPI (Life Technologies) was used. Sections were imaged using a Nikon Eclipse Ti-U microscope equipped with a CCD camera (Andor Zyla 5.5) and NIS-Elements software.

Metabolic Profiling

The use of TEP1 cells for Seahorse metabolic profiling was started by pilot experiments for optimal starting cell number, duration of differentiation, differentiation medium etc. Accordingly, 15,000 cells/well were cultured for 9 days using standard MDI differentiation protocol (31). This was followed by the evaluation of their metabolic profile using the Seahorse XF 96 platform (Seahorse Bioscience). Cells were plated into Seahorse cell plates at confluence and were left to attach overnight. The next day, cells were subject to oxymetry measurement. After recording baseline oxygen consumption cells were treated with butyril-cAMP (500 μM), oligomycin (2 μM), and antimycin (10 μM). Antimycin-resistant oxygen consumption was considered as background and was subtracted from all values. Baseline oxygen consumption, membrane leak (OCR, after oligomycin treatment) was calculated. Glycolysis was assessed through the extracellular acidification value (ECAR, before oligomycin treatment) and the ECAR/OCR values were calculated. Negative values were omitted in calculations.

RNA Isolation, cDNA Preparation, qRT-PCR, TaqMan Array

Total RNA of enriched thymic epithelial cells, TEP1 and 1889c cells was isolated with the NucleoSpin RNAII kit (Macherey-Nagel). cDNA was prepared using the High Capacity cDNA Reverse Transcription kit (Applied Biosystems). For qPCR analysis the StepOnePlus (Applied Biosystems) platform was used with SensiFAST SYBR Hi-ROX Mix (Bioline) as well as PikoReal™ Real-Time PCR System (Thermo Fisher Scientific) using Luminaris Color HiGreen qPCR Master Mix (Thermo Fisher Scientific) (for primer list see **Table 1**). Gene expression was normalized to β-actin, GUSB and HPRT1 housekeeping genes. Reverse transcription of 1889c RNA samples for miRNA analysis was completed with Megaplex™ RT Primers specific to human Pool A (Cat. No.: 4399966) and Pool B (Cat. No.: 4444281). MiRNA profiling was performed on Applied Biosystems Quantstudio™ 12K Flex Real-Time PCR System platform using TaqMan™ Array Human MicroRNA A (Applied Biosystems, Cat. No.: 4398965) and B Card (Applied Biosystems, Cat. No.: 4444910) containing 6 housekeeping genes (RNU44, RNU48, ath-miR159a and 4 U6 snRNAs) and 377 human miRNAs. Additionally 600 ng of total RNA was mixed with TaqMan™ Fast Universal PCR Master Mix (2X), no AmpErase™ UNG (Applied Biosystems, Cat. No.: 4364103) for each array

TABLE 1 | List of mouse and human primer sequences.

Gene Name	Mouse primer sequence	Human primer sequence
Actin-for	GGGAGGGTGAGGGACTTCC	GCGCGGCTACAGCTTCA
Actin-rev	TGGGCGCTTTTGACTCAGGA	CTTAATGTCACGCACGATTTCC
GUSB-for	AAATGGAGTGCGTGTTGGGT	GATGCTGTACCCCCAGGA
GUSB-rev	CGGTACCATTGCTGCTCGAA	GTCGGTTGTCAGAGAAGTCG
HPRT-for	TTGCTCGAGATGTCATGAAGGA	CTGGCGTCGTGATTAGTGAT
HPRT-rev	ATGTAATCCAGCAGGTCAGCA	ACATCTCGAGCAAGACGTTC
CD137-for	CGTGCAGAACTCCTGTGATAAC	CCTGAGCTACAAAGAGGACAC
CD137-rev	CTCCACCTATGCTGGAGAAGG	GTGCAGCGCAAGTGAAAC
Ear2-for	CCTGTACCCCAGAACTCCA	GCAAGCATTACGGTGTCTTC
Ear2-rev	CAGATGAGCAAAGGTGCAAA	GATCTGGCAGTCACGGTTG
PPARg-for	TGTCTCACAATGCCATCAGGT	GGTGGCCATCCGCATCT
PPARg-rev	TCTTTCCTGTCAAGATCGCCC	GCTTTTGGCATACTCTGTGATCTC
TBX1-for	GGCAGGCAGACGAATGTTC	CTACGACCACTATCTCGGGG
TBX1-rev	TTGTCATCTACGGGCACAAAG	TGGGGCAATAGTCGTAGGAG
UCP1-for	GGCCTCTACGACTCAGTCCA	ACAATCACCGCTGTGGTAAA
UCP1-rev	TAAGCCGGCTGAGATCTTGT	GTAGAGGCCGATCCTGAGAG

card. Gene expressions were analyzed using Expression Suite Software version 1.1.

NanoString System Assay

One hundred nanogram of total RNA was used to detect up to 800 miRNA targets with nCounter SPRINT Profiler (NanoString Technologies) using nCounter® Human v3 miRNA Expression Assay. Sample preparation was performed with nCounter® CodeSet (NanoString Technologies) following annealing, ligation and purification. Hybridization protocol was completed at 65°C and 12 h long according to the manufacturer's instructions. Quantified data was analyzed using nSolver™ Analysis Software version 4.0. Threshold count was determined using negative controls as background noise. Gene expression changes were visualized on heat map using GraphGad Prism version 7.04.

Statistical Analysis

All experiments were performed at least on three occasions, representative experiments are shown. Measures were obtained in triplicates, data are presented as mean and ±SD as error bars. For statistical analysis GraphPad Prism software and SPSS Statistics version 22.0 was used. To evaluate the kinetics of TBX-1 expression with age in both mouse and human samples normality distribution was tested using Shapiro-Wilk test ($n < 50$). In case of human samples our data met the assumption of homogeneity of variances, so parametric one-way ANOVA with Tukey's honestly significant difference (HSD) *post hoc* test was used. To determine the significant differences of mouse samples non-parametric Kruskal-Wallis test was used. For further cases two-tailed student's *t*-test was applied. Significant differences are shown by asterisks (ns for $p > 0.05$, $^{*}p \leq 0.05$, $^{**}p \leq 0.01$, $^{***}p \leq 0.001$).

RESULTS

Aging and Steroid-Induced TECS Show Beige Adipocyte Markers

Thymic senescence is accompanied by the appearance of adipose tissue. Mediastinal location and local FGF21 production are characteristic to the thymus and both were reported to promote beige adipose tissue development (23–25). For this reason we searched for the up-regulation of beige adipocyte markers in the adult thymus tissue and its model system: steroid-induced TECs.

Aging Up-Regulates key Beige Adipocyte Marker in Human Thymus Tissue

Using a pilot set of human thymic FFPE samples of various adult ages (18, 23, 42, 44, and 58 years) we performed immune-histochemistry staining for beige adipose tissue-specific marker TBX-1 (**Figures 1A–E**). TBX-1 expression (enzyme reaction in brown) appears to persist throughout adulthood. Normalization to hematoxylin nuclear counterstain (in blue) shows that TBX-1 staining intensity transiently decreases at young adult age (23 years) to show rebound at later ages (**Figure 1F**). In other words: TBX-1 expression may present a bimodal nature with elevations at both young and adulthood ages and an in-between transient decrease during young adulthood. The histological appearance of adipocytes is observed from 44 years of age onwards in this series.

Further Beige Adipocyte Markers Are Also Up-Regulated in Steroid-Induced Human TECs

As reported previously molecular level events are similar in the aging thymus and steroid-induced TECs in the mouse setting (4, 6). Accordingly, Dx-treatment significantly up-regulated ($p < 0.01$) pan-adipocyte marker PPAR-gamma expression in the human 1889c TEC line (**Figures 2A,B,I**). We have evaluated 1889c human TECs for the expression of beige-specific and beige-indicative protein markers as well following Dx-treatment. Similar to human thymus sections above, 1889c cells showed persistent and increasing ($p < 0.05$) TBX-1 expression following Dx-treatment (**Figures 2C,D,I**). UCP-1 expression showed only indicative (not significant) increase upon Dx-treatment (**Figures 2E,F,I**). Lipid accumulation was also tested, using a fluorescent dye (LipidTox Red) specific for neutral lipid deposits. The staining showed that Dx-treatment triggers significant ($p < 0.05$) accumulation of neutral lipid deposits (**Figures 2G–I**) in harmony with our previous reports (4, 6).

Aging Up-Regulates key Beige Adipocyte Marker in Mouse Thymus Tissue

Using a pilot set of mouse thymic cryosections of various ages (1, 6, 8, 12, 14, 18, and 21 months) we performed immune-fluorescent staining for beige adipose tissue-specific marker TBX-1 (**Figures 3A–G**). TBX-1 expression (in red) appears to persist throughout adulthood in the mouse similar to human above. EpCAM-1 staining (in green) shows medullary areas to demonstrate histological organization. Normalization

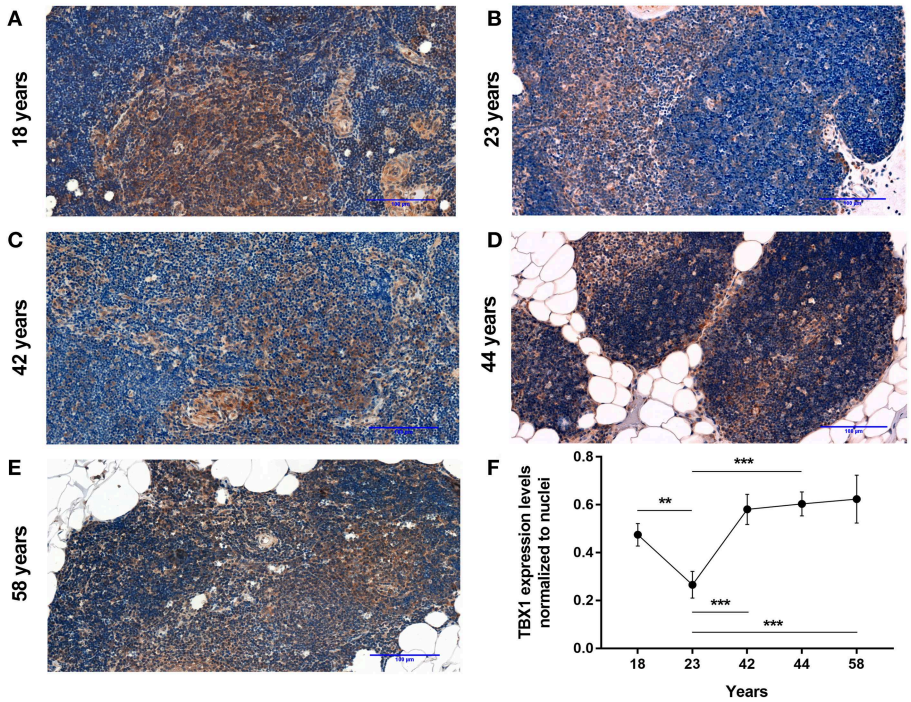

FIGURE 1 | Kinetics of TBX-1 expression in the adult human thymus with age. Human thymic FFPE sections from different ages (18, 23, 42, 44, and 58 years) were evaluated by immune-histochemical staining **(A–E)**, respectively. Brown color reaction (DAB) shows TBX-1 expression along with hematoxylin nuclear counter-staining. Please note signs of adipose degeneration (vacuoles) at elevated ages. TBX-1 staining was normalized to nuclear counter-stain and is shown as relative value **(F)**. Please note that relative TBX-1 expression shows a transient decrease at young adult age (23 years of age). Significant differences are shown by asterisks (**$p \leq 0.01$, ***$p \leq 0.001$). Data were calculated from three slides and representative slide is shown. For exact numerical values and standard error of mean please refer to **Supplementary Data Sheet**.

to DAPI nuclear counterstain (in blue, not shown here) reveals that TBX-1 staining intensity transiently decreases at adult mid-term (12–14 months) to show rebound at senior ages (**Figure 3H**). In other terms: TBX-1 expression potentially appears to be bimodal in the mouse as well showing elevation at both young and senior ages with a transient in-between decrease during adulthood. Murine kinetics of TBX-1 expression resembles the previously shown human kinetics but with higher resolution in time. Please note medullary involution observed from 14 months of age onwards in line with our previous reports (4, 6).

Further Beige Adipocyte Markers Are Also Up-Regulated in Steroid-Induced Mouse TECs

As reported previously focusing on PPARgamma expression molecular level events are similar in the aging thymus and steroid-induced TECs in the mouse setting (4, 6). We have evaluated TEP1 mouse TECs for the expression of beige-specific and beige-indicative protein markers after Dx-treatment. TEP1 cells showed persistent, unchanged TBX-1 expression following Dx-treatment (**Figures 4A,B,I**). UCP-1 expression showed significant ($p < 0.01$) increase following Dx-treatment (**Figures 4C,D,I**). Lipid accumulation was also tested (LipidTox Red as above). The staining showed that Dx-treatment results in significant ($p < 0.05$) accumulation of neutral lipid deposits (**Figures 4E,F,I**) in accordance with our previous reports (4, 6). Ultra-structural imaging by TEM shows the appearance of multi-locular intracellular lipid deposits (indicated by asterisks) upon Dx-treatment, reminiscent of beige adipose tissue (**Figures 4G,H**).

Steroid-Induced TECs Show Beige Adipocyte Metabolic Profile

There is a significant difference between white, brown and beige adipose tissue metabolic traits. In search of further evidence we have characterized the metabolic fingerprint of Dx-induced mouse TECs (TEP1).

The metabolic fingerprint of TEP1 cells treated with Dx (as part of MDI differentiation medium) was assayed using the Seahorse platform (**Figure 5**). MDI cells showed significantly higher basal OCR values compared to control cells ($p < 0.001$) (**Figure 5A**). Of note cAMP-induced OCR was rapid (30 min post-treatment) and lasted shorter than in previous reports (32, 33). In line with elevated UCP-1 expression oligomycin-resistant respiration was significantly higher in MDI cells than in control cells ($p < 0.001$) (**Figure 5B**). Although we have recorded increased glycolysis marked by significantly increased ECAR values ($p < 0.001$) (**Figure 5C**), the significantly increased ratio of basal OCR and ECAR ($p < 0.001$) (**Figure 5D**) in MDI cells suggests their dependence on mitochondrial oxidation.

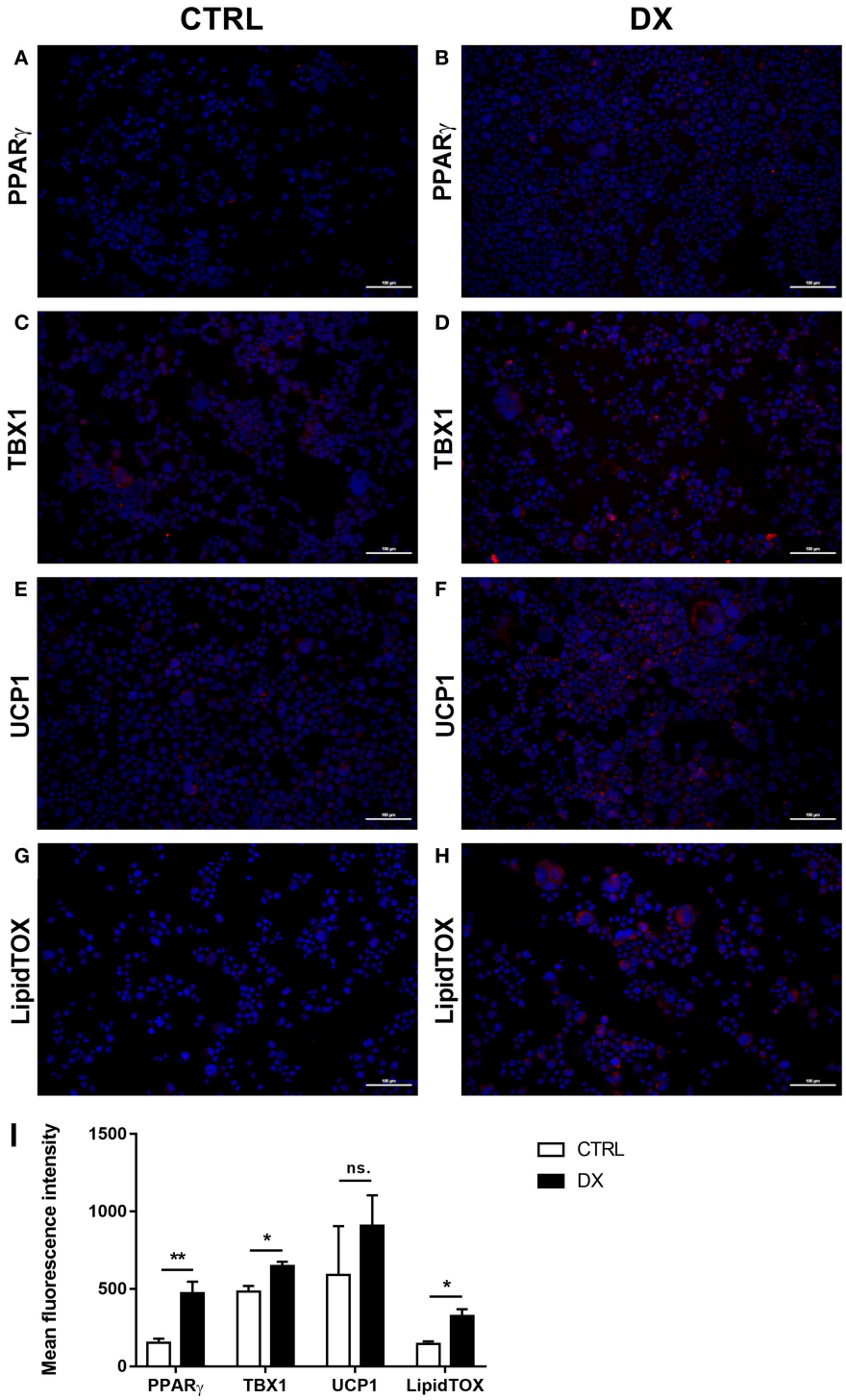

FIGURE 2 | Beige adipocyte marker expression and lipid accumulation in steroid-induced human TECs. Cytospin slides of control (Ctrl) and steroid-induced (Dx) 1889c cells were stained by immune-fluorescence. Adipose tissue mastermind transcription factor PPARgamma **(A,B)**, beige-specific marker TBX-1 **(C,D)** and beige-indicative marker UCP-1 **(E,F)** was evaluated in red (Alexa555). Neutral lipid deposits were stained with LipidTOX Red dye **(G,H)**. DAPI staining was also applied as fluorescent nuclear counter stain in all cases. PPAR-gamma, TBX-1, UCP-1 and LipidTOX staining relative to DAPI staining is also shown by histograms **(I)**. PPAR-gamma and TBX-1 show significant increase, UCP-1 remains unchanged, while neutral lipid deposits show significant increase following Dx-induction. Significant differences are shown by asterisks ($^{*}p \leq 0.05$, $^{**}p \leq 0.01$). Data were calculated from six slides, representative slide is shown. For exact numerical values and standard error of mean please refer to **Supplementary Data Sheet**.

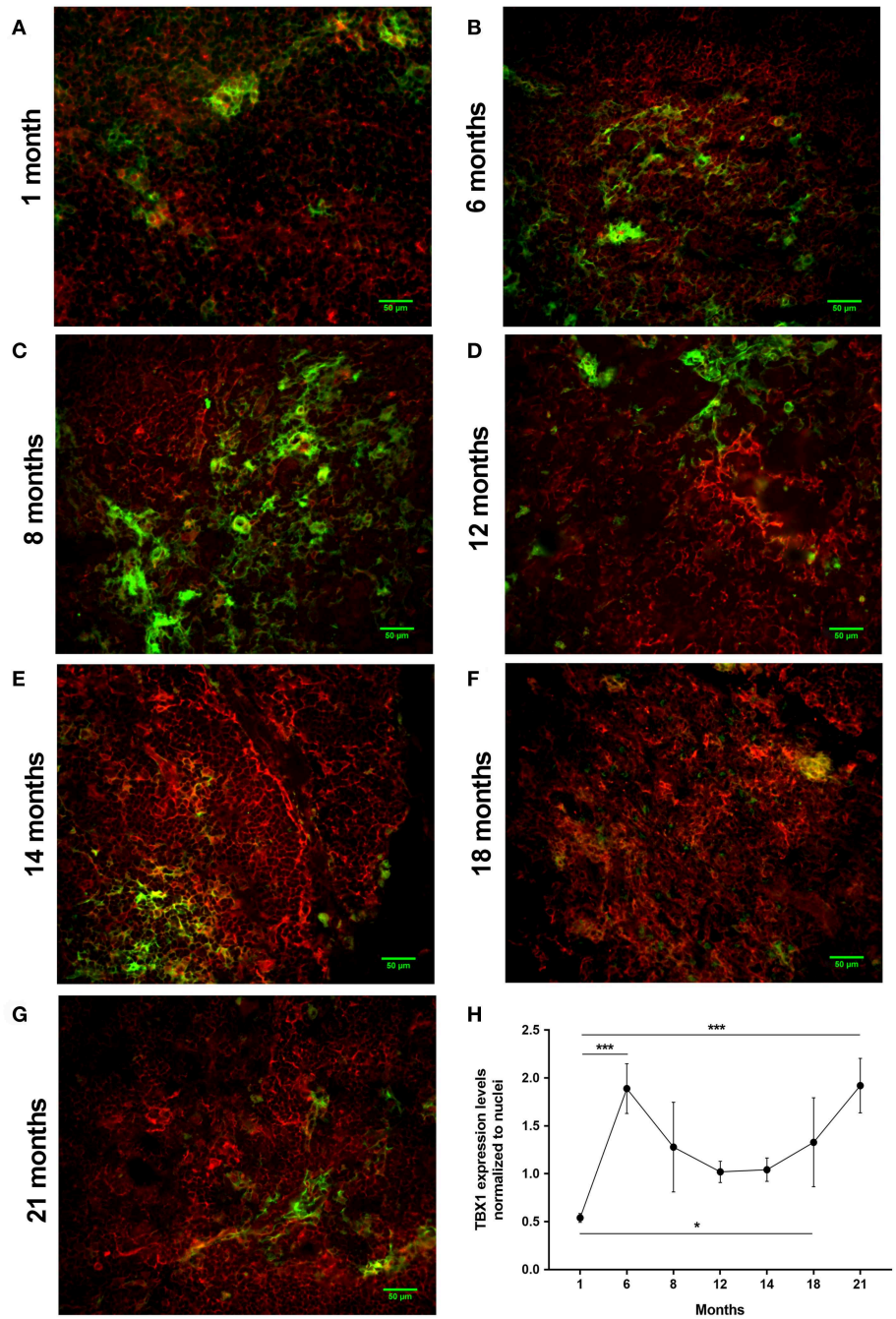

FIGURE 3 | Kinetics of TBX-1 expression in the adult mouse thymus with age. Murine thymic frozen sections from different ages (1, 6, 8, 12, 14, 18, and 21 months) were evaluated by immune-fluorescent staining **(A–G)**, respectively. Epithelial network is shown in green (EpCAM1-FITC) while TBX-1 expression is shown in red (TBX1-Alexa555) fluorescence. Please note signs of degeneration (auto-fluorescence) at elevated ages. Please also note that TBX-1 staining pattern localizes to both nuclear and cytoplasmic bodies in accordance with The Human Protein Atlas: http://www.proteinatlas.org/ENSG00000184058-TBX1/cell. TBX-1 staining was normalized to DAPI nuclear counter-stain (not shown) and is presented as relative value **(H)**. Please note that relative TBX-1 expression shows a transient decrease at adult age (12 months of age). Significant differences are shown by asterisks (*$p \leq 0.05$, ***$p \leq 0.001$). Data were calculated from three slides, representative slide is shown. For exact numerical values and standard error of mean please refer to **Supplementary Data Sheet**.

Taking the observed increase in basal OCR value, OCR/ECAR ratio, cAMP-response, and oligomycin-resistant respiration into consideration, these suggest that MDI-differentiated TECs possess a beige metabolic fingerprint in accordance with the up-regulation of beige-specific and beige-indicative markers shown above.

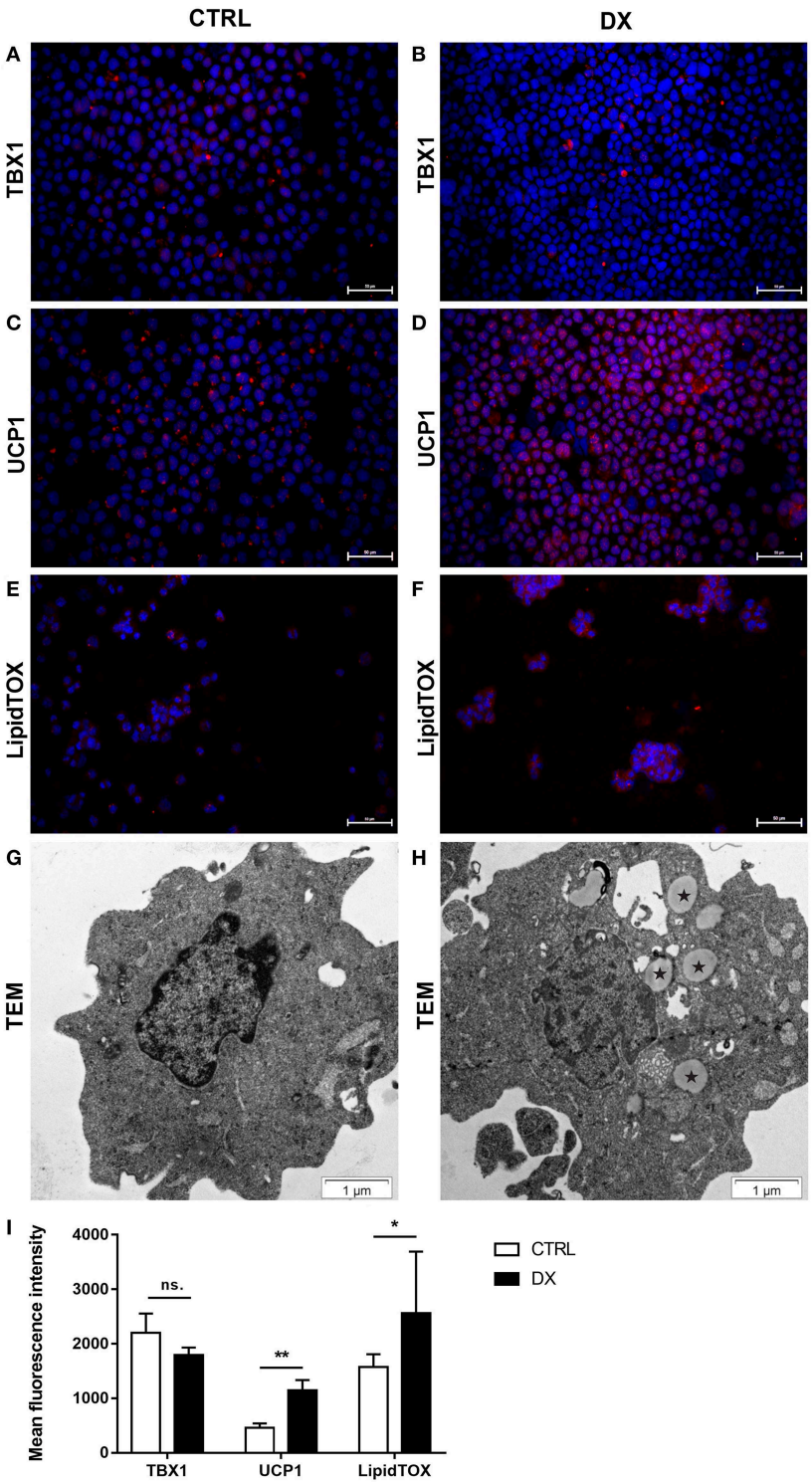

FIGURE 4 | Beige adipocyte marker expression and lipid accumulation in steroid-induced mouse TECs. Cytospin slides of control (Ctrl) and steroid-induced (Dx) TEP1 cells were stained by immune-fluorescence. Beige-specific marker TBX-1 **(A,B)** and beige-indicative marker UCP-1 **(C,D)** was evaluated in red (Alexa555). Neutral lipid deposits were stained with LipidTOX Red dye **(E,F)**. DAPI staining was also applied as nuclear counter-stain. TBX-1, UCP-1, and LipidTOX staining relative to DAPI staining is also shown by histograms **(I)**. TBX-1 shows unaltered expression, while UCP-1 and lipid accumulation show significant increase following Dx-induction. Significant differences are shown by asterisks (*$p \leq 0.05$, **$p \leq 0.01$). Data were calculated from six slides, representative slide is shown. For exact numerical values and standard error of mean please refer to **Supplementary Data Sheet**. Ultrastructure of control (Ctrl) and steroid-induced (Dx) TEP1 cells was also evaluated by transmission electron microscopy (TEM) **(G,H)**, respectively. Asterisks (*) show intracellular multi-locular lipid deposits following Dx-induction.

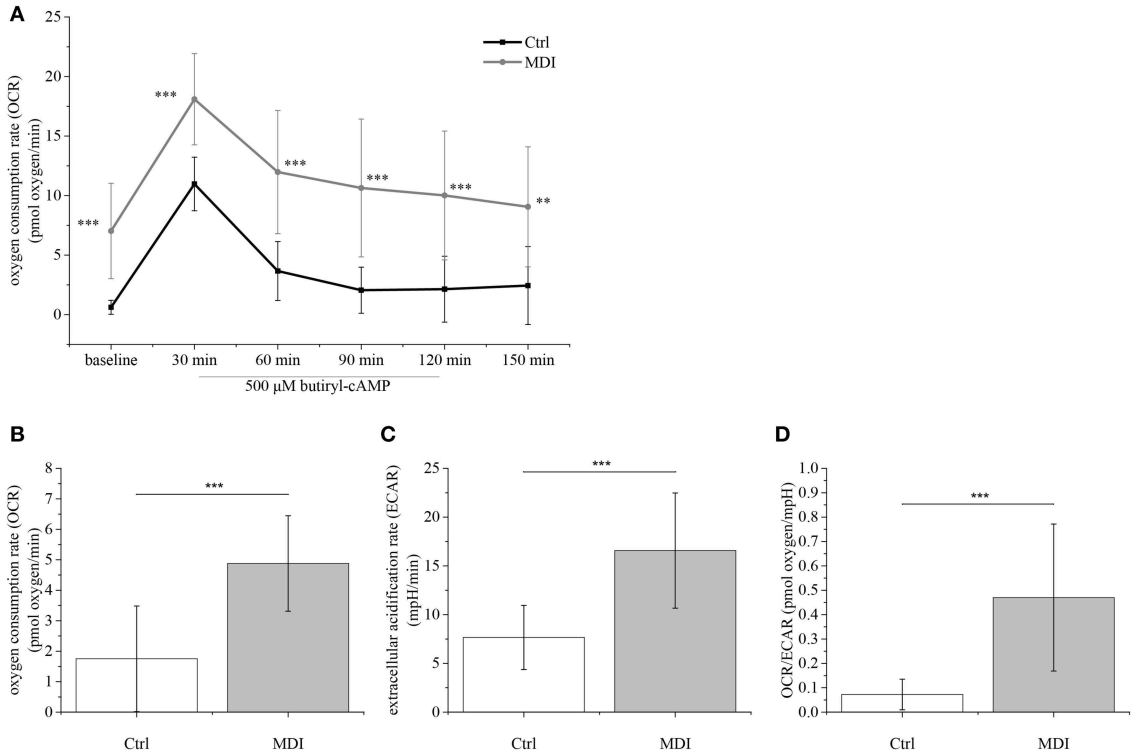

FIGURE 5 | Metabolic parameters of steroid-induced TECs. Following pilot experiments, 15,000 cells / well were cultured for 9 days in MDI (or control) medium prior to Seahorse measurements. Baseline OCR was recorded followed by induction with cAMP (readings every 30 min) **(A)**. Cells were treated with oligomycin to show oligomycin-resistant respiration indicating mitochondrial inner membrane leakage **(B)**. ECAR was also determined **(C)** and the OCR/ECAR ratio was calculated **(D)**. Significant differences are shown by asterisks (**$p \leq 0.01$, ***$p \leq 0.001$). Data were calculated from forty measurements, mean is shown. For exact numerical values and standard error of mean please refer to **Supplementary Data Sheet**.

Aged and Steroid-Induced TECs Show Beige Adipocyte Gene Expression Profile

Adult human and mouse thymus sections showed similar histological changes with age. Likewise, mouse and human steroid-induced TECs were also similar by immune-fluorescent staining. Next, TECs enriched from adult mice or Dx-treated (murine or human) TECs were subjected to gene expression analysis.

Changes in gene expression were further tested at the mRNA level in EpCAM1-enriched primary murine thymic epithelial cells from senior adult age (12 m) and steroid-induced TEP1 or 1889c cells for beige-specific (TBX1) and beige-indicative genes (UCP1, CD137, EAR2) (21–26). Enriched cells showed the up-regulation of both beige-specific and beige-indicative genes with age (1 vs. 12 months) as TBX1, UCP1, and EAR2 all showed significant elevation ($p < 0.05$ for all, **Figure 6A**), while CD137 activity remained unchanged. Gene expression analysis of mouse TEC line following Dx-treatment showed a similar tendency. as significant increase of TBX1 and UCP1 expression was detected ($p < 0.01$ and $p < 0.05$, respectively, **Figure 6B**), while CD137 and EAR2 were not altered. Likewise, the steroid-induced human TEC line showed significantly increased PPAR-gamma expression ($p < 0.01$) as reported previously for mouse TECs (4) and also significant increase of UCP-1 expression ($p < 0.05$) (**Figure 6C**), while CD137 and EAR2 remained identical. Please note the harmony of *in vivo* and *in vitro* data in both mouse and human species supporting our observations.

Steroid-Induced TECs Show Beige Adipocyte miRNA Profile

There is a significant difference between white, brown and beige adipose tissue miRNA profile. Seeking further evidence we have characterized the miRNA profile of Dx-induced human TECs (1889c).

We have elaborated two distinct platforms (**Figure 7**) for complete human miRNome analysis. For both platforms increased copy numbers are shown in red, while decreased copy numbers are shown in green (heat map). QuantStudio miRNA (QS) panels (A and B, **Figures 7A,B**) evaluate 768 miRNA entities, while the NanoString (NS) cartridge measures copy numbers of 880 miRNA entries (**Figure 7C**). Of note QS is amplification- (PCR) based while NS is amplification free. QS provides enhanced sensitivity, NS ensures unmatched signal-to-noise ratio. Accordingly, QS identified more miRNA species with occasional out-of-scale activities (shown in white) while NS recognized less species with a compressed scale of activities relative to QS. An overlap of the recognized miRNA species identified by at least one platform or evaluated by both

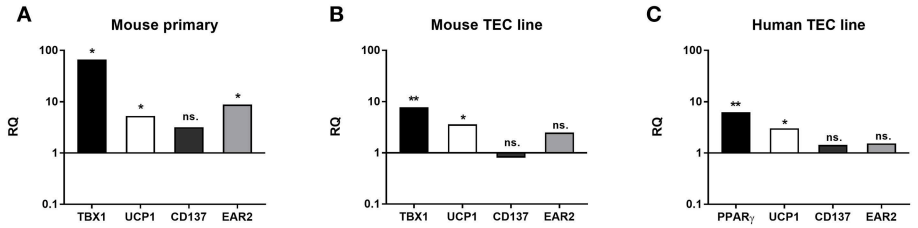

FIGURE 6 | Beige adipocyte marker expression in aged or steroid-induced, mouse, and human TECs. Marker expression was evaluated by qRT-PCR from sorted TECs of mice **(A)**. TBX-1, UCP-1 and EAR-2 showed significant increase with age (1 m vs 12 m). CD137 remained unchanged. Marker expression was evaluated by qRT-PCR in Dx-induced mouse TEP1 cells **(B)** and human 1889c cells **(C)**, respectively. In mouse TEP1 cells TBX-1 and UCP-1 showed significant increase with Dx-induction. CD137 and EAR-2 did not present significant difference. In human 1889c cells PPAR-gamma and UCP-1 showed significant increase with Dx-induction. CD137 and EAR-2 did not present significant difference. Relative quantity values (RQ) are shown where Y = 1 represents young adult **(A)** or control expression levels **(B,C)**, respectively. Significant differences are shown by asterisks (*$p \leq 0.05$, **$p \leq 0.01$). Please not that Y-axis is logarithmic. For exact numerical values and standard error of mean please refer to **Supplementary Data Sheet** containing both RQ and Ct/SD values for all experiments and target genes.

platforms similarly is summarized by **Table 2**. The table connects the identified miRNA species with context-relevant function based on literature search. Of note, several of the recognized species have relevance to thymus senescence with special focus on adipose tissue development, epithelial-to-mesenchymal transition, cell proliferation and senescence.

DISCUSSION

Thymic Tissue Samples and Steroid-Induced TECs Show Beige Adipocyte Markers

TBX-1 has been extensively studied for its role in the thymic context during embryonic organogenesis, but not in the adult thymus undergoing adipose involution (11–15). Using human and mouse thymus sections we show that TBX-1 expression persists throughout adulthood with a transient decrease in expression (23 years of age in human and 12 months of age in mouse) based on our pilot studies. This persistence of thymic TBX-1 expression raises the possibility of an alternative role in adulthood. This hypothesis is supported by reports showing that (1) once the thymus has been formed TBX-1 suppresses FoxN1 (key transcription factor of thymic epithelial identity) and (2) TBX-1 has a key and specific role in beige adipose tissue development (17–21). This plausible connection is supported by our results as further beige-indicative markers (UCP-1, EAR2) show increasing mRNA levels with age. This is in harmony with the fact that the thymus resides in the mediastinum and secretes FGF21, both reported to promote the emergence of beige adipose tissue (25). The *in vitro* model system of aging (Dx-treated mouse TEP1 or human 1889c cells) show similar molecular and cellular changes. Immune-fluorescent histology shows the presence of TBX-1 both in control conditions and following Dx-treatment. UCP-1 protein expression, on the other hand, significantly increases following Dx-treatment. Protein level data are in accordance with mRNA results as both TBX-1 and UCP-1 showed an increase following Dx-treatment (both in mouse and human). The above molecular changes are accompanied by evident phenotypical changes: the appearance of typical intracellular multi-locular neutral lipid deposits (characteristic to brown/beige adipose tissue) as shown by LipidTox staining and transmission electron microscopy. Taken together, these data suggest that thymic adipose tissue emerging with senescence and modeled by steroid-induced TECs show beige adipocyte features.

Steroid-Induced TECs Show Beige Adipocyte Metabolic Profile

There is profound difference between white and brown/beige adipose tissues with respect to metabolic traits (23). Basal respiration (OCR) is significantly lower in white fat cells than in brown/beige fat cells. Also, UCP-mediated uncoupled respiration rate (resistant to inhibition by oligomycin) is characteristic to brown/beige fat cells and not observed in white fat cells (32). Furthermore, in brown/beige fat cells cAMP-induced mitochondrial oxidation is elevated compared to white fat cells (33). Having analyzed these metabolic parameters, our data suggest that adipocyte differentiation in our model system shows beige bias as indicated by elevated basal OCR, increased OCR/ECAR ratio, enhanced cAMP-response and oligomycin-resistant respiration. Our metabolic readouts are in accordance with the recorded beige adipose tissue markers, morphological characteristics and gene expression profiles.

Steroid-Induced TECs Show Beige Adipocyte miRNA Profile

Unbiased dual platform complete miRNome analysis identified a number of context-relevant miRNA copy number alterations. Of note, miR-27a and miR-106b are beige adipose tissue regulators and miR-155 is an inhibitor of brown/beige adipose tissue formation (36, 46, 53). From a broad pan-adipocyte perspective, miR-128a-3p, miR-1825, miR-301a-5p, miR-30d, miR-425-5p, miR-550a, and miR92b-3p also influence adipose tissue formation and show changes in the current experimental setting (40, 43, 48, 49, 54, 55, 62, 66, 67). Furthermore, a cornerstone of thymus adipose involution: epithelial-to-mesenchymal transition (EMT), operates via miR-105-5p, miR-200a-3p, miR-597-5p, miR-888, and miR-99b, all demonstrating

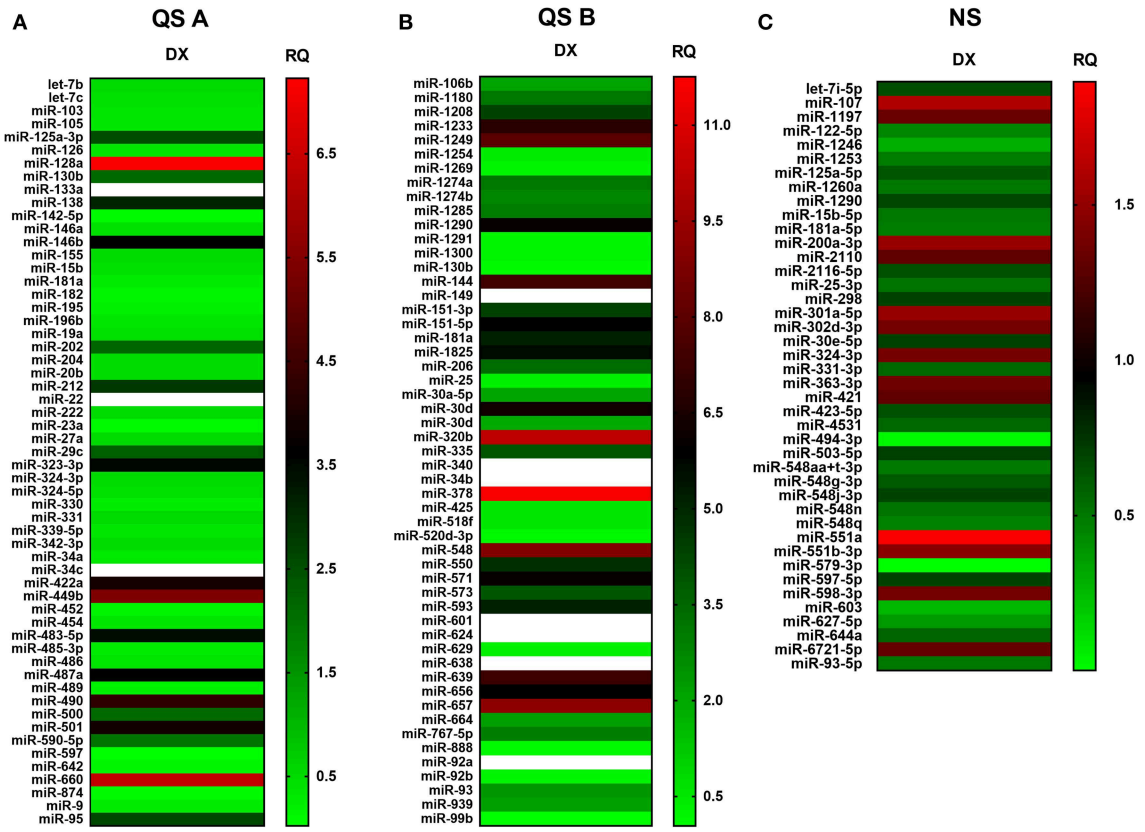

FIGURE 7 | miRNA profile of steroid-induced TECs. miRNA profile of Dx-treated human 1889c cells measured by Quantstudio 12K Flex Pool A **(A)**, Pool B **(B)** and NanoString nCounter SPRINT Profiler **(C)**. Heat-map representation shows miRNA species with most significant changes in copy number. Relative quantity values are presented (ctrl = 1). Up-regulation of miRNA species is shown in red while down-regulation is shown in green. Out-of-scale RQ values are shown in white. Pilot study is shown, for exact numerical values please refer to **Supplementary Data Sheet**.

changes in copy number in steroid-induced TECs (35, 36, 50, 63, 65, 69, 70). Taking a final expansion of interest, from a senescent perspective miR-125a-3p, miR-125a-5p, miR-15b-5p, miR-181a-5p, miR-323-3p, and miR-331-3p affect cellular / tissue level senescence with focus on the thymus and also show significant changes (36, 39, 40, 45, 47, 56–58). In summary, steroid-treatment in TECs affects the same miRNA species that were reported in connection with senescence-related thymus adipose involution that apparently yields beige adipose tissue.

Expanding Overlap Between Metabolism and Immunity

Overlap of metabolism and immunity has already been raised decades ago, and this inter-disciplinary field has recently become a prominent research area. For example, both previous and recent papers discussed overlap between the neuroendocrine and immune systems with regard to melatonin (71–73). Melatonin—mainly produced by the pineal gland, but also expressed by the thymus in small amounts—has been reported to have an immune-modulatory effect, enhancing immune functions with Th1 bias. Accordingly, anti-viral and anti-cancer defense is boosted by melatonin and age-related loss of melatonin production partly explains elevated incidence of infection and cancer observed with senescence. Protection from cancer metastasis development in the central nervous system (CNS) implies proper blood-brain barrier (BBB) function (74–76). BBB function, CNS function and immune status are all controlled by metabolic interplays involving small molecules such as lactate. Local tissue lactate concentration has been reported to have important role in immune regulation, its accumulation promoting autoimmune reactions (77, 78). Intercellular immune modulatory signals triggered by metabolically active small molecules are transmitted in cells through signaling pathways. An important pathway connecting metabolism and immunity utilizes mechanistic target of rapamycin (mTOR). It was shown that mTOR senses certain small nutrients (amino acids) and thus affects immune tolerance through regulatory T-cells (79, 80). Mammalian immunity heavily relies on both the innate and the adaptive branch. Within innate immunity macrophages have an important role in connecting metabolism and immunity. It has also been reported that carbohydrate metabolism significantly affects inflammation via macrophages (81).

Carbohydrates are also basic metabolic fuels. The mammalian immune system is a costly defense system with regard to T-cell

TABLE 2 | Overlap of QS- and NS-based miRNA results with functional and literature annotation.

Name	Up/down regulation	QS/ NS	Function	References
miR-103a-3p		QS A	Inactivation upregulates insulin receptors in adipocytes	(34)
miR-105-5p		QS A, NS	Epithelial to mesenchymal transition	(35)
miR-106b		QS B	Beige adipose tissue regulator	(36)
miR-1208		QS B	Targets TGFB2 (involved in adipose tissue development)	(37)
miR-1246		NS	Promotes cell proliferation	(38)
miR-125a-3p		QS A	Tissue-specific senescence	(39)
miR-125a-5p		QS A, NS	Regulation of epithelial cell differentiation	(40)
miR-126-3p		QS A	Insulin/IGF1 signaling pathway	(41)
miR-1274a		QS B	Potential biomarker for Alzheimer's Disease	(42)
miR-1274b		QS B	Potential biomarker for Alzheimer's Disease	(42)
miR-128a-3p		QS A	Regulatory effect on PPARg	(43)
miR-138-5p		QS A	Negative regulation of apoptosis	(44)
miR-15b-5p		QS A, NS	Characteristic of senescent cell derived EVs	(36, 45)
miR-155		QS A	Induces brown adipocyte differentiation from white adipocytes	(46)
miR-181a-5p		QS A, NS	Stress-related thymic involution	(47)
miR-1825		QS B	Lipid signaling	(48, 49)
miR-200a-3p		NS	Regulates epithelial cell transformation (EMT and MET)	(50)
miR-2110		NS	Cellular development, cell-mediated immune response	(51)
miR-2116-5p		NS	Regulatory function in colorectal cancer	(52)
miR-25-3p		QS A, B, NS	Modulator of the Wnt pathway	(47)
miR-27a		QS A, B	Negative regulator in beige adipose tissue	(36, 53)
miR-301a-5p		NS	Role in adipogenesis	(54)
miR-30d		QS B	Upregulation in adipose tissue	(55)
miR-323-3p		QS A	Regulation of senescence through IGF signaling pathway	(56)
miR-331-3p		NS, QS A	Induces senescence and cell cycle arrest	(57, 58)
miR-421		NS	Upregulation modulates oxidant stress and lipid metabolism	(59)
miR-425-5p		QS A, B	Inhibits differentiation and proliferation of preadipocytes	(40)
miR-4531		NS	Involved in type 1 diabetes mellitus	(60)
miR-520d-3p		NS, QS B	Regulatory function in colorectal cancer	(52)
miR-548q		NS	Possible biomarker of nasopharyngeal carcinoma	(61)
miR-550a		QS B	Adipogenic differentiation	(62)
miR-597-5p		NS, QS A	Drives EMT	(63)
miR-657		QS B	Regulates IL-37/NF-κB signaling	(64)
miR-6721-5p		NS	Unknown	
miR-888		QS B, NS	Downregulates E-cadherin	(65)
miR-92a-3p		QS A, NS	Replicative and organismal human aging	(36)
miR-92b-3p		QS B, NS	Regulation of lipid deposition	(66, 67)
miR-939-5p		QS B, NS	Inhibits cell proliferation	(68)
miR-99b		QS A, B, NS	Regulates epithelial cell differentiation	(36, 69, 70)

development and selection taking place in the thymus, where approx. Ninety-five percent of developing thymocytes are deleted being useless or potentially autoimmune. However, the adaptive branch heavily relies on the constant supply of fresh naïve and scrupulously selected T-cells to prevent infection, cancer and autoimmunity from developing. Severe negative imbalance in energy expenditure (due to fasting or malnutrition) has long been known to hamper thymus function and immunity (82). In contrast, currently, global human population is more threatened by obesity than fasting/malnutrition along with its reported negative effects on thymus function (1, 83). Fashionable countermeasures of obesity include e.g., applying diet to induce ketosis. Ketosis has been reported to enhance FGF21 secretion, known to promote white adipose tissue browning especially in the mediastinal context, where the thymus also resides (25, 84). Further options of white adipose tissue browning include interventions e.g., irisin (exercise hormone) treatment (32). However, since irisin promotes beige adipose tissue development it may also impair thymus function via promoting adipose involution identical to thymus senescence.

Our study highlights another potential intersection of immunity and metabolism via the dual role of TBX-1 during thymus development and senescence. TBX-1 shows bimodal expression (high expression in early and late ages, with a transient decrease in-between) in both mouse and human. It is conceivable that TBX-1 plays a role in thymus organogenesis early on (early "immune" peak) and thymic adipose involution later on (late "metabolic" peak). This dualism may be unique to the thymus due to the observed "beige" adipose involution process.

With senescence the thymus suffers adipose involution. Impaired thymic niche leads to decreased naïve T-cell output. This in turn weakens T cell-mediated anti-viral and anti-cancer defense, and elevates the chances of autoimmune disorders due to dysfunctional T-cell selection. Therefore, thymic adipose tissue emerging with age impairs immune homeostasis and the maintenance of tolerance. Our results indicate that thymic adipose tissue shows "beige" characteristics by molecular, cellular and metabolic profiling. Our research contributes to the breadth of overlap between metabolism and immune homeostasis.

DATA AVAILABILITY

All datasets generated for this study are included in the manuscript and/or the **Supplementary Files**.

ETHICS STATEMENT

Mice were kept in the Laboratory Animal Core Facility of the University. Experimental procedures were carried out according to the 1988/XXVIII act of the Hungarian Parliament on Animal Protection (243/1988) which complies with recommendations of the Helsinki Declaration. All animal experiments were performed with the consent of the Ethics Committee on Animal Research of the University (ref. no.: #BA02/2000-46/2016). Formalin-fixed, paraffin-embedded (FFPE) human thymus samples from 18, 23, 42, 44, and 58 years of age were provided by the Department of Pathology, Faculty of Medicine, University of Pecs, Hungary. Experiments involving human samples were performed with the consent of the Regional and Local Ethics Committee of Clinical Centre of the University (ref. no.: 6069/2016) according to their guidelines. All subjects gave written informed consent in accordance with the Declaration of Helsinki.

AUTHOR CONTRIBUTIONS

KB performed most histological, molecular biology, and statistics work in the project and was involved in manuscript preparation. DE performed all human IHC work. AP and PB were responsible for preparative Seahorse measurements. KG performed statistical analysis. DB was involved in experiments performed on human 1889c cells. JP was involved in planning experiments and manuscript preparation as well as local supervision of respective department. KK was involved in histological, molecular biology, and statistics work, also in planning experiments and manuscript preparation, and supervised the project.

FUNDING

Scientific research support was provided by the Hungarian National Science Foundation (No. 78310) and PTE AOK KA-2016-16 to KK. The project was also supported by the University of Pecs in the frame of Pharmaceutical Talent Center program and the Viral Pathogenesis Talent Center program via KK. The Janos Bolyai Scholarship of the Hungarian Academy of Sciences and Bolyai+ 2018/2019 (UNKP-18-4 2018/2019 new national excellence program of the ministry of human capacities) also supported KK. JP was also supported by the European Union and the State of Hungary, co-financed by the European Social Fund in the framework of, TAMOP-4.2.2. A-11/1/KON-2012-0024 and TAMOP-4.2.4.A/2-11/1-2012-0001 National Excellence Program and PTE AOK-KA-2013/22. Further grant support was provided to PB by NKFIH K108308, C120732, TAMOP-4.2.2.A-11/1/KONV-2012-0025. The project was also supported by the UNKP-18-3 2018/2019 new national excellence program of the ministry of human capacities to KG. Research funding was also provided by University of Pecs Biomedical Engineering Project to JP and KK.

ACKNOWLEDGMENTS

The authors wish to thank Hajnalka Abraham MD, PhD (Central Electron Microscope Laboratory, University of Pecs, Hungary) for the technical aid in taking transmission electron microscope images. The thymic carcinoma cell line 1889c was kindly provided by Prof Ralf J. Riecker (Institute of Pathology, University Hospital, Heidelberg, Germany). The authors wish to thank Ricky Odedra (Humeltis Ltd) and prof. Mary Keen (University of Birmingham, UK) for improving the manuscript using their native speaker skills. The present scientific contribution is dedicated to the 650th anniversary of the foundation of the University of Pecs, Hungary.

SUPPLEMENTARY MATERIAL

The Supplementary Material for this article can be found online at: https://www.frontiersin.org/articles/10.3389/fendo.2019.00369/full#supplementary-material

REFERENCES

1. Yang H, Youm Y-H, Vandanmagsar B, Rood J, Kumar KG, Butler AA, et al. Obesity accelerates thymic aging. *Blood*. (2009) 114:3803–12. doi: 10.1182/blood-2009-03-213595
2. Dixit VD. Thymic fatness and approaches to enhance thymopoietic fitness in aging. *Curr Opin Immunol.* (2010) 22:521–8. doi: 10.1016/j.coi.2010.06.010
3. Yang H, Youm Y-H, Dixit VD. Inhibition of thymic adipogenesis by caloric restriction is coupled with reduction in age-related thymic involution. *J Immunol*. (2009) 183:3040–52. doi: 10.4049/jimmunol.0900562

4. Talaber G, Kvell K, Varecza Z, Boldizsar F, Parnell SM, Jenkinson EJ, et al. Wnt-4 protects thymic epithelial cells against dexamethasone-induced senescence. *Rejuvenation Res*. (2011) 14:241–8. doi: 10.1089/rej.2010.1110
5. Youm Y-H, Yang H, Amin R, Smith SR, Leff T, Dixit VD. Thiazolidinedione treatment and constitutive-PPARgamma activation induces ectopic adipogenesis and promotes age-related thymic involution. *Aging Cell*. (2010) 9:478–89. doi: 10.1111/j.1474-9726.2010.00574.x
6. Kvell K, Varecza Z, Bartis D, Hesse S, Parnell S, Anderson G, et al. Wnt4 and LAP2alpha as pacemakers of thymic epithelial senescence. *PLoS ONE*. (2010) 5:e10701. doi: 10.1371/journal.pone.0010701
7. Ernszt D, Banfai K, Kellermayer Z, Pap A, Lord JM, Pongracz JE, et al. PPARgamma deficiency counteracts thymic senescence. *Front Immunol*. (2017) 8:1515. doi: 10.3389/fimmu.2017.01515
8. Palmer DB. The effect of age on thymic function. *Front Immunol*. (2013) 4:316. doi: 10.3389/fimmu.2013.00316
9. Bertho JM, Demarquay C, Moulian N, Van Der Meeren A, Berrih-Aknin S, Gourmelon P. Phenotypic and immunohistological analyses of the human adult thymus: evidence for an active thymus during adult life. *Cell Immunol*. (1997) 179:30–40. doi: 10.1006/cimm.1997.1148
10. George AJ, Ritter MA. Thymic involution with ageing: obsolescence or good housekeeping? *Immunol Today*. (1996) 17:267–72. doi: 10.1016/0167-5699(96)80543-3
11. Steinmann GG. Changes in the human thymus during aging. *Curr Top Pathol*. (1986) 75:43–88. doi: 10.1007/978-3-642-82480-7_2
12. Gao S, Li X, Amendt BA. Understanding the role of Tbx1 as a candidate gene for 22q11.2 deletion syndrome. *Curr Allergy Asthma Rep*. (2013) 13:613–21. doi: 10.1007/s11882-013-0384-6
13. Farley AM, Morris LX, Vroegindeweij E, Depreter MLG, Vaidya H, Stenhouse FH, et al. Dynamics of thymus organogenesis and colonization in early human development. *Development*. (2013) 140:2015–26. doi: 10.1242/dev.087320
14. Jerome LA, Papaioannou VE. DiGeorge syndrome phenotype in mice mutant for the T-box gene, Tbx1. *Nat Genet*. (2001) 27:286–91. doi: 10.1038/85845
15. Sirianni MC, Businco L, Seminara R, Aiuti F. Severe combined immunodeficiencies, primary T-cell defects and DiGeorge syndrome in humans: characterization by monoclonal antibodies and natural killer cell activity. *Clin Immunol Immunopathol*. (1983) 28:361–70. doi: 10.1016/0090-1229(83)90103-4
16. Reeh KAG, Cardenas KT, Bain VE, Liu Z, Laurent M, Manley NR, et al. Ectopic TBX1 suppresses thymic epithelial cell differentiation and proliferation during thymus organogenesis. *Development*. (2014) 141:2950–8. doi: 10.1242/dev.111641
17. Wu J, Boström P, Sparks LM, Ye L, Choi JH, Giang A-H, et al. Beige adipocytes are a distinct type of thermogenic fat cell in mouse and human. *Cell*. (2012) 150:366–76. doi: 10.1016/j.cell.2012.05.016
18. Giralt M, Villarroya F. White, brown, beige/brite: different adipose cells for different functions? *Endocrinology*. (2013) 154:2992–3000. doi: 10.1210/en.2013-1403
19. Symonds ME. Brown adipose tissue growth and development. *Scientifica*. (2013) 2013:305763. doi: 10.1155/2013/305763
20. Cinti S. Adipocyte differentiation and transdifferentiation: plasticity of the adipose organ. *J Endocrinol Invest*. (2002) 25:823–35. doi: 10.1007/BF03344046
21. Berg JM, Tymoczko JL, Stryer L. *Biochemistry*. 5th ed, section 18.6. New York, NY: WH Freeman and Co (2002).
22. Peláez-García A, Barderas R, Batlle R, Viñas-Castells R, Bartolomé RA, Torres S, et al. A proteomic analysis reveals that Snail regulates the expression of the nuclear orphan receptor nuclear receptor subfamily 2 group F member 6 (Nr2f6) and interleukin 17 (IL-17) to inhibit adipocyte differentiation. *Mol Cell Proteomics*. (2015) 14:303–15. doi: 10.1074/mcp.M114.045328
23. Cereijo R, Giralt M, Villarroya F. Thermogenic brown and beige/brite adipogenesis in humans. *Ann Med*. (2015) 47:169–77. doi: 10.3109/07853890.2014.952328
24. Poher A-L, Altirriba J, Veyrat-Durebex C, Rohner-Jeanrenaud F. Brown adipose tissue activity as a target for the treatment of obesity/insulin resistance. *Front Physiol*. (2015) 6:4. doi: 10.3389/fphys.2015.00004
25. Gaborit B, Venteclef N, Ancel P, Pelloux V, Gariboldi V, Leprince P, et al. Human epicardial adipose tissue has a specific transcriptomic signature depending on its anatomical peri-atrial, peri-ventricular, or peri-coronary location. *Cardiovasc Res*. (2015) 108:62–73. doi: 10.1093/cvr/cvv208
26. Langhi LGP, Andrade LR, Shimabukuro MK, van Ewijk W, Taub DD, Borojevic R, et al. Lipid-laden multilocular cells in the aging thymus are phenotypically heterogeneous. *PLoS ONE*. (2015) 10:e0141516. doi: 10.1371/journal.pone.0141516
27. Beardsley TR, Pierschbacher M, Wetzel GD, Hays EF. Induction of T-cell maturation by a cloned line of thymic epithelium (TEPI). *Proc Natl Acad Sci USA*. (1983) 80:6005–9. doi: 10.1073/pnas.80.19.6005
28. Ehemann V, Kern MA, Breinig M, Schnabel PA, Gunawan B, Schulten H-J, et al. Establishment, characterization and drug sensitivity testing in primary cultures of human thymoma and thymic carcinoma. *Int J cancer*. (2008) 122:2719–25. doi: 10.1002/ijc.23335
29. Belharazem D, Grass A, Paul C, Vitacolonna M, Schalke B, Rieker RJ, et al. Increased cFLIP expression in thymic epithelial tumors blocks autophagy via NF-κB signalling. *Oncotarget*. (2017) 8:89580–94. doi: 10.18632/oncotarget.15929
30. Meggyes M, Lajko A, Palkovics T, Totsimon A, Illes Z, Szereday L, et al. Feto-maternal immune regulation by TIM-3/galectin-9 pathway and PD-1 molecule in mice at day 14.5 of pregnancy. *Placenta*. (2015) 36:1153–60. doi: 10.1016/j.placenta.2015.07.124
31. Gratzner HG, Ahmad PM, Stein J, Ahmad F. Flow cytometric analysis of DNA replication during the differentiation of 3T3-L1 preadipocytes. *Cytometry*. (1985) 6:563–9. doi: 10.1002/cyto.990060610
32. Kristóf E, Doan-Xuan Q-M, Bai P, Bacso Z, Fésüs L. Laser-scanning cytometry can quantify human adipocyte browning and proves effectiveness of irisin. *Sci Rep*. (2015) 5:12540. doi: 10.1038/srep12540
33. Abdul-Rahman O, Kristóf E, Doan-Xuan Q-M, Vida A, Nagy L, Horváth A, et al. AMP-Activated Kinase (AMPK) activation by AICAR in human white adipocytes derived from pericardial white adipose tissue stem cells induces a partial beige-like phenotype. *PLoS ONE*. (2016) 11:e0157644. doi: 10.1371/journal.pone.0157644
34. Trajkovski M, Hausser J, Soutschek J, Bhat B, Akin A, Zavolan M, et al. MicroRNAs 103 and 107 regulate insulin sensitivity. *Nature*. (2011) 474:649–53. doi: 10.1038/nature10112
35. Jin X, Yu Y, Zou Q, Wang M, Cui Y, Xie J, et al. MicroRNA-105 promotes epithelial-mesenchymal transition of nonsmall lung cancer cells through upregulating Mcl-1. *J Cell Biochem*. (2019) 120:5880–8. doi: 10.1002/jcb.27873
36. Goody D, Pfeifer A. MicroRNAs in brown and beige fat. *Biochim Biophys Acta Mol Cell Biol Lipids*. (2019) 1864:29–36. doi: 10.1016/j.bbalip.2018.05.003
37. Kolhe R, Mondal AK, Pundkar C, Periyasamy-Thandavan S, Mendhe B, Hunter M, et al. Modulation of miRNAs by vitamin C in human bone marrow stromal cells. *Nutrients*. (2018) 10:186. doi: 10.3390/nu10020186
38. Li XJ, Ren ZJ, Tang JH, Yu Q. Exosomal MicroRNA MiR-1246 promotes cell proliferation, invasion and drug resistance by targeting CCNG2 in breast cancer. *Cell Physiol Biochem*. (2017) 44:1741–8. doi: 10.1159/000485780
39. Holly AC, Grellscheid S, van de Walle P, Dolan D, Pilling LC, Daniels DJ, et al. Comparison of senescence-associated miRNAs in primary skin and lung fibroblasts. *Biogerontology*. (2015) 16:423–34. doi: 10.1007/s10522-015-9560-5
40. Du J, Xu Y, Zhang P, Zhao X, Gan M, Li Q, et al. MicroRNA-125a-5p affects adipocytes proliferation, differentiation and fatty acid composition of porcine intramuscular fat. *Int J Mol Sci*. (2018) 19:501. doi: 10.3390/ijms19020501
41. Tryggestad JB, Vishwanath A, Jiang S, Mallappa A, Teague AM, Takahashi Y, et al. Influence of gestational diabetes mellitus on human umbilical vein endothelial cell miRNA. *Clin Sci*. (2016) 130:1955–67. doi: 10.1042/CS20160305
42. Kumar S, Reddy PH. Are circulating microRNAs peripheral biomarkers for Alzheimer's disease? *Biochim Biophys Acta*. (2016) 1862:1617–27. doi: 10.1016/j.bbadis.2016.06.001
43. Wotschofsky Z, Gummlich L, Liep J, Stephan C, Kilic E, Jung K, et al. Integrated microRNA and mRNA signature associated with the transition from the locally confined to the metastasized clear cell renal cell carcinoma exemplified by miR-146-5p. *PLoS ONE*. (2016) 11:e0148746. doi: 10.1371/journal.pone.0148746
44. Dhahbi JM, Spindler SR, Atamna H, Yamakawa A, Guerrero N, Boffelli D, et al. Deep sequencing identifies circulating mouse miRNAs that are functionally implicated in manifestations of aging and responsive to calorie restriction. *Aging*. (2013) 5:130–41. doi: 10.18632/aging.100540

45. Terlecki-Zaniewicz L, Lämmermann I, Latreille J, Bobbili MR, Pils V, Schosserer M, et al. Small extracellular vesicles and their miRNA cargo are anti-apoptotic members of the senescence-associated secretory phenotype. *Aging*. (2018) 10:1103–32. doi: 10.18632/aging.101452
46. Chen Y, Siegel F, Kipschull S, Haas B, Fröhlich H, Meister G, et al. miR-155 regulates differentiation of brown and beige adipocytes via a bistable circuit. *Nat Commun*. (2013) 4:1769. doi: 10.1038/ncomms2742
47. Xu M, Zhang X, Hong R, Su D-M, Wang L. MicroRNAs regulate thymic epithelium in age-related thymic involution via down- or upregulation of transcription factors. *J Immunol Res*. (2017) 2017:2528957. doi: 10.1155/2017/2528957
48. Raghavachari N, Liu P, Barb JJ, Yang Y, Wang R, Nguyen QT, et al. Integrated analysis of miRNA and mRNA during differentiation of human CD34+ cells delineates the regulatory roles of microRNA in hematopoiesis. *Exp Hematol*. (2014) 42:14–27.e1–2. doi: 10.1016/j.exphem.2013.10.003
49. Stace CL, Ktistakis NT. Phosphatidic acid- and phosphatidylserine-binding proteins. *Biochim Biophys Acta*. (2006) 1761:913–26. doi: 10.1016/j.bbalip.2006.03.006
50. Becker LE, Takwi AAL, Lu Z, Li Y. The role of miR-200a in mammalian epithelial cell transformation. *Carcinogenesis*. (2015) 36:2–12. doi: 10.1093/carcin/bgu202
51. Chen Y-J, Chang W-A, Huang M-S, Chen C-H, Wang K-Y, Hsu Y-L, et al. Identification of novel genes in aging osteoblasts using next-generation sequencing and bioinformatics. *Oncotarget*. (2017) 8:113598–613. doi: 10.18632/oncotarget.22748
52. http://exocarta.org
53. Kim SY, Kim AY, Lee HW, Son YH, Lee GY, Lee J-W, et al. miR-27a is a negative regulator of adipocyte differentiation via suppressing PPARγ expression. *Biochem Biophys Res Commun*. (2010) 392:323–8. doi: 10.1016/j.bbrc.2010.01.012
54. Nowak WN, Taha H, Kachamakova-Trojanowska N, Stepniewski J, Markiewicz JA, Kusienicka A, et al. Murine bone marrow mesenchymal stromal cells respond efficiently to oxidative stress despite the low level of heme oxygenases 1 and 2. *Antioxid Redox Signal*. (2018) 29:111–27. doi: 10.1089/ars.2017.7097
55. Nunez Lopez YO, Garufi G, Pasarica M, Seyhan AA. Elevated and correlated expressions of miR-24, miR-30d, miR-146a, and SFRP-4 in human abdominal adipose tissue play a role in adiposity and insulin resistance. *Int J Endocrinol*. (2018) 2018:7351902. doi: 10.1155/2018/7351902
56. Nidadavolu LS, Niedernhofer LJ, Khan SA. Identification of microRNAs dysregulated in cellular senescence driven by endogenous genotoxic stress. *Aging*. (2013) 5:460–73. doi: 10.18632/aging.100571
57. Maes OC, Sarojini H, Wang E. Stepwise up-regulation of microRNA expression levels from replicating to reversible and irreversible growth arrest states in WI-38 human fibroblasts. *J Cell Physiol*. (2009) 221:109–19. doi: 10.1002/jcp.21834
58. Morita K, Fujii T, Itami H, Uchiyama T, Nakai T, Hatakeyama K, et al. NACC1, as a target of MicroRNA-331-3p, regulates cell proliferation in urothelial carcinoma cells. *Cancers*. (2018) 10:347. doi: 10.3390/cancers10100347
59. Cheng Y, Mai J, Hou T, Ping J. MicroRNA-421 induces hepatic mitochondrial dysfunction in non-alcoholic fatty liver disease mice by inhibiting sirtuin 3. *Biochem Biophys Res Commun*. (2016) 474:57–63. doi: 10.1016/j.bbrc.2016.04.065
60. de Almeida RC, Chagas VS, Castro MAA, Petzl-Erler ML. Integrative analysis identifies genetic variants associated with autoimmune diseases affecting putative MicroRNA binding sites. *Front Genet*. (2018) 9:139. doi: 10.3389/fgene.2018.00139
61. Zhuo X, Zhou W, Li D, Chang A, Wang Y, Wu Y, et al. Plasma microRNA expression signature involving miR-548q, miR-630 and miR-940 as biomarkers for nasopharyngeal carcinoma detection. *Cancer Biomark*. (2018) 23:579–87. doi: 10.3233/CBM-181852
62. Heilmeier U, Hackl M, Skalicky S, Weilner S, Schroeder F, Vierlinger K, et al. Serum miRNA signatures are indicative of skeletal fractures in postmenopausal women with and without type 2 diabetes and influence osteogenic and adipogenic differentiation of adipose tissue-derived mesenchymal stem cells *in vitro*. *J Bone Miner Res*. (2016) 31:2173–92. doi: 10.1002/jbmr.2897
63. Xie L, Jiang T, Cheng A, Zhang T, Huan P, Li P, et al. MiR-597 targeting 14-3-3σ enhances cellular invasion and EMT in Nasopharyngeal carcinoma cells. *Curr Mol Pharmacol*. (2018) 12:105–114. doi: 10.2174/1874467212666181218113930
64. Wang P, Wang H, Li C, Zhang X, Xiu X, Teng P, et al. Dysregulation of microRNA-657 influences inflammatory response via targeting interleukin-37 in gestational diabetes mellitus. *J Cell Physiol*. (2019) 234:7141–8. doi: 10.1002/jcp.27468
65. Huang S, Cai M, Zheng Y, Zhou L, Wang Q, Chen L. miR-888 in MCF-7 side population sphere cells directly targets E-cadherin. *J Genet Genomics*. (2014) 41:35–42. doi: 10.1016/j.jgg.2013.12.002
66. Maes OC, An J, Sarojini H, Wu H, Wang E. Changes in MicroRNA expression patterns in human fibroblasts after low-LET radiation. *J Cell Biochem*. (2008) 105:824–34. doi: 10.1002/jcb.21878
67. Wang Z, Li Q, Chamba Y, Zhang B, Shang P, Zhang H, et al. Identification of genes related to growth and lipid deposition from transcriptome profiles of pig muscle tissue. *PLoS ONE*. (2015) 10:e0141138. doi: 10.1371/journal.pone.0141138
68. Chen G, Du C, Shen Z, Peng L, Xie H, Zang R, et al. MicroRNA-939 inhibits cell proliferation via targeting LRSAM1 in Hirschsprung's disease. *Aging*. (2017) 9:2471–9. doi: 10.18632/aging.101331
69. Dalmasso G, Thu Nguyen HT, Yan Y, Laroui H, Srinivasan S, Sitaraman SV, et al. MicroRNAs determine human intestinal epithelial cell fate. *Differentiation*. (2010) 80:147–54. doi: 10.1016/j.diff.2010.06.005
70. Li Y-J, Wang Y, Wang Y-Y. MicroRNA-99b suppresses human cervical cancer cell activity by inhibiting the PI3K/AKT/mTOR signaling pathway. *J Cell Physiol*. (2019) 234:9577–91. doi: 10.1002/jcp.27645
71. Mocchegiani E, Malavolta M, Costarelli L, Giacconi R, Piacenza F, Lattanzio F, et al. Is there a possible single mediator in modulating neuroendocrine-thymus interaction in ageing? *Curr Aging Sci*. (2013) 6:99–107. doi: 10.2174/1874609811306010013
72. Srinivasan V, Spence DW, Trakht I, Pandi-Perumal SR, Cardinali DP, Maestroni GJ. Immunomodulation by melatonin: its significance for seasonally occurring diseases. *Neuroimmunomodulation*. (2008) 15:93–101. doi: 10.1159/000148191
73. Espino J, Pariente JA, Rodríguez AB. Oxidative stress and immunosenescence: therapeutic effects of melatonin. *Oxid Med Cell Longev*. (2012) 2012:670294. doi: 10.1155/2012/670294
74. Mauro C, De Rosa V, Marelli-Berg F, Solito E. Metabolic syndrome and the immunological affair with the blood-brain barrier. *Front Immunol*. (2014) 5:677. doi: 10.3389/fimmu.2014.00677
75. Tang C-Y, Mauro C. Similarities in the metabolic reprogramming of immune system and endothelium. *Front Immunol*. (2017) 8:837. doi: 10.3389/fimmu.2017.00837
76. Wang T, Liu G, Wang R. The intercellular metabolic interplay between tumor and immune cells. *Front Immunol*. (2014) 5:358. doi: 10.3389/fimmu.2014.00358
77. Pucino V, Bombardieri M, Pitzalis C, Mauro C. Lactate at the crossroads of metabolism, inflammation, and autoimmunity. *Eur J Immunol*. (2017) 47:14–21. doi: 10.1002/eji.201646477
78. Haas R, Smith J, Rocher-Ros V, Nadkarni S, Montero-Melendez T, D'Acquisto F, et al. Lactate regulates metabolic and pro-inflammatory circuits in control of T cell migration and effector functions. *PLoS Biol*. (2015) 13:e1002202. doi: 10.1371/journal.pbio.1002202
79. Howie D, Waldmann H, Cobbold S. Nutrient sensing via mTOR in T cells maintains a tolerogenic microenvironment. *Front Immunol*. (2014) 5:409. doi: 10.3389/fimmu.2014.00409
80. Cobbold SP, Adams E, Farquhar CA, Nolan KF, Howie D, Lui KO, et al. Infectious tolerance via the consumption of essential amino acids and mTOR signaling. *Proc Natl Acad Sci USA*. (2009) 106:12055–60. doi: 10.1073/pnas.0903919106
81. Nagy C, Haschemi A. Time and demand are two critical dimensions of immunometabolism: the process of macrophage activation and the pentose phosphate pathway. *Front Immunol*. (2015) 6:164. doi: 10.3389/fimmu.2015.00164

82. Faulk WP, Paes RP, Marigo C. The immunological system in health and malnutrition. *Proc Nutr Soc*. (1976) 35:253–61. doi: 10.1079/PNS19760044
83. Castro É, Silva TEO, Festuccia WT. Critical review of beige adipocyte thermogenic activation and contribution to whole-body energy expenditure. *Horm Mol Biol Clin Investig*. (2017) 31. doi: 10.1515/hmbci-2017-0042
84. Ryan KK, Packard AEB, Larson KR, Stout J, Fourman SM, Thompson AMK, et al. Dietary manipulations that induce ketosis activate the HPA axis in male rats and mice: a potential role for fibroblast growth factor-21. *Endocrinology*. (2018) 159:400–13. doi: 10.1210/en.2017-00486

Conflict of Interest Statement: The authors declare that the research was conducted in the absence of any commercial or financial relationships that could be construed as a potential conflict of interest.

frontiers in Endocrinology

REVIEW
published: 11 July 2019
doi: 10.3389/fendo.2019.00466

Regulation of Adaptive Immune Cells by Sirtuins

Jonathan L. Warren[1] *and Nancie J. MacIver*[1,2,3]*

[1] Department of Pediatrics, Duke University School of Medicine, Durham, NC, United States, [2] Department of Immunology, Duke University School of Medicine, Durham, NC, United States, [3] Department of Pharmacology and Cancer Biology, Duke University School of Medicine, Durham, NC, United States

It is now well-established that the pathways that control lymphocyte metabolism and function are intimately linked, and changes in lymphocyte metabolism can influence and direct cellular function. Interestingly, a number of recent advances indicate that lymphocyte identity and metabolism is partially controlled via epigenetic regulation. Epigenetic mechanisms, such as changes in DNA methylation or histone acetylation, have been found to alter immune function and play a role in numerous chronic disease states. There are several enzymes that can mediate epigenetic changes; of particular interest are sirtuins, protein deacetylases that mediate adaptive responses to a variety of stresses (including calorie restriction and metabolic stress) and are now understood to play a significant role in immunity. This review will focus on recent advances in the understanding of how sirtuins affect the adaptive immune system. These pathways are of significant interest as therapeutic targets for the treatment of autoimmunity, cancer, and transplant tolerance.

Keywords: adaptive immunity, T cells, epigenetics, sirtuins, metabolism

OPEN ACCESS

Edited by:
Jie Chen,
Xiamen University, China

Reviewed by:
Terrence Deak,
Binghamton University, United States
Xiaoqiang Tang,
Sichuan University, China

***Correspondence:**
Nancie J. MacIver
nancie.maciver@duke.edu

Specialty section:
This article was submitted to Experimental Endocrinology, a section of the journal Frontiers in Endocrinology

Received: *02 February 2019*
Accepted: *26 June 2019*
Published: *11 July 2019*

Citation:
Warren JL and MacIver NJ (2019) Regulation of Adaptive Immune Cells by Sirtuins. Front. Endocrinol. 10:466. doi: 10.3389/fendo.2019.00466

INTRODUCTION

The adaptive immune system is critical for responding to and eliminating foreign pathogens. T cells are important members of the adaptive immune system, and are generally responsible for recruiting additional inflammatory machinery to the site of infection or tumor. T cells develop within the thymus and, upon maturation, are classified broadly by their expression of either CD4 or CD8 receptor. Both $CD4^+$ and $CD8^+$ T cells exist as a number of subsets that perform unique functions within the immune milieu and exhibit unique surface receptors, produce lineage-specific cytokines, and express lineage-defining transcription factors. $CD4^+$ T effector cells (Teff) are a broad class of T cells that are further divided into unique subsets with distinct effector functions. T helper 1 (Th1) cells are necessary for combating intracellular bacteria and viruses and for producing cytokines (most notably IFNγ and IL-2, but also TNFα) to promote cellular immunity, macrophage activation, and phagocytosis (1). Th2 cells are important for responses to helminthic and other gastrointestinal parasitic infections, producing IL-4, IL-5, and IL-10, and stimulating B cell differentiation (2). Th9 cells are a relatively newly defined subset, and are known to primarily produce IL-9 and facilitate the immune response against intestinal worms (3). Th17 cells are broadly involved in inflammation as well as host response to infection, producing IL-17, IL-6, and TNFα to recruit additional immune cell types to the site (4). In contrast with the pro-inflammatory nature of Teff cells, regulatory T (Treg) cells are responsible for immunosuppression, preventing overactive inflammatory responses and autoimmunity (5). This subset secretes key anti-inflammatory cytokines, notably TGFβ and IL-10, and Treg differentiation is driven by the

transcription factor Foxp3. $CD8^+$ cytotoxic T cells are primarily responsible for killing infected or malignant cells through the release of cytotoxic cytokines (TNFα, IFNγ) and granules (perforin, granzymes), and by initiating apoptotic processes mediated by the caspase cascade (6). Lastly, B cells are lymphocytes derived from bone marrow and are also major players within the adaptive immune system, supporting humoral immunity upon activation by producing large quantities of antibodies (7).

The metabolic profile of each of these specialized T cell subsets is optimized to support their unique functions (8). For example, activated $CD4^+$ Teff cells, including Th1, Th2, Th17, and $CD8^+$ cytotoxic T cells upregulate glucose uptake and glycolysis to promote rapid growth, proliferation, and effector function. Teff cells also rely on increased glutamine uptake and metabolism to support cell growth and proliferation, although the requirement for glutamine metabolism varies among T cell subsets (9). In contrast, Treg cells rely primarily on lipid oxidation to support their suppressive activity. While considerably less is known about B cell metabolism relative to T cell metabolism, there are some similarities such that naïve B cells are relatively quiescent, but following stimulation, have increased metabolic demand, likely to support proliferation and antibody production (10). Additionally, B cell subsets tend to display unique metabolic phenotypes as a product of their environment and function (11). Thus, the pathways that control adaptive immune cell function and metabolism are intimately linked (12–14). A number of recent advances indicate that immune cell identity, function, and metabolism are controlled, at least in part, via epigenetic mechanisms.

EPIGENETICS

While DNA sequence is the same from cell to cell within an organism, the transcription (or lack thereof) of certain genes contributes greatly to the differentiation of the myriad of cell types that are present within an organism. This variation is controlled in large part by epigenetic mechanisms that result in dynamic but heritable changes in gene expression that do not involve changes in DNA sequence (15). There are several mechanisms by which this kind of transcriptome regulation may occur. One example of these mechanisms is DNA methylation, the addition of a methyl group to cysteine residues within DNA by various DNA methyltransferases typically in regions rich in cysteine-guanine dinucleotides. Generally, DNA methylation can act to either inhibit gene transcription (if methylation occurs within a promoter region) or promote transcription (if methylation occurs within the gene body) (16). Another mechanism of epigenetic regulation occurs via non-coding RNA. These single-stranded RNA fragments seek out complementary sites within the mRNA of target genes and degrade RNA, ultimately preventing translation (17). Lastly, the modification of histones is a highly prevalent mechanism of epigenetic control and contributes to genetic regulation by altering the physical structure of chromatin to improve or impair the accessibility of DNA to various transcription factors and transcription machinery. Histones form the backbone of the nucleosome, providing structure and stability. In contrast with the stability of DNA methylation, histone modifications can be more fluid over acute periods of time (18). Deacetylated histones form a densely packed chromatin structure, known as heterochromatin, physically preventing transcription. Histone acetylation maintains a more loose and fluid chromatin structure. Other common histone modifications can occur by methylation, phosphorylation, and deamination. Moreover, all of these mechanisms likely work synergistically to regulate the epigenome (19).

SIRTUINS

Among the four defined classes of histone deacetylases, sirtuins (class III) are a unique family of highly conserved, NAD^+-dependent protein deacetylases with important implications on the epigenome. In addition to their deacetylase activity, sirtuins display some additional enzymatic function on other substrates, including ADP-ribosyltransferase and desuccinylase activity (20, 21). Mammalian sirtuins are orthologs of the silent information regulatory 2 (Sir2) protein, which was first identified in yeast as a significant contributor to the life-span extending effects of calorie restriction (22). These effects were further observed in *C. elegans* and *Drosophila* (23), suggesting that this pathway is conserved across species. Given the NAD^+-dependent activity of sirtuins, they are activated in periods of catabolism and low nutrient availability, and were thus thought to be a novel target for mimicking the life-span extending effects of calorie restriction in humans.

Mammals ubiquitously express seven sirtuins (SIRT1-SIRT7) with different subcellular locations and functions. Sirtuins are currently gaining widespread attention in the context of a number of disease states associated with inflammation, including autoimmunity (24), cardiometabolic diseases (25), and cancers (26). Further, the mammalian sirtuins have been found to mediate cellular metabolism and adaptive responses to a variety of stresses, including calorie restriction and other metabolic stress (27). Given the relationship between nutrient availability and the function of the adaptive immune system (28), sirtuins are currently of great interest as mediators of tumor proliferation, autoimmunity, and the ability of an organism to respond to foreign pathogens.

The idea that sirtuins might be involved in immunity was posited over a decade ago (23), following the early finding that SIRT1 can regulate NF-κB (29), a transcription factor well-known to regulate inflammation and immune cell proliferation (30). Indeed, further study has begun to elucidate the link between this family of proteins and immune cell function. While each of the sirtuins has since been broadly studied, the most intense attention has been given to SIRT1 (primarily localized to the nucleus) and SIRT3 (primarily in mitochondria) with respect to adaptive immune cells, and will thus be the focus of this review (**Figure 1**). Further, considerations for the use of sirtuin-modifying drugs to manipulate immune activity are explored.

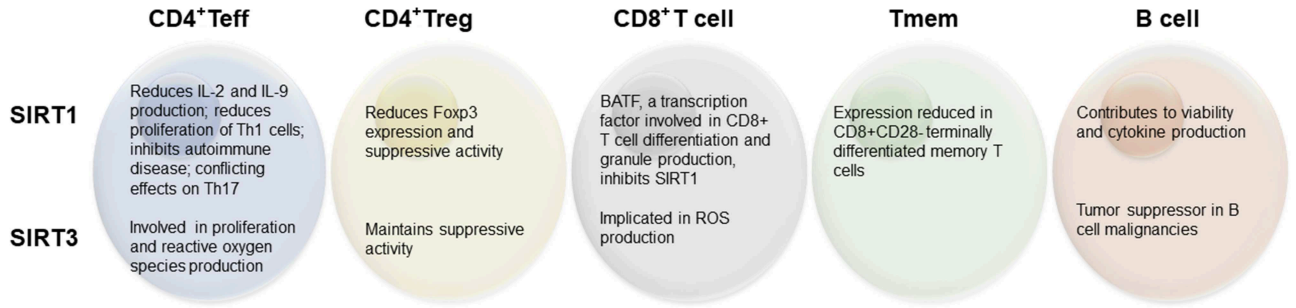

FIGURE 1 | Summary of reported effects of SIRT1 and SIRT3 on lymphocyte populations.

EFFECTOR CD4$^+$ T CELLS

Activation of T cells occurs seconds after stimulation of the T cell antigen receptor (TCR) by a ligand, along with co-stimulatory signals, which initiate a number of signaling pathways that promote differentiation and growth. This activation is supported by a transition from a relatively quiescent oxidative metabolism to an intense glycolytic metabolic signature to support proliferation and cytokine production (12). This metabolic switch is likely driven, at least in part, by sirtuin activity, however there presently appears to be a number of incongruous effects reported across the various CD4$^+$ T cell subsets.

SIRT1 appears to play a significant role in the regulation of Teff cell activation (31, 32). Early studies into the function of SIRT1 on Teff cells indicated that SIRT1 inhibits the immune response by acting as an antagonist against transcription factors that support IL-2 production (32) and thereby decreasing Th1 cell activation. This relationship may contribute in part to the link between fasting/calorie restriction and poor immune performance (28), given that SIRT1 is generally activated in response to fasting (33). The direct role of sirtuins within adaptive immune cells has also begun to be studied using knockout (KO) animal models. T cells from a SIRT1 KO mouse model are more proliferative, produce more IL-2 both *in vitro* and *in vivo*, and these mice are more susceptible to experimental autoimmune encephalomyelitis (EAE), indicating a more inflammatory immune phenotype (32). Studies in SIRT1 KO animals also found that T cells without SIRT1 can be activated solely via the T cell receptor (TCR), without co-stimulation by CD28, suggesting a hyper-sensitivity to activation signals when SIRT1 is not present (32). Follow-up studies indicated that IL-2 is involved in a feedback response to reduce further SIRT1 gene transcription and allow for proliferation in response to the activation cascade (34). Hyper-responsive Teff cells can contribute to an environment prone to autoimmune disease. In fact, earlier studies in SIRT1-null mice detailed the development of a mild autoimmune condition that resembled systemic lupus erythematosus, characterized by deposition of immune complexes within liver and kidneys, with some mice going on to spontaneously develop a diabetes insipidus-like autoimmune disorder after 2 years of age, altogether suggesting a preventative role of SIRT1 in autoimmunity (35).

SIRT1 also inhibits Bcl-2 Associated Transcription Factor 1 (Bclaf1) (36). Bclaf1 was originally identified as a promoter of apoptosis (37); however, subsequent studies revealed further reaching effects of Bclaf1 on T cell development, activation, and proliferation (38), perhaps by promoting hypoxia-inducible factor 1-α (HIF-1α) transcription (39). SIRT1-mediated inhibition of Bclaf1 is thought to occur by the binding of SIRT1 to the promoter region of Bclaf1 after stimulation of the TCR, suppressing acetylation of the histone 3 lysine 56 residue (H3K56) (36). When SIRT1 was knocked out of T cells, there was greater expression of the gene coding for Bclaf1, and specific knockdown of Bclaf was able to suppress the increase in IL-2 production and proliferation seen in SIRT1 KO mice (36).

SIRT1 inhibition can also depress the adaptive response and differentiation of Th2 cells. Pharmacological SIRT1 inhibition contributed to decreased allergic inflammation in BALB/c mice exposed to ovalbumin via aerosol (40). In addition, mice that exhibit KO of a transcriptional activator essential for Th2 differentiation (B-cell lymphoma/leukemia 11B; Bcl11b) have been found to be protected against EAE (41). Bcl11b is a transcriptional repressor and likely functions by recruiting SIRT1 for histone deacetylase activity (42). Although T helper 9 (Th9) cells exhibit a number of similarities to Th2 cells, SIRT1 inhibition has been found to promote Th9 cell differentiation and IL-9 production by these cells (43).

The implications of SIRT1 on Th17 cells have been more equivocal. Pharmacological induction of SIRT1 using resveratrol, low dose metformin, or the inhibitor SRT1720 has been shown to impair Th17 cell differentiation with decreased expression of IL-17 and RORγt, in a STAT3-dependent manner (44). The same study further describes anti-tumor effects of metformin by its action in reducing Th17 differentiation and STAT3 acetylation. In a separate study, *in vivo* activation of SIRT1 through treatment with NAD$^+$ contributed to a delayed onset of EAE. This protection was hypothesized to be conferred by enhanced SIRT1 expression within the spinal cord of mice exposed to the EAE stimulus, which may suppress inflammatory responses by Th1 and Th17 cells (45). However, others have shown that SIRT1 is necessary for the production of pro-inflammatory Th17 cells

through the deacetylation of transcription factor RORγt, which suggests that SIRT1 inhibitors could confer protection against autoimmunity (46). Clearly, more studies are needed to dissect out the role of SIRT1 in Th17 cell differentiation, proliferation, and cytokine response.

SIRT3 is a mitochondrial sirtuin that supports the structure, function, and biogenesis of the mitochondria (47). SIRT3 is elevated in fasting and calorie restriction in liver, muscle, and brown adipose tissue, and is known to modify cellular metabolism in those tissues (48, 49). In a model of experimental allogenic bone marrow transplantation, total T cells from donor animals that exhibit a whole-body SIRT3 KO were less likely to promote graft-vs.-host disease relative to T cells from control mice, but did not affect the graft-vs.-tumor effect, suggesting that targeted inhibition of SIRT3 in allogenic T cells can improve outcomes after transplant (50). Further, while SIRT3 KO did not affect the composition of peripheral naïve T cell subsets, it was determined that SIRT3 KO Teff cells were less proliferative and produced less reactive oxygen species (ROS) in response to non-specific TCR stimulation (50). However, a SIRT3 KO mouse model did not affect the development of immune cells or immune responses to various endotoxins (51), suggesting SIRT3 may play a limited role in Teff cell function.

Little is known about the role of the other sirtuins on Teff cell development and function. SIRT6 may be a negative regulator of glycolytic activity, notably through the inhibition of glucose transporter 1 (GLUT1) and the transcriptional regulator HIF-1α (52), suggesting a potential role for SIRT6 in downregulating Teff cell activation. HIF-1α is a transcriptional regulator of glycolysis and is known to regulate the production of a number of cytokines (53) and enhance Th17 cell differentiation (54). Relatively little work has been done on SIRT2 in adaptive immunity. However, SIRT2 has been identified as a potential suppressor of colitis through its deacetylase activity on NF-κB within bone marrow-derived macrophages in a mouse model (55). Further, this study observed a greater proportion of activated ($CD4^+CD69^+$) T cell populations at the mesenteric lymph nodes of SIRT2 KO mice in response to DSS-induced colitis, indicative of enhanced inflammatory action (55), and ascribing a role for SIRT2, similar to SIRT1, in limiting $CD4^+$ Teff cell inflammation.

REGULATORY $CD4^+$ T CELLS

SIRT1 has been found to reduce the activity of Foxp3, contributing to an overall more inflammatory immune phenotype (46). Further, inhibiting SIRT1 can promote greater Treg suppressive activity (56, 57). While the regulation of Treg metabolism by sirtuins has not been widely studied, Treg function has been shown to be regulated in part by sirtuin activity. In addition, Foxp3 itself has been found to be a regulator of epigenetic activity to support the Treg phenotype, and is regulated in part by the deacetylase activity of SIRT1 (56). A previous review has outlined the role of demethylation and histone modifications that occur in order to promote and stabilize the expression of Foxp3 during Treg cell development (58). Briefly, three conserved non-coding sequences are primary targets for epigenetic mechanisms that regulate Foxp3 expression in response to external environmental stimulus.

Given the localization of SIRT3 to the mitochondria and its role in oxidative metabolism and mitochondrial function, it is not surprising that the loss of SIRT3 in Treg cells has been shown to impair their suppressive activity (59). Indeed, deletion of histone deacetylase 9 was found to be sufficient to increase Treg suppressive activity, by increasing the expression of SIRT3. Further, Treg cells from SIRT3 KO mice had impaired suppressive function both in an *in vitro* suppression assay and an *in vivo* cardiac allograft model, likely due to the role of SIRT3 in promoting oxidative metabolism (59).

$CD8^+$ T CELLS

Activation and differentiation of $CD8^+$ T cells leads to markedly variable chromatin accessibility (60), which is likely critical to facilitate the transition between naïve, effector, and memory $CD8^+$ T cells. SIRT1 appears to play a crucial role in $CD8^+$ T cell differentiation. Basic leucine zipper ATF-like transcription factor (BATF) has been shown to inhibit the expression of SIRT1, contributing to increased histone acetylation, particularly at the T-bet locus (61). This has been shown to affect $CD8^+$ T cell differentiation and activity, as $CD8^+$ T cells from BATF KO animals exhibited lower ATP production and lower mRNA expression of perforin and IFNγ (61). SIRT3 is also involved in $CD8^+$ T cell function. Toubai et al. found that SIRT3-null activated $CD8^+$ T cells produced less ROS upon activation (50). This impairment in ROS production may lead to impairments in sulfenylation, a process known to play a role in the regulation of histone deacetylases (62). Further SIRT3-null donor cells were able to attenuate graft-vs.-host disease within the gastrointestinal tract and the authors hypothesize this may be due, in part, to decreased $CD8^+$ T cell trafficking to site (50).

MEMORY T CELLS

Following the primary immune response, a portion of T cells ($CD4^+$ and $CD8^+$) can become memory cells that remain ready to respond rapidly in the event that they re-encounter their antigen. These cells are relatively long-lived and therefore exhibit a relatively quiescent oxidative metabolism similar to that of a naïve immune cell until they are re-activated. Little is known about the role of sirtuins in mediating the generation or longevity of memory T cells; however, given the role of sirtuins in promoting oxidative metabolism, this is a potentially interesting area for further study. Though not specific to memory T cells, SIRT1 has distinct effects on PGC-1α and PGC-1β, both proteins with roles in facilitating mitochondrial biogenesis and oxidative metabolism. Thus, the return to a more oxidative metabolism in memory cells may be mediated in part by SIRT1, given the role of SIRT1-mediated deacetylation on transcription of PGC-1α and PGC-1β (63, 64). In support of this hypothesis, SIRT1 expression has been shown to be decreased in terminally differentiated $CD8^+CD28^-$ memory T cells, driving the downregulation of forkhead box protein O1 (FoxO1), a transcription factor that mediates T cell homing and differentiation (65). Further,

these authors demonstrate that these SIRT1-low $CD8^+CD28^-$ memory cells have an enhanced glycolytic capacity in the resting state, which can support effector function upon reactivation.

B CELLS

Naïve B cells exhibit a relatively inert epigenetic status with high levels of DNA methylation and histone deacetylation. However, upon activation and maturation toward a germinal center B cell phenotype, B cells exhibit dramatic shifts in methylation status and become hypomethylated with increased histone acetylation and expression of various miRNAs (66, 67). Thus far, the limited literature on sirtuin activity in B cells indicates sirtuins support B cell viability, proliferation, and function. SIRT1 overexpression by viral transfection in BaF3 B cells (a murine B cell line) has been shown to support enhanced viability (mediated in part by a decrease in p53) and increased cytokine production (68). A short, non-coding microRNA, miR-132, is increased in B cells of patients with multiple sclerosis (MS) concurrent with a reduced expression of SIRT1 (69). SIRT3 also has been found to be a tumor suppressor in the context of B cell malignancies, as a number of malignant B cell lines display decreased SIRT3 protein expression and higher ROS levels, and overexpression of SIRT3 in these lines decreased proliferative activity (70). SIRT4 has also been shown to act as a tumor suppressor by inhibiting glutamine metabolism, which is necessary to conserve resources for repairing DNA damage (71). Further, SIRT4 overexpression can inhibit proliferation of Burkitt lymphoma cells, a model of B cell lymphoma (72). Inhibition of SIRT1 and SIRT2 increased apoptotic activity and ROS production in cells from patients with B cell chronic lymphotic leukemia (73). While not specific to sirtuins, histone deacetylase inhibitors have been shown to be effective in preventing B cell malignancies (74).

MODULATING SIRTUIN ACTIVITY TO ALTER IMMUNE OUTCOMES *IN VIVO*

A number of novel drugs with sirtuin modulatory activity have been studied in the context of immune function. However, it will be critical to determine whether to induce or inhibit sirtuin activity and, further, how to target specific sirtuins (perhaps even within a particular lymphocyte subset), in order to reach desired immune outcomes. For instance, promoting SIRT3 activity in Treg cells to improve suppressive capabilities and temper inflammation could be a novel means to treat autoimmunity. On the other hand, SIRT1 generally inhibits Teff inflammation, suggesting that activators of SIRT1 could be useful for the treatment of autoimmune disease; however, the effects of SIRT1 on T cells vary by subset and are context-dependent. As sirtuins are proteins with functions in a wide array of cell types, targeting specific sirtuins in specific tissues (and immune cell subsets) will remain an immense challenge.

Despite the challenges with tissue-specificity, drugs to modify sirtuin activity have been studied in cell culture and animal models. Inhibition of SIRT1 *in vivo* (using a SIRT1-specific inhibitor, EX-527) increased complications of sepsis at 12 h despite conferring dramatic protection at 24 h (75). EX-527 and sirtinol (another commonly studied sirtuin inhibitor with specificity against SIRT1 and SIRT2) also have been found to reduce platelet count (76). Metformin, classically prescribed as a medication for the management of type 2 diabetes, has been well-documented to have anticancer effects (77); however, the precise mechanism of action is largely unknown, though there is speculation that these effects may be due to the stimulatory effect of metformin on sirtuins. SIRT1 activation by metformin has been shown to decrease Th17 cell populations promoting a less inflammatory environment (44). SIRT1 knockdown has also been shown to promote apoptotic processes in leukemia cells (78), suggesting the exact mechanisms for sirtuin modulation in cancers is still being determined.

Resveratrol, a polyphenol compound with anti-inflammatory properties, is a compound with sirtuin modifying effects that is currently of intense interest within both the scientific and lay communities. Resveratrol increases SIRT1 activity and impedes acetylation of c-Jun, thereby limiting T cell activation (79). Further, resveratrol has been shown to improve outcomes in two well-characterized murine models of autoimmunity: EAE (80) and colitis (81). Additionally, resveratrol confers protection against a murine model of rheumatoid arthritis, by inhibiting Th17 expansion and IL-17 production, as well as autoantibody production from B cells (82). Resveratrol has also been shown to increase the ratio of $CD4^+$ to $CD8^+$ T cells and increase total Treg cells in the context of diet-induced obesity in mice while also conferring benefits on glucose homeostasis by activating phosphoinositide 3-kinase (PI3K) signaling pathways (83). Dosages necessary to produce these effects in humans are likely impossible to obtain exclusively through diet, but could realistically be obtained through supplementation.

The role of sirtuins in promoting organ transplant tolerance is also an area of intense investigation. While advances have been made in long-term survival following transplantation, current immunosuppressive therapies are known to promote infections and cancer. There is speculation that SIRT1 inhibitors may enhance the function of Treg cells to support immune suppression and allograft tolerance (84). Additionally, SIRT1 inhibitors may also confer prolonged allograft survival through the suppression of Th17 activity, as evidenced by decreased IL-17A (85); however, these results are in direct opposition to the SIRT1-activating and anti-tumor properties of metformin described above (44), and further studies are needed.

CONCLUDING REMARKS

The wide-ranging effects of sirtuins and the availability of a number of sirtuin-modifying compounds provide a significant opportunity for future study to improve immune cell phenotypes. However, there are significant challenges ahead in developing drugs with targeted tissue-specific effects given the ubiquity of these mechanisms within the body. The development of tissue-specific and sirtuin-specific therapies remains an intriguing possibility to treat the myriad of autoimmune diseases, cancers, and other chronic diseases associated with inflammation that are now understood to be regulated by some degree of protein acetylation.

AUTHOR CONTRIBUTIONS

All authors listed have made a substantial, direct and intellectual contribution to the work, and approved it for publication.

FUNDING

This work was supported by the National Institutes of Health (R01-DK106090) and the Derfner Foundation.

REFERENCES

1. Romagnani S. T-cell subsets (Th1 versus Th2). *Ann Allergy Asthma Immunol.* (2000) 85:9–18. doi: 10.1016/S1081-1206(10)62426-X
2. Smith KM, Pottage L, Thomas ER, Leishman AJ, Doig TN, Xu D, et al. Th1 and Th2 CD4+ T cells provide help for B cell clonal expansion and antibody synthesis in a similar manner *in vivo*. *J Immunol.* (2000) 165:3136–44. doi: 10.4049/jimmunol.165.6.3136
3. Vyas SP, Goswami R. A Decade of Th9 Cells: Role of Th9 cells in inflammatory bowel disease. *Front Immunol.* (2018) 9:1139. doi: 10.3389/fimmu.2018.01139
4. Tesmer LA, Lundy SK, Sarkar S, Fox DA. Th17 cells in human disease. *Immunol Rev.* (2008) 223:87–113. doi: 10.1111/j.1600-065X.2008.00628.x
5. Schmidt A, Oberle N, Krammer PH. Molecular mechanisms of treg-mediated T cell suppression. *Front Immunol.* (2012) 3:51. doi: 10.3389/fimmu.2012.00051
6. Alam A, Cohen LY, Aouad S, Sékaly RP. Early activation of caspases during T lymphocyte stimulation results in selective substrate cleavage in nonapoptotic cells. *J Exp Med.* (1999) 190:1879–90. doi: 10.1084/jem.190.12.1879
7. Hoffman W, Lakkis FG, Chalasani G. B cells, antibodies, and more. *Clin J Am Soc Nephrol.* (2016) 11:137–54. doi: 10.2215/CJN.09430915
8. Michalek RD, Gerriets VA, Jacobs SR, Macintyre AN, MacIver NJ, Mason EF,et al. Cutting edge: distinct glycolytic and lipid oxidative metabolic programs are essential for effector and regulatory CD4+ T cell subsets. *J Immunol.* (2011) 186:3299–303. doi: 10.4049/jimmunol.1003613
9. Johnson MO, Wolf MM, Madden MZ, Andrejeva G, Sugiura A, Contreras DC, et al. Distinct regulation of Th17 and Th1 cell differentiation by glutaminase-dependent metabolism. *Cell.* (2018) 175:1780–95.e19. doi: 10.1016/j.cell.2018.10.001
10. Caro-Maldonado A, Wang R, Nichols AG, Kuraoka M, Milasta S, Sun LD, et al. Metabolic reprogramming is required for antibody production that is suppressed in anergic but exaggerated in chronically BAFF-exposed B cells. *J Immunol.* (2014) 192:3626–36. doi: 10.4049/jimmunol.1302062
11. Clarke AJ, Riffelmacher T, Braas D, Cornall RJ, Simon AK. B1a B cells require autophagy for metabolic homeostasis and self-renewal. *J Exp Med.* (2018) 215:399–413. doi: 10.1084/jem.20170771
12. MacIver NJ, Michalek RD, Rathmell JC. Metabolic regulation of T lymphocytes. *Annu Rev Immunol.* (2013) 31:259–83. doi: 10.1146/annurev-immunol-032712-095956
13. Buck MD, O'Sullivan D, Pearce EL. T cell metabolism drives immunity. *J Exp Med.* (2015) 212:1345–60. doi: 10.1084/jem.20151159
14. Buck MD, Sowell RT, Kaech SM, Pearce EL. Metabolic instruction of immunity. *Cell.* (2017) 169:570–86. doi: 10.1016/j.cell.2017.04.004
15. Xu W, Wang F, Yu Z, Xin F. Epigenetics and cellular metabolism. *Gene Epigene.* (2016) 8:43–51. doi: 10.4137/GEG.S32160
16. Maunakea AK, Chepelev I, Cui K, Zhao K. Intragenic DNA methylation modulates alternative splicing by recruiting MeCP2 to promote exon recognition. *Cell Res.* (2013) 23:1256–69. doi: 10.1038/cr.2013.110
17. Frías-Lasserre D, Villagra CA. The importance of ncRNAs as epigenetic mechanisms in phenotypic variation and organic evolution. *Front Microbiol.* (2017) 8:2483. doi: 10.3389/fmicb.2017.02483
18. Hansen JC, Nyborg JK, Luger K, Stargell LA. Histone chaperones, histone acetylation, and the fluidity of the chromogenome. *J Cell Physiol.* (2010) 224:289–99. doi: 10.1002/jcp.22150
19. Rose NR, Klose RJ. Understanding the relationship between DNA methylation and histone lysine methylation. *Biochim Biophys Acta.* (2014) 1839:1362–72. doi: 10.1016/j.bbagrm.2014.02.007
20. Hawse WF, Wolberger C. Structure-based mechanism of ADP-ribosylation by sirtuins. *J Biol Chem.* (2009) 284:33654–61. doi: 10.1074/jbc.M109.024521
21. Du J, Zhou Y, Su X, Yu JJ, Khan S, Jiang H, et al. Sirt5 is a NAD-dependent protein lysine demalonylase and desuccinylase. *Science.* (2011) 334:806–9. doi: 10.1126/science.1207861
22. Guarente L. Diverse and dynamic functions of the Sir silencing complex. *Nat Genetics.* (1999) 23:281–5. doi: 10.1038/15458
23. Guarente L. Sirtuins in aging and disease. *Cold Spring Harbor Symp Quant Biol.* (2007) 72:483–8. doi: 10.1101/sqb.2007.72.024
24. Kong S, McBurney MW, Fang D. Sirtuin 1 in immune regulation and autoimmunity. *Immunol Cell Biol.* (2012) 90:6–13. doi: 10.1038/icb.2011.102
25. Tang X, Chen XF, Chen HZ, Liu DP. Mitochondrial Sirtuins in cardiometabolic diseases. *Clin Sci.* (2017) 131:2063–78. doi: 10.1042/CS20160685
26. Jeong SM, Haigis MC. Sirtuins in cancer: a balancing act between genome stability and metabolism. *Mol Cells.* (2015) 38:750–8. doi: 10.14348/molcells.2015.0167
27. Haigis MC, Guarente LP. Mammalian sirtuins–emerging roles in physiology, aging, and calorie restriction. *Genes Dev.* (2006) 20:2913–21. doi: 10.1101/gad.1467506
28. Alwarawrah Y, Kiernan K, MacIver NJ. Changes in nutritional status impact immune cell metabolism and function. *Front Immunol.* (2018) 9:1055. doi: 10.3389/fimmu.2018.01055
29. Yeung F, Hoberg JE, Ramsey CS, Keller MD, Jones DR, Frye RA, et al. Modulation of NF-kappaB-dependent transcription and cell survival by the SIRT1 deacetylase. *EMBO J.* (2004) 23:2369–80. doi: 10.1038/sj.emboj.7600244
30. Hayden MS, West AP, Ghosh S. NF-kappaB and the immune response. *Oncogene.* (2006) 25:6758–80. doi: 10.1038/sj.onc.1209943
31. Gao X, Xu YX, Janakiraman N, Chapman RA, Gautam SC. Immunomodulatory activity of resveratrol: suppression of lymphocyte proliferation, development of cell-mediated cytotoxicity, and cytokine production. *Biochem Pharmacol.* (2001) 62:1299–308. doi: 10.1016/s0006-2952(01)00775-4
32. Zhang J, Lee SM, Shannon S, Gao B, Chen W, Chen A, et al. The type III histone deacetylase Sirt1 is essential for maintenance of T cell tolerance in mice. *J Clin Investig.* (2009) 119:3048–58. doi: 10.1172/JCI38902
33. Rodgers JT, Lerin C, Haas W, Gygi SP, Spiegelman BM, Puigserver P. Nutrient control of glucose homeostasis through a complex of PGC-1alpha and SIRT1. *Nature.* (2005) 434:113–8. doi: 10.1038/nature03354.
34. Gao B, Kong Q, Kemp K, Zhao YS, Fang D. Analysis of sirtuin 1 expression reveals a molecular explanation of IL-2-mediated reversal of T-cell tolerance. *Proc Natl Acad Sci USA.* (2012) 109:899–904. doi: 10.1073/pnas.1118462109
35. Sequeira J, Boily G, Bazinet S, Saliba S, He X, Jardine K, et al. sirt1-null mice develop an autoimmune-like condition. *Exp Cell Res.* (2008) 314:3069–74. doi: 10.1016/j.yexcr.2008.07.011
36. Kong S, Kim SJ, Sandal B, Lee SM, Gao B, Zhang DD, et al. The type III histone deacetylase Sirt1 protein suppresses p300-mediated histone H3 lysine 56 acetylation at Bclaf1 promoter to inhibit T cell activation. *J Biol Chem.* (2011) 286:16967–75. doi: 10.1074/jbc.M111.218206
37. Haraguchi T, Holaska JM, Yamane M, Koujin T, Hashiguchi N, Mori C, et al. Emerin binding to Btf, a death-promoting transcriptional repressor, is disrupted by a missense mutation that causes Emery-Dreifuss muscular dystrophy. *Eur J Biochem.* (2004) 271:1035–45. doi: 10.1111/j.1432-1033.2004.04007.x
38. McPherson JP, Sarras H, Lemmers B, Tamblyn L, Migon E, Matysiak-Zablocki E, et al. Essential role for Bclaf1 in lung development and immune system function. *Cell Death Differ.* (2009) 16:331–9. doi: 10.1038/cdd.2008.167

39. Wen Y, Zhou X, Lu M, He M, Tian Y, Liu L, et al. Bclaf1 promotes angiogenesis by regulating HIF-1alpha transcription in hepatocellular carcinoma. *Oncogene.* (2018) 38:1845–59. doi: 10.1038/s41388-018-0552-1
40. Legutko A, Marichal T, Fievez L, Bedoret D, Mayer A, de Vries H, et al. Sirtuin 1 promotes Th2 responses and airway allergy by repressing peroxisome proliferator-activated receptor-gamma activity in dendritic cells. *J Immunol.* (2011) 187:4517–29. doi: 10.4049/jimmunol.1101493
41. Lorentsen KJ, Cho JJ, Luo X, Zuniga AN, Urban JF Jr, Zhou L, et al. Bcl11b is essential for licensing Th2 differentiation during helminth infection and allergic asthma. *Nat Commun.* (2018) 9:1679. doi: 10.1038/s41467-018-04111-0
42. Senawong T, Peterson VJ, Avram D, Shepherd DM, Frye RA, Minucci S, et al. Involvement of the histone deacetylase SIRT1 in chicken ovalbumin upstream promoter transcription factor (COUP-TF)-interacting protein 2-mediated transcriptional repression. *J Biol Chem.* (2003) 278:43041–50. doi: 10.1074/jbc.M307477200
43. Wang Y, Bi Y, Chen X, Li C, Li Y, Zhang Z, et al. Histone deacetylase SIRT1 negatively regulates the differentiation of interleukin-9-producing CD4(+) T cells. *Immunity.* (2016) 44:1337–49. doi: 10.1016/j.immuni.2016.05.009
44. Limagne E, Thibaudin M, Euvrard R, Berger H, Chalons P, Vegan F, et al. Sirtuin-1 activation controls tumor growth by impeding Th17 differentiation via STAT3 deacetylation. *Cell Reports.* (2017) 19:746–59. doi: 10.1016/j.celrep.2017.04.004
45. Wang J, Zhao C, Kong P, Sun H, Sun Z, Bian G, et al. Treatment with NAD(+) inhibited experimental autoimmune encephalomyelitis by activating AMPK/SIRT1 signaling pathway and modulating Th1/Th17 immune responses in mice. *Int Immunopharmacol.* (2016) 39:287–94. doi: 10.1016/j.intimp.2016.07.036
46. Lim HW, Kang SG, Ryu JK, Schilling B, Fei M, Lee IS, et al. SIRT1 deacetylates RORgammat and enhances Th17 cell generation. *J Exp Med.* (2015) 212:607–17. doi: 10.1084/jem.20132378
47. Giralt A, Villarroya F. SIRT3, a pivotal actor in mitochondrial functions: metabolism, cell death and aging. *Biochem J.* (2012) 444:1–10. doi: 10.1042/BJ20120030
48. Hirschey MD, Shimazu T, Goetzman E, Jing E, Schwer B, Lombard DB, et al. SIRT3 regulates mitochondrial fatty-acid oxidation by reversible enzyme deacetylation. *Nature.* (2010) 464:121–5. doi: 10.1038/nature08778
49. Newman JC, He W, Verdin E. Mitochondrial protein acylation and intermediary metabolism: regulation by sirtuins and implications for metabolic disease. *J Biol Chem.* (2012) 287:42436–43. doi: 10.1074/jbc.R112.404863
50. Toubai T, Tamaki H, Peltier DC, Rossi C, Oravecz-Wilson K, Liu C, et al. Mitochondrial deacetylase SIRT3 plays an important role in donor T cell responses after experimental allogeneic hematopoietic transplantation. *J Immunol.* (2018) 201:3443–55. doi: 10.4049/jimmunol.1800148
51. Ciarlo E, Heinonen T, Lugrin J, Acha-Orbea H, Le Roy D, Auwerx J, et al. Sirtuin 3 deficiency does not alter host defenses against bacterial and fungal infections. *Sci Reports.* (2017) 7:3853. doi: 10.1038/s41598-017-04263-x
52. Zhong L, D'Urso A, Toiber D, Sebastian C, Henry RE, Vadysirisack DD, et al. The histone deacetylase Sirt6 regulates glucose homeostasis via Hif1alpha. *Cell.* (2010) 140:280–93. doi: 10.1016/j.cell.2009.12.041
53. Krzywinska E, Stockmann C. Hypoxia, metabolism and immune cell function. *Biomedicines.* (2018) 6:56. doi: 10.3390/biomedicines6020056
54. Dang EV, Barbi J, Yang HY, Jinasena D, Yu H, Zheng Y, et al. Control of T(H)17/T(reg) balance by hypoxia-inducible factor 1. *Cell.* (2011) 146:772–84. doi: 10.1016/j.cell.2011.07.033
55. Lo Sasso G, Menzies KJ, Mottis A, Piersigilli A, Perino A, Yamamoto H, et al. SIRT2 deficiency modulates macrophage polarization and susceptibility to experimental colitis. *PLoS ONE.* (2014) 9:e103573. doi: 10.1371/journal.pone.0103573
56. van Loosdregt J, Vercoulen Y, Guichelaar T, Gent YY, Beekman JM, van Beekum O, et al. Regulation of Treg functionality by acetylation-mediated Foxp3 protein stabilization. *Blood.* (2010) 115:965–74. doi: 10.1182/blood-2009-02-207118
57. Kwon HS, Lim HW, Wu J, Schnolzer M, Verdin E, Ott M. Three novel acetylation sites in the Foxp3 transcription factor regulate the suppressive activity of regulatory T cells. *J Immunol.* (2012) 188:2712–21. doi: 10.4049/jimmunol.1100903
58. Huehn J, Beyer M. Epigenetic and transcriptional control of Foxp3+ regulatory T cells. *Semin Immunol.* (2015) 27:10–8. doi: 10.1016/j.smim.2015.02.002
59. Beier UH, Angelin A, Akimova T, Wang L, Liu Y, Xiao H, et al. Essential role of mitochondrial energy metabolism in Foxp3(+) T-regulatory cell function and allograft survival. *FASEB J.* (2015) 29:2315–26. doi: 10.1096/fj.14-268409
60. Scott-Browne JP, López-Moyado IF, Trifari S, Wong V, Chavez L, Rao A, et al. Dynamic changes in chromatin accessibility occur in CD8(+) T cells responding to viral infection. *Immunity.* (2016) 45:1327–40. doi: 10.1016/j.immuni.2016.10.028
61. Kuroda S, Yamazaki M, Abe M, Sakimura K, Takayanagi H, Iwai Y. Basic leucine zipper transcription factor, ATF-like (BATF) regulates epigenetically and energetically effector CD8 T-cell differentiation via Sirt1 expression. *Proc Natl Acad Sci USA.* (2011) 108:14885–9. doi: 10.1073/pnas.1105133108
62. Franchina DG, Dostert C, Brenner D. Reactive oxygen species: involvement in T Cell signaling and metabolism. *Trends Immunol.* (2018) 39:489–502. doi: 10.1016/j.it.2018.01.005
63. Cantó C, Auwerx J. PGC-1alpha, SIRT1 and AMPK, an energy sensing network that controls energy expenditure. *Curr Opin Lipidol.* (2009) 20:98–105. doi: 10.1097/MOL.0b013e328328d0a4
64. Kelly TJ, Lerin C, Haas W, Gygi SP, Puigserver P. GCN5-mediated transcriptional control of the metabolic coactivator PGC-1beta through lysine acetylation. *J Biol Chem.* (2009) 284:19945–52. doi: 10.1074/jbc.M109.015164
65. Jeng MY, Hull PA, Fei M, Kwon HS, Tsou CL, Kasler H, et al. Metabolic reprogramming of human CD8(+) memory T cells through loss of SIRT1. *J Exp Med.* (2018) 215:51–62. doi: 10.1084/jem.20161066
66. Wu H, Deng Y, Feng Y, Long D, Ma K, Wang X, et al. Epigenetic regulation in B-cell maturation and its dysregulation in autoimmunity. *Cell Mol Immunol.* (2018) 15:676–84. doi: 10.1038/cmi.2017.133
67. Shaknovich R, Cerchietti L, Tsikitas L, Kormaksson M, De S, Figueroa ME, et al. DNA methyltransferase 1 and DNA methylation patterning contribute to germinal center B-cell differentiation. *Blood.* (2011) 118:3559–69. doi: 10.1182/blood-2011-06-357996
68. Wang Q, Yan C, Xin M, Han L, Zhang Y, Sun M. Sirtuin 1 (Sirt1) overexpression in BaF3 cells contributes to cell proliferation promotion, apoptosis resistance and pro-inflammatory cytokine production. *Med Sci Monit.* (2017) 23:1477–82. doi: 10.12659/MSM.900754
69. Miyazaki Y, Li R, Rezk A, Misirliyan H, Moore C, Farooqi N, et al. A novel microRNA-132-sirtuin-1 axis underlies aberrant B-cell cytokine regulation in patients with relapsing-remitting multiple sclerosis [corrected]. *PLoS ONE.* (2014) 9:e105421. doi: 10.1371/journal.pone.0105421
70. Yu W, Denu RA, Krautkramer KA, Grindle KM, Yang DT, Asimakopoulos F, et al. Loss of SIRT3 provides growth advantage for B cell malignancies. *J Biol Chem.* (2016) 291:3268–79. doi: 10.1074/jbc.M115.702076
71. Jeong SM, Xiao C, Finley LW, Lahusen T, Souza AL, Pierce K, et al. SIRT4 has tumor-suppressive activity and regulates the cellular metabolic response to DNA damage by inhibiting mitochondrial glutamine metabolism. *Cancer Cell.* (2013) 23:450–63. doi: 10.1016/j.ccr.2013.02.024
72. Jeong SM, Lee A, Lee J, Haigis MC. SIRT4 protein suppresses tumor formation in genetic models of Myc-induced B cell lymphoma. *J Biol Chem.* (2014) 289:4135–44. doi: 10.1074/jbc.M113.525949
73. Bhalla S, Gordon LI. Functional characterization of NAD dependent de-acetylases SIRT1 and SIRT2 in B-cell chronic lymphocytic leukemia (CLL). *Cancer Biol Ther.* (2016) 17:300–9. doi: 10.1080/15384047.2016.1139246
74. Waibel M, Christiansen AJ, Hibbs ML, Shortt J, Jones SA, Simpson I, et al. Manipulation of B-cell responses with histone deacetylase inhibitors. *Nat Commun.* (2015) 6:6838. doi: 10.1038/ncomms7838
75. Vachharajani VT, Liu T, Brown CM, Wang X, Buechler NL, Wells JD, et al. SIRT1 inhibition during the hypoinflammatory phenotype of sepsis enhances immunity and improves outcome. *J leukocy Biol.* (2014) 96:785–96. doi: 10.1189/jlb.3MA0114–034RR.
76. Kumari S, Chaurasia SN, Nayak MK, Mallick RL, Dash D. Sirtuin inhibition induces apoptosis-like changes in platelets and thrombocytopenia. *J Biol Chem.* (2015) 290:12290–9. doi: 10.1074/jbc.M114.615948
77. Saini N, Yang X. Metformin as an anti-cancer agent: actions and mechanisms targeting cancer stem cells. *Acta Biochim Biophys Sin.* (2018) 50:133–43. doi: 10.1093/abbs/gmx106

78. Zhang W, Wu H, Yang M, Ye S, Li L, Zhang H, et al. SIRT1 inhibition impairs non-homologous end joining DNA damage repair by increasing Ku70 acetylation in chronic myeloid leukemia cells. *Oncotarget.* (2016) 7:13538–50. doi: 10.18632/oncotarget.6455
79. Zou T, Yang Y, Xia F, Huang A, Gao X, Fang D, et al. Resveratrol Inhibits CD4+ T cell activation by enhancing the expression and activity of Sirt1. *PLoS ONE.* (2013) 8:e75139. doi: 10.1371/journal.pone.0075139
80. Imler TJ Jr, Petro TM. Decreased severity of experimental autoimmune encephalomyelitis during resveratrol administration is associated with increased IL-17+IL-10+ T cells, CD4(-) IFN-gamma+ cells, and decreased macrophage IL-6 expression. *Int Immunopharmacol.* (2009) 9:134–43. doi: 10.1016/j.intimp.2008.10.015
81. Sanchez-Fidalgo S, Cardeno A, Villegas I, Talero E, de la Lastra CA. Dietary supplementation of resveratrol attenuates chronic colonic inflammation in mice. *Eur J Pharmacol.* (2010) 633:78–84. doi: 10.1016/j.ejphar.2010.01.025
82. Xuzhu G, Komai-Koma M, Leung BP, Howe HS, McSharry C, McInnes IB, et al. Resveratrol modulates murine collagen-induced arthritis by inhibiting Th17 and B-cell function. *Ann Rheum Dis.* (2012) 71:129–35. doi: 10.1136/ard.2011.149831
83. Wang B, Sun J, Li L, Zheng J, Shi Y, Le G. Regulatory effects of resveratrol on glucose metabolism and T-lymphocyte subsets in the development of high-fat diet-induced obesity in C57BL/6 mice. *Food Funct.* (2014) 5:1452–63. doi: 10.1039/C3FO60714C
84. Welsh KJ, Zhao B, Buja LM, Brown RE. Sirt1-positive lymphocytes in acute cellular cardiac allograft rejection: contributor to pathogenesis and a therapeutic target. *ASAIO J.* (2016) 62:349–53. doi: 10.1097/MAT.0000000000000338
85. Ye Q, Zhang M, Wang Y, Fu S, Han S, Wang L, et al. Sirtinol regulates the balance of Th17/Treg to prevent allograft rejection. *Cell Biosci.* (2017) 7:55. doi: 10.1186/s13578-017-0182-2

Conflict of Interest Statement: The authors declare that the research was conducted in the absence of any commercial or financial relationships that could be construed as a potential conflict of interest.

frontiers in Endocrinology

ORIGINAL RESEARCH
published: 06 August 2019
doi: 10.3389/fendo.2019.00536

The Association of Hypoglycemia Assessed by Continuous Glucose Monitoring With Cardiovascular Outcomes and Mortality in Patients With Type 2 Diabetes

Wei Wei[1], Shi Zhao[1], Sha-li Fu[1], Lan Yi[1], Hong Mao[1], Qin Tan[2], Pan Xu[3] and Guo-liang Yang[4]*

[1] Department of Endocrinology, Tongji Medical College, The Central Hospital of Wuhan, Huazhong University of Science and Technology, Wuhan, China, [2] Department of Cardiology, Tongji Medical College, The Central Hospital of Wuhan, Huazhong University of Science and Technology, Wuhan, China, [3] Department of Neurology, Tongji Medical College, The Central Hospital of Wuhan, Huazhong University of Science and Technology, Wuhan, China, [4] Department of Information, Tongji Medical College, The Central Hospital of Wuhan, Huazhong University of Science and Technology, Wuhan, China

Objective: Hypoglycemia has been shown to promote inflammation, a common pathogenic process, in many chronic health conditions including diabetes and cardiovascular disease. The aim of this study was to investigate the association of hypoglycemia, assessed by continuous glucose monitoring (CGM) with major adverse cardiovascular event (MACE) outcomes and all-cause mortality.

Methods: A retrospective cohort study was conducted with 1,520 patients with type 2 diabetes mellitus (T2DM). The severity of hypoglycemia event was assessed by CGM system.

Results: Three hundred and forty-seven participants experienced hypoglycemia events (323 with mild hypoglycemia and 24 with severe hypoglycemia). A fraction of 72.62% hypoglycemia was asymptomatic. During a median follow-up of 31 months, 380 participants reached the primary outcome of MACE (61 cardiovascular death, 50 non-fatal myocardial infarction [MI], 116 non-fatal stroke, 153 unstable angina requiring hospitalization), 80 participants died before the end of the study. In multivariate Cox regression models, hypoglycemia was associated with cardiovascular death (HR 2.642[95CI% 1.398–4.994]), non-fatal stroke (HR 1.813 [95CI% 1.110–2.960]) and all-cause mortality (HR 1.960 [95 CI% 1.124- 3.418]) after the full adjustment. Hypoglycemia was not associated with non-fatal MI and unstable angina. The HR of severe hypoglycemia was higher than mild hypoglycemia for cardiovascular death. Patients with symptomatic and asymptomatic hypoglycemia had similar MACE outcomes and all-cause mortality.

Conclusions: CGM is effective to detect asymptomatic and nocturnal hypoglycemia. Hypoglycemia is associated with an increased risk of non-fatal stroke, cardiovascular related death, and total mortality. The cardiovascular mortality is dose-dependent on the severity of hypoglycemia.

Keywords: T2DM, hypoglycemia, CGM system, MACE, all-cause mortality

OPEN ACCESS

Edited by:
Jie Chen,
Xiamen University, China

Reviewed by:
Youlian Wang,
Jiangxi Provincial People's Hospital, China
Edward Narayan,
Western Sydney University, Australia

***Correspondence:**
Shi Zhao
zhaoshiwuhan@126.com

Specialty section:
This article was submitted to Experimental Endocrinology, a section of the journal Frontiers in Endocrinology

Received: *23 April 2019*
Accepted: *18 July 2019*
Published: *06 August 2019*

Citation:
Wei W, Zhao S, Fu S, Yi L, Mao H, Tan Q, Xu P and Yang G (2019) The Association of Hypoglycemia Assessed by Continuous Glucose Monitoring With Cardiovascular Outcomes and Mortality in Patients With Type 2 Diabetes. Front. Endocrinol. 10:536. doi: 10.3389/fendo.2019.00536

INTRODUCTION

Chronic low grade inflammation is a common feature underlying many chronic diseases and conditions such as insulin resistance and cardiovascular disease. Studies have suggested that hypoglycemia is able to promote inflammatory processes in patients with or without diabetes (1, 2). Hypoglycemia is a frequent adverse effect of anti-diabetic therapy in diabetic patients, and severe hypoglycemia has been identified as a potential risk factor for cardiovascular events in patients with type 2 diabetes mellitus (T2DM). Previous studies have reported an increased hazard ratio (HR) for adverse cardiovascular outcomes and total mortality in diabetic patients with hypoglycemia (3–6). However, these conclusions were drawn from the secondary analyses of randomized clinical trials (7, 8) or retrospective analyses of medical claims databases (9, 10), which a clear definition of hypoglycemia was lacking. Continuous glucose monitoring (CGM) system is an effective tool for the assessment of hypoglycemic status, particularly for the asymptomatic nocturnal hypoglycemia (11). Using CGM system, researchers found out that hypoglycemia is more common in T2DM patients than previously thought (12), and the frequency of hypoglycemia in those previous studies may be underestimated.

In the present study, using glucose data collected from CGMs, we investigated the relationships of hypoglycemia with total mortality and major adverse cardiovascular events (MACE), including non-fatal stroke, non-fatal myocardial infarction (MI), unstable angina leading to hospitalization, and cardiovascular death.

MATERIALS AND METHODS

Subjects

In this retrospective cohort study, we recruited 1,520 patients admitted to our hospital between January 2013 and December 2017.

The inclusion criteria were: (1) T2DM according to 2013 American Diabetes Association standards (13). Patients with other types of diabetes, such as type 1 diabetes, gestational diabetes, and secondary diabetes were excluded from the study. (2) Patients without the acute phase of illness, such as acute coronary syndrome, uncontrolled infection, etc. (3) CGM (iPro®2 CGM System Gold, Medtronic MiniMed, Inc., Northridge, CA) was used to monitor blood glucose within 3 days of admission without changing medications before the patients were discharged from hospital.

The CGM devices used in this study continuously measured the glucose level in the interstitial fluids within the range of 2.2–22.2 mmol/L (40–400 mg/dL). The glucose level was determined every 5 min, 288 times maximum per day. The CGM system was calibrated with blood glucometer measurements (ACCU-CHEK® Aviva, Roche, Mannheim, Germany) four times daily according to the manufacturer's instruction. Participants were instructed to keep a diary about the occurrence of hypoglycemic symptoms. The CGM system used in our study measured interstitial glucose in a blinded manner, and data analysis was performed after disconnection of the device.

This clinical study was approved by the ethics committee boad of The Central Hospital of Wuhan. All participants had signed the informed consent form during the enrollment and before the start the study.

Clinical Data Collection

A clinical data warehouse was created as a collaborative program between Wuhan Central Hospital (Wuhan, China) and Shanghai Lejiu Healthcare Technology Co., Ltd. Data were extracted every 24 h by Lex Clinical Data Application 3.2 (Shanghai Lejiu Healthcare Technology Co., Ltd) from the Hospital Health Information System (HIS) to a designated clinical data warehouse including admission/transfer/discharge, laboratory orders/results, medication orders, discharge summary, administration events, flow sheet entries, procedures, medical reports, etc. All original unstructured data (i.e., pathology report, radiology report, admit/discharge summary etc.) were exclusively converted to a uniformed structured format. Core elements of the data warehouse were completely de-identified so that all queries and analytics could be carried out without exposing the confidential health data, allowing the investigators with sufficient privilege to re-identify data. Lex Clinical Data Application 3.2 was a self-service data access tool designed to query the clinical data warehouse and return tabular data for analysis and visualization.

Definition of Hypoglycemia

A hypoglycemia event was defined as an interstitial glucose level below 3.9 mmol/L (70 mg/dl) for at least 15 min and recovery when the interstitial glucose concentration had been continuously above the threshold for 15 min or more (11). Percent time at interstitial glucose level below 3.9 mmol/L was evaluated. A severe hypoglycemia event was defined as cognitive impairment requiring external assistance for recovery. A mild hypoglycemia event was defined as a glucose level below 3.9 mmol/L without cognitive impairment and external assistance for recovery. Nocturnal hypoglycemia was defined as an episode occurring between 00:00 a.m. and 06:00 a.m.

Follow-Ups and Outcomes

After discharging from the hospital, participants were invited to join the out-patient blood glucose management system, which was run by the professional medical staff. Routine self-blood glucose (at least four times per week) and HbA1c (every 3 month) monitoring were demanded in order to know the glucose control condition and clinical medication. The median duration of follow-ups was 31 months (inter-quartile range, 22–56). Eighteen patients (1.18%) with new episodes of severe hypoglycemic events during follow-up were excluded from the study, and 41 (2.70%) patients were lost before follow-ups due to various reasons.

The primary outcome was the first occurrence of an adjudicated MACE, including non-fatal MI, non-fatal stroke, cardiovascular death, and unstable angina leading to hospitalization. The secondary outcome was death of any

cause. The diagnoses of MACE outcomes were ascertained according to the hospitalization records, discharge summary and certification of death, which were adjudicated by an independent committee. The members of the committee were from the cardiovascular and neurology departments of our hospital, who were unaware of the CGM results. Follow-up time was calculated from the date of hypoglycemia event to the onset date of the MACE event, death, or end of study (31 August 2018). Cause of death was classified as cardiovascular death and all other causes of death.

Statistical Analysis

The differences between groups were compared using *t*-test for continuous variables and Chi-square test for categorical data. Cox proportional models were used to evaluate the association between hypoglycemia and either MACE or all-cause mortality. We progressively adjusted the models for potential confounders. Model 1 was a crude model. Model 2 included age, sex, eGFR, HbA1c, BMI, and duration of diabetes. Model 3 included all variables in model 2 plus smoking status, alcohol history, past medical history (hepatic disease, renal disease, malignancy, coronary heart disease, and stroke), all diabetic medications (insulin, sulfonylureas, metformin, alpha-glucosidase inhibitors, pioglitazone, glinides, and DPP-4 inhibitors), hypertension medication, lipid-lowering medication, and antiplatelet agents.

TABLE 1 | Baseline characteristics of the study population (n = 1,520).

Outcome	Number of patients
Severity of hypoglycemia	
No hypoglycemia	1173 (77.17%)
Mild hypoglycemia	323 (21.25%)
Severe hypoglycemia	24 (1.58%)
Numbers of hypoglycemia events	
1	94 (27.09%)
2	87 (25.07%)
3	66 (19.02%)
4	40 (11.53%)
≥5	60 (17.29%)
Symptoms of hypoglycemia	
Asymptomatic hypoglycemia	265 (76.37%)
Symptomatic hypoglycemia	82 (23.63%)
Time of hypoglycemia	
Nocturnal hypoglycemia	155 (44.67%)
Diurnal hypoglycemia	192 (55.33%)
MACE outcomes	380
Non-fatal myocardial infraction	50 (13.16%)
Non-fatal stroke	116 (30.53%)
Cardiovascular death	61 (16.05%)
Unstable angina requiring hospitalization	153 (40.26%)
All-cause mortality	80

Dates are presented as numbers (percentages).
MACE, major adverse cardiovascular event.

TABLE 2 | Clinical characteristics of participants by the occurrence of hypoglycemia.

	No hypoglycemia n = 1,173	Hypoglycemia n = 347	*P*-value
Age, years	58.59 ± 11.26	62.27 ± 11.58	<0.001
Gender, Male (*n* %)	592 (50.5)	191 (55)	0.142
Diabetes duration, years	6.46 ± 6.00	7.78 ± 7.37	0.002
Mean glucose of CGM, mmol/L	8.97 ± 2.17	7.81 ± 2.06	<0.001
SD of CGM, mmol/L	2.64 ± 1.30	3.29 ± 1.71	<0.001
FPG, mmol/L	9.15 ± 3.81	8.36 ± 3.86	0.001
HbA1c, %	8.19 ± 2.10	7.73 ± 1.96	<0.001
BMI, kg/m^2	24.50 ± 2.88	24.75 ± 2.90	0.173
eGFR	95.18 ± 20.29	89.09 ± 21.78	0.001
TG, mmol/L	1.83 ± 1.80	1.84 ± 1.58	0.924
TC, mmol/L	4.58 ± 1.06	4.62 ± 1.02	0.616
HDL, mmol/L	2.61 ± 0.85	2.60 ± 0.84	0.750
LDL, mmol/L	1.13 ± 0.33	1.14 ± 0.29	0.844
Systolic blood pressure, mmHg	130.46 ± 17.03	132.00 ± 19.84	0.154
Diastolic blood pressure, mmHg	78.67 ± 9.78	77.70 ± 11.09	0.116
Smoking status	340 (29)	102 (29.4)	0.893
Alcohol history	151 (12.9)	59 (17)	0.052
Previous hypoglycemia	73 (6.2)	57 (16.4)	< 0.001
History of hepatic disease	160 (13.6)	48 (13.8)	0.624
History of renal disease	32 (2.7)	23 (6.6)	0.002
History of malignancy	29 (2.5)	12 (3.5)	0.089
History of coronary heart disease	191 (16.3)	66 (19.0)	0.254
History of stroke	79 (6.7)	26 (7.5)	0.630
Diabetic Complication			
Diabetic nephropathy	331 (28.2)	106 (30.5)	0.418
Diabetic retinopathy	283 (24.1)	91 (26.2)	0.436
Diabetic peripheral neuropathy	246 (21.0)	78 (22.5)	0.551
Peripheral arterial disease	8 (0.7)	4 (1.2)	0.487
Diabetic Medications			
Insulin	444 (37.9)	179 (51.6)	0.000
Sulfonylureas	167 (14.2)	59 (17.0)	0.229
Metformin	407 (34.7)	55 (15.9)	< 0.001
Alpha-glucosidase inhibitors	437 (37.3)	124 (35.7)	0.613
Pioglitazone	112 (9.5)	19 (5.5)	0.016
Glinides	73 (6.2)	23 (6.6)	0.802
DPP-4 inhibitors	87 (7.4)	12 (3.5)	0.009
Hypertension medication	527 (44.9)	176 (50.7)	0.058
Lipid-lowering medication	269 (22.9)	78 (22.5)	0.884
Antiplatelet agents	358 (30.5)	132 (38.0)	0.009

Continuous variables are shown as mean ± SD. Categorical data are presented as numbers (percentages).
CGM, continuous glucose monitoring; SD, standard deviation; FPG, fasting plasma glucose; BMI, body mass index; GFR, glomerular filtration rate; TG, triglyceride; TC, total cholesterol; LDL, low density lipoprotein; HDL, high density lipoprotein; DPP-4, dipeptidylpeptidse 4.

For further analysis, we evaluated the risk of MACE outcomes and total mortality according to the severity of hypoglycemia and the appearance of hypoglycemic symptoms. The severity of hypoglycemia was classified into three categories: no hypoglycemia, mild hypoglycemia, and severe hypoglycemia. The group of no hypoglycemia served as the reference group, and adjusted for models described before. The survival curves of the three groups were estimate by Kaplan-Meier method, and the homogeneity between survival curves was tested by log-rank test.

All analyses were performed using State software (version 13.1, Stata Corp, College Station, TX). $P < 0.05$ was considered as statistical significance.

RESULT

Characteristics of Study Population

Baseline characteristics of the study population were presented in **Table 1**. The total number of patients included in the study was 1,520, with 347 (22.83%) patients experiencing hypoglycemic events. A total of 1,028 hypoglycemic events were recorded, corresponding to 250 h in hypoglycemia status. Of all the hypoglycemia, 24 patients were with severe hypoglycemia and 323 with mild hypoglycemia. The overall fraction of asymptomatic hypoglycemia was 72.62%, and the fraction of nocturnal hypoglycemia was 44.67%.

Compared to patients without hypoglycemia, those who experienced hypoglycemia were significantly older, had a longer duration of diabetes, and a lower eGFR. They were more likely to have experienced hypoglycemia events previously. They also took less anti-diabetic medications of metformin, pioglitazone, and DPP-4 inhibitors; meanwhile they were more often treated with insulin and anti-platelet agents (**Table 2**). Patients with severe hypoglycemia were even older, and more likely to be a smoker. They experienced hypoglycemia earlier than those with mild hypoglycemia (**Supplementary Table 1**).

Patients with hypoglycemia were further divided into two groups according to the appearance of hypoglycemic symptoms. Compared to patients with symptomatic hypoglycemia, patients experiencing asymptomatic hypoglycemia had lower mean glucose of CGM and smaller glycemic variability, were more likely to experience nocturnal hypoglycemia, and had longer periods of hypoglycemic events (**Supplementary Table 2**). The other baseline clinical characteristics of patients with symptomatic hypoglycemia were similar to those with asymptomatic hypoglycemia, except that patients experiencing asymptomatic hypoglycemia had a higher proportion of diabetic peripheral neuropathy (**Supplementary Table 3**).

Association Between Hypoglycemia and MACE Outcomes

During the follow-up, 380 diabetic patients had developed MACE (61 cardiovascular deaths, 153 unstable angina requiring hospitalization, 50 non-fatal MI, 116 non-fatal strokes). Eighty patients died before the end of our study. Of the 347 patients with hypoglycemia, the median time between hypoglycemia events and MACE outcomes was 21 (inter-quartile range, 11–38) months.

The crude incidence of MACE outcomes in people with hypoglycemia was higher than the incidence in people without hypoglycemia. These estimated results still remained significant (model 2: HR 1.592, 95%CI, 1.233-2.056; model 3: HR 1.615, 95% CI, 1.239-2.106) after further adjustments for potential confounding factors.

TABLE 3 | Association between hypoglycemia and MACE outcomes and all-cause mortality.

	Events/ N			Model 1	Model 2	Model 3
	With hypoglycemia	Without hypoglycemia	*p*	HR (95%CI)	HR (95%CI)	HR (95%CI)
MACE	117/333	263/1,128	<0.001	1.501 (1.207, 1.866)	1.592 (1.233, 2.056)	1.615 (1.239, 2.106)
Cardiovascular death	23/333	38/1,128	0.006	2.033 (1.211, 3.413)	2.652 (1.433, 4.914)	2.642 (1.398, 4.994)
Unstable angina requiring hospitalization	41/333	112/1,128	0.300	1.226 (0.857, 1.753)	1.172 (0.774, 1.774)	1.218 (0.794, 1.869)
Non-fatal MI	18/333	32/1,128	0.030	1.901 (1.067, 3.389)	1.634 (0.828, 3.226)	1.549 (0.768, 3.124)
Non-fatal stroke	35/333	81/1,128	0.060	1.691 (1.144, 2.499)	1.755 (1.099, 2.803)	1.813 (1.110, 2.960)
All-cause mortality	34/333	46/1,128	<0.001	2.501 (1.605, 3.898)	2.259 (1.323, 3.858)	1.960 (1.124, 3.418)

Hypoglycemia was modeled as a time-dependent exposure.
Model 1 was a crude model.
Model 2 included age, sex, eGFR, HbA1c, BMI, and duration of diabetes.
Model 3 included all variables in model 2 plus smoking status, alcohol history, past medical history (hepatic disease, renal disease, malignancy, coronary heart disease, and stroke), all diabetic medications (insulin, sulfonylureas, metformin, alpha-glucosidase inhibitors, pioglitazone, glinides, and DPP-4 inhibitors), hypertension medication, lipid-lowering medication, and antiplatelet agents.
MACE, major adverse cardiovascular event; MI, myocardial infarction.

Furthermore, we examined the findings by subtypes of MACE outcomes. Compared to patients without hypoglycemia, those with hypoglycemia had a higher rate for non-fatal stroke, cardiovascular death and total mortality (**Table 3**). The associations were still persistent after additional adjustment in model 2 and model 3. In the minimally adjusted models, hypoglycemia was associated with an increased risk of non-fatal MI, which was no longer observed after further adjustment (model 3: HR 1.549, 95%CI 0.768–3.124). No association with hypoglycemia was found for unstable angina requiring hospitalization in any model.

Patients with severe hypoglycemia had a higher risk of cardiovascular death than those with mild hypoglycemia (**Figure 1A**). For subtypes of MACE outcomes, the values of HRs had a trend of rising in the severe hypoglycemia group compared with those in the hypoglycemia group, but the difference did not reach statistical significance (**Figure 2**). Patients with symptomatic and asymptomatic hypoglycemia had similar MACE outcomes and all-cause mortality (**Figures 1B**, **3**).

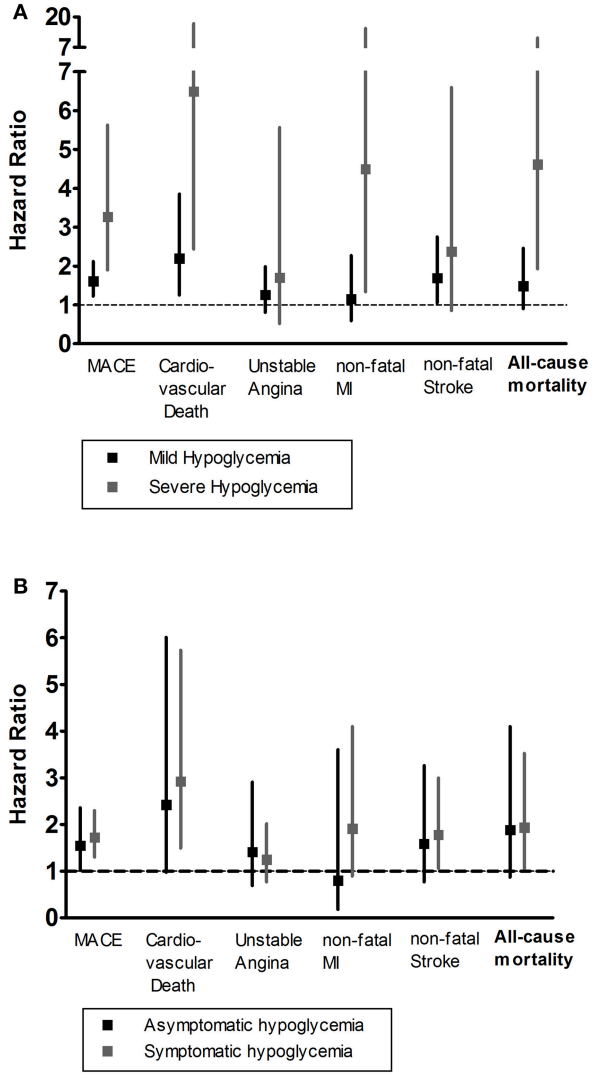

FIGURE 1 | (A) The HR and 95% CIs of MACE outcomes and all-cause mortality according to the severity of hypoglycemia. **(B)** The HR and 95% CIs of MACE outcomes and all-cause mortality according to the appearance of hypoglycemic symptoms. The severity of hypoglycemia was classified into three categories: no hypoglycemia, mild hypoglycemia, and severe hypoglycemia. The appearance of hypoglycemic symptoms was classified into three categories: no hypoglycemia, asymptomatic hypoglycemia, and symptomatic hypoglycemia. The group of no hypoglycemia served as the reference group, and adjusted for models including age, sex, duration of diabetes, HbA1c, BMI, eGFR, past medical history, diabetes medications, hypertension medication, lipid-lowering medication, and antiplatelet agents. HR, Hazard Ratios; MACE, major adverse cardiovascular event; MI, myocardial infarction.

DISCUSSION

The results of our study showed that hypoglycemia events detected by CGM were strongly associated with subsequent MACE outcomes and all-cause mortality. This association persisted after adjustment for a wide range of confounders. Furthermore, the risk of cardiovascular death and all-cause mortality was the highest after severe hypoglycemia events during CGM monitoring, especially in the first year, suggesting that health care providers should pay particular attention to the potential for morbidity and mortality after a severe hypoglycemic event. CGMs also detected a high proportion of asymptomatic hypoglycemic events, which appeared to have a similarly effect on MACE outcomes and all-cause mortality like the symptomatic hypoglycemia.

The Action to Control Cardiovascular Risk in Diabetes (ACCORD) study reported that intensive glycemic control was associated with increased risk of cardiovascular-related death (3, 4). Since the premature closure of the ACCORD study, the hypoglycemia-related cardiovascular adverse outcomes have led to considerable debate. The impacts of hypoglycemia on cardiovascular events in diabetic patients have been evaluated in several large prospective clinical trials, which have different conclusions (5, 6, 14). Also, there were many observational studies, with inconsistent results of the association between hypoglycemia and MACE outcomes (7, 15). A subsequent meta-analysis including 10 studies suggested that severe hypoglycemia was associated with an almost two fold increased risk of cardiovascular events (17). Consistent with parts of those previous studies, the results of our analyses showed that hypoglycemia was associated with cardiovascular-related death and all-cause mortality. However, due to the insufficient cases of non-cardiovascular mortality ($n = 19$), we were unable to analyze the association between the cause-specific mortality and hypoglycemia like the Trail Comparing Cardiovascular Safety of Insulin Degludec vs. Insulin Glargine in Patients with Type 2 Diabetes at High Risk of Cardiovascular Events (DEVOTE)study (16). In analysis of other subtypes of MACE outcomes, we can only see the association between hypoglycemia and an increased risk of developing non-fatal stroke. There was only a trend between hypoglycemia and non-fatal MI and unstable angina requiring hospitalization, which contrasted with the previous analyses (10, 14).

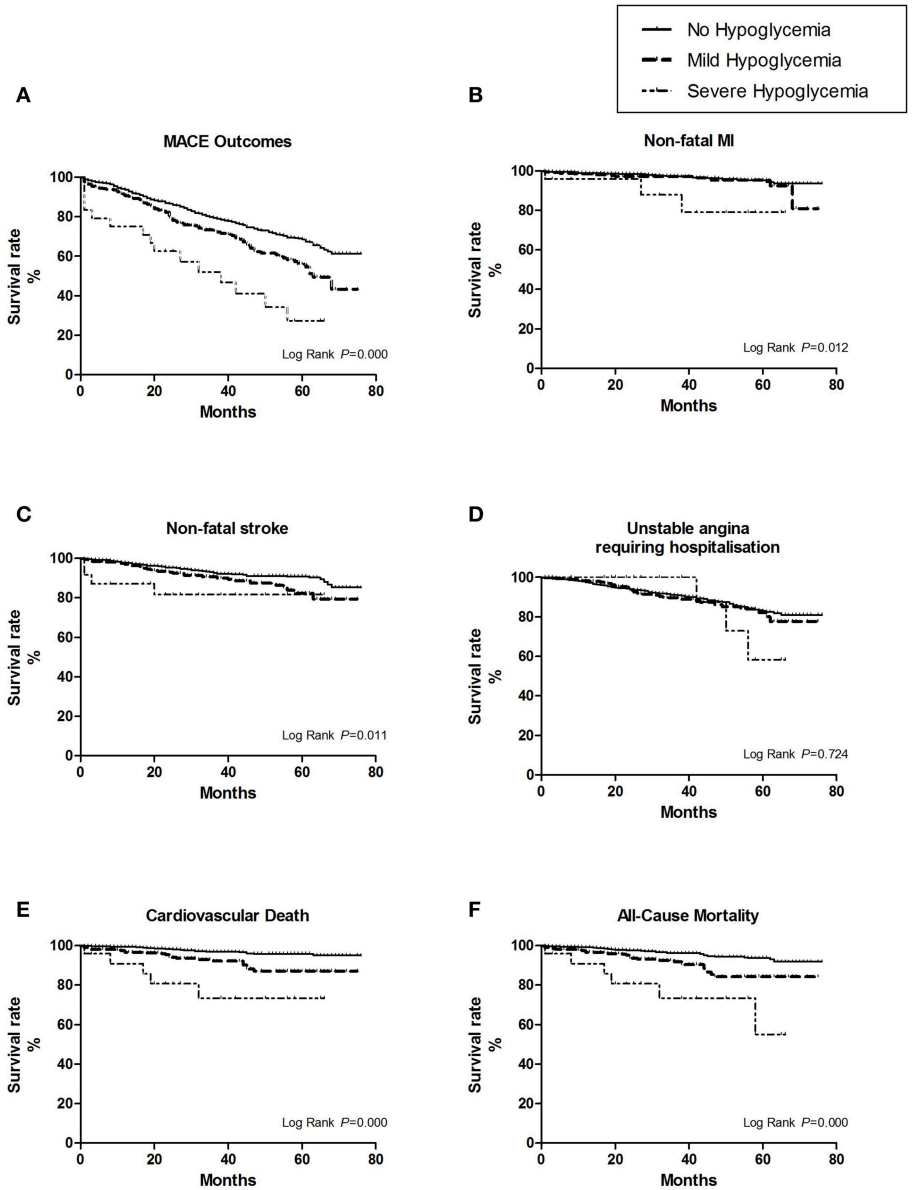

FIGURE 2 | The survival curves of the hypoglycemic severity were estimate by Kaplan-Meier method, and the homogeneity between survival curves was tested by log-rank test. **(A)** For overall MACE outcomes, the risk of MACE was the highest in the first year after severe hypoglycemia (25%, 6/24). **(B)** For the subtype of non-fatal myocardial infarction (MI). **(C)** For the subtype of non-fatal stroke. **(D)** For the subtype of unstable angina leading to hospitalization. **(E)** For the subtype of cardiovascular death. **(F)** For all cause-mortality.

This can be explained by the different definitions of hypoglycemia, resulting in variable frequencies of hypoglycemia across studies. For most large epidemiological studies, hypoglycemia cases were collected by self-report (5, 6) or ICD-codes from medical electronic data (9, 10, 14), which may underestimate the prevalence of hypoglycemia. In our study, a fraction of 76.37% hypoglycemic episodes were asymptomatic, which was also supported by earlier studies using CGM system (18, 19). Such a high proportion of asymptomatic hypoglycemia in diabetic patients with reduced awareness is worth our serious attention in clinical management. CGM is an effective way to detect hypoglycemia events, especially nocturnal and asymptomatic hypoglycemia, which could play an important role in reducing hypoglycemia events and is worth promoting in clinical applications.

We found some evidence of a dose-dependent relationship between the severity of hypoglycemia and cardiovascular death and all-cause mortality. Our assumption is that the cardiovascular outcomes of severe hypoglycemia may be worse than that of mild hypoglycemia. A sub-analysis of the ACCORD

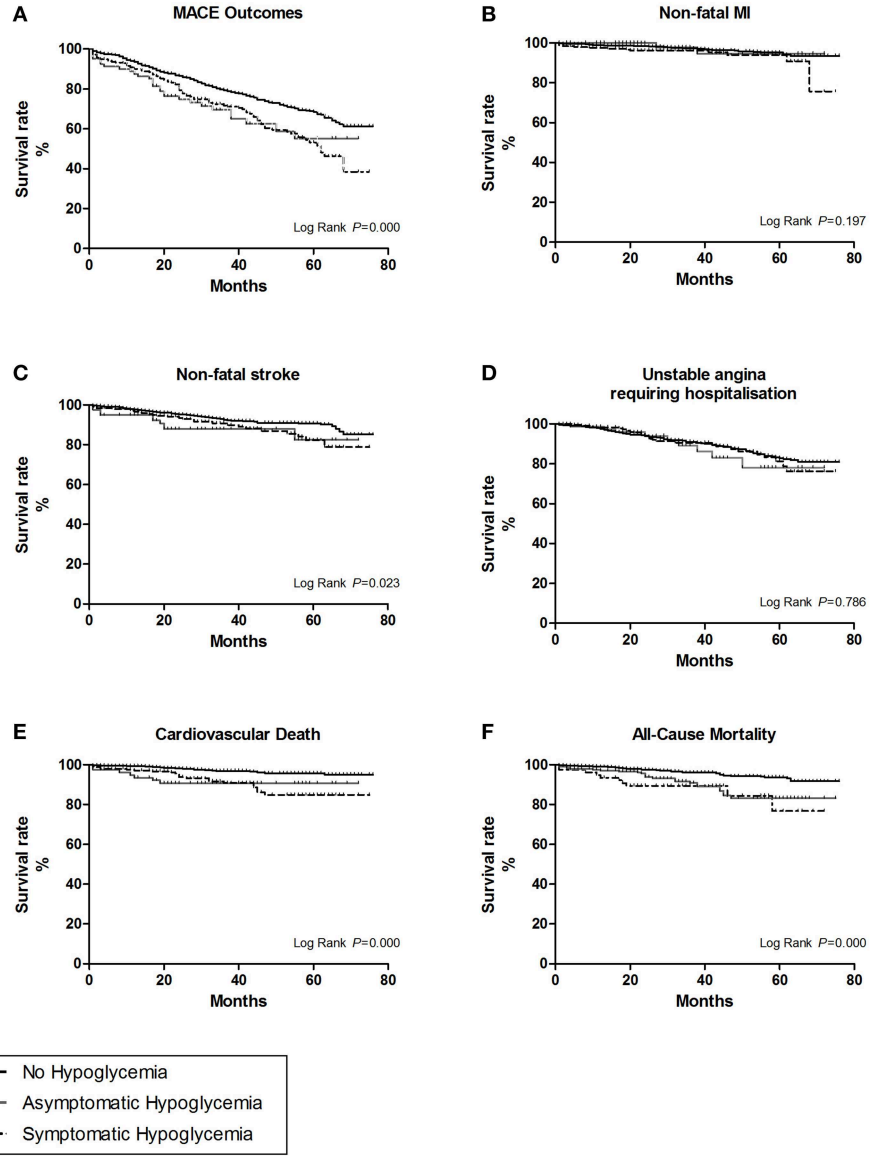

FIGURE 3 | The survival curves of the hypoglycemic symptoms were estimate by Kaplan-Meier method, and the homogeneity between survival curves was tested by log-rank test. **(A)** For overall MACE outcomes. **(B)** For the subtype of non-fatal myocardial infarction (MI). **(C)** For the subtype of non-fatal stroke. **(D)** For the subtype of unstable angina leading to hospitalization. **(E)** For the subtype of cardiovascular death. **(F)** For all cause-mortality.

study found that the protective effect of recurrent mild hypoglycemia was more pronounced than severe hypoglycemia (20). It is suggested that exposure to mild hypoglycemia may offer better preparation against the adverse cardiovascular outcomes caused by severe hypoglycemia through prior blunting of sympathetic responses (21). In contrast to the findings of our study, several observational studies (22, 23) found out that mild hypoglycemia events have no association with mortality. Differences in methods of defining mild hypoglycemia may contribute to discrepancies. However, given the small number of participants with severe hypoglycemia ($n = 24$) in our study, these results may be limited by low statistical power.

The clinical management of T2DM emphasizes the importance of glycemic control to reduce the risk of chronic complications associated with diabetes (24). However, a too-intensive glucose management therapy also puts patients at increased risk of hypoglycemia, which could be life-threatening. Given the concern that hypoglycemia might be a risk factor for cardiovascular disease, avoiding hypoglycemia remains a significant goal in optimizing glucose control. Individualizing glycemic targets should be considered for people with T2DM who are at high risk for hypoglycemia.

Currently, the standard of care in clinical practice is self-monitoring of capillary blood glucose (SMBG),

which only provides a single point of time measurement and often fails to detect nocturnal and asymptomatic hypoglycemia. With the ability to measure glucose levels continuously and reflect glycemic variability, CGM technology is gaining increasing interest in clinical management. Numerous studies using CGM have demonstrated significant improvements in reducing hypoglycemia (25, 26). Future incorporation of CGMs in large clinical trials may provide precise information on the severity of hypoglycemia, as well as the glucose level at the occurrence of a hypoglycemic event.

Our study has two important strengths. First, to our knowledge, this is the first study of applying CGM to reveal the relationship between hypoglycemia and the increased risk of CVD. Previous epidemiologic investigations without an accurate definition of hypoglycemia may underestimate the prevalence of hypoglycemia events. Both the severity and time of hypoglycemia can be collected precisely through the CGM system to make a precise diagnosis of hypoglycemia. Second, we were able to adjust for numerous standardized and high-quality covariates, including the duration of diabetes, personal habits (smoking and drinking), BMI, and kidney function. In most large clinical trials, the ICD-code extracted from electronic medical records may be inaccurate, possibly leading to misclassification of exposure and confounding factors.

There were several limitations in our research. Firstly, the number of events for some outcomes may limit the precision of our estimations. Secondly, our study had a relatively short duration of follow-up with a median time of 31 months, which may limit the power to detect a significant association. Thirdly, the study only recruited participants of T2DM during hospitalization, which may not be generalizable beyond this population. Finally, the retrospective nature of our study precludes the possibility to explain the direct causal effect between hypoglycemia and MACE outcomes. Thus, well-designed prospective cohort studies with the primary intention are needed to evaluate the association between hypoglycemia and cardiovascular outcomes.

In conclusion, through the analysis of glucose data collected by using CGMs, our results add to the accumulating evidence that hypoglycemia is associated with an increased risk of non-fatal stroke, cardiovascular death, and all-cause mortality. We also revealed a dose-dependent relationship between the severity of hypoglycemia and cardiovascular outcomes. Therefore, effective measurements should be taken to prevent severe hypoglycemia in patients with T2DM, especially those at high risk of cardiovascular problems.

DATA AVAILABILITY

The raw data supporting the conclusions of this manuscript will be made available by the authors, without undue reservation, to any qualified researcher.

ETHICS STATEMENT

This clinical study was approved by the ethics committee broad of The Central Hospital of Wuhan. All participants had signed the informed consent form during the enrollment and before the start the study.

AUTHOR CONTRIBUTIONS

WW and SZ conceived and designed the study. WW conducted the statistical analyses and wrote the manuscript. SZ provided guidance for the statistical analysis and made critical revisions to the manuscript for important intellectual content. HM provided guidance for the statistical analysis. GY collaborated with Shanghai Lejiu Healthcare Technology Co., Ltd. and took responsibility for the integrity of the data. QT and PX adjudicated the MACE outcomes and the cause of death. LY and SF took charge of the patients' follow-up.

FUNDING

This work was supported by the National Natural Science Foundation of China [No. 81370942] and the project of Regenerative Medicine Clinical Research Center of Hubei Province.

ACKNOWLEDGMENTS

The authors thank the participants of this study for their contributions.

SUPPLEMENTARY MATERIAL

The Supplementary Material for this article can be found online at: https://www.frontiersin.org/articles/10.3389/fendo.2019.00536/full#supplementary-material

REFERENCES

1. Gogitidze Joy N, Hedrington MS, Briscoe VJ, Tate DB, Ertl AC, Davis SN. Effects of acute hypoglycemia on inflammatory and pro-atherothrombotic biomarkers in individuals with type 1 diabetes and healthy individuals. *Diabetes Care*. (2010) 33:1529–35. doi: 10.2337/dc09-0354
2. Ratter JM, Rooijackers HM, Tack CJ, Hijmans AG, Netea MG, de Galan BE, et al. Proinflammatory effects of hypoglycemia in humans with or without diabetes. *Diabetes*. (2017) 66:1052–61. doi: 10.2337/db16-1091
3. ACCORD Study Group, Gerstein HC, Miller ME, Byington RP, Goff DC Jr, Bigger JT, et al. Effects of intensive glucose lowering in type 2 diabetes. *N Engl J Med*. (2008) 358:2545–59. doi: 10.1056/NEJMoa0802743
4. ACCORD Study Group, Gerstein HC, Miller ME, Genuth S, Ismail-Beigi F, Buse JB, et al. Long-term effects of intensive glucose lowering on cardiovascular outcomes. *N Engl J Med*. (2011) 364:818–28. doi: 10.1056/NEJMoa1006524
5. Zoungas S, Patel A, Chalmers J, de Galan BE, Li Q, Billot L, et al. Severe hypoglycemia and risks of vascular events and death. *N Engl J Med*. (2010) 363:1410–8. doi: 10.1056/NEJMoa1003795

6. Duckworth WC, Abraira C, Moritz TE, Davis SN, Emanuele N, Goldman S, et al. The duration of diabetes affects the response to intensive glucose control in type 2 subjects: the VA diabetes trial. *J Diabetes Compl.* (2011) 25:355–61. doi: 10.1016/j.jdiacomp.2011.10.003
7. ORIGIN Trial Investigators, Mellbin LG, Rydén L, Riddle MC, Probstfield J, Rosenstock J, et al. Does hypoglycaemia increase the risk of cardiovascular events? A report from the ORIGIN trial. *Eur Heart J.* (2013) 34:3137–44. doi: 10.1093/eurheartj/eht332
8. Heller SR, Bergenstal RM, White WB, Kupfer S, Bakris GL, Cushman WC, et al. Relationship of glycatedhaemoglobin and reported hypoglycaemia to cardiovascular outcomes in patients with type 2 diabetes and recent acute coronary syndrome events: the EXAMINE trial. *Diabetes Obes Metab.* (2017) 19: 664–71. doi: 10.1111/dom.12871
9. Hsu PF, Sung SH, Cheng HM, Yeh JS, Liu WL, Chan WL, et al. Association of clinical symptomatic hypoglycemia with cardiovascular events and total mortality in type 2 diabetes: a nationwide population-based study. *Diabetes Care.* (2013) 36: 894–900. doi: 10.2337/dc12-0916
10. Goto A, Goto M, Terauchi Y, Yamaguchi N, Noda M. Association between severe hypoglycemia and cardiovascular disease risk in Japanese patients with type 2 diabetes. *J Am Heart Assoc.* (2016) 5:e002875. doi: 10.1161/JAHA.115.002875
11. Danne T, Nimri R, Battelino T, Bergenstal RM, Close KL, DeVries JH, et al. International consensus on use of continuous glucose monitoring. *Diabetes Care.* (2017) 40:1631–40. doi: 10.2337/dc17-1600
12. Gehlaut RR, Dogbey GY, Schwartz FL, Marling CR, Shubrook JH. Hypoglycemia in type 2 diabetes–more common than you think: a continuous glucose monitoring study. *J Diabetes Sci Technol.* (2015) 9:999–1005. doi: 10.1177/1932296815581052
13. American Diabetes Association. Standards of medical care in diabetes—2013. *Diabetes Care.* (2013) 36(Suppl. 1):S11–66. doi: 10.2337/dc13-S011
14. Lee AK, Warren B, Lee CJ, McEvoy JW, Matsushita K, Huang ES, et al. The association of severe hypoglycemia with incident cardiovascular events and mortality in adults with type 2 diabetes. *Diabetes Care.* (2018) 41:104–11. doi: 10.2337/dc17-1669
15. Khunti K, Davies M, Majeed A, Thorsted BL, Wolden ML, Paul SK. Hypoglycemia and risk of cardiovascular disease and all-cause mortality in insulin-treated people with type 1 and type 2 diabetes: a cohort study. *Diabetes Care.* (2015) 38:316–22. doi: 10.2337/dc14-0920
16. Pieber TR, Marso SP, McGuire DK, Zinman B, Poulter NR, Emerson SS, et al. DEVOTE 3: temporal relationships between severe hypoglycemia, cardiovascular outcomes and mortality. *Diabetologia.* (2018) 61:58–65. doi: 10.1007/s00125-017-4422-0
17. Goto A, Arah OA, Goto M, Terauchi Y, Noda M. Severe hypoglycaemia and cardiovascular disease: systematic review and meta-analysis with bias analysis. *BMJ.* (2013) 347:f4533. doi: 10.1136/bmj.f4533
18. Henriksen MM, Andersen HU, Thorsteinsson B, Pedersen-Bjergaard U. Hypoglycemic exposure and risk of asymptomatic hypoglycemia in type 1 diabetes assessed by continuous glucose monitoring. *J Clin Endocrinol Metab.* (2018) 103: 2329–35. doi: 10.1210/jc.2018-00142
19. Uemura F, Okada Y, Torimoto K, Tanaka Y. Relation between hypoglycemia and glycemic variability in type 2 diabetes patients with insulin therapy: a study based on continuous glucose monitoring. *Diabetes Technol Ther.* (2018) 20: 140–6. doi: 10.1089/dia.2017.0306
20. Seaquist ER, Miller ME, Bonds DE, Feinglos M, Goff DC Jr, Peterson K, et al. The impact of frequent and unrecognized hypoglycemia on mortality in the ACCORD study. *Diabetes Care.* (2012) 35:409–14. doi: 10.2337/dc11-0996
21. Reno CM, Daphna-Iken D, Chen YS, Vander Weele J, Jethi K, Fisher SJ. Severe hypoglycemia-induced lethal cardiac arrhythmias are mediated by sympathoadrenal activation. *Diabetes.* (2013) 62:3570–81. doi: 10.2337/db13-0216
22. McCoy RG, Van Houten HK, Ziegenfuss JY, Shah ND, Wermers RA, Smith SA. Increased mortality of patients with diabetes reporting hypoglycemia. *Diabetes Care.* (2012) 35:1897–901. doi: 10.2337/dc11-2054
23. Luk AO, Ho TS, Lau ES, Ko GT, Ozaki R, Tsang CC, et al. Association of self-reported recurrent mild hypoglycemia with incident cardiovascular disease and all-cause mortality in patients with type 2 diabetes: prospective analysis of the Joint Asia diabetes evaluation registry. *Medicine.* (2016) 95:e5183. doi: 10.1097/MD.0000000000005183
24. Holman RR, Paul SK, Bethel MA, Matthews DR, Neil HA. 10-year follow-up of intensive glucose control in type 2 diabetes. *N Engl J Med.* (2008) 359:1577–89. doi: 10.1056/NEJMoa0806470
25. Bolinder J, Antuna R, Geelhoed-Duijvestijn P, Kröger J, Weitgasser R. Novel glucose-sensing technology and hypoglycaemia in type 1 diabetes: a multicentre, non-masked, randomised controlled trial. *Lancet.* (2016) 388:2254–63. doi: 10.1016/S0140-6736(16)31535-5
26. Haak T, Hanaire H, Ajjan R, Hermanns N, Riveline JP, Rayman G. Flash glucose-sensing technology as a replacement for blood glucose monitoring for the management of insulin-treated type 2diabetes: a multicenter, open-label randomized controlled trial. *Diabetes Ther.* (2017) 8:55–73. doi: 10.1007/s13300-016-0223-6

Conflict of Interest Statement: The authors declare that the research was conducted in the absence of any commercial or financial relationships that could be construed as a potential conflict of interest.

frontiers in Endocrinology

ORIGINAL RESEARCH
published: 20 May 2020
doi: 10.3389/fendo.2020.00272

Characteristics of the Urinary Microbiome From Patients With Gout: A Prospective Study

Yaogui Ning[1,2], Guomei Yang[1], Yangchun Chen[3], Xue Zhao[1], Hongyan Qian[3], Yuan Liu[3], Shiju Chen[3] and Guixiu Shi[3]**

[1] School of Medicine, Xiamen University, Xiamen, China, [2] Department of Intensive Care Unit, The First Affiliated Hospital of Xiamen University, Xiamen, China, [3] Department of Rheumatology and Clinical Immunology, The First Affiliated Hospital of Xiamen University, Xiamen, China

The role of host microbes in the pathogenesis of several diseases has been established, and altered microbiomes have been related to diseases. However, the variability of the urinary microbiome in individuals with gout has not been evaluated to date. Therefore, we conducted the present prospective study to characterize the urinary microbiome and its potential relation to gout. Urine samples from 30 patients with gout and 30 healthy controls were analyzed by Illumina MiSeq sequencing of the 16S rRNA hypervariable regions, and the microbiomes were compared according to alpha-diversity indices, complexity (beta diversity) with principal component analysis, and composition with linear discriminant analysis effect size. The most significantly different taxa at the phylum and genus levels were identified, and their potential as biomarkers for discriminating gout patients was assessed based on receiver operating characteristic (ROC) curve analysis. Compared with the healthy controls, there was a dramatic decrease in microbial richness and diversity in the urine of gout patients. The phylum Firmicutes and its derivatives (Lactobacillus_iners, Family_XI, and Finegoldia), the phylum Actinobacteria and its derivatives (unidentified_Actinobacteria, Corynebacteriales, Corynebacteriale, Corynebacterium_1, and Corynebacterium_tuberculostearicum), and the genera *Prevotella* and Corynebacterium_1 were significantly enriched in the urine of gout patients. ROC analysis indicated that the top five altered microbial genera could be reliable markers for distinguishing gout patients from healthy individuals. These findings demonstrate that there are specific alterations in the microbial diversity of gout patients. Thus, further studies on the causal relationship between gout and the urinary microbiome will offer new prospects for diagnosing, preventing, and treating gout.

Keywords: gout, urine, microbiome, 16S rRNA, high-throughput sequencing, biomarker

OPEN ACCESS

Edited by:
Wen Kong,
Huazhong University of Science and Technology, China

Reviewed by:
Zhiguang Su,
Sichuan University, China
Xue Xu,
The Affiliated Drum Tower Hospital of Nanjing University Medical School, China

***Correspondence:**
Shiju Chen
shiju@xmu.edu.cn
Guixiu Shi
gshi@xmu.edu.cn

Specialty section:
This article was submitted to Experimental Endocrinology, a section of the journal Frontiers in Endocrinology

Received: *16 July 2019*
Accepted: *14 April 2020*
Published: *20 May 2020*

Citation:
Ning Y, Yang G, Chen Y, Zhao X, Qian H, Liu Y, Chen S and Shi G (2020) Characteristics of the Urinary Microbiome From Patients With Gout: A Prospective Study. Front. Endocrinol. 11:272. doi: 10.3389/fendo.2020.00272

INTRODUCTION

The human microbiome is increasingly considered an important contributor to both health and diseases (1, 2). Advanced technologies for the sequencing of bacterial 16S rRNA alleles have revealed the existence of culture-independent microbes in areas of the human body previously considered to be microbe-free, including urine (3–6). Indeed, several studies have demonstrated a diverse microbiome in the human mouth, skin, respiratory system, gastrointestinal tract, and urine,

including previously uncharacterized and uncultivated species (7, 8). Moreover, accumulating evidence since the completion of the National Institutes of Health Human Microbiome Project points to an association between dysbiosis of the microbiome and the pathogenesis of multiple diseases, including gastrointestinal diseases, pulmonary diseases, cancer, metabolic diseases, and inflammatory diseases (1, 9, 10). Thus, further comprehensive study of the microbiome characteristics related to diseases can provide new insights into the pathogenic mechanism or inform new strategies for diagnosis and treatment.

Gout is one of the most common auto-inflammatory diseases, which is characterized by elevated levels of serum uric acid (UA) with consequent deposition of urate in and around the joints. The prevalence of gout is around 3.9% in the USA and 2.5% in Europe (11–13). Although the specific pathogenic mechanism of gout remains unclear, disruption of purine metabolism and inflammation regulation has been implicated. Treatment options are also limited, and patients with gout require the use of long-term drugs to decrease the UA level. UA is excreted through the kidneys and intestine, and several studies have indicated the abnormal excretion of UA in gout, which could potentially alter the microbiome. Moreover, the microbiome itself might contribute to the abnormal UA metabolism or inflammation regulation in gout. Thus, understanding the characteristics of the microbiome in gout patients might provide potential new strategies for diagnosis and help elucidate the pathogenic mechanisms.

A previous study demonstrated the presence of intestinal bacterial dysbiosis in gout patients compared with a healthy population (14). However, the characteristics of the microbiome in the urine of gout patients remain unclear. In this study, Illumina MiSeq sequencing was employed to investigate the microbial community in urinary extracts from gout patients and healthy volunteers to explore the urinary microbiome alterations associated with gout. These results can serve as a resource for further research to gain a better understanding of the role of bacterial dysbiosis in the pathogenic mechanism and identify candidate diagnostic biomarkers for gout.

MATERIALS AND METHODS

Study Design and Subject Recruitment

The study cohort consisted of two groups (**Table 1**): the gout group ($n = 30$) and the healthy group ($n = 30$). Gout was diagnosed by rheumatologists according to the American College of Rheumatology (ACR)/EULAR 2015 criteria (15). The patients and healthy volunteers were (all males) were recruited from the First Affiliated Hospital of Xiamen University, China, from March to October 2017. The exclusion criteria were follows: (1) any comorbid disorders and (2) taking antibiotics within 1 month prior to enrolment in the study. The study was approved by the Ethics Committee of the First Affiliated Hospital of Xiamen University, and informed consent was obtained from all participants. Demographic characteristics, including age, body mass index, smoking, alcohol intake, or dietary habits, and laboratory data were recorded for all subjects.

TABLE 1 | Characteristics of gout patients and healthy controls.

Characteristic	Gout patients ($n = 30$)	Healthy controls ($n = 30$)	*P*-value
Age	45.86 ± 9.84	41.36 ± 14.30	0.161
BMI (kg/m^2)	24.09 ± 1.41	23.12 ± 1.30	0.203
UA (μmol/L)	456.30 ± 72.94	265.73 ± 68.19	0.038
BUN (mmol/L)	6.62 ± 1.40	4.43 ± 1.00	0.000
Cr (μmol/L)	73.00 ± 15.08	69.23 ± 16.97	0.426
Average reads	79,785.03 ± 3982.98	78,727.63 ± 5892.81	0.430

Values are presented as mean ± SD. BMI, body mass index; UA, ureic acid; BUN, urea nitrogen; Cr, creatinine.

Sample Preparation and DNA Extraction

Mid-stream urine samples freshly collected from each individual were immediately frozen at −20°C and transported to the laboratory with an ice pack. Total bacterial DNA from samples was extracted at Novogene Bioinformatics Technology Co., Ltd. using a TIANGEN kit according to the manufacturer's protocols. The quality of the extracted DNA was determined by 1% agarose gel electrophoresis, and the optical density value at 260/280 nm was measured on a spectrophotometer. According to the concentration, the DNA was diluted to 1 ng/μL using sterile water and stored at −20°C for Illumina MiSeq sequencing analysis.

Polymerase Chain Reaction (PCR) Amplification of the Bacterial 16S rRNA V3–V4 Region and Illumina Pyrosequencing

The V3–V4 hypervariable region of the 16S rRNA gene was amplified from the diluted DNA extracts with the forward primer 341F and reverse primer 806R. All PCRs were carried out in 30 μL reactions with 15 μL of Phusion® High-Fidelity PCR Master Mix (New England Biolabs), 0.2 μM of forward and reverse primers, and about 10 ng of template DNA. The thermal cycling program consisted of initial denaturation at 98°C for 1 min, followed by 30 cycles of denaturation at 98°C for 10 s, annealing at 50°C for 30 s, and elongation at 72°C for 30 s, followed by a final extension step at 72°C for 5 min. The same volume of 1X loading buffer (containing SYBR Green) was mixed with the PCR products and subjected to electrophoresis on a 2% agarose gel for detection. Samples with a bright main strip between 400 and 450 bp were chosen for further analysis.

The PCR products were mixed at equidensity ratios and purified with GeneJET Gel Extraction Kit (Thermo Scientific). Sequencing libraries were generated using TruSeq® DNA PCR-Free Sample Preparation Kit according to the manufacturer's recommendations, and index codes were added. The library quality was assessed on a Qubit® 2.0 fluorometer (Thermo Scientific) and an Agilent Bioanalyzer 2100 system. Finally, the

Abbreviations: UA, ureic acid; ROC, receiver operating characteristic; LDA, linear discriminant analysis; LEfSe, linear discriminant analysis effect size; PCoA, principal coordinates analysis; AUC, area under the curve.

library was sequenced on an Illumina HiSeq 2500 system, and 250-bp paired-end reads were generated.

Statistics

Clinical Data Analysis

Quantitative demographic data with a normal distribution are expressed as mean ± standard deviation, and the *t*-test was used for comparisons between the two groups. All statistical tests were two-sided, and $P < 0.05$ was regarded as statistically significant. Statistical analyses were performed using SPSS 19 (SPSS, Chicago, IL, USA).

Bioinformatics Analysis

Alpha diversity was used to analyze the complexity of species diversity for a sample through six indices: observed-species, Chao1, Shannon, Simpson, ACE, and Good's coverage. All indices in our samples were calculated with QIIME (version 1.7.0), and the results were displayed with the R software (version 2.15.3). Chao1 and observed-species represent bacterial richness, whereas the Shannon and Simpson indices are quantitative measures of bacterial diversity reflecting both species richness and evenness. The difference in alpha diversity was evaluated by the Kruskal–Wallis test.

Beta diversity was used to evaluate differences in species complexity among samples. Beta diversity on both weighted and unweighted UniFrac distances was calculated by the QIIME software (version 1.7.0). Principal coordinates analysis (PCoA) was performed to obtain principal coordinates and reduce the complex, multidimensional data for visualization of patterns and to assess whether urinary microbial species could be differentiated between gout patients and healthy controls. A distance matrix of weighted or unweighted UniFrac distances among samples was transformed to a new set of orthogonal axes, by which the maximum variation factor is reflected by the first principal coordinate, the second maximum factor is reflected by the second principal coordinate, and so on. PCoA results were displayed using the WGCNA package, stat packages, and ggplot2 package in the R software (version 2.15.3).

Each sample was mapped based on the overall microbial composition and assessed for similarities. To identify significantly different bacteria as biomarkers between groups, the online software linear discriminant analysis effect size (LEfSe) (16) was utilized to select and demonstrate differentially abundant taxonomic groups based on the Kruskal–Wallis test and linear discriminant analysis (LDA) score.

Moreover, receiver operating characteristic (ROC) curves were constructed using the statistical programming language R (V.3.1.2) to visualize the potential of significantly altered genera as gout biomarkers. ROC curves are used to evaluate the performance or the quality of diagnostic tests and are widely used to evaluate the performance of many microbial biomarkers in gut microbiome analyses (17, 18). Area under the curves (AUCs) of ROC was generated to evaluate the performance of the fitted logistic regression models. It was based on the predicted probability of gout for each individual by the multivariate logistic regression coefficient estimates and the individual's transformed relative abundances for each bacterial taxon included in the analysis to predict the probability of gout for each individual.

RESULTS

Subject Characteristics

The basic characteristics of the patients ($n = 30$) and healthy controls ($n = 30$) are summarized in **Table 1**. All of the subjects were male, with no significant differences between the two groups in terms of age, smoking history, alcohol intake, or dietary patterns. No significant difference between the groups was found in the laboratory data except for the serum levels of UA and blood urea nitrogen, which were both significantly elevated in the gout group.

Urinary Dysbiosis in Gout Patients

The urine samples of all 60 subjects were analyzed to assess overall differences in the microbial community structure in urine between gout patients and healthy individuals. After optimization, a total of 4,755,380 sequence reads were included in the final analysis. The results of Illumina MiSeq sequencing showed at least 64,967 valid reads of each sample for operational taxonomic unit (OTU) analysis.

The urinary microbiota of gout patients was significantly different from that of healthy controls. Most of the alpha-diversity indices (ACE, Chao1, Shannon, Simpson, and observed-species) of the urinary microbiota from the gout group were significantly lower than those of the healthy group (**Figure 1**). Good's coverage was higher in the gout patients than in the healthy controls, but there was no statistical difference ($P = 0.058$). These results indicate that gout patients have a lower diversity and richness in the urinary microbiome, but the evenness of the urinary microbiome is similar to that of healthy controls.

The difference in beta diversity according to the weighted UniFrac distance was assessed by PCoA, which indicated that most of the samples from the two groups clustered together (**Figure 2A**). However, the ordination plot demonstrates difference between the gout patients and healthy controls. Further examination showed that a total of 1606 OTUs were shared between the gout patients and healthy controls, which accounted for 84.34 and 78.84% of the total OTUs in healthy controls and gout patients, respectively (**Figure 2B**).

Major Differences Between the Microbiomes of Healthy Individuals and Gout Patients

The range of sequence reads obtained per subject varied from 64,967 to 90,070. A total of 30,488 OTUs were observed across all subjects, and the range of OTU numbers varied from 255 to 769. A total of 10 bacterial phyla accounted for >90% of all sequence reads in the two groups (**Figure 3A**). At the phylum level, the relative abundances of Firmicutes and Actinobacteria in the gout group were significantly higher than those in the controls ($P < 0.001$) (**Figures 3B,C**). However, the other dominant phyla

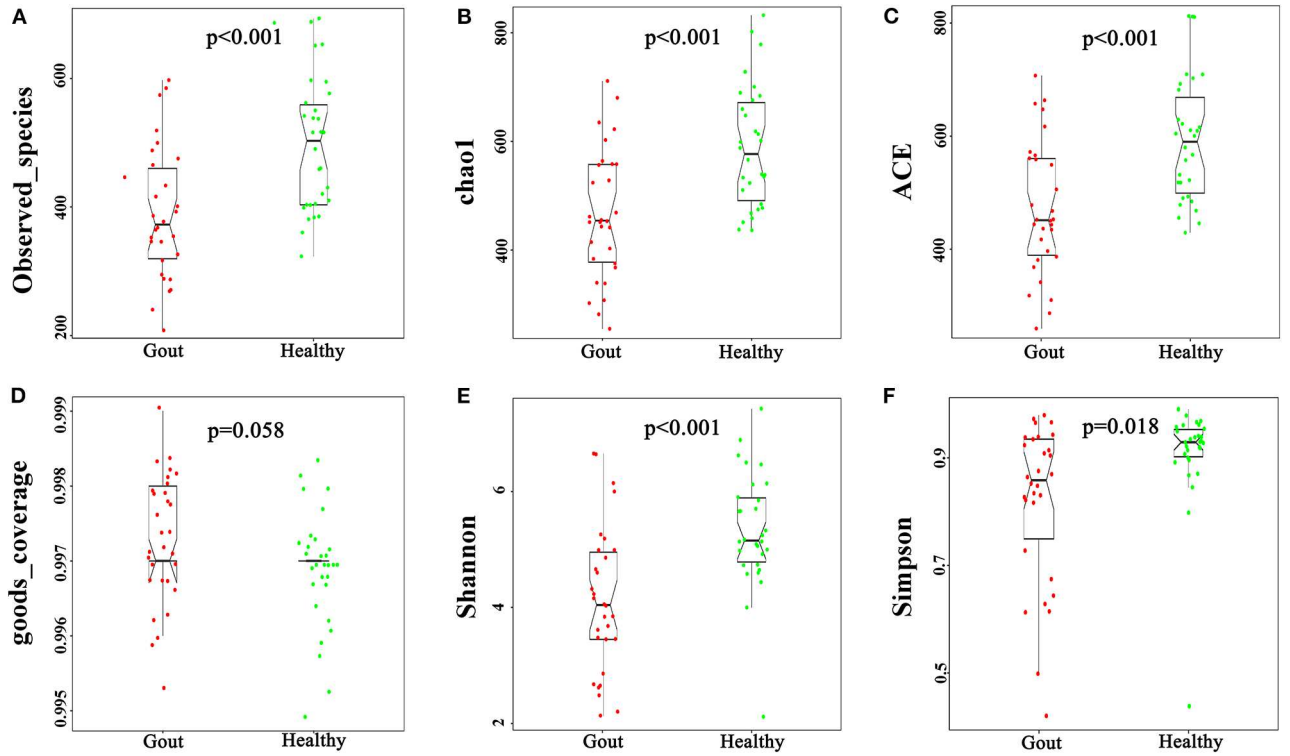

FIGURE 1 | Variation in alpha-diversity indices between gout patients (red) and healthy controls (green). Six indices of alpha-diversity were analyzed. The results demonstrate that ACE, Chao1, Shannon, Simpson, and observed-species of the urinary microbiota from the gout group were significantly lower than those of the healthy group **(A–C,E,F)**, while no statistical difference in Good's coverage was found **(D)**.

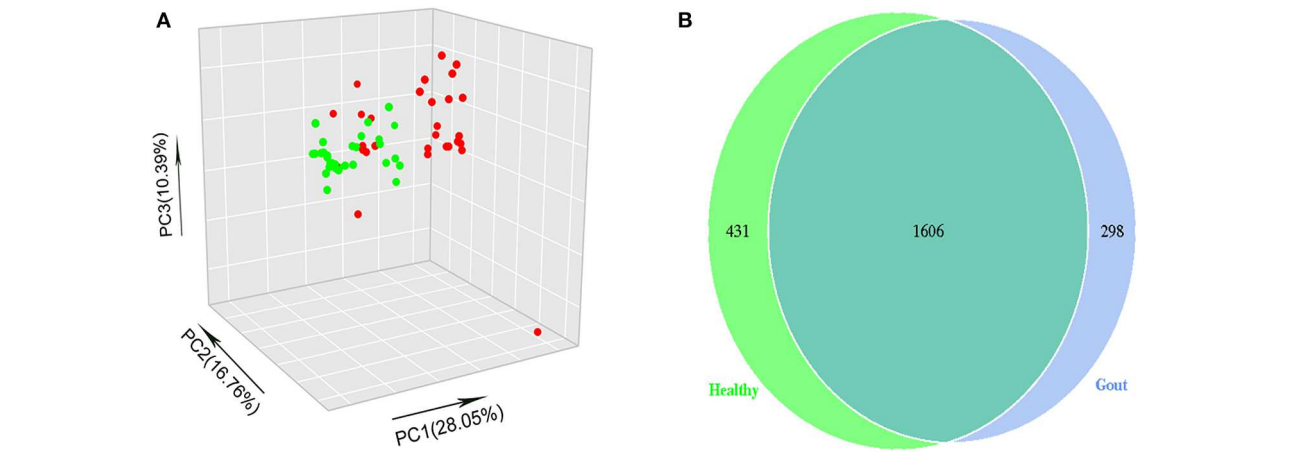

FIGURE 2 | (A) The beta-diversity indices between gout patients (red) and healthy controls (green) are shown in PCoA analysis. The ordination plot shows a clear difference between the two groups. **(B)** Venn diagrams show the percentage of shared OTUs between gout patients and healthy controls. The results show that a total of 1606 OTUs were shared between two groups, which accounted for 84.34% of the total OTUs in healthy controls and 78.84% of the total OTUs in gout patients.

showed lower abundances in the gout group, especially the relative abundance of Proteobacteria (**Figure 3D**).

At the genus level, Corynebacterium_1 was clearly enriched in the gout patients ($P = 0.004$), which possibly inflated the total Actinobacteria abundance observed at the phylum level. Another minor genus that was also significantly more abundant in the gout patients was *Prevotella*, which belongs to the phylum Bacteroidetes ($P = 0.04$). The relative abundances of other genera, including *Novosphingobium*, *Derxia*, *Curvibacter*, *Methylobacterium*, *Caulobacter*, *Skermanella*,

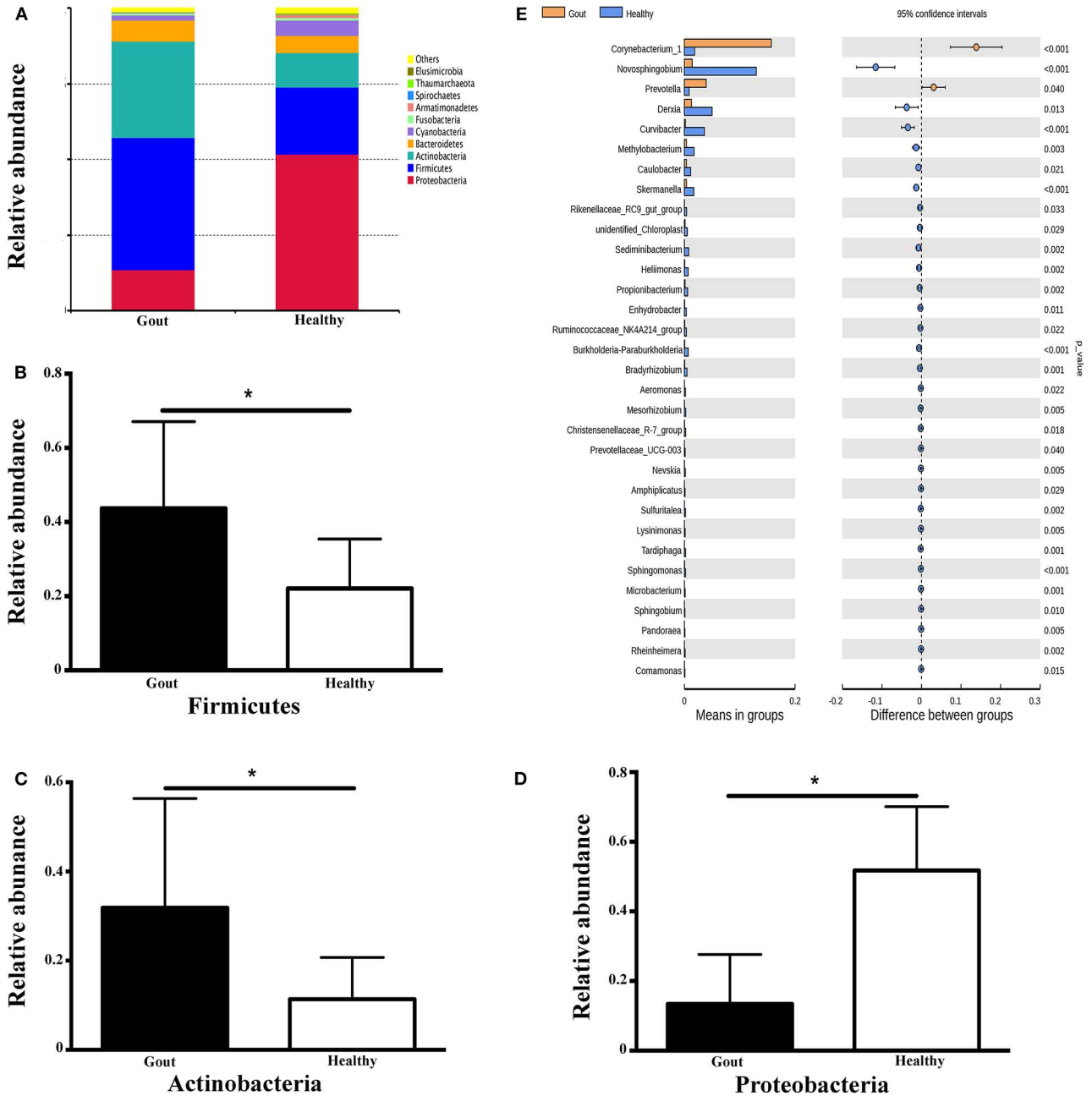

FIGURE 3 | Microbiota composition at the phylum and genus levels. **(A)** Relative abundances of the 10 dominant bacterial phyla found across the two groups shown as histograms. A *t*-test was used to detect the difference between the two groups. **(B–D)** Phyla with significantly different relative abundances between two groups, $^*P < 0.05$. **(E)** Genus with significantly different relative abundances between two groups. Different genera were assigned only to those presenting minimum variation at a significance level of $P < 0.05$.

unidentified_Chloroplast, and Rikenellaceae_RC9_gut_group, were significantly decreased in gout patients (**Figure 3E**).

Potential Biomarkers to Differentiate Gout Patients From Healthy Patients

To explore the potential gout-associated biomarkers, the urinary microbiome sequence data were subjected to LEfSe analysis. A cladogram representative of the structure of the urinary microbiota and the predominant bacteria is shown in **Figure 4**, which also displays the taxa with the greatest differences between the two groups and the discrepant microbial species with a reduced significance threshold (LDA score > 2). The LEfSe method revealed that the phylum Firmicutes and its derivatives (Lactobacillus_iners, Family_XI, and Finegoldia), the phylum

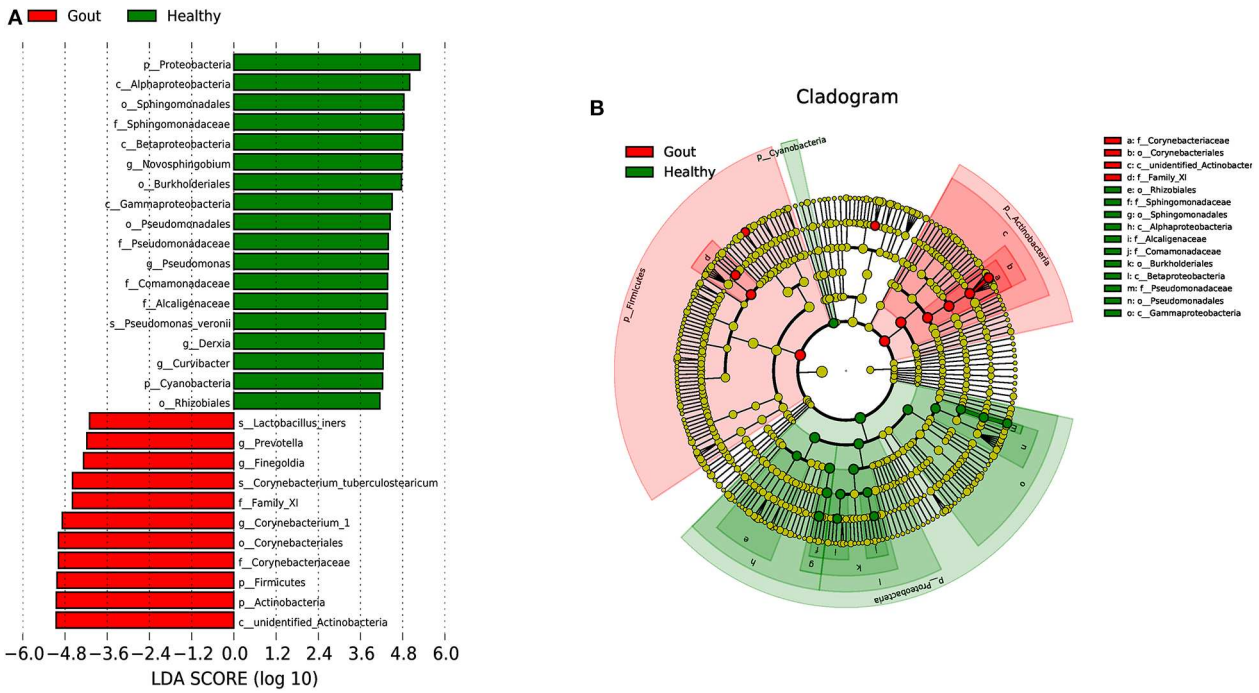

FIGURE 4 | A cladogram representative of the structure of the urinary microbiota and the predominant bacteria. **(A)** Histograms of LDA score; red and green represent gout samples and healthy controls, respectively. **(B)** Cladogram showing differentially abundant taxa of urinary microbiota in gout patients and healthy controls.

Actinobacteria and its derivatives (unidentified_Actinobacteria, Corynebacteriales, Corynebacteriale, Corynebacterium_1, and Corynebacterium_tuberculostearicum), and the genus *Prevotella* all showed higher relative abundances in the urinary microbiota from the gout patients, suggesting these taxa as candidate biomarkers for potential distinguishing between gout patients and healthy controls.

Five of the significantly altered genera (*Pandoraea*, *Curvibacter*, *Skermanella*, *Novosphingobium*, and *Sulfuritalea*) were screened for their abilities in distinguishing gout patients and healthy controls in the ROC analysis. Complete results of the training and test validation subjects using leave-one-out cross-validation are shown in **Figure 5**. This combination of significantly altered genera could effectively differentiate between gout patients and healthy controls with AUC values of 0.971 [95% confidence interval (CI) 89.22–100%] in the test validation subjects (**Figure 5A**) and 0.934 (95% CI 86.28–100%) in the training validation subjects (**Figure 5B**).

DISCUSSION

In this prospective pilot study, we first characterized the urinary microbiome of male patients with gout and healthy individuals using high-throughput sequencing of the V3–V4 region of the 16S rRNA gene. The results showed clear differences in the microbiomes between the groups, with lower diversity and richness in the gout patients, which might contribute to the abnormal UA metabolism and inflammation regulation in gout. The combination of significantly altered genera showed good ability to differentiate gout patients from healthy controls, which might provide a new non-invasive biomarker for improving gout diagnosis.

Our results further highlight the polymicrobial composition of human urine, with evident individual variation. The OTU analysis suggested that the microbiota of gout samples showed over 79% similarity with that of healthy controls. The alpha-diversity (observed-species, Chao1, ACE, Shannon, and Simpson) indices of the urinary microbiota from the gout group were all lower than those of the healthy controls, suggesting a decrease in the overall richness and ecological diversity in gout patients. These slight differences spanned from the phylum level to the species level. All of the urine samples were predominantly composed of bacteria from four phyla, Firmicutes, Proteobacteria, Actinobacteria, and Bacteroidetes, which is consistent with the findings of Karstens et al. (19). The most abundant phylum in healthy controls was Proteobacteria, whereas Firmicutes was the most abundant phylum in the gout group. Firmicutes is considered as the most abundant bacteria in normal urine samples (19–23), although Proteobacteria has also been reported to be the most common in healthy urine (24). This overall similarity at the phylum level could suggest a relatively stable bacterial community in gout. However, at the genus level, more specific and clear shifts were observed, especially for genera in Actinobacteria and Bacteroidetes. The predominant ecological structure of the urine microbiomes showed slight variations in relative abundance in the two groups. In particular, *Prevotella* increased in the gout patients, which belongs to Bacteroidetes, and was reported to be the second and/or third most abundant or

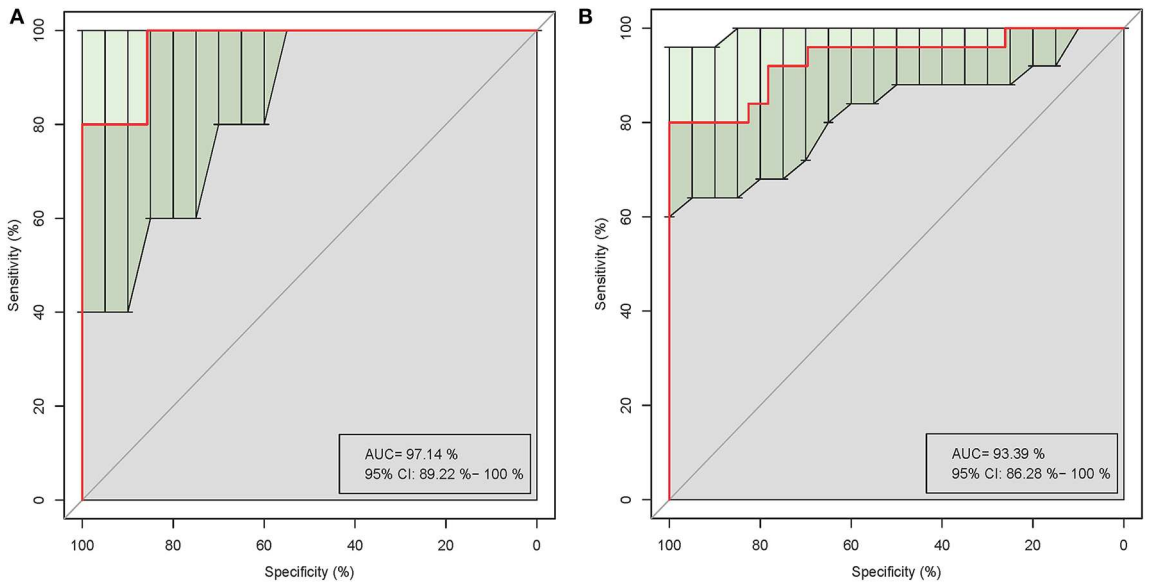

FIGURE 5 | Receiver operating characteristic (ROC) curves demonstrating the performance of significantly altered microbial genera for the test **(A)** and training **(B)** validation subjects using leave-one-out cross-validation.

even lower in rank in healthy individuals (21, 22, 25). A previous study also demonstrated that the family Bacteroidaceae and its genus *Bacteroides* were enriched in the gut of male gout patients (26). *Prevotella* has been regarded as pathogenic in the vaginal microbiome (27). This genus was also found to be was enriched in patients with type 2 diabetes (24) and in general non-healthy individuals (21, 25). *Prevotella* was also found to be increased in the gut microbiome of patients with kidney stones compared with non-stone controls (28). Bacteria selectively aggregate to crystals in the urinary tract, which suggests a proper mechanistic role for bacteria in stone formation. Gout is a high-risk factor for the formation of kidney stones; however, the role of *Prevotella* in gout and/or uric acid stone formation remains unknown.

Corynebacterium_1 was also a predominant genus detected in the gout group, whereas *Novosphingobium* was more predominant in the urine of healthy controls. The abundance of Corynebacterium_1 was previously demonstrated to be correlated with serum concentrations of interleukin-6 and C-reactive protein in cancer patients (29). Gout not only is a metabolic condition but is also an auto-inflammatory disease associated with an increased inflammatory reaction. Therefore, these findings could suggest an association between urinary microbiota such as Corynebacterium_1 and an inflammatory reaction. The relative abundance of Corynebacterium_1 was previously reported to be increased in patients with prostate cancer (30). Both gout and prostate cancer are clinical conditions that mainly occur in male patients; therefore, it would be interesting to investigate a potential sex-specific pattern of Corynebacterium_1 abundance. The urine samples of the present study were all from male subjects since gout is predominant in men. However, previous studies have demonstrated a difference in the healthy urine microbiome of males and females (31). Therefore, these conclusions should be interpreted with caution when applied to elderly female patients suffering from gout.

There is previous evidence of an association of the gut microbiota with gout (14, 26, 32), suggesting that the altered metabolites of gout patients may play a role not only in inflammation disorders but also in purine metabolism and UA excretion. The intestinal microbiota composition also markedly varies according to dietary intake (33), which could induce differences in both the microbiota composition and microbial metabolites (34). Consequently, the urinary microbiota can be indirectly influenced by gut microbiota alterations caused by dietary patterns (35).

Here, we found some specific alterations of the urinary microbiome with potential to distinguish gout patients from healthy controls. In particular, the combination of five genera that were significantly altered in the urine of gout patients, *Pandoraea*, *Curvibacter*, *Skermanella*, *Novosphingobium*, and *Sulfuritalea*, could effectively distinguish gout patients from healthy controls with a high predictive value. To the best of our knowledge, this is the first attempt to characterize the urinary signatures of gout by integrating the microbiome. The significantly altered urine microbiome could serve as a biomarker to discriminate between gout patients and healthy controls, thereby improving diagnosis and allowing for early intervention. Further exploration of the underlying mechanisms to explain these associations could also provide insight into the pathogenesis of gout and suggest new treatment strategies.

DATA AVAILABILITY STATEMENT

Raw Illumina data reads are available in the NCBI Sequence Read Archive database of GenBank under accession ID SRP153570.

ETHICS STATEMENT

The studies involving human participants were reviewed and approved by the Ethics Committee of the First Affiliated Hospital of Xiamen University. The patients/participants provided their written informed consent to participate in this study. Written informed consent was obtained from the individual(s) for the publication of any potentially identifiable images or data included in this article.

AUTHOR CONTRIBUTIONS

GS participated in the research design and data analysis, reviewed and revised the manuscript, and provided general supervision and financial support. YL revised the manuscript. YN performed data acquisition, sample collection and analysis, and interpretation and contributed to article drafting and revision. SC performed sample collection, data analysis, and article revision and provided financial support. GY, XZ, HQ, and YC performed data acquisition and sample collection. All authors contributed to the study and approved the final submitted manuscript.

ACKNOWLEDGMENTS

We appreciate all of the patients and volunteers for their participation. We also thank the postgraduate researchers Xining Liao, Mi Zhou, Xiaoqin Yuan, and Yingling Xiong for their contribution in sample collection. This work was partly supported by the Natural Science of China (Grant Numbers 81501369, 81971536, and 81601384), and Young Grant from Health and Family Planning Commission of Fujian Province (Grant Number 2015-2-40).

REFERENCES

1. Cho I, Blaser MJ. The human microbiome: at the interface of health and disease. *Nat Rev Genet*. (2012) 13:260–70. doi: 10.1038/nrg3182
2. Wu P, Chen Y, Zhao J, Zhang G, Chen J, Wang J, et al. Urinary microbiome and psychological factors in women with overactive bladder. *Front Cell Infect Microbiol*. (2017) 7:488. doi: 10.3389/fcimb.2017.00488
3. Arthur JC, Perez-Chanona E, Mühlbauer M, Tomkovich S, Uronis JM, Fan TJ, et al. Intestinal inflammation targets cancer-inducing activity of the microbiota. *Science*. (2012) 338:120–3. doi: 10.1126/science.1224820
4. Caporaso JG, Kuczynski J, Stombaugh J, Bittinger K, Bushman FD, et al. QIIME allows analysis of high-throughput community sequencing data. *Nat Methods*. (2010) 7:335–6. doi: 10.1038/nmeth.f.303
5. Langmead B, Salzberg SL. Fast gapped-read alignment with Bowtie 2. *Nat Methods*. (2012) 9:357–9. doi: 10.1038/nmeth.1923
6. Edgar RC. Search and clustering orders of magnitude faster than BLAST. *Bioinformatics*. (2010) 26:2460–1. doi: 10.1093/bioinformatics/btq461
7. Robinson CJ, Bohannan BJ, Young VB. From structure to function: the ecology of host-associated microbial communities. *Microbiol Mol Biol Rev*. (2010) 74:453–76. doi: 10.1128/MMBR.00014-10
8. Nelson DE, Van Der Pol B, Dong Q, Revanna KV, Fan B, Easwaran S, et al. Characteristic male urine microbiomes associate with asymptomatic sexually transmitted infection. *PLoS ONE*. (2010) 5:e14116. doi: 10.1371/journal.pone.0014116
9. Kau AL, Ahern PP, Griffin NW, Goodman AL, Gordon JI. Human nutrition, the gut microbiome and the immune system. *Nature*. (2011) 474:327–36. doi: 10.1038/nature10213
10. Pflughoeft KJ, Versalovic J. Human microbiome in health and disease. *Annu Rev Pathol*. (2012) 7:99–122. doi: 10.1146/annurev-pathol-011811-132421
11. Wijnands JM, Viechtbauer W, Thevissen K, Arts IC, Dagneli PC, Stehouwer CD, et al. Determinants of the prevalence of gout in the general population: a systematic review and meta-regression. *Eur J Epidemiol*. (2015) 30:19–33. doi: 10.1007/s10654-014-9927-y
12. Kuo CF, Grainge MJ, Mallen C, Zhang W, Doherty M. Rising burden of gout in the UK but continuing suboptimal management: a nationwide population study. *Ann Rheum Dis*. (2015) 74:661–7. doi: 10.1136/annrheumdis-2013-204463
13. Zhu Y, Pandya BJ, Choi HK. Prevalence of gout and hyperuricemia in the US general population: the National Health and Nutrition Examination Survey 2007-2008. *Arthritis Rheum*. (2011) 63:3136–41. doi: 10.1002/art.30520
14. Guo Z, Zhang J, Wang Z, Ang KY, Huang S, Hou Q, et al. Intestinal microbiota distinguish gout patients from healthy humans. *Sci Rep*. (2016) 6:20602. doi: 10.1038/srep20602
15. Neogi T, Jansen TL, Dalbeth N, Fransen J, Schumacher HR, Berendsen D, et al. 2015 Gout classification criteria: an American College of Rheumatology/European League Against Rheumatism collaborative initiative. *Ann Rheum Dis*. (2015) 74:1789–98. doi: 10.1136/annrheumdis-2015-208237
16. Segata N, Izard J, Waldron L, Gevers D, Miropolsky L, Garrett WS, et al. Metagenomic biomarker discovery and explanation. *Genome Biol*. (2011) 12:R60. doi: 10.1186/gb-2011-12-6-r60
17. He Z, Shao T, Li H, Xie Z, Wen C. Alterations of the gut microbiome in Chinese patients with systemic lupus erythematosus. *Gut Pathog*. (2016) 8:64. doi: 10.1186/s13099-016-0146-9
18. Xu J, Xiang C, Zhang C, Xu B, Wu J, Wang R, et al. Microbial biomarkers of common tongue coatings in patients with gastric cancer. *Microb Pathog*. (2019) 127:97–105. doi: 10.1016/j.micpath.2018.11.051
19. Karstens L, Asquith M, Davin S, Stauffer P, Fair D, Gregory WT, et al. Does the urinary microbiome play a role in urgency urinary incontinence and its severity? *Front Cell Infect Microbiol*. (2016) 6:78. doi: 10.3389/fcimb.2016.00078
20. Siddiqui H, Nederbragt AJ, Lagesen K, Jeansson SL, Jakobsen KS. Assessing diversity of the female urine microbiota by high throughput sequencing of 16S rDNA amplicons. *BMC Microbiol*. (2011) 11:244. doi: 10.1186/1471-2180-11-244
21. Siddiqui H, Lagesen K, Nederbragt AJ, Jeansson SL, Jakobsen KS. Alterations of microbiota in urine from women with interstitial cystitis. *BMC Microbiol*. (2012) 12:205. doi: 10.1186/1471-2180-12-205
22. Pearce MM, Hilt EE, Rosenfeld AB, Zilliox MJ, Thomas-White K, Fok C, et al. The female urinary microbiome: a comparison of women with and without urgency urinary incontinence. *MBio*. (2014) 5:e01283–14. doi: 10.1128/mBio.01283-14
23. Thomas-White KJ, Kliethermes S, Rickey L, Lukacz ES, Richter HE, Moalli P, et al. Evaluation of the urinary microbiota of women with uncomplicated stress urinary incontinence. *Am J Obstet Gynecol*. (2017) 216:55.e1–16. doi: 10.1016/j.ajog.2016.07.049
24. Liu F, Ling Z, Xiao Y, Lv L, Yang Q, Wang B, et al. Dysbiosis of urinary microbiota is positively correlated with type 2 diabetes mellitus. *Oncotarget*. (2017) 8:3798–810. doi: 10.18632/oncotarget.14028
25. Pearce MM, Zilliox MJ, Rosenfeld AB, Thomas-White KJ, Richter HE, Nager CW, et al. The female urinary microbiome in urgency urinary incontinence. *Am J Obstet Gynecol*. (2015) 213:347.e1–11. doi: 10.1016/j.ajog.2015.07.009
26. Shao T, Shao L, Li H, Xie Z, He Z, Wen C. Combined signature of the fecal microbiome and metabolome in patients with gout. *Front Microbiol*. (2017) 8:268. doi: 10.3389/fmicb.2017.00268
27. Xia Q, Cheng L, Zhang H, Sun S, Liu F, Li H, et al. Identification of vaginal bacteria diversity and it's association with clinically diagnosed bacterial vaginosis by denaturing gradient gel electrophoresis

and correspondence analysis. *Infect Genet Evol*. (2016) 44:479–86. doi: 10.1016/j.meegid.2016.08.001
28. Stern JM, Moazami S, Qiu Y, Kurland I, Chen Z, Agalliu I, et al. Evidence for a distinct gut microbiome in kidney stone formers compared to non-stone formers. *Urolithiasis*. (2016) 44:399–407. doi: 10.1007/s00240-016-0882-9
29. Reunanen J, Kainulainen V, Huuskonen L, Ottman N, Belzer C, Huhtinen H, et al. *Akkermansia muciniphila* adheres to enterocytes and strengthens the integrity of the epithelial cell layer. *Appl Environ Microbiol*. (2015) 81:3655–62. doi: 10.1128/AEM.04050-14
30. Shrestha E, White JR, Yu SH, Kulac I, Ertunc O, De Marzo AM, et al. Profiling the urinary microbiome in men with positive versus negative biopsies for prostate cancer. *J Urol*. (2018) 199:161–71. doi: 10.1016/j.juro.2017.08.001
31. Fouts DE, Pieper R, Szpakowski S, Pohl H, Knoblach S, Suh MJ, et al. Integrated next-generation sequencing of 16S rDNA and metaproteomics differentiate the healthy urine microbiome from asymptomatic bacteriuria in neuropathic bladder associated with spinal cord injury. *J Transl Med*. (2012) 10:174. doi: 10.1186/1479-5876-10-174
32. Kim JK, Kwon JY, Kim SK, Han SH, Won YJ, Lee JH, et al. Purine biosynthesis, biofilm formation, and persistence of an insect-microbe gut symbiosis. *Appl Environ Microbiol*. (2014) 80:4374–82. doi: 10.1128/AEM.00739-14
33. Jang HB, Choi MK, Kang JH, Park SI, Lee HJ. Association of dietary patterns with the fecal microbiota in Korean adolescents. *BMC Nutr*. (2017) 3:20. doi: 10.1186/s40795-016-0125-z
34. Sheflin AM, Melby CL, Carbonero F, Weir TL. Linking dietary patterns with gut microbial composition and function. *Gut Microbes*. (2017) 8:113–29. doi: 10.1080/19490976.2016.1270809
35. Remer T. Influence of nutrition on acid-base balance–metabolic aspects. *Eur J Nutr*. (2001) 40:214–20. doi: 10.1007/s394-001-8348-1

Conflict of Interest: The authors declare that the research was conducted in the absence of any commercial or financial relationships that could be construed as a potential conflict of interest.

Advantages of publishing in Frontiers

OPEN ACCESS
Articles are free to read for greatest visibility and readership

FAST PUBLICATION
Around 90 days from submission to decision

HIGH QUALITY PEER-REVIEW
Rigorous, collaborative, and constructive peer-review

TRANSPARENT PEER-REVIEW
Editors and reviewers acknowledged by name on published articles

Frontiers
Avenue du Tribunal-Fédéral 34
1005 Lausanne | Switzerland

Visit us: www.frontiersin.org
Contact us: info@frontiersin.org | +41 21 510 17 00

REPRODUCIBILITY OF RESEARCH
Support open data and methods to enhance research reproducibility

DIGITAL PUBLISHING
Articles designed for optimal readership across devices

FOLLOW US
@frontiersin

IMPACT METRICS
Advanced article metrics track visibility across digital media

EXTENSIVE PROMOTION
Marketing and promotion of impactful research

LOOP RESEARCH NETWORK
Our network increases your article's readership